NASA Contractor Report 168288

RESULTS OF AN EXPERIMENTAL PROGRAM INVESTIGATING THE EFFECTS OF SIMULATED ICE ON THE PERFORMANCE OF THE NACA 63A415 AIRFOIL WITH FLAP

R. J. Zaguli, M. B. Bragg, and G. M. Gregorek

The Ohio State University
Columbus, Ohio

January 1984

Prepared for

NATIONAL AERONAUTICS AND SPACE ADMINISTRATION
Lewis Research Center
Under Grant NAG3-28

TABLE OF CONTENTS

N84-16145 #

NOMENCLATURE

c	Airfoil chord length, m
C_d	Drag coefficient, $D/q_\infty c$
C_ℓ	Lift coefficient, $L/q_\infty c$
C_m	Moment coefficient about the quarter chord, $M/q_\infty c^2$
C_p	Pressure coefficient, $(P - P_\infty)/q_\infty$
K/c	Roughness height
P	Local static pressure, N/m^2
P_∞	Free stream static pressure, N/m^2
q_∞	Free stream dynamic pressure, N/m^2
T	Temperature, ^oF
V	Velocity in knots
x/c	Horizontal coordinate
z/c	Vertical coordinate
α, AOA	Angle of attack, degrees
δ_f	Flap deflection, degrees

INTRODUCTION

The test program described in this report is an extension of a study begun in 1981 to provide needed information on the performance degradation of airfoil sections resulting from rime and glaze ice accretions. Its primary objectives were:

1) To expand the current database of performance data on the 63A415 with simulated ice to include flap deflection.

2) To further study the flowfield in the area of the ice accretion through pressure distributions and flow visualization techniques, which can then be used to evaluate the accuracy of the theoretical analysis methods currently being developed.

3) To obtain data on a simulated glaze ice shape that scales down to a 6 inch chord model and will be tested in the OSU Transonic Airfoil Wind Tunnel Facility. These data will be used to compare the aerodynamic qualities of the NASA Icing Research Tunnel and the OSU tunnel, and to evaluate a lift measuring system based on wall pressures.

Mr. Richard Freuler, Senior Computer Specialist at the Aeronautical and Astronautical Research Laboratory, developed the software needed for the data acquisition system. Mr. Steven Thompson, an under-graduate research assistant, modified the software and performed the data reduction for this test.

EXPERIMENTAL METHOD

Equipment

Testing was performed in the NASA Lewis 6' x 9' Icing Research Tunnel (IRT). The airfoil model used was the NACA 63_2-A415 with a 1.36 m chord and a moveable flap with deflections of 10°, 20°, and 30°. The airfoil and flap were pressure tapped using 1/8" OD strip-a-tube attached to the airfoil surface. In addition, the model was fitted with five simulated ice shapes (Figures 1A-1E):

1) Generic Glaze
2) Glaze 3°
3) Rime 3°
4) Glaze 7°
5) Rime 7°

Aerodynamic data were taken on the first three shapes and flow visualization was performed on all five. The Generic Glaze shape was derived from the work of Ingelman-Sundberg[1]. This shape was chosen because it scales to a convenient size on the 6" chord model which will be tested in the OSU Transonic Airfoil Wind Tunnel Facility.

The Glaze 3, Rime 3, Glaze 7, and Rime 7 shapes were chosen from a series of ice growths generated during an actual ice accretion study in the NASA Lewis Icing Research Tunnel[2]. They represent typical climb, high angle of attack and low velocity, and cruise, low angle of attack and high velocity conditions.

In order to add the surface roughness characteristic of natural ice shapes, aluminum oxide grit with a K/C = .00058 was attached to the glaze shapes with a spray acrylic adhesive. A grit with a K/C = .0012 was added to the rime shapes.

On-line data acquisition and reduction were accomplished using the OSU Digital Data Acquisition and Reduction System[3] (DDARS -

figure 2). The central processing unit is the DEC LSI-11 microcomputer. Input and output is through a teletype terminal and mass data storage through a twin floppy disc drive system. Analog data signals from the transducers and wake probe slidewire systems are fed into an analog front end which conditions the signal and converts it into a digital format.

Airfoil pressures were obtained through a Scanivalve transducer arrangement, while drag data were measured using a wake probe with total and static ports. The voltages from these systems as well as those from tunnel total and tunnel static transducers were input to the analog box and then to the computer for on-line reduction (figure 3).

In order to visualize the flow in the leading edge region, a splitter plate[4] was constructed which could be positioned between the upper and lower segments of the attached ice shape. (See figure 4). Small drops of oil-based paint were then applied to the plate in the regions of interest and the tunnel then brought up to speed. Videotape was made of the movement of the drops and still photographs were taken after no further movement was observed.

Data Reduction

The DDARS system provides the test engineer quick-look pressure distributions as well as integrated values of C_ℓ, C_m, and C_d. This permits maximum use of tunnel time.

An interactive computer program was written for the final data reduction on the OSU Harris/6 computer system. The raw data files from the IRT test were transferred to the Harris from the LSI-11 microcomputer. The program converts Scanivalve voltage from each model tap into a pressure coefficient. The user is given a plot of the final C_p distribution for each element (main and flap) on a Tektronix CRT and can control any re-reduction required using the terminal cursors. The program then integrates the distribution to get lift and moment coefficients.

The drag coefficient is calculated using the Jones Equation[5]. The wake is displayed on the graphics terminal and the user enters the integration limits using cursors. If the operator sees that the probe traverse was not large enough to capture the full wake, that run reduction can be bypassed.

RESULTS AND DISCUSSION

Aerodynamic Measurements

Data were taken on the following simulated ice accretions as well as the clean airfoil;

1) Rime 3 Rough
2) Glaze 3 Rough
3) Generic Glaze Smooth
4) Generic Glaze Rough

In addition, for each configuration flap deflection was varied from 0-30 degrees.

The glaze ice C_p distributions show the characteristic adverse pressure gradient where the flow is forced to negotiate the large change in surface slope at the tip of the horns. These pressure spikes promote separation and tend to decrease $C_{\ell_{max}}$ and increase the drag coefficient. The separated zone is clearly seen as a region of constant pressure in the C_p distribution in the area behind the glaze ice horn.

From the pressure distributions, it is observed that the flap was stalled for most of the runs. This separation is again characterized by a region of constant C_p. A previous investigation by W. R. Krolak[6] on the Beechcraft Sundowner, equipped with a NACA 63A415 airfoil, shows this same trend in flight test data.

From Table I and figure 5, it is clear that the penalties associated with ice show up in reductions in $C_{\ell_{max}}$ and α_{stall}. The G3 shape showed a reduction in $C_{\ell_{max}}$ over the clean case of 0.2 - 0.4, and a reduction in α_{stall} of as much as 4° for the $\delta_f = 30^{\circ}$ case. Similar reductions were seen for the generic and rime shapes.

Due to the position of the wake probe, drag data could only be taken on $\delta_f = 0^{\circ}$ cases. Cumulative plots of C_ℓ vs. C_d show

TABLE I

PERFORMANCE DEGRADATION WITH SIMULATED ICE

	CLEAN			G3			GEN			R3		
δ_f	10	20	30	10	20	30	10	20	30	10	20	30
$C_{\ell max}$	1.8	2.0	2.2	1.4	1.7	2.0	1.2	1.5	1.7	1.5	1.75	1.95
α_{stall}	14.0	12.5	11.5	10.5	9.5	7.5	7.5	-	5.5	10.5	8.5	6.5
α_{LO}	-6.5	-10.0	-13.0	-6.0	-	-12.5	-6.0	-	-10.0	-6.0	-	-11.0

the increase in drag caused by the ice shapes. For example, at $C_\ell = .4$, a 20% increase in drag over the clean airfoil was observed when the R3 rough shape was attached, and a 30% increase for the G3 rough shape. Interestingly, the presence of roughness on the Generic Glaze shape was not found to be very crucial. This is due to the large laminar separation bubble in the region of the ice shape, which tends to be the prominent source of pressure drag.

From the cumulative plots of C_m vs C_ℓ, it is observed that at the lower lift coefficients the effect of the ice shape is almost negligible. However, at the higher C_ℓ's, for example at low speed with the flap deflected, more positive C_m's were observed with the simulated ice than for the clean airfoil.

<u>Flow Visualization</u>

Using the splitter plate arrangement, discussed previously, the flow about the simulated shapes was recorded. Of particular interest were the separated zones observed with the glaze shapes. These laminar separation zones were photographed and later the coordinates of the separated streamline were digitized from these records. Figures 6 and 7 are representative of the observed flow patterns. Figure 6 clearly shows the Generic Glaze shape at $\alpha = 1.7^{\circ}$ with its separated zone behind the horn. Figure 6 is of the same configuration but at $\alpha = 5.6^{\circ}$, and clearly shows the characteristic recirculation region. Figure 8 shows the G3 shape at $\alpha = 5.6^{\circ}$.

The authors discovered during the analysis of the photos that the splitter plate extended too far into the flow ahead of the stagnation region between the glaze ice horns. The splitter plate boundary layer then separated due to the adverse gradient from the airfoil flowfield. This 3-D flowfield created vortices which were shed downstream and affected the flow patterns recorded. This is particularly evident in figure 7 where the streamlines converge due to the influence of these shed vortices. However, qualitatively the data provides some interesting clues to the shape and extent of the laminar separation bubble.

Further investigation was performed at Ohio State using two different splitter plate configurations. A scaled-down version of the splitter plate utilized in the Lewis IRT and a smaller one with the leading edge reduced were tested on a GAW-1 airfoil with a simulated ice shape. Flow visualization techniques confirmed the authors' hypotheses that vortices were shed downstream due to the severe pressure gradient induced by the ice shape on the splitter plate. It was observed that the reattachment point was shortened by as much as 3% under these test conditions as a result of the larger splitter plate. This value cannot however, be directly applied to the 63A415 airfoil in the Lewis test. Rather, the reader should realize that qualitatively this shows that the observed reattachment point was moved forward due to the presence of the splitter plate. In addition, it must be pointed out that this method of visualization does not actually display the position of the separated streamline. Rather a position above the zero velocity line in the separated zone between the recirculating flow is measured.

Presentation of Data

A tabulated run summary is included in the appendix of this report. It is organized by configuration: 1) clean, 2) rime 3 rough, 3) glaze 3 rough, 4) generic glaze rough and 5) generic glaze smooth. Following these tables are the cumulative plots of C_ℓ vs α, C_m vs C_ℓ, and C_ℓ vs C_d. Lastly, the pressure distributions are included and ordered in the same sequence as the run summary tables.

Data reported with zero flap deflection was taken at approximately $Re = 4.2 \times 10^6$ and $M = 0.13$. Due to the large loads on the model, data at all flap deflection angles greater than zero, were taken at approximately $Re = 3.3 \times 10^6$ and $M = 0.10$. No tunnel wall corrections have been made in the data.

SUMMARY AND CONCLUSIONS

A typical general aviation airfoil, the NACA 63_2-A415, was outfitted with simulated ice accretions and tested in the NASA Icing Research Tunnel. Pressure distributions were obtained for a variety of flap deflections and angles of attack. As a result of this study, the following observations can be made;

1) The airfoils with simulated ice shapes showed large increases in drag and heavy penalties in $C_{\ell max}$ and α_{stall}. A shift in α_{LO} was also observed. These reductions in performance would be of particular importance to the pilot in a landing configuration with the flap deployed and power reduced.

2) Measured pressure distributions and flow visualization show the separated zone behind the horn of the glaze shapes and the severe adverse pressure gradients which lead to the separation.

3) Surface roughness for the Generic Glaze shape was not a crucial factor in the drag observed. Rather, the prominent effect was the large separated zone.

Further investigation is necessary to document the flow characteristics reported. More detailed pressure distributions should be obtained, particularly in the region behind and between the glaze ice horns. Also, while flow visualization provides valuable insight into the flow in the separated zones, quantitative data must be gathered here before an analytical model can be developed.

REFERENCES

1. Ingelman-Sundberg, M., Trunov, O. K. and Ivaniko, A., "Methods for Prediction of the Influence of Ice on Aircraft Flying Characteristics," Swedish-Soviet Working Group on Flight Safety, 6th Meeting, 1977.

2. Bragg, M. B., Zaguli, R. J. and Gregorek, G. M., "Wind Tunnel Evaluation of Airfoil Performance Using Simulated Ice Shapes," NASA Contractor Report 167960, November 1982.

3. Freuler, R. J. and Hoffmann, M. J., "Experiences with an Airborne Digital Computer System for General Aviation Flight Testing," AIAA Paper No. 79-1834, presented at the AIAA Aircraft Systems and Technology Meeting, New York, New York, August 20-22, 1979.

4. Pfeiffer, N. J. and Zumwalt, G. W., "A Computational Model for Low Speed Flows Past Airfoils with Spoilers," AIAA Paper No. 81-0253, Presented at the 19th Aerospace Sciences Meeting, St. Louis, Missouri, January 12-15, 1981.

5. Schlichting, H., Boundary-Layer Theory, Sixth Edition, McGraw-Hill, New York, 1968.

6. Krolak, W. R., "In-Flight Investigation of the Aerodynamic Characteristics of a Wing Equipped with an Upper Surface Leading Edge Modification," Master's Thesis, Ohio State University, 1981.

7. Kunchal, David, "Splitter Plate Analysis," Final Report for AAE 693, Ohio State University Aeronautical and Astronautical Engineering Department, October 1982.

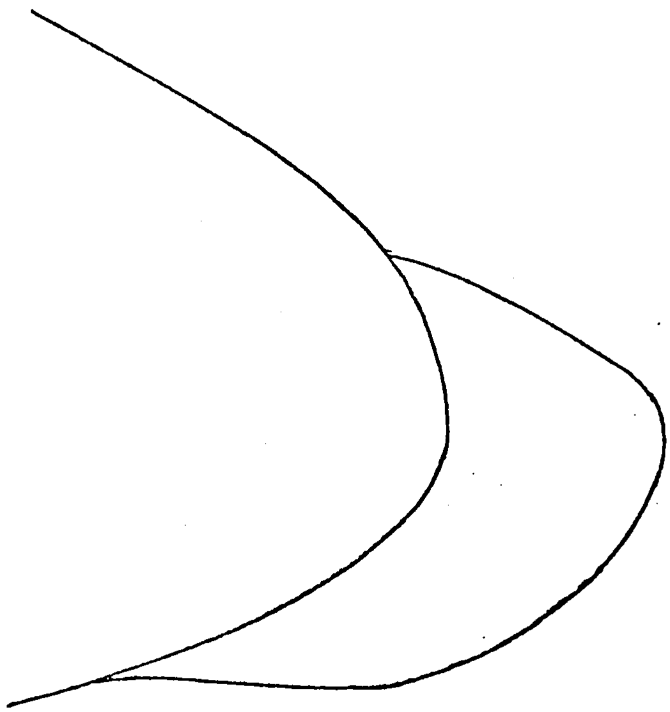

x/c	z/c
0.004455	0.01982
-0.00278	0.01815
-0.01204	0.01426
-0.01889	0.00963
-0.02454	0.00278
-0.02593	-0.00389
-0.02296	-0.01019
-0.01593	-0.01315
-0.00796	-0.01407
0.00093	-0.01463

FIGURE 1A. R3 ICE SHAPE

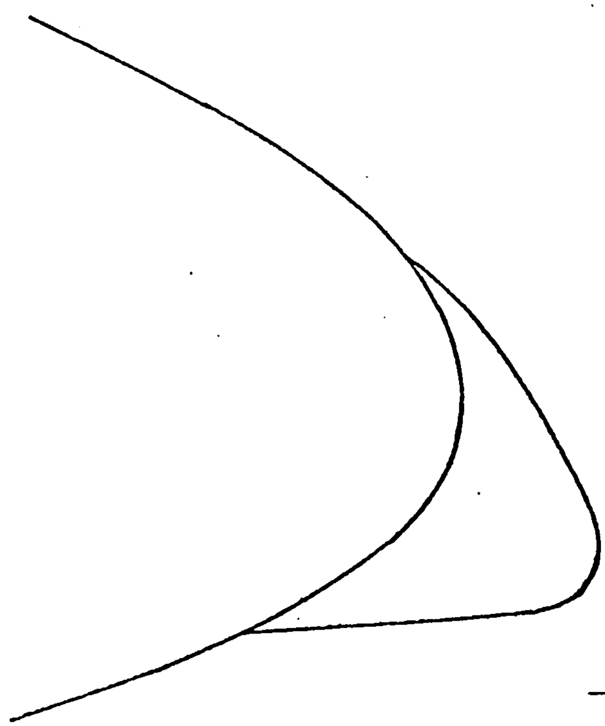

x/c	z/c
0.00000	0.01157
-0.00417	-.00630
-0.00815	0.00000
-0.01157	-0.00602
-0.01315	-0.01167
-0.01130	-0.01519
-0.00778	-0.01685
-0.00139	-0.01759
0.00370	-0.01815
0.01000	-0.01852

FIGURE 1B. R7 ICE SHAPE

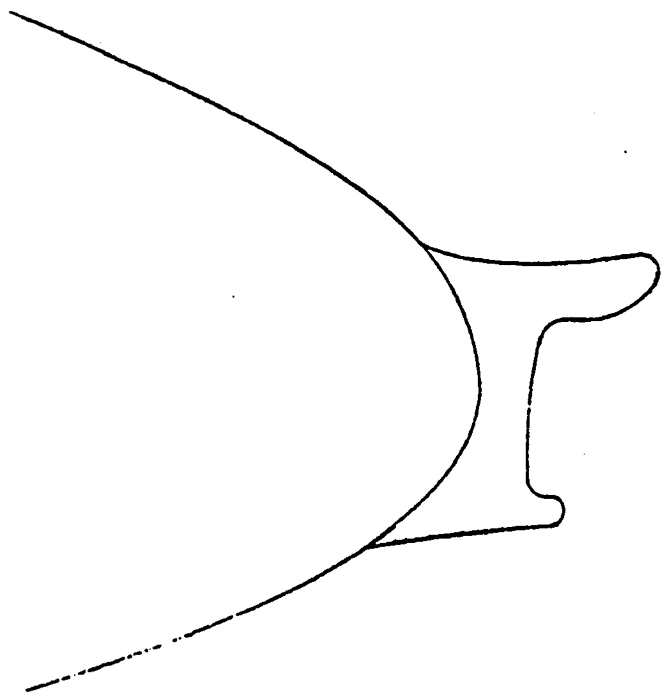

X/C	Z/C
-.00232	.01435
-.01019	.01389
-.01667	.01407
-.01944	.01315
-.01907	.01019
-.00648	.00241
-.00556	-.00593
-.00889	-.01204
-.00389	-.01389
.00667	-.01482

FIGURE 1C. GLAZE 3 SIMULATED ICE ACCRETION AND PRESSURE TAP LOCATIONS

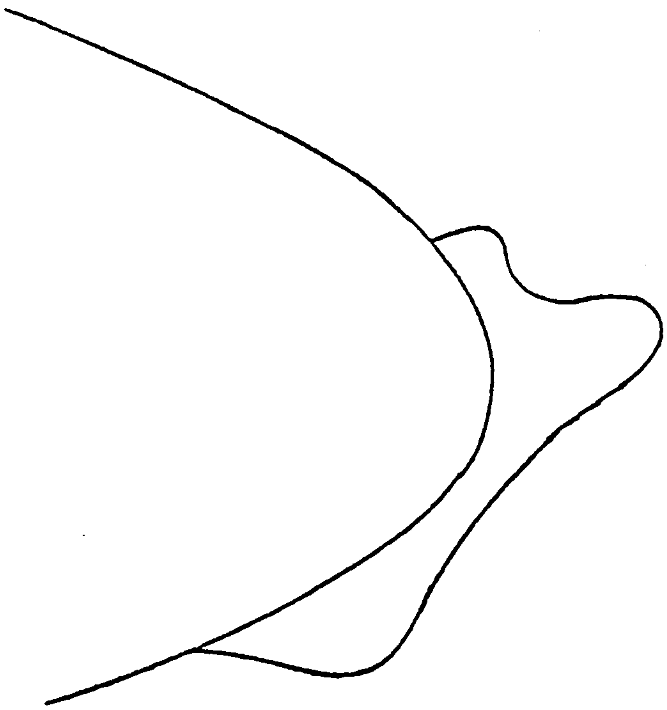

X/C	Z/C
.00093	.01759
-.00278	.01620
-.00648	.00972
-.01667	.00778
-.01796	.00519
-.01157	-.00093
-.00509	-.00602
.00556	-.01759
.01435	-.02732
.02500	-.02593

FIGURE 1D. GLAZE 7 SIMULATED ICE ACCRETION AND PRESSURE TAP LOCATIONS

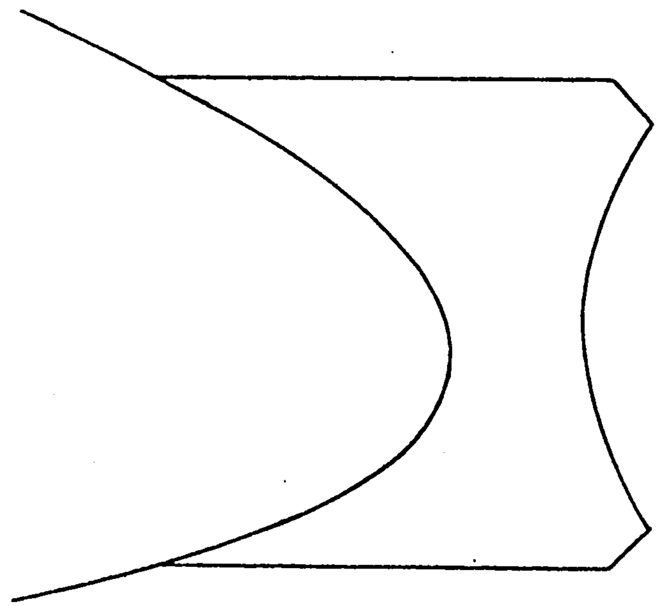

X/C	Z/C
0.01985	0.03807
0.00427	0.03807
- 0.01133	0.03807
- 0.02452	0.03584
- 0.02136	0.02264
- 0.01857	0.00706
- 0.02099	- 0.00854
- 0.02452	- 0.02229
- 0.00613	- 0.02414
0.01467	- 0.02414

FIGURE 1E. GENERIC GLAZE SIMULATED ICE ACCRETION AND PRESSURE TAP LOCATIONS

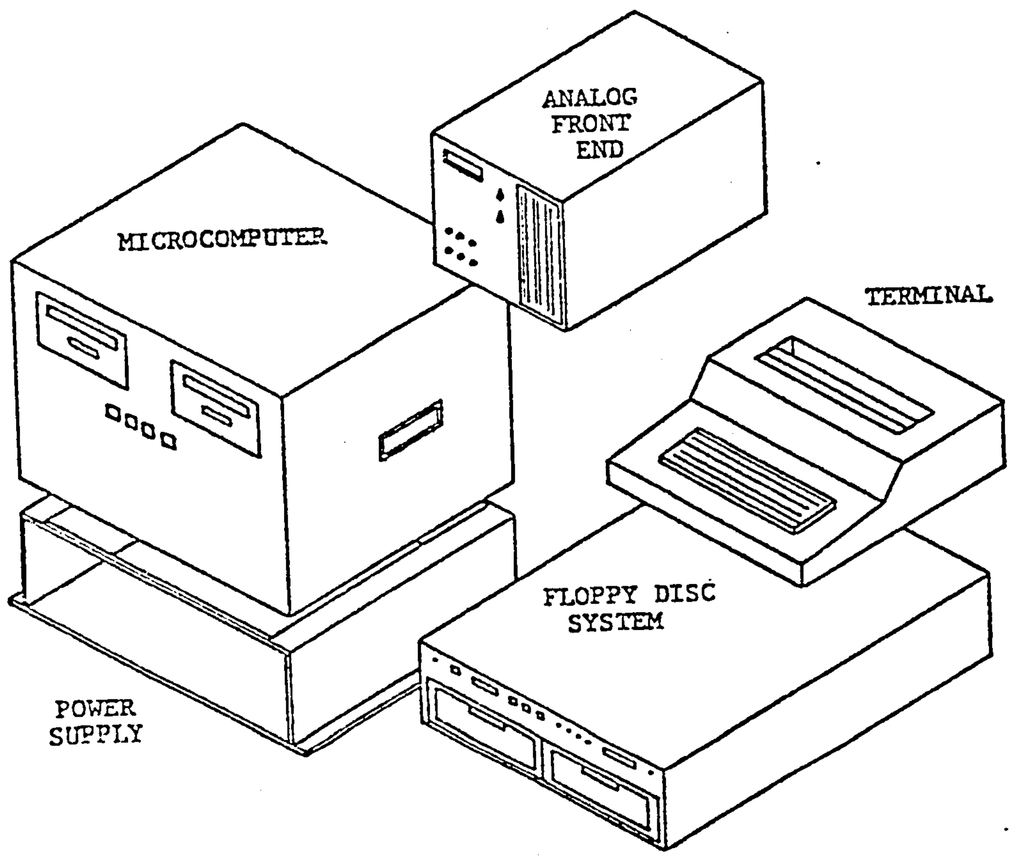

FIGURE 2. OSU DIGITAL DATA ACQUISITION
AND REDUCTION SYSTEM

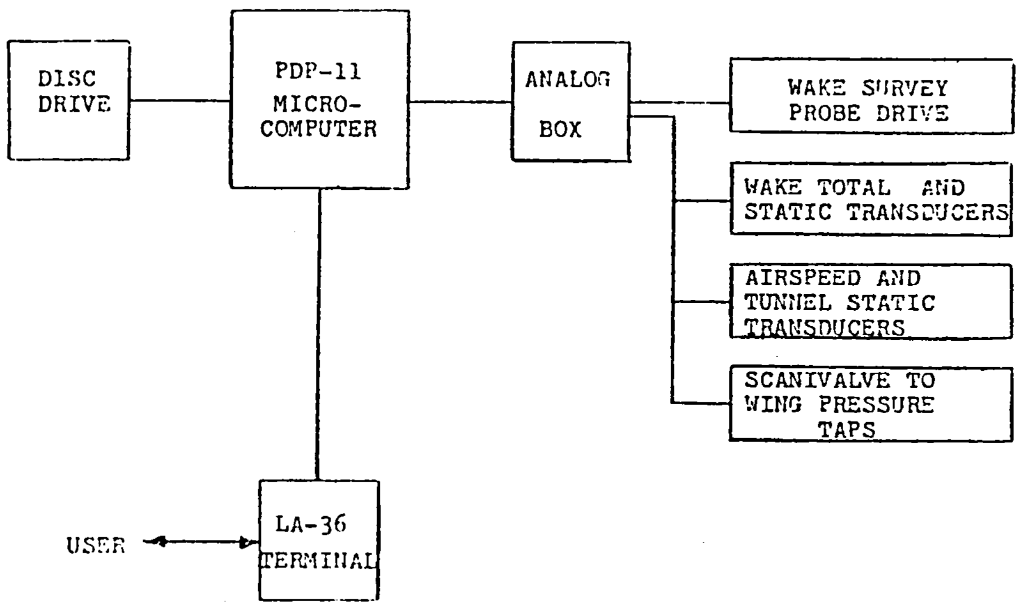

FIGURE 3. OSU DATA ACQUISITION SYSTEM
AS USED IN THE NASA LEWIS IRT

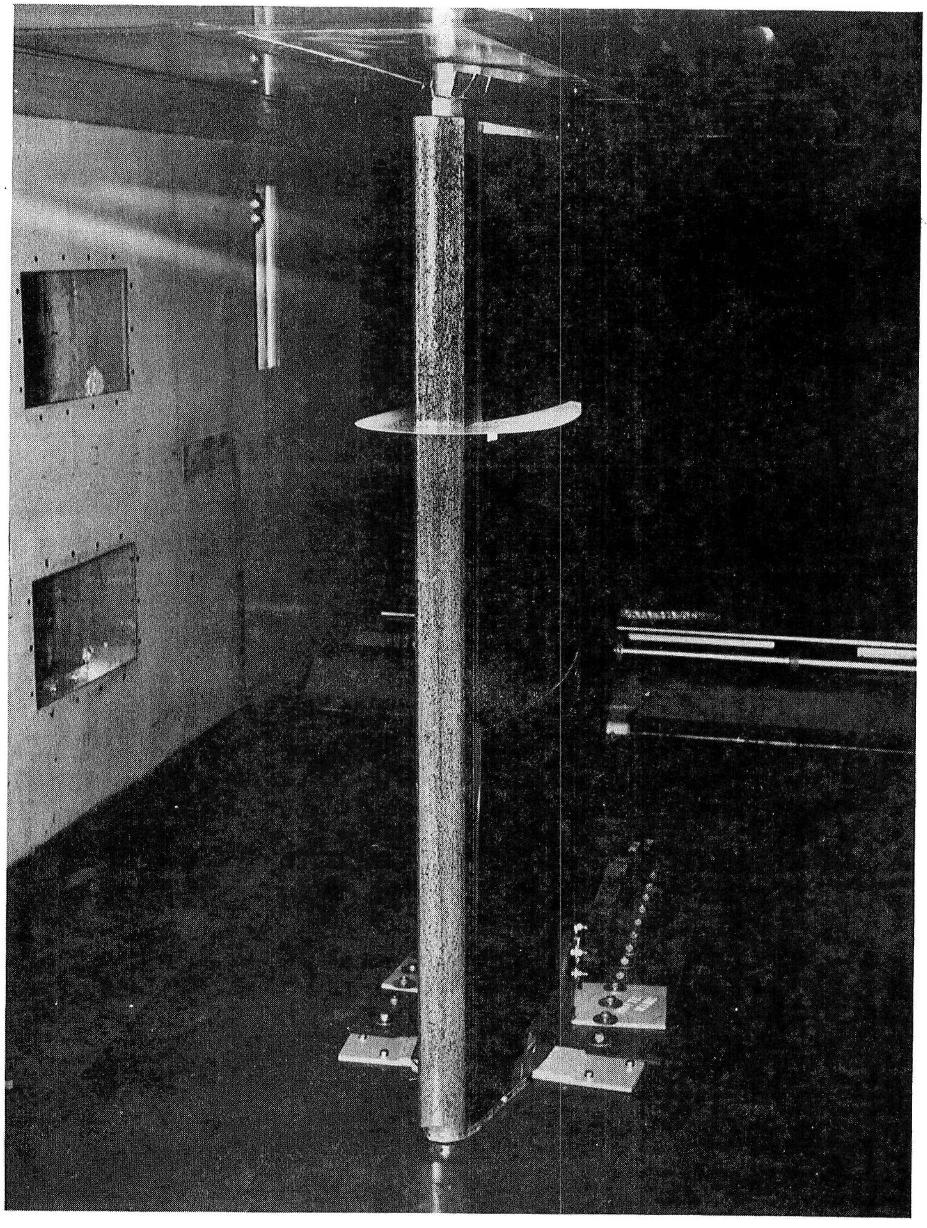

FIGURE 4. 63A415 WING WITH SPLITTER PLATE
IN LEWIS ICING RESEARCH TUNNEL

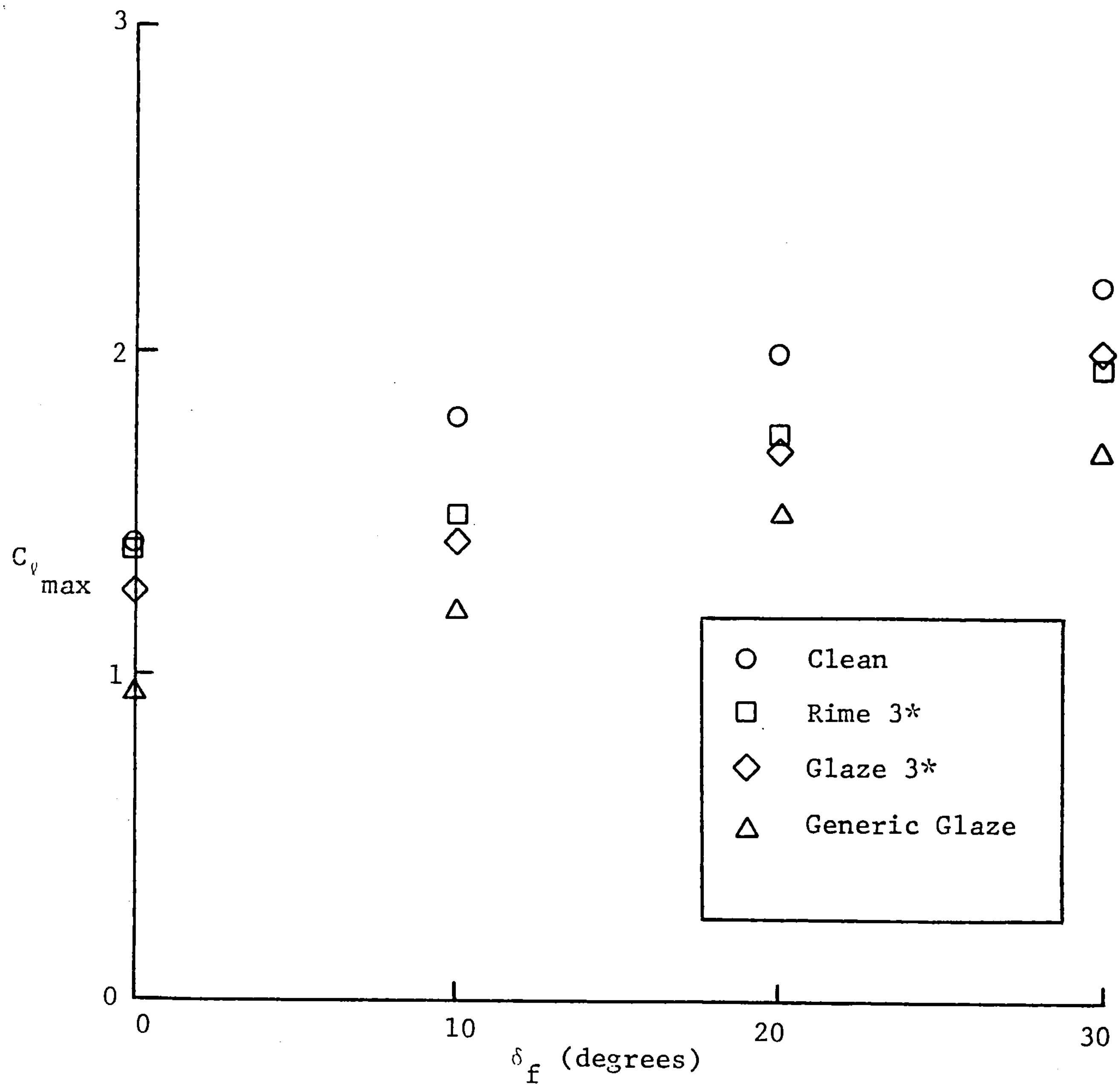

FIGURE 5. CHANGE IN $C_{\ell_{max}}$ WITH SIMULATED ICE SHAPES
($\delta_f = 0^o$ Cases from 1982 IRT Test[2])

$\alpha = 1.6^{\circ}$
$M = 0.152$
$Re = 4.7 \times 10^{6}$

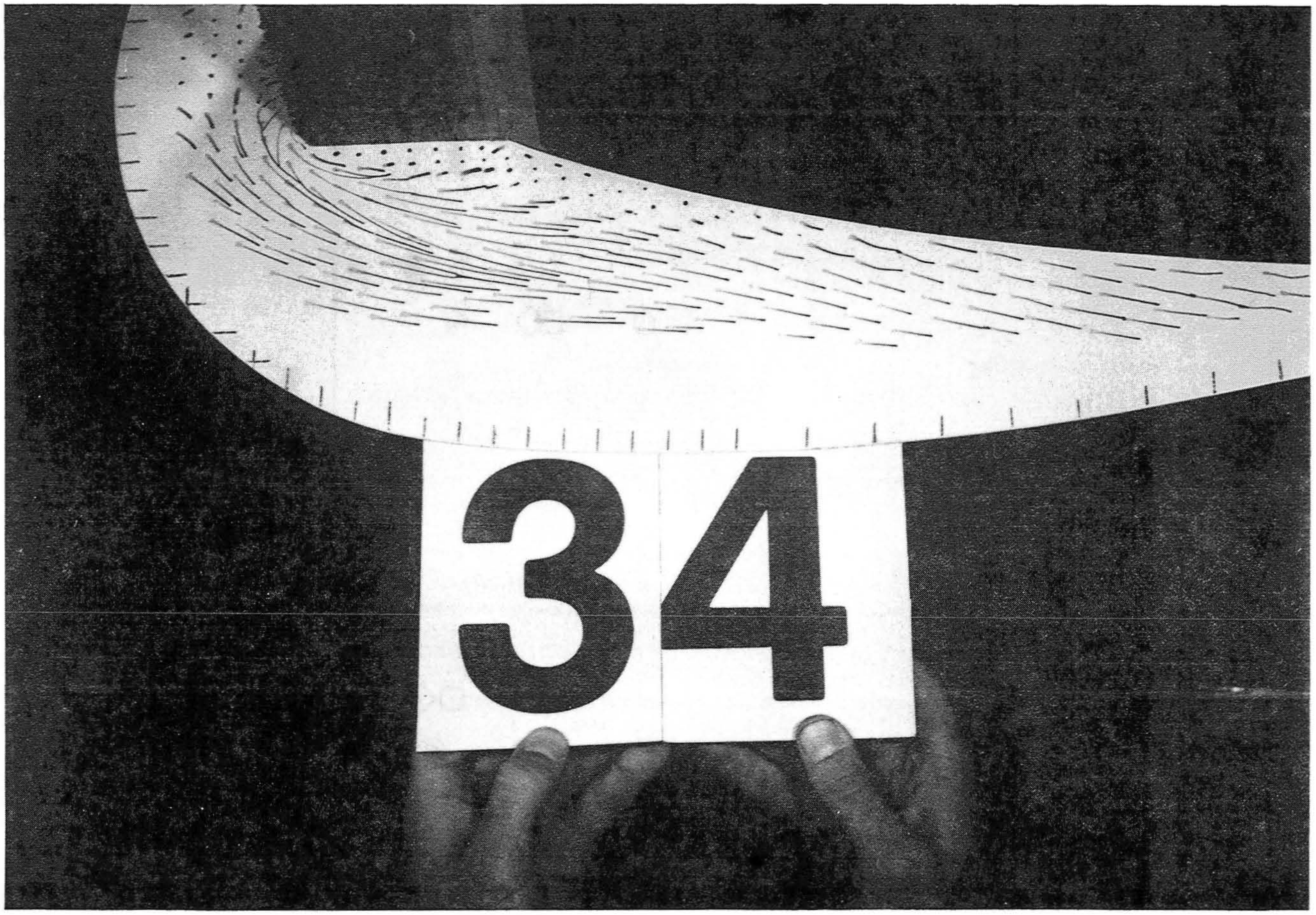

FIGURE 6. SPLITTER PLATE PHOTOGRAPH OF UPPER SURFACE OF THE GENERIC GLAZE ROUGH ICE SHAPE

$\alpha = 5.6^{\circ}$
$M = 0.152$
$Re = 4.7 \times 10^{6}$

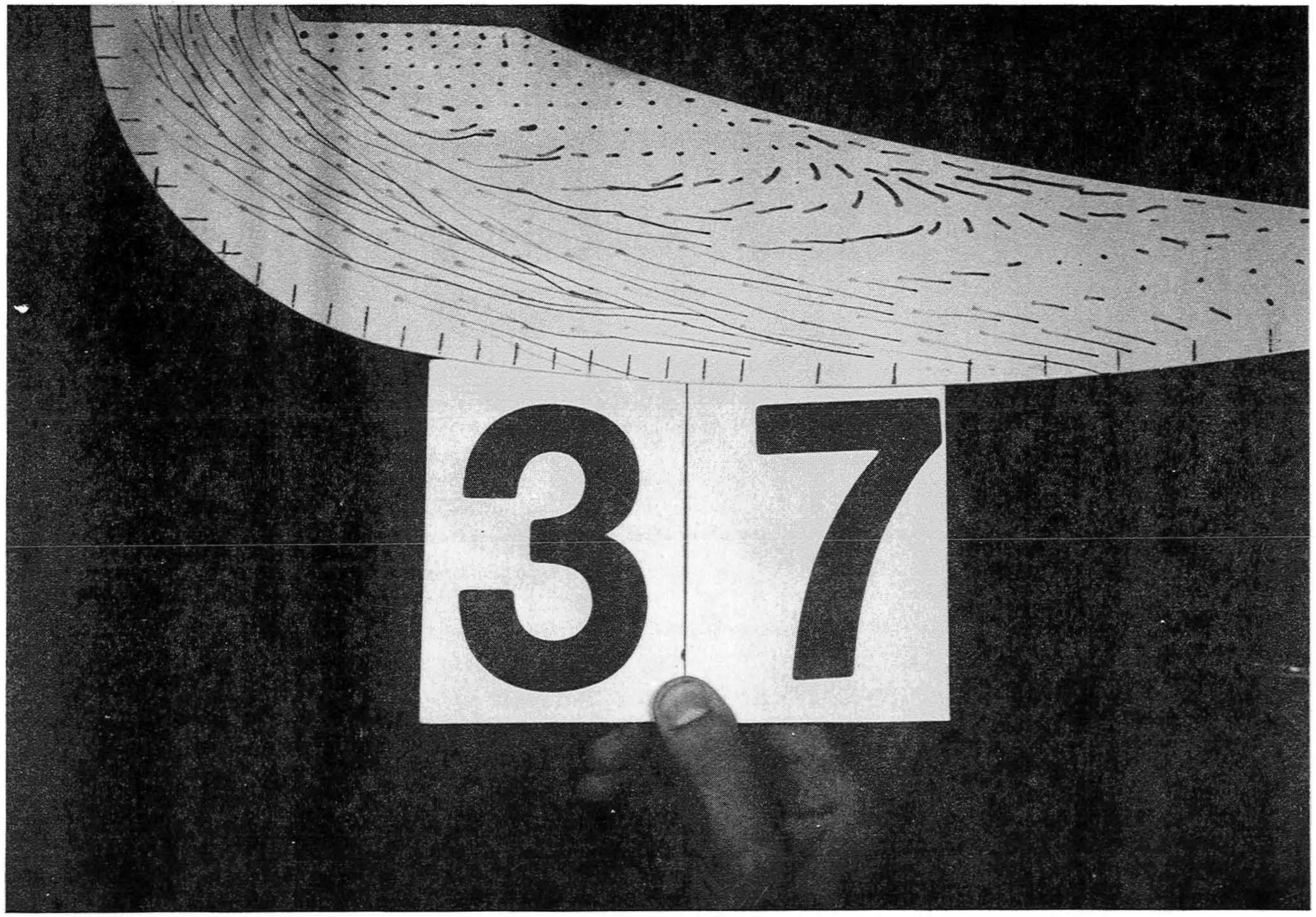

FIGURE 7. SPLITTER PLATE PHOTOGRAPH OF UPPER SURFACE OF THE GENERIC CLAZE ROUGH ICE SHAPE

$\alpha=5.6^{\circ}$
$M=0.153$
$Re=4.6 \times 10^{6}$

FIGURE 8. SPLITTER PLATE PHOTOGRAPH OF UPPER SURFACE OF THE G3 ROUGH ICE SHAPE

APPENDIX

Run Summary

RUN #	AOA	FLAP DEF	V (KT)	$T^o(F)$	PRESS. ALT. (FT)	CL	CD	CM
CLEAN								
48	10.6	0.0	103.43	77.0	838.0	1.3393	0.0256	-0.095
49	11.6	0.0	101.92	75.0	832.3	1.4410	------	-0.108
60	-5.4	0.0	102.23	50.0	852.9	-0.2326	0.0110	-0.044
61	-2.4	0.0	101.39	52.0	844.3	0.0710	0.0105	-0.046
62	-0.4	0.0	100.18	69.0	839.2	0.3126	0.0108	-0.049
63	1.6	0.0	102.84	75.0	869.4	0.5431	0.0112	-0.059
64	3.6	0.0	101.05	67.0	857.2	0.7220	0.0128	-0.059
65	5.6	0.0	102.25	70.0	870.5	0.9020	0.0144	-0.059
66	7.6	0.0	101.64	72.0	869.9	1.1002	0.0169	-0.075
67	8.6	0.0	101.03	74.0	871.1	1.1691	0.0196	-0.077
68	9.6	0.0	103.57	75.0	892.1	1.2279	0.0220	-0.075
69	10.6	0.0	101.74	71.0	878.5	1.3198	0.0275	-0.092
70	11.6	0.0	101.25	73.0	880.2	1.4225	0.0300	-0.090
81	-2.4	0.0	102.59	62.0	1083.5	0.0881	0.0118	-0.049
82	-0.4	0.0	101.79	57.0	1079.6	0.3017	0.0124	-0.051
83	1.6	0.0	102.24	68.0	1087.2	0.5059	0.0125	-0.056
84	-6.4	10.0	78.01	73.0	907.7	-0.0097	------	-0.117
85	-2.4	10.0	78.31	70.0	902.1	0.4352	------	-0.129
86	-0.4	10.0	78.74	70.0	903.7	0.6694	------	-0.132
87	1.6	10.0	80.30	69.0	915.4	0.9075	------	-0.142
88	3.6	10.0	78.15	69.0	906.1	1.1058	------	-0.142
89	5.6	10.0	78.51	67.0	906.8	1.2202	------	-0.133
90	7.6	10.0	79.29	68.0	914.0	1.3540	------	-0.136
91	9.6	10.0	77.68	67.0	902.1	1.5255	------	-0.153
92	11.6	10.0	80.53	67.0	924.2	1.7296	------	-0.178
93	12.6	10.0	79.26	65.0	917.8	1.7155	------	-0.178
94	13.6	10.0	78.44	66.0	910.8	1.8233	------	-0.196
95	-6.4	20.0	81.20	64.0	930.0	0.4258	------	-0.219
96	-2.4	20.0	79.75	65.0	922.5	0.8938	------	-0.231
98	9.6	20.0	78.67	68.0	914.1	1.8714	------	-0.255
99	3.6	20.0	77.82	66.0	909.8	1.4635	------	-0.231
100	-10.4	30.0	78.35	64.0	917.7	0.3084	------	-0.288
101	-6.4	30.0	78.57	66.0	913.7	0.7973	------	-0.304
102	-2.4	30.0	79.80	66.0	921.2	1.2287	------	-0.303
103	1.6	30.0	78.09	65.0	907.6	1.7413	------	-0.317
104	5.6	30.0	78.86	64.0	910.5	1.9171	------	-0.311
105	9.6	30.0	78.96	66.0	913.2	2.1071	------	-0.328
106	10.6	30.0	77.39	65.0	905.2	2.2760	------	-0.349
107	11.6	30.0	79.75	65.0	921.8	2.1741	------	-0.346
135	13.6	10.0	78.26	79.0	708.8	1.7906	------	-0.125
136	14.6	10.0	79.20	79.0	717.7	1.8024	------	-0.134
137	11.6	20.0	79.00	67.0	716.8	1.9553	------	-0.209
138	12.6	20.0	80.18	67.0	726.3	1.9723	------	-0.208
139	13.6	20.0	79.77	73.0	728.2	1.9275	------	-0.213

RUN #	AOA	FLAP DEF	V (KT)	$T^{o}(F)$	PRESS. ALT. (FT)	CL	CD	CM
RIME 3 ROUGH								
76	-2.4	0.0	101.48	73.0	929.7	0.0544	0.0163	-0.053
77	-0.4	0.0	102.49	74.0	937.0	0.3458	0.0140	-0.058
78	1.6	0.0	101.67	73.0	931.1	0.5213	0.0146	-0.048
79	3.6	0.0	101.06	73.0	926.3	0.7468	0.0170	-0.049
80	5.6	0.0	102.67	74.0	941.7	0.9326	------	-0.046
159	-10.4	30.0	78.76	73.0	753.7	-0.0371	------	-0.208
160	-6.4	30.0	79.60	73.0	757.8	0.7000	------	-0.286
161	-2.4	30.0	78.40	72.0	750.0	1.1937	------	-0.295
162	1.6	30.0	79.96	72.0	762.9	1.6685	------	-0.294
163	5.6	30.0	79.28	72.0	758.6	1.9713	------	-0.274
164	7.6	30.0	79.32	72.0	754.6	1.9211	------	-0.238
165	7.6	20.0	79.39	72.0	763.2	1.7497	------	-0.190
166	9.6	20.0	78.57	71.0	759.4	1.7519	------	-0.173
167	8.6	20.0	79.10	72.0	763.6	1.7041	------	-0.176
168	6.6	20.0	77.92	72.0	757.8	1.6702	------	-0.190
169	-6.4	10.0	78.30	66.0	766.3	-0.0732	------	-0.110
170	-2.4	10.0	79.19	66.0	772.2	0.4180	------	-0.119
171	1.6	10.0	78.61	66.0	769.3	0.8904	------	-0.116
172	5.6	10.0	79.15	64.0	774.1	1.2159	------	-0.109
173	7.6	10.0	79.29	64.0	773.9	1.3934	------	-0.110
174	9.6	10.0	79.00	64.0	772.2	1.4241	------	-0.088
175	10.6	10.0	78.22	62.0	769.3	1.5164	------	-0.098
176	11.6	10.0	78.91	63.0	771.5	1.4800	------	-0.093
GLAZE 3 ROUGH								
71	-2.4	0.0	102.00	66.0	905.0	0.0816	0.0161	-0.050
72	-0.4	0.0	101.95	73.0	911.9	0.3061	0.0153	-0.049
73	1.6	0.0	101.88	73.0	914.9	0.5276	0.0163	-0.039
74	3.6	0.0	101.46	72.0	915.7	0.7521	0.0226	-0.044
75	5.6	0.0	100.09	71.0	907.1	0.8933	0.0323	-0.025
140	-6.4	10.0	78.01	64.0	727.3	-0.0546	------	-0.118
141	-2.4	10.0	79.61	75.0	740.3	0.3881	------	-0.122
142	1.6	10.0	78.88	79.0	734.8	0.8908	------	-0.108
143	5.6	10.0	78.86	81.0	738.6	1.2350	------	-0.093
144	7.6	10.0	78.33	81.0	733.0	1.3459	------	-0.088
145	9.6	10.0	79.18	80.0	739.2	1.3892	------	-0.088
146	10.6	10.0	78.24	79.0	733.0	1.4311	------	-0.117
147	11.6	10.0	80.30	76.0	746.4	1.4188	------	-0.148
148	7.6	20.0	79.96	76.0	746.4	1.7196	------	-0.166
149	9.6	20.0	79.58	74.0	743.2	1.6808	------	-0.202
150	8.6	20.0	77.88	75.0	735.5	1.6640	------	-0.173
151	10.6	20.0	79.20	75.0	747.3	1.6806	------	-0.243
152	6.6	20.0	79.54	74.0	747.5	1.6647	------	-0.163
153	-6.4	30.0	78.10	72.0	740.0	0.6960	------	-0.288
154	-2.4	30.0	79.59	72.0	750.5	1.2116	------	-0.288
155	1.6	30.0	77.67	73.0	743.3	1.6481	------	-0.276
156	5.6	30.0	78.66	73.0	747.6	1.9344	------	-0.250
157	7.6	30.0	77.33	74.0	740.0	1.9626	------	-0.260
158	8.6	30.0	78.96	72.0	750.8	1.9028	------	-0.277

RUN #	AOA	FLAP DEF	V (KT)	$T^{o}(F)$	PRESS. ALT. (FT)	CL	CD	CM
GENERIC GLAZE ROUGH								
50	-2.4	0.0	103.14	72.0	846.8	0.0546	0.0338	-0.060
51	-0.4	0.0	102.21	69.0	842.4	0.2948	0.0366	-0.041
52	1.6	0.0	102.60	72.0	848.6	0.5537	0.0443	-0.035
53	3.6	0.0	101.58	74.0	843.6	0.7346	0.0677	-0.021
GENERIC GLAZE SMOOTH								
55	-2.4	0.0	102.28	70.0	849.2	0.1027	0.0353	-0.059
56	-0.4	0.0	101.98	72.0	846.8	0.3227	0.0359	-0.042
57	1.6	0.0	101.96	71.0	845.4	0.5319	0.0433	-0.030
58	3.6	0.0	103.09	69.0	855.1	0.7267	0.0616	-0.019
59	5.6	0.0	102.09	69.0	847.2	0.8491	------	-0.024
108	-2.4	30.0	79.16	65.0	920.5	1.2403	------	-0.271
109	-8.4	30.0	79.27	66.0	923.3	0.2044	------	-0.209
110	-5.4	30.0	79.31	67.0	927.6	0.8411	------	-0.283
111	1.6	30.0	79.24	67.0	918.3	1.6462	------	-0.252
112	5.6	30.0	79.31	66.0	912.5	1.7384	------	-0.299
113	7.6	30.0	79.77	66.0	912.1	1.7132	------	-0.343
114	-6.4	10.0	79.96	67.0	907.6	-0.1021	------	-0.113
115	-2.4	10.0	78.91	63.0	904.4	0.4485	------	-0.111
124	5.6	10.0	81.39	50.0	712.8	1.1937	------	-0.097
125	7.6	10.0	78.92	57.0	699.4	1.2161	------	-0.136
126	5.6	10.0	79.54	63.0	702.9	1.1910	------	-0.094
127	9.6	10.0	79.66	64.0	702.6	1.1447	------	-0.181
128	5.6	20.0	81.74	63.0	715.3	1.4608	------	-0.202
129	7.6	20.0	79.65	66.0	703.9	1.5527	------	-0.251
130	9.6	20.0	79.63	66.0	704.7	1.3729	------	-0.290
131	-2.4	20.0	79.26	66.0	706.0	0.8024	------	-0.174
132	7.6	0.0	78.22	73.0	1000.0	0.9037	------	-0.036
133	9.6	0.0	79.77	66.0	1000.0	0.9364	------	-0.092
134	11.6	0.0	80.21	71.0	1000.0	0.7749	------	-0.116

Cumulative Plots

C_ℓ vs α

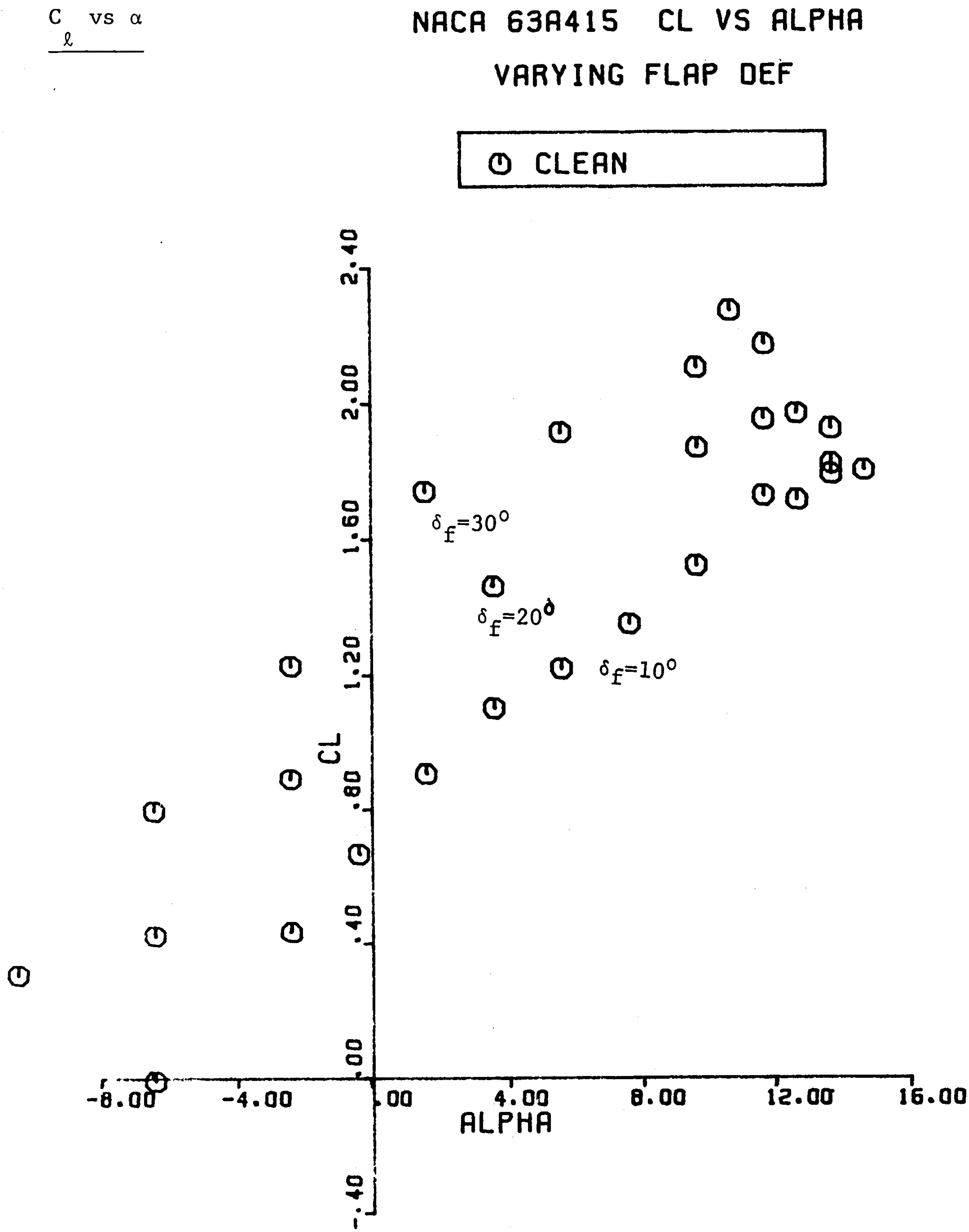

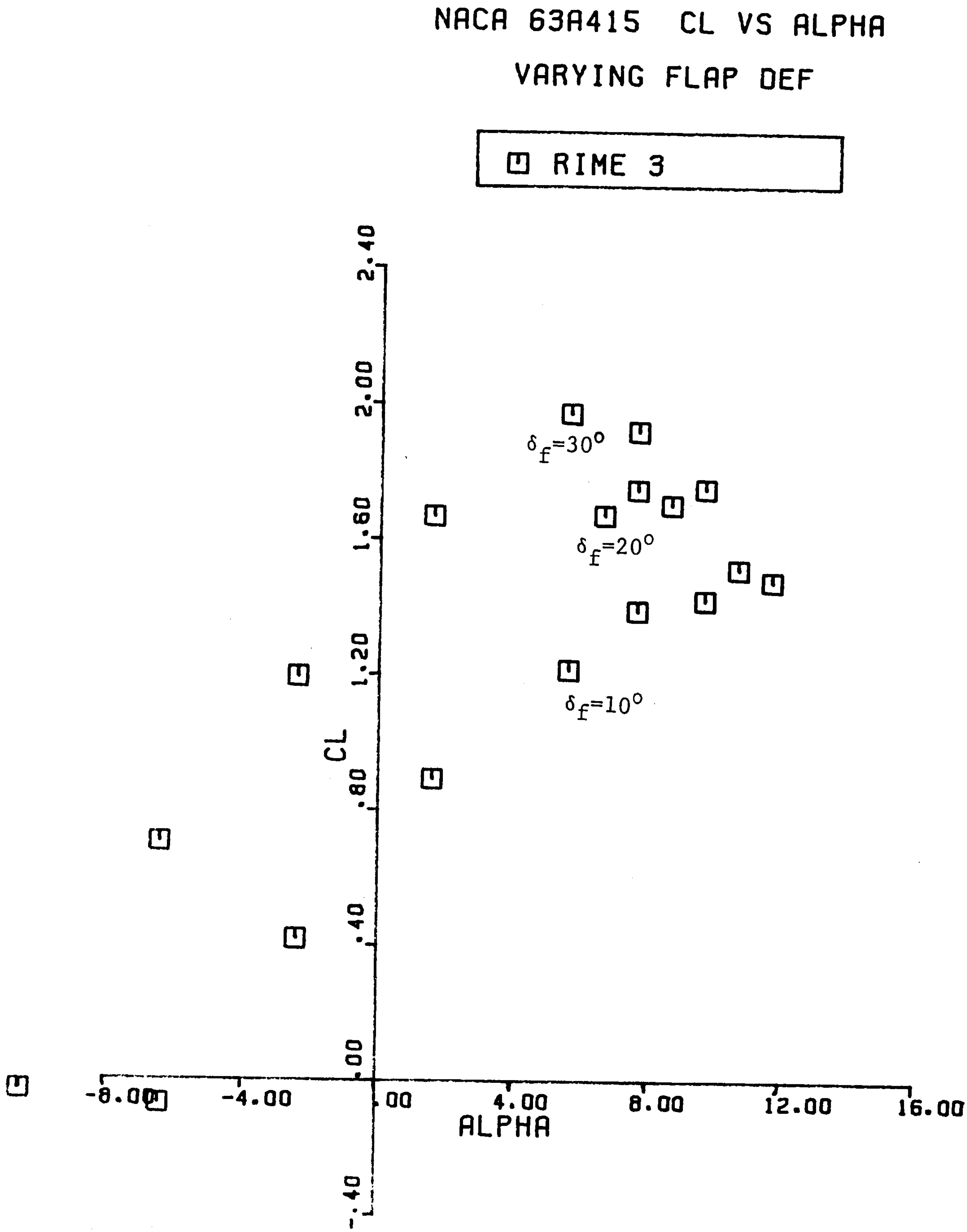

NACA 63A415 CL VS ALPHA
VARYING FLAP DEF
RIME 3
CL
ALPHA
2.40
2.00
1.60
1.20
.80
.40
.00
-.40
-8.00
-4.00
.00
4.00
8.00
12.00
16.00
δf=30°
δf=20°
δf=10°

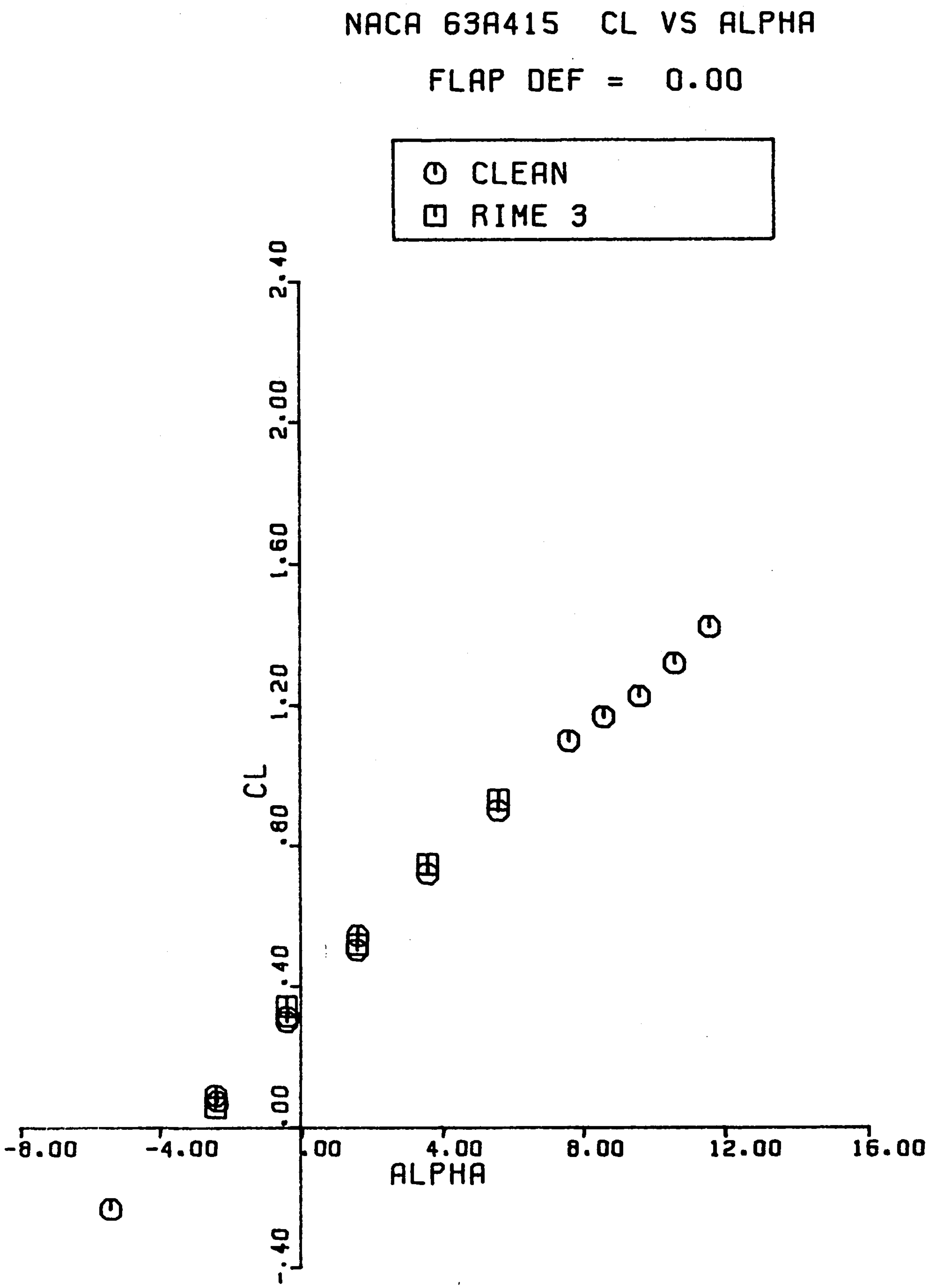
NACA 63A415 CL VS ALPHA
FLAP DEF = 0.00
CLEAN
RIME 3
CL
ALPHA
2.40
2.00
1.60
1.20
.80
.40
.00
-.40
-8.00
-4.00
.00
4.00
8.00
12.00
16.00

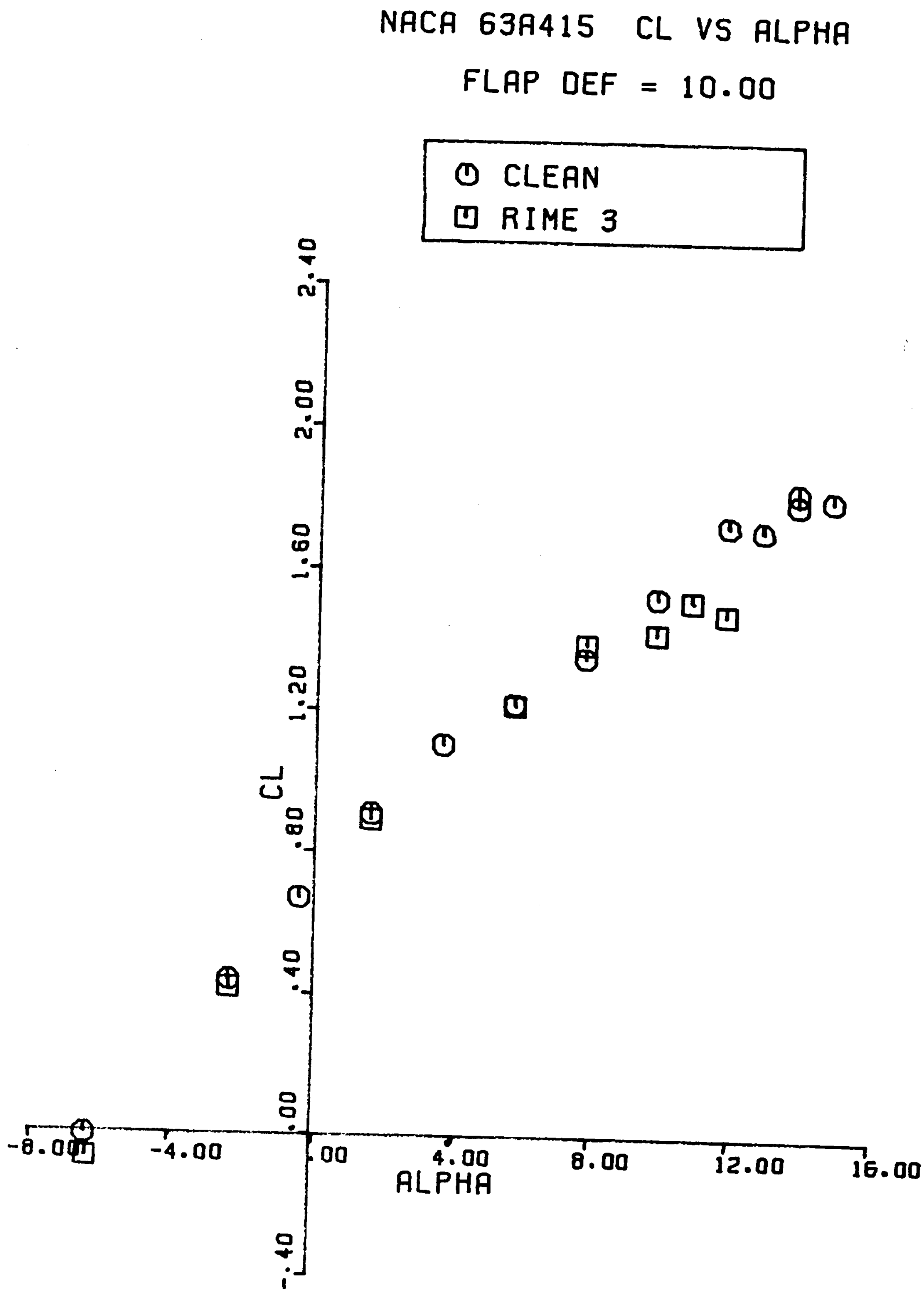
NACA 63A415 CL VS ALPHA
FLAP DEF = 10.00
CLEAN
RIME 3
CL
ALPHA
2.40
2.00
1.60
1.20
.80
.40
.00
-.40
-8.00
-4.00
.00
4.00
8.00
12.00
16.00

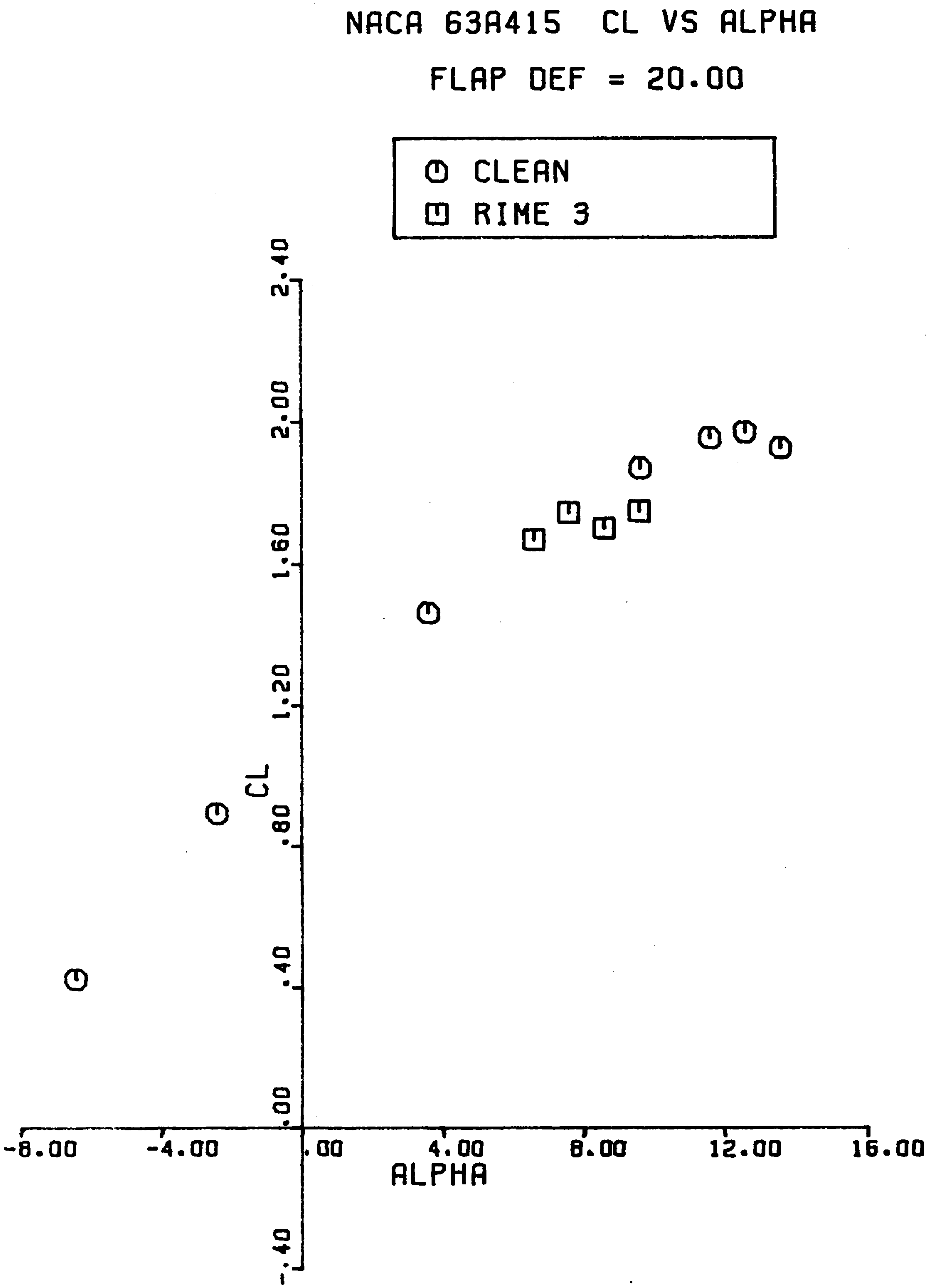
NACA 63A415 CL VS ALPHA
FLAP DEF = 20.00
CLEAN
RIME 3
CL
ALPHA
2.40
2.00
1.60
1.20
.80
.40
.00
-.40
-8.00
-4.00
.00
4.00
8.00
12.00
16.00

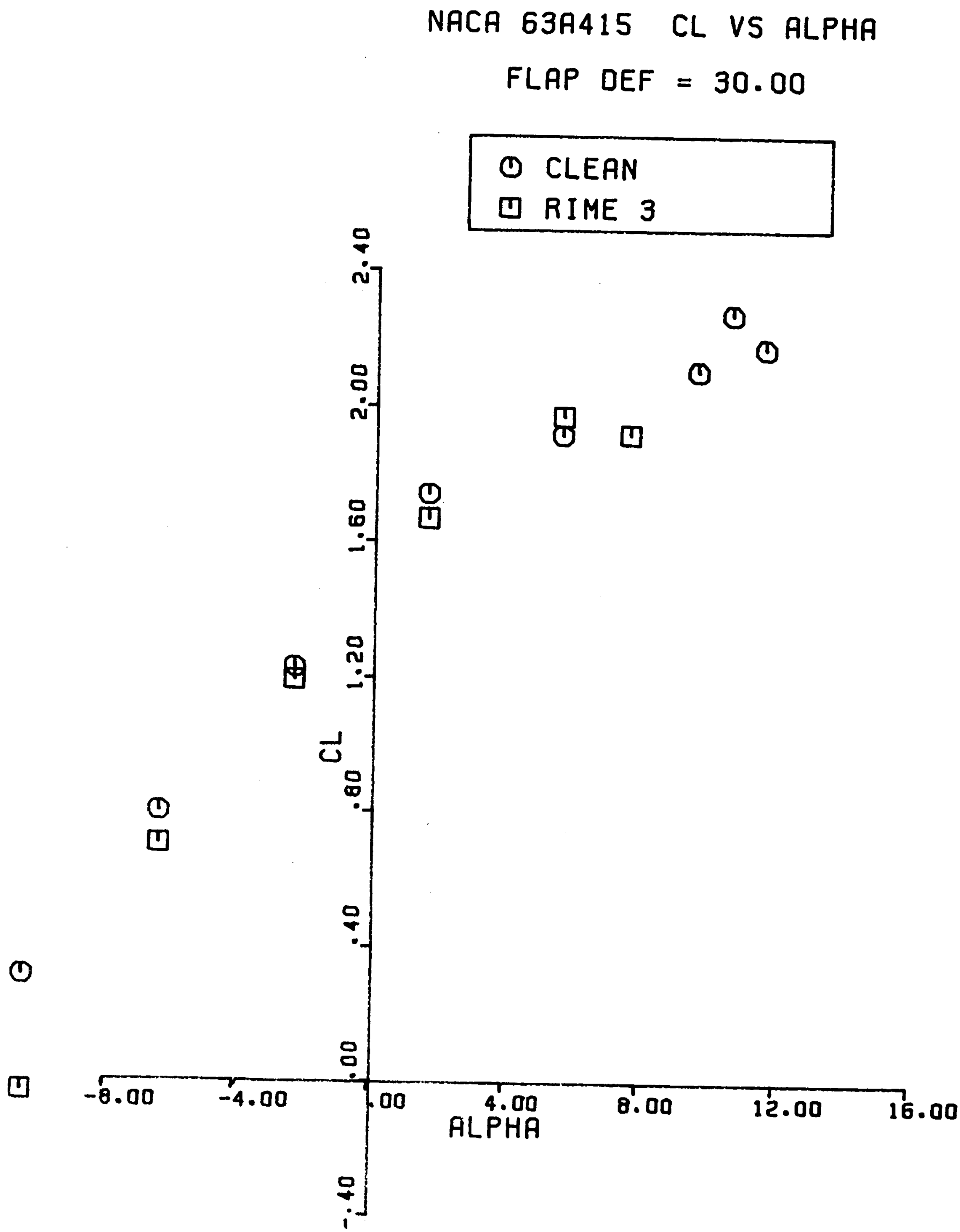
NACA 63A415 CL VS ALPHA
FLAP DEF = 30.00
CLEAN
RIME 3
CL
ALPHA
2.40
2.00
1.60
1.20
.80
.40
.00
-.40
-8.00
-4.00
.00
4.00
8.00
12.00
16.00

NACA 63A415 CL VS ALPHA

VARYING FLAP DEF

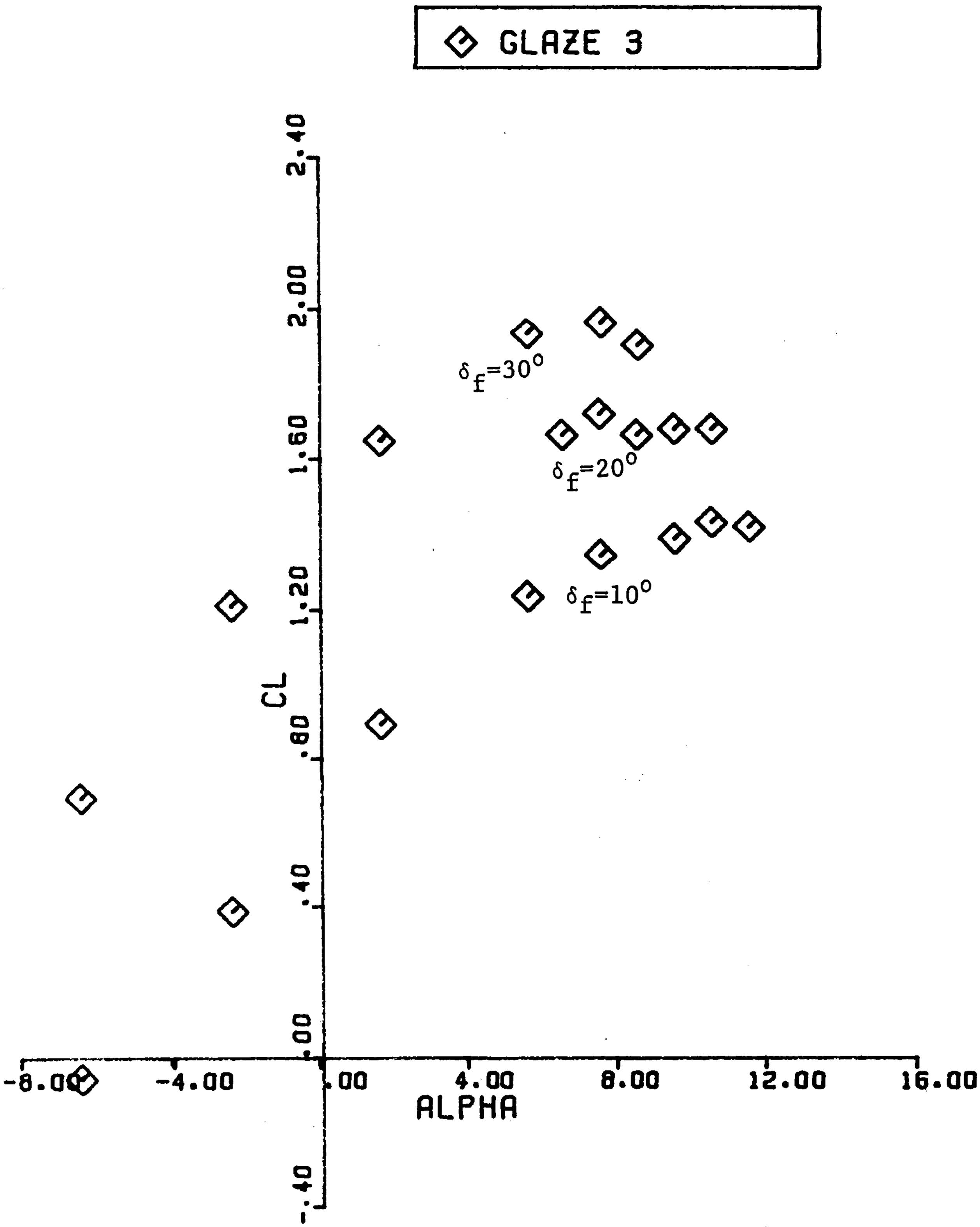

NACA 63A415 CL VS ALPHA

FLAP DEF = 0.00

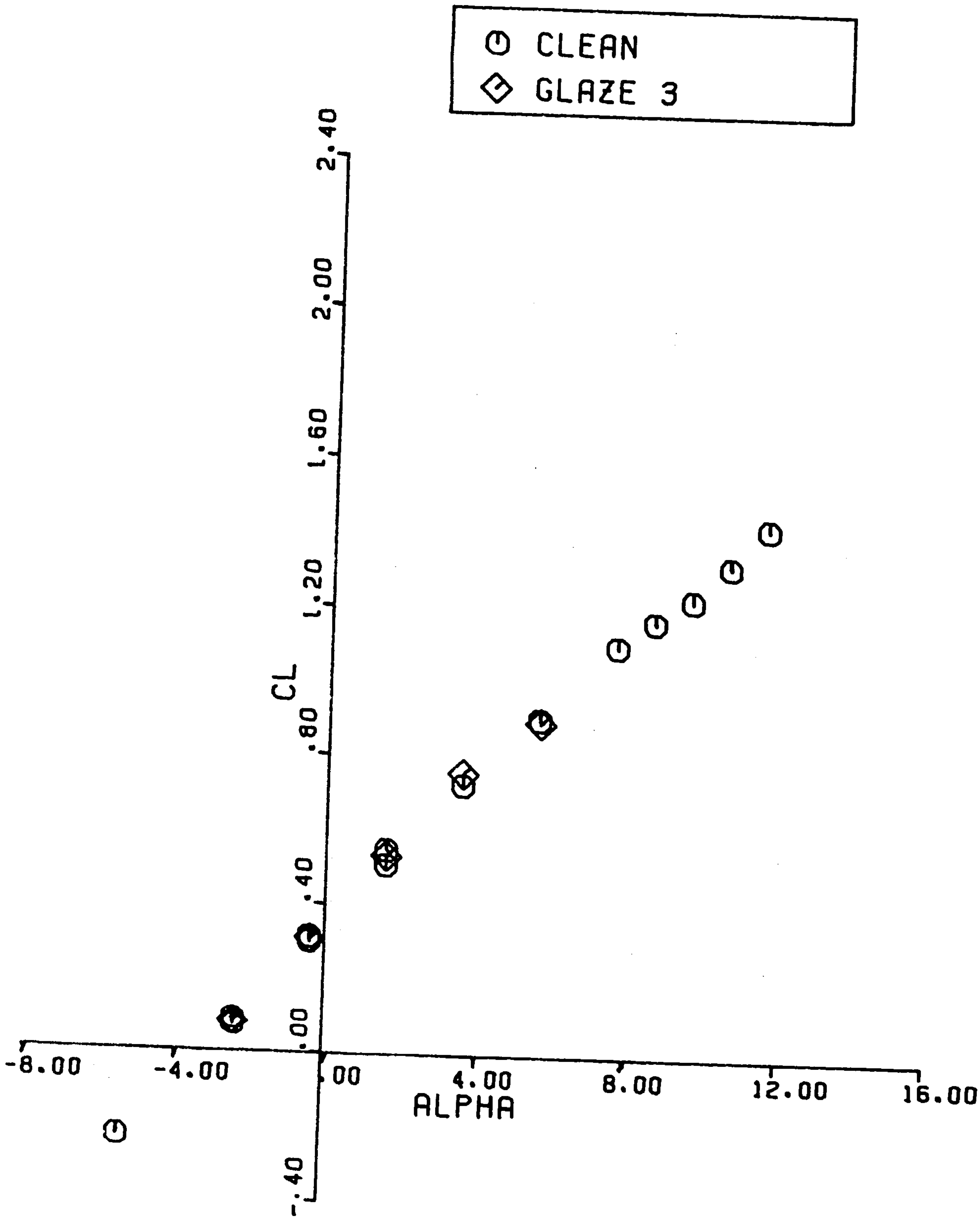

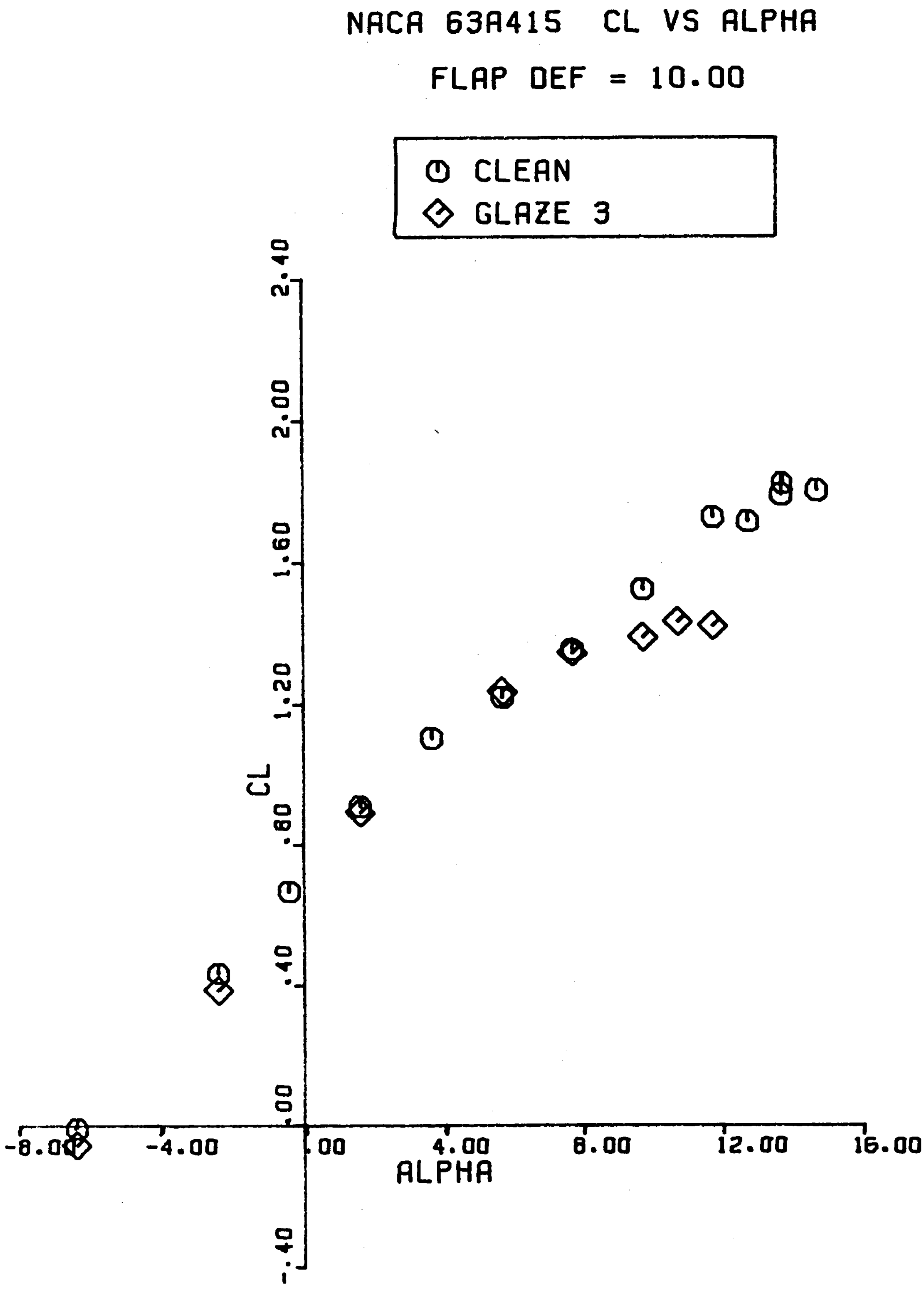
NACA 63A415 CL VS ALPHA
FLAP DEF = 10.00
CLEAN
GLAZE 3
2.40
2.00
1.60
1.20
.80
.40
.00
-.40
CL
-8.00
-4.00
.00
4.00
8.00
12.00
16.00
ALPHA

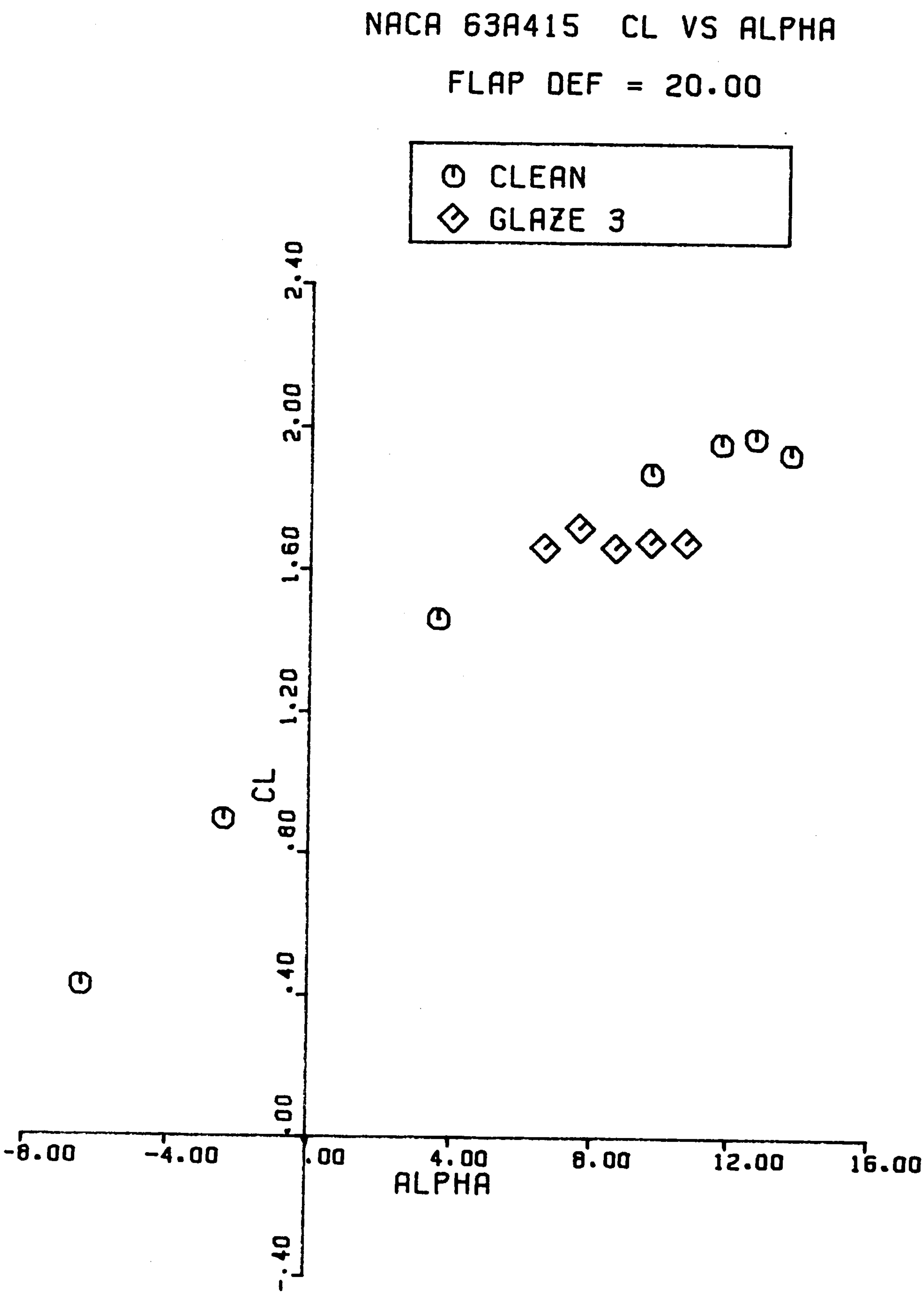

NACA 63A415 CL VS ALPHA
FLAP DEF = 20.00
CLEAN
GLAZE 3
CL
ALPHA
2.40
2.00
1.60
1.20
.80
.40
.00
-.40
-8.00
-4.00
.00
4.00
8.00
12.00
16.00

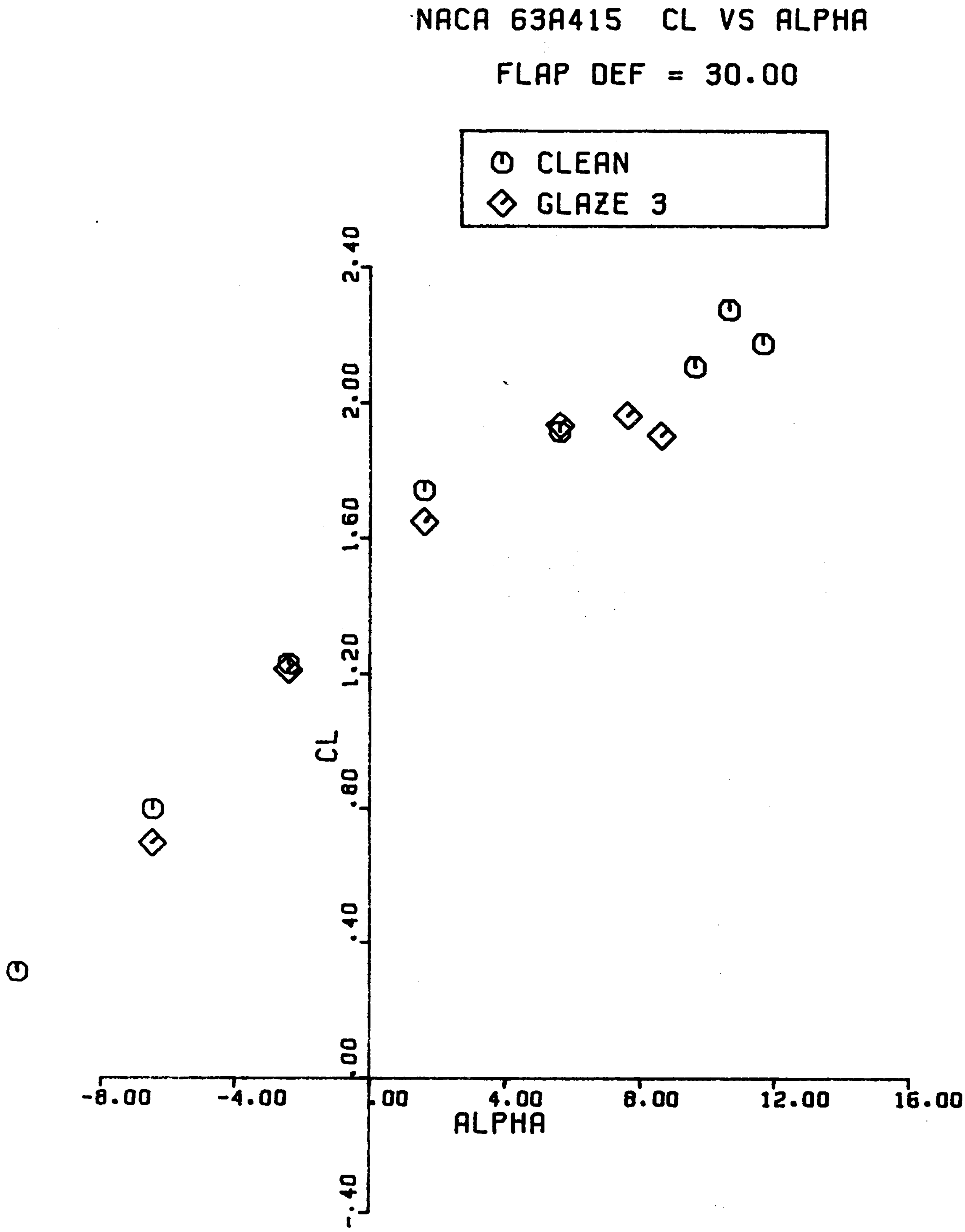
NACA 63A415 CL VS ALPHA
FLAP DEF = 30.00
CLEAN
GLAZE 3
CL
2.40
2.00
1.60
1.20
.80
.40
.00
-.40
-8.00
-4.00
.00
4.00
8.00
12.00
16.00
ALPHA

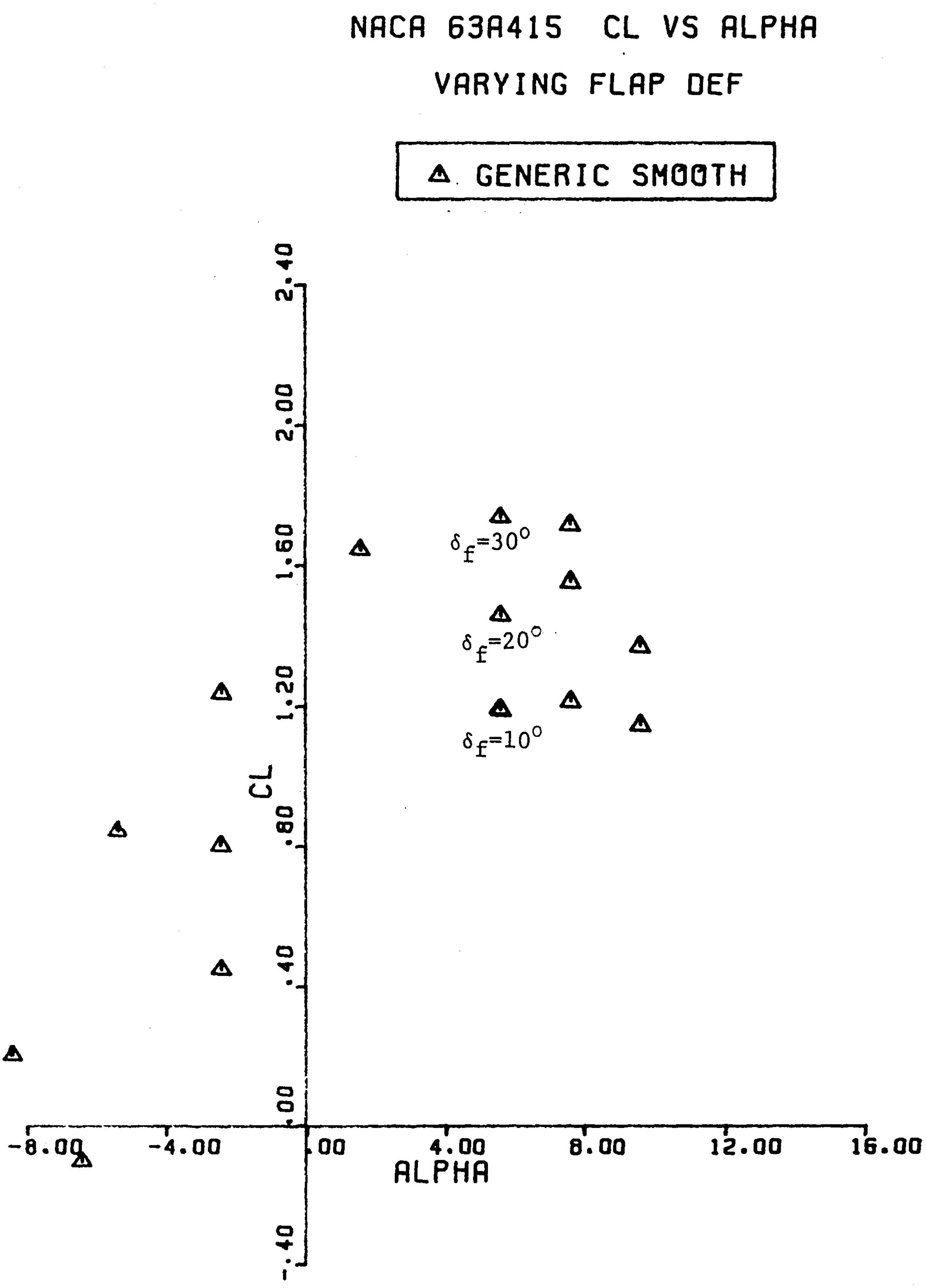

NACA 63A415 CL VS ALPHA
VARYING FLAP DEF
GENERIC SMOOTH
δ_f=30°
δ_f=20°
δ_f=10°
CL
ALPHA
2.40
2.00
1.60
1.20
.80
.40
.00
-.40
-8.00
-4.00
.00
4.00
8.00
12.00
16.00

NACA 63A415 CL VS ALPHA

FLAP DEF = 0.00

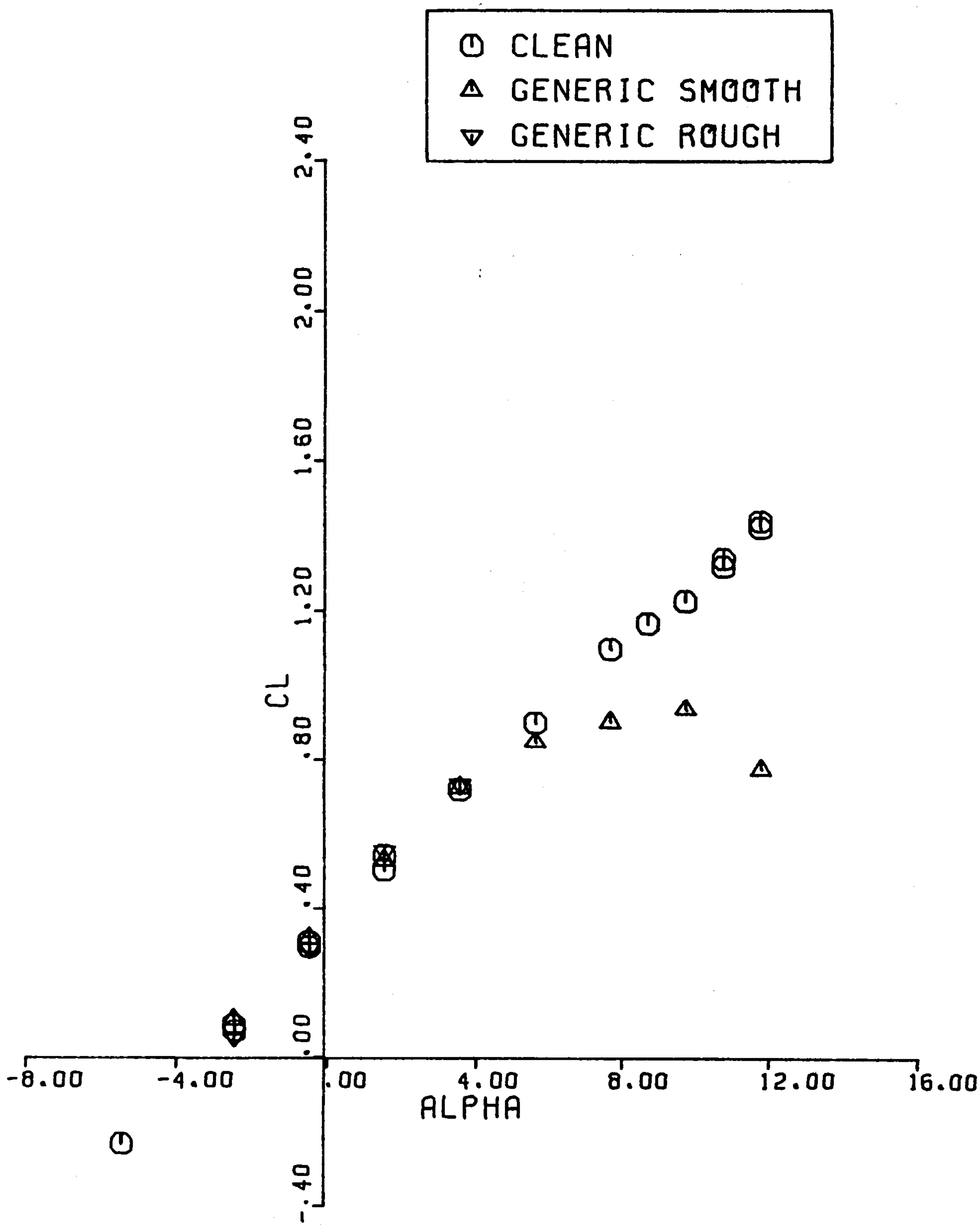

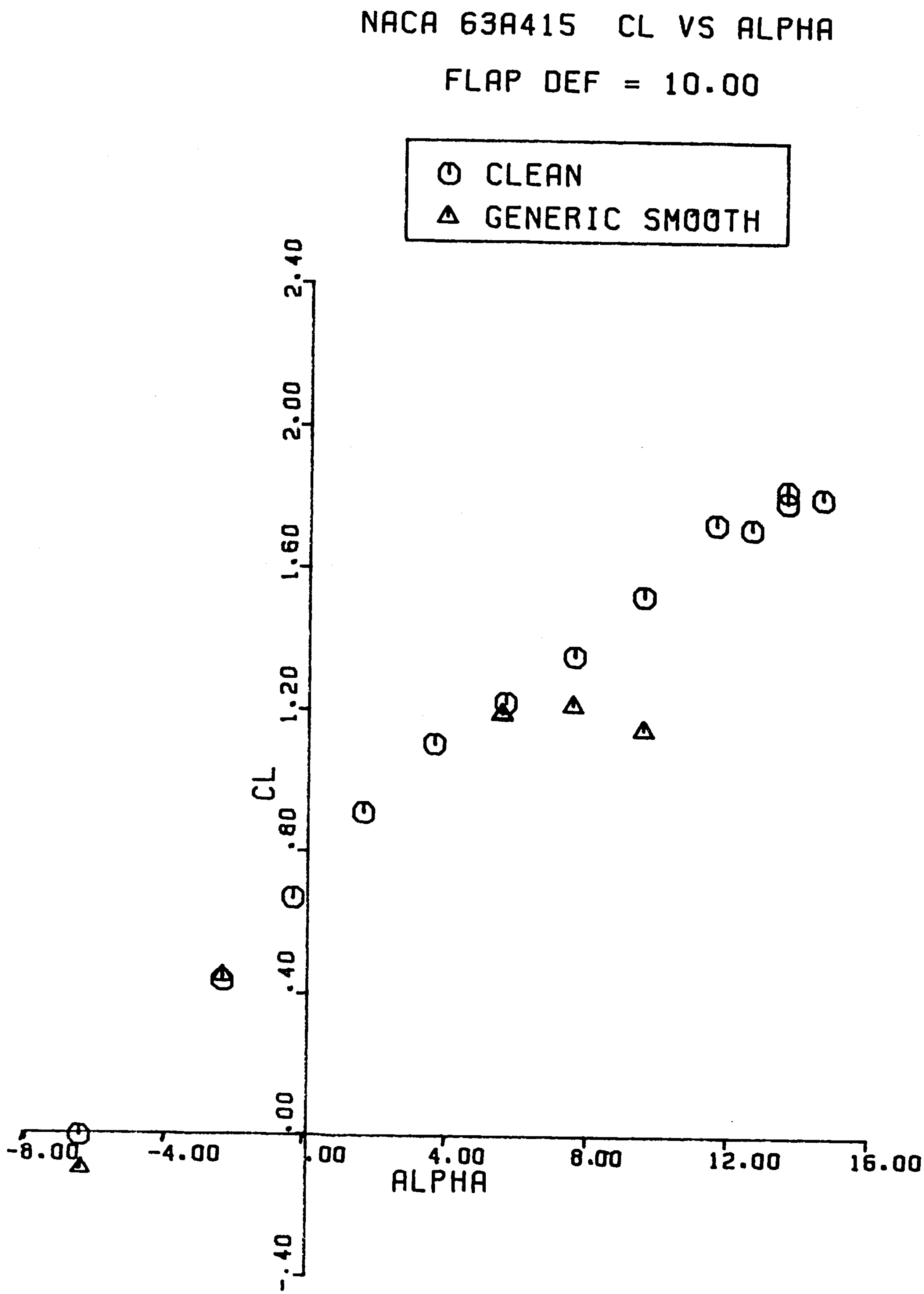
NACA 63A415 CL VS ALPHA
FLAP DEF = 10.00
CLEAN
GENERIC SMOOTH
2.40
2.00
1.60
1.20
.80
.40
.00
-.40
CL
-8.00
-4.00
.00
4.00
8.00
12.00
16.00
ALPHA

NACA 63A415 CL VS ALPHA

FLAP DEF = 20.00

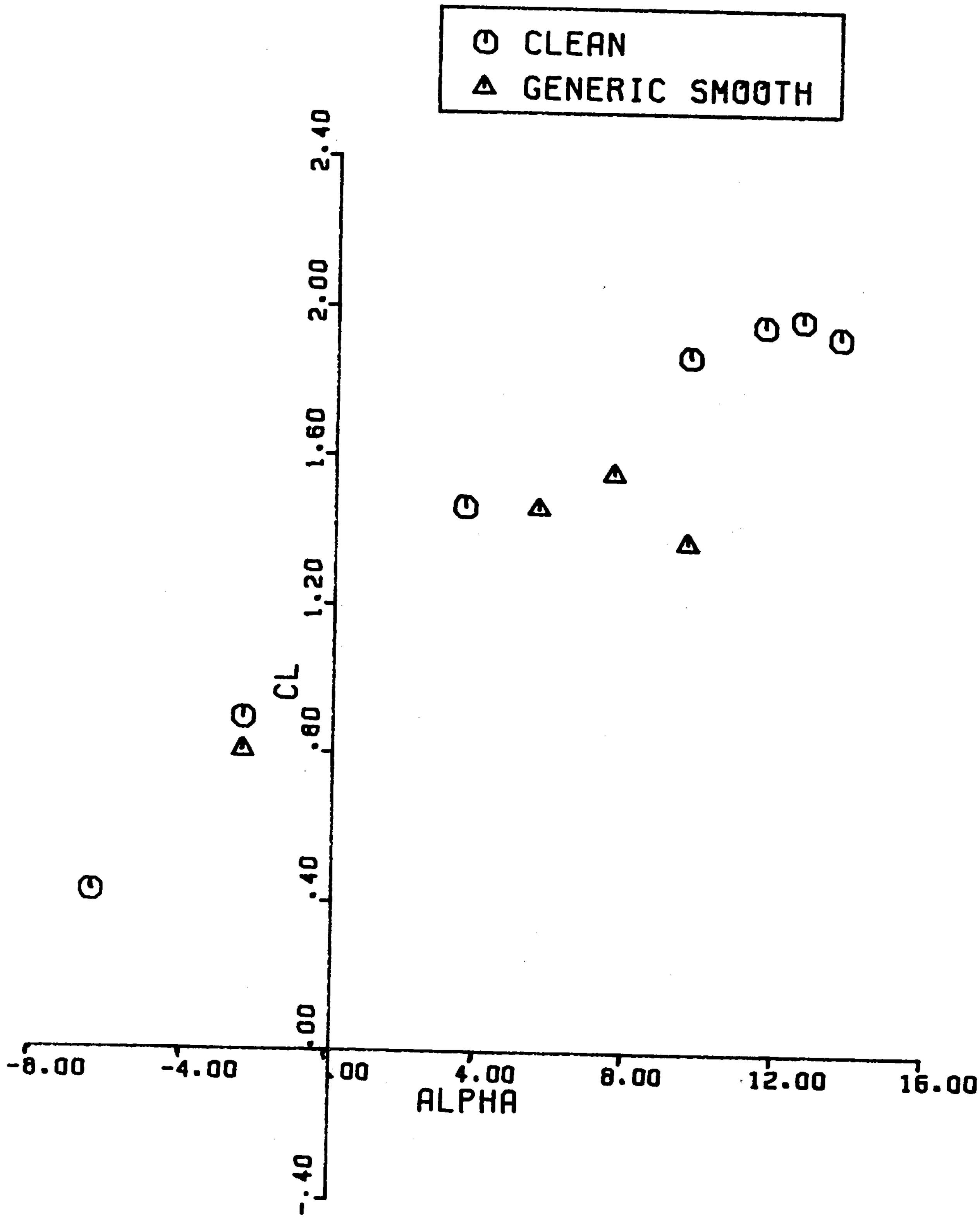

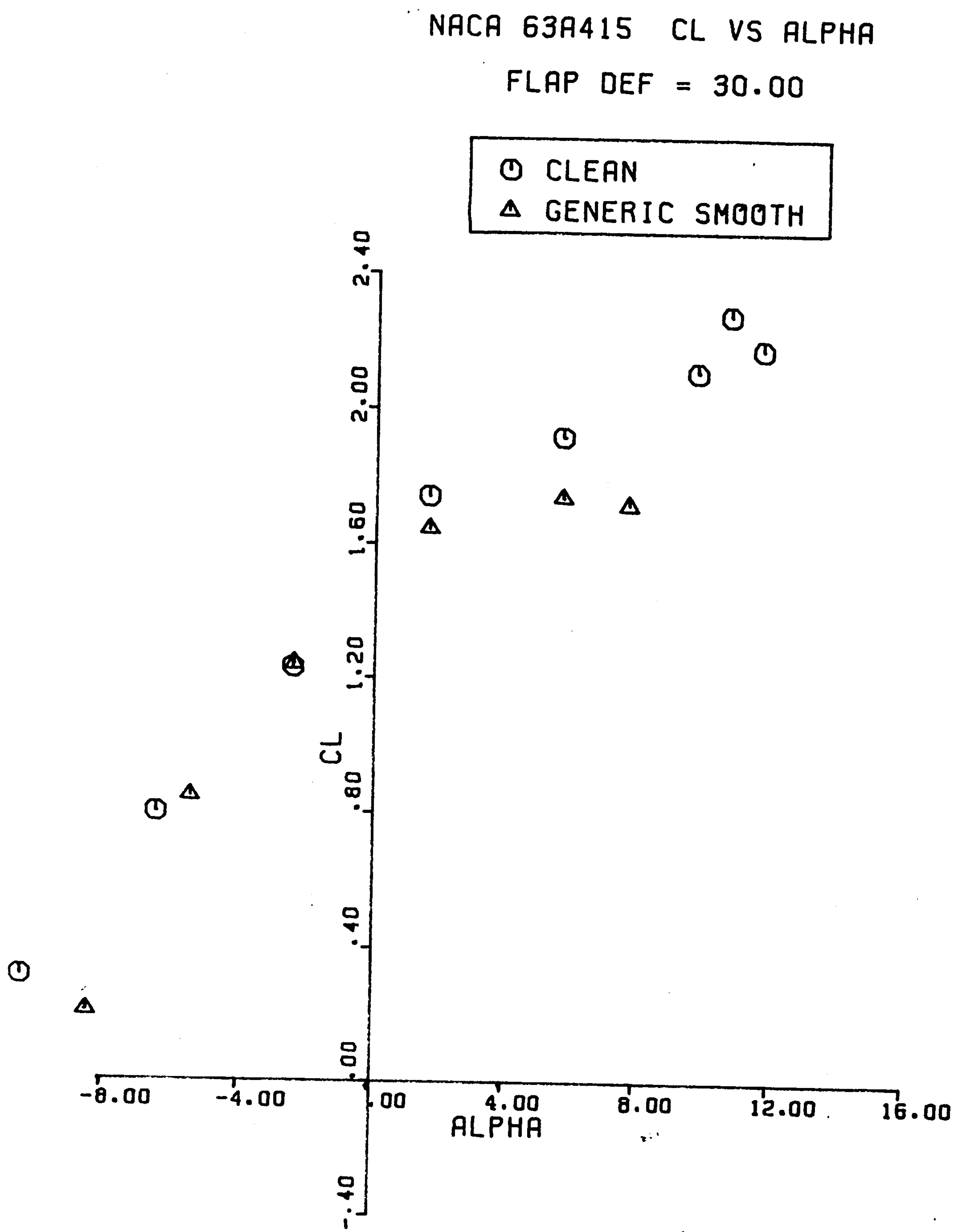
NACA 63A415 CL VS ALPHA
FLAP DEF = 30.00
CLEAN
GENERIC SMOOTH
2.40
2.00
1.60
1.20
CL
.80
.40
.00
-.40
-8.00
-4.00
.00
4.00
8.00
12.00
16.00
ALPHA

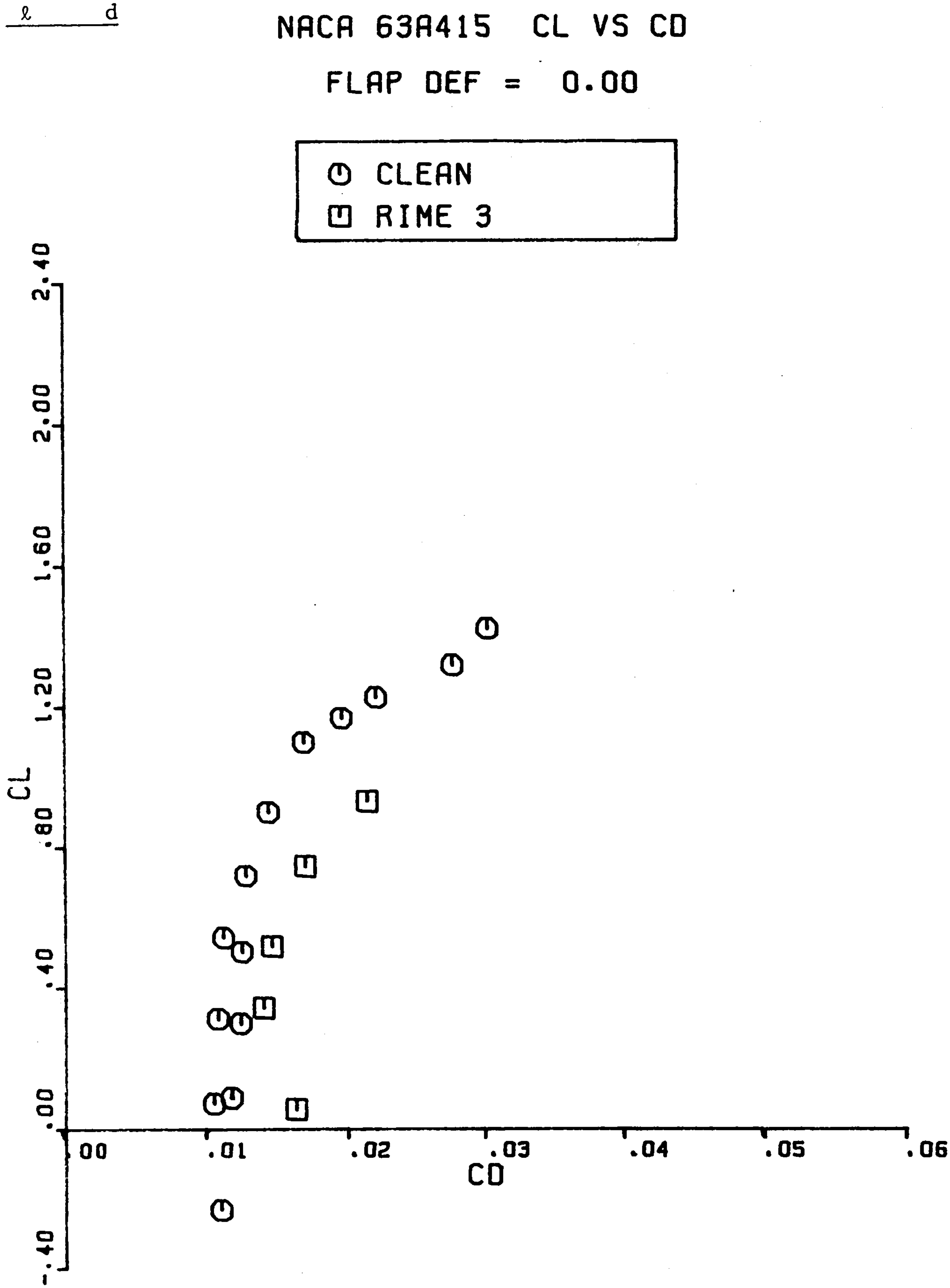
NACA 63A415 CL VS CD
FLAP DEF = 0.00
CLEAN
RIME 3
CL
CD
2.40
2.00
1.60
1.20
.80
.40
.00
-.40
.00
.01
.02
.03
.04
.05
.06

NACA 63A415 CL VS CD

FLAP DEF = 0.00

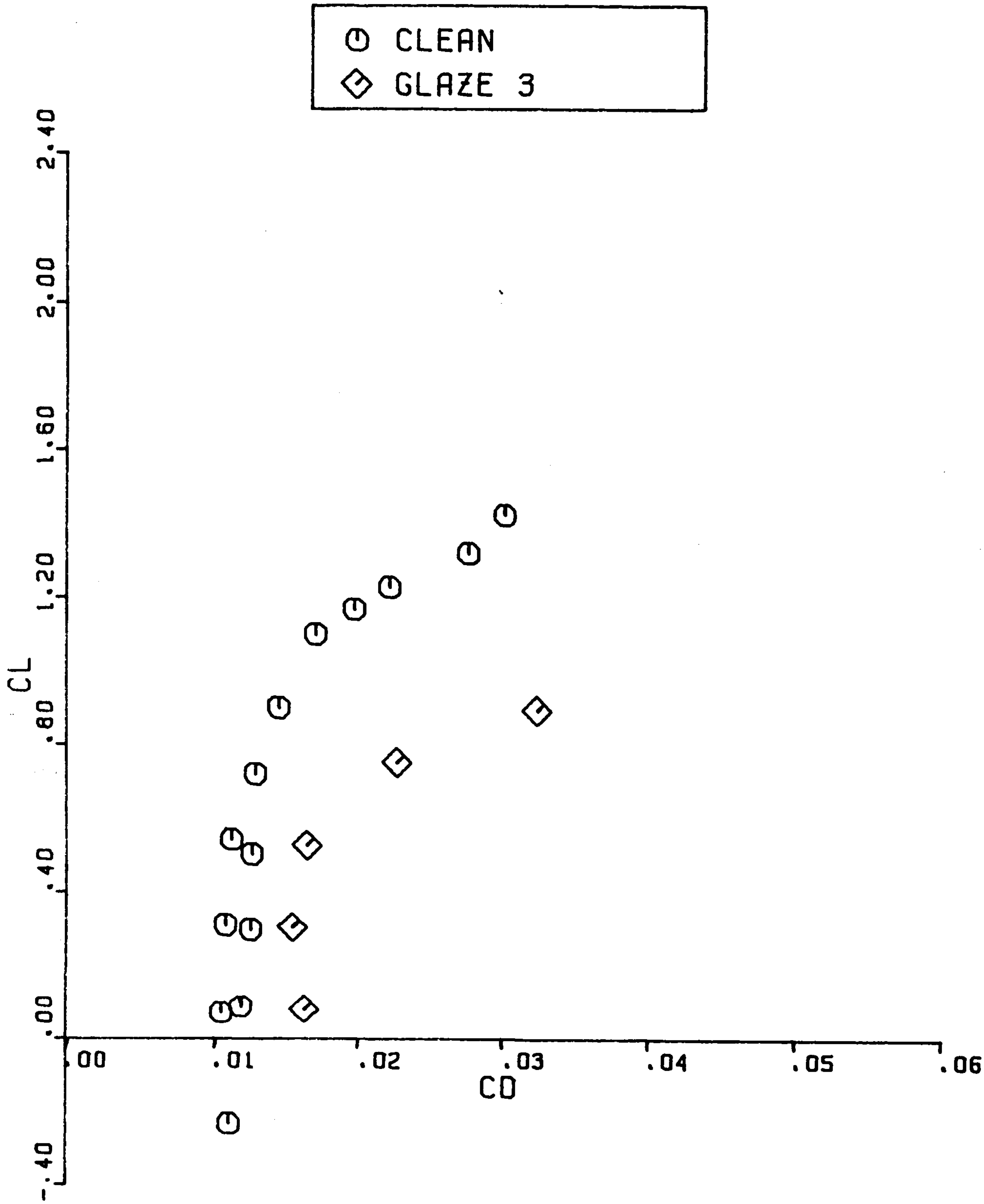

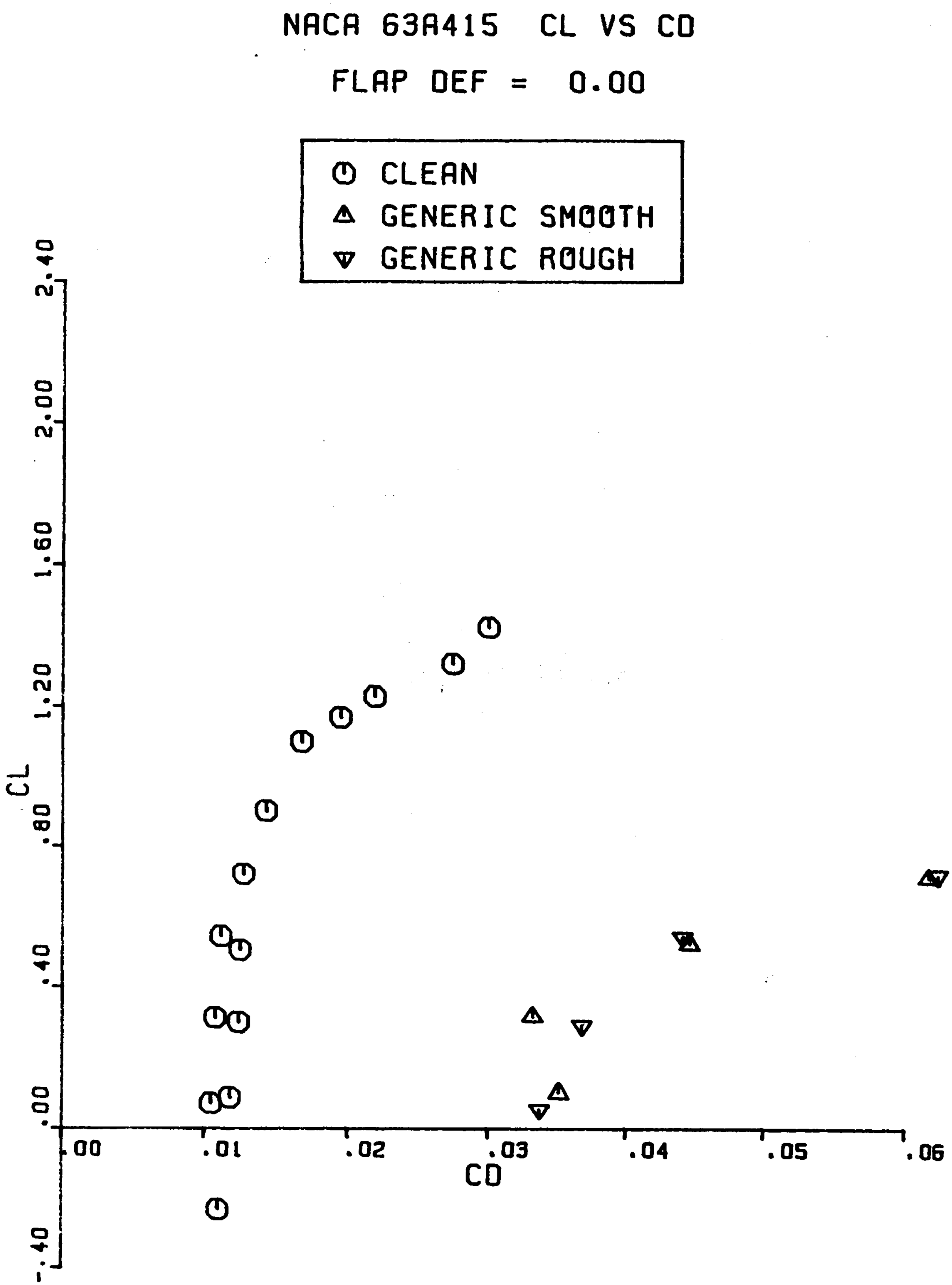
NACA 63A415 CL VS CD
FLAP DEF = 0.00
CLEAN
GENERIC SMOOTH
GENERIC ROUGH
CL
2.40
2.00
1.60
1.20
.80
.40
.00
-.40
CD
.00
.01
.02
.03
.04
.05
.06

C_m vs C_ℓ

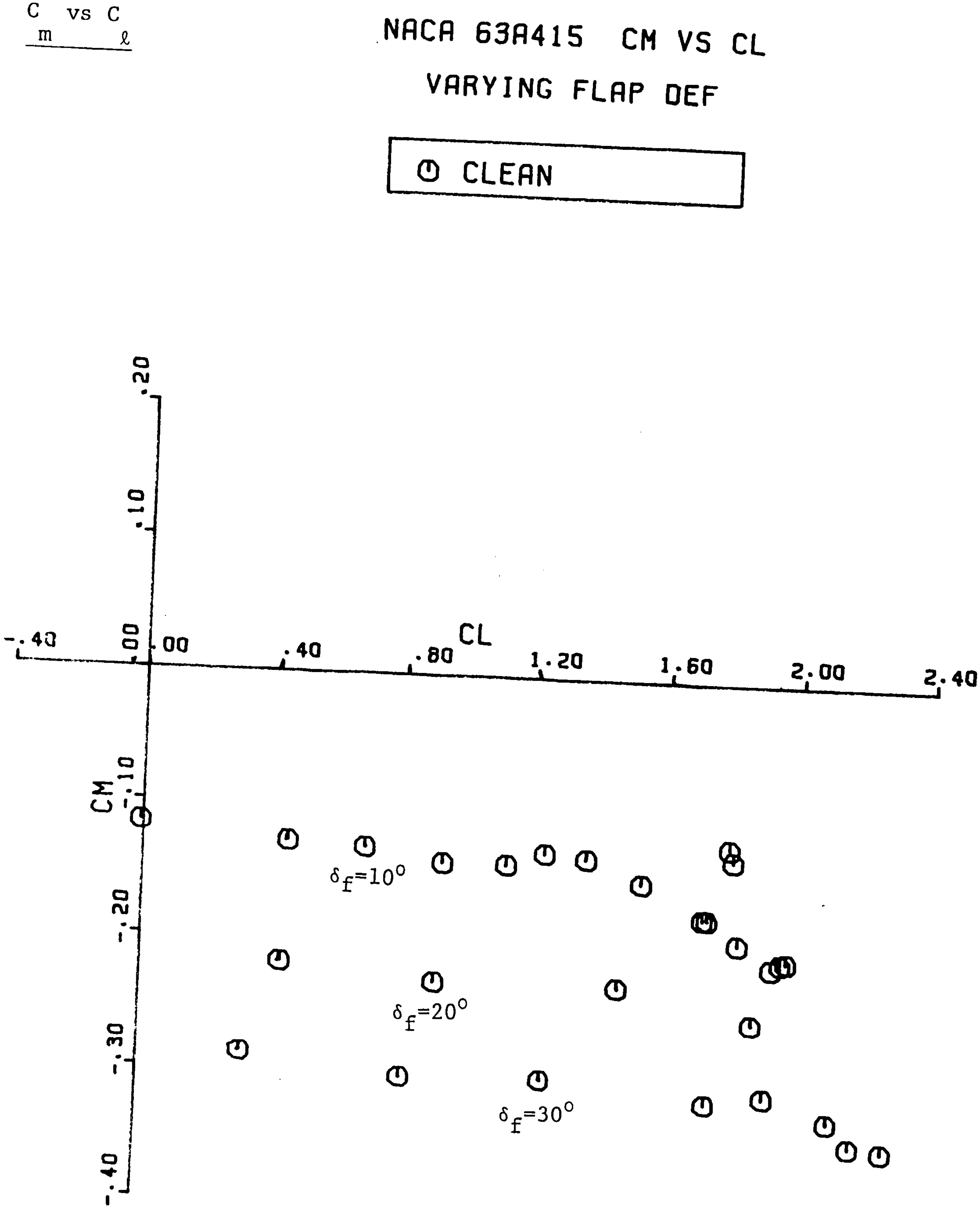

NACA 63A415 CM VS CL
VARYING FLAP DEF
CLEAN
CL
CM
-.40
.00
.40
.80
1.20
1.60
2.00
2.40
.20
.10
.00
-.10
-.20
-.30
-.40
δf=10°
δf=20°
δf=30°

NACA 63A415 CM VS CL

VARYING FLAP DEF

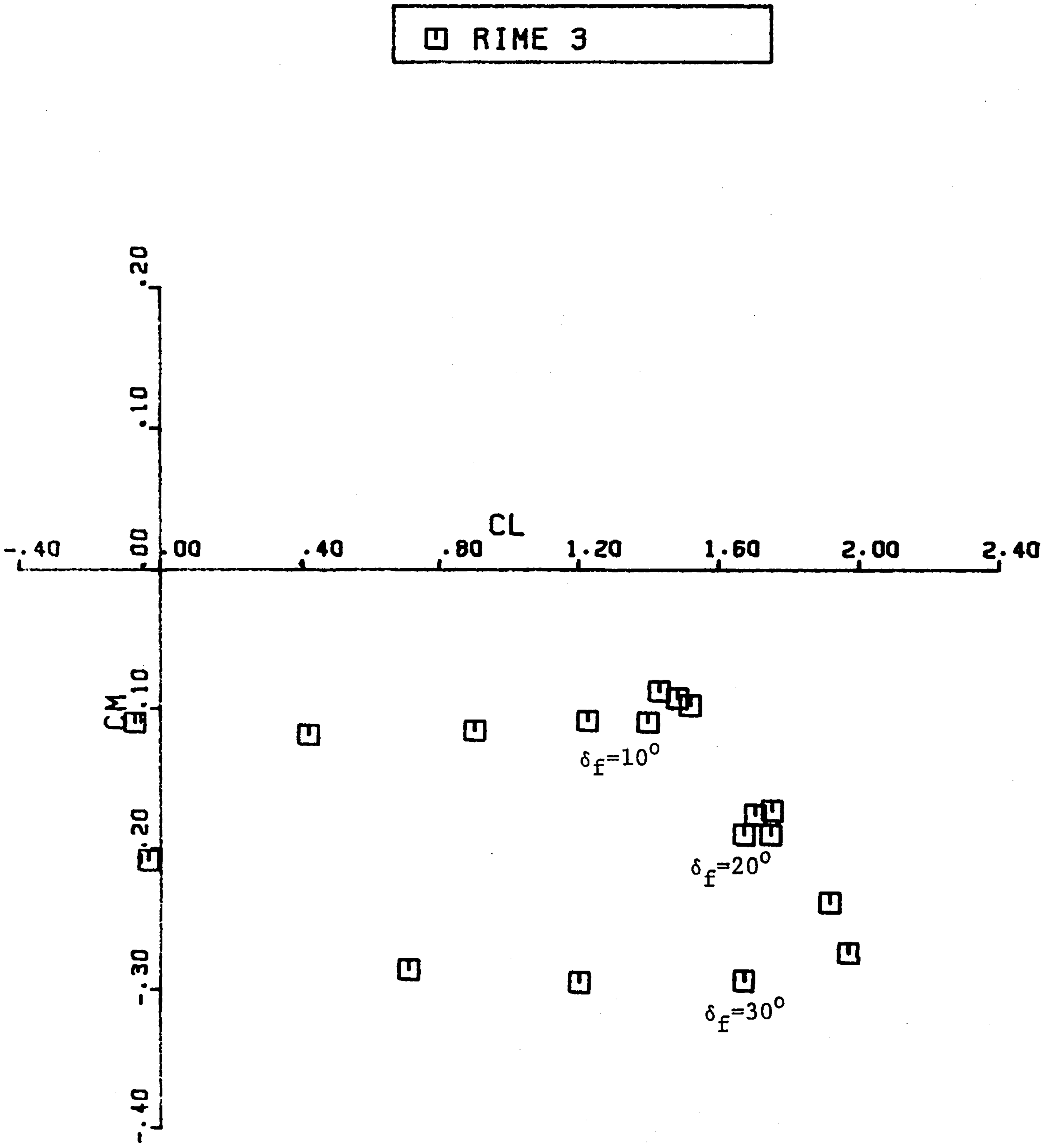

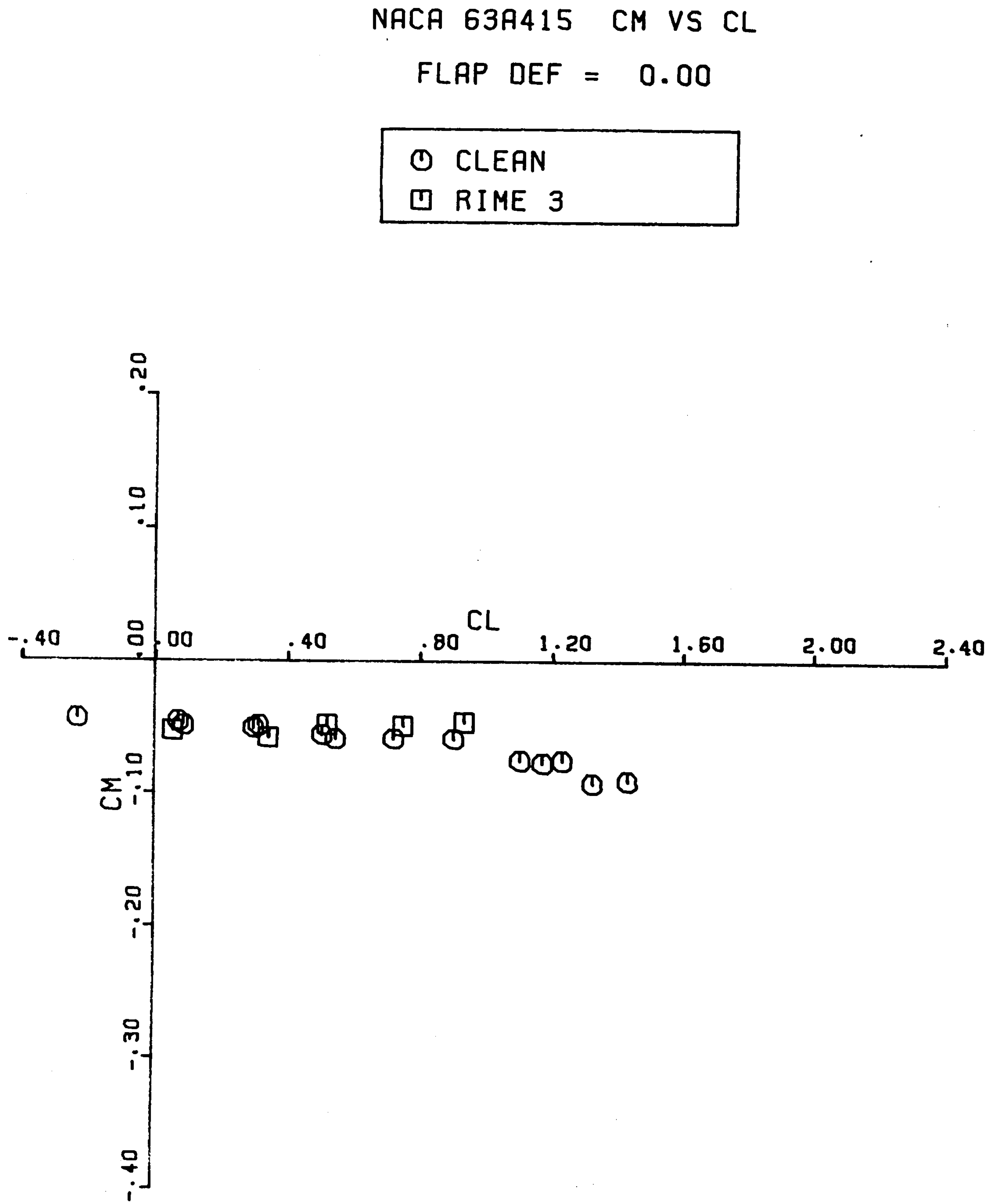

NACA 63A415 CM VS CL
FLAP DEF = 0.00
CLEAN
RIME 3
CL
CM
-.40
.00
.40
.80
1.20
1.60
2.00
2.40
.20
.10
.00
-.10
-.20
-.30
-.40

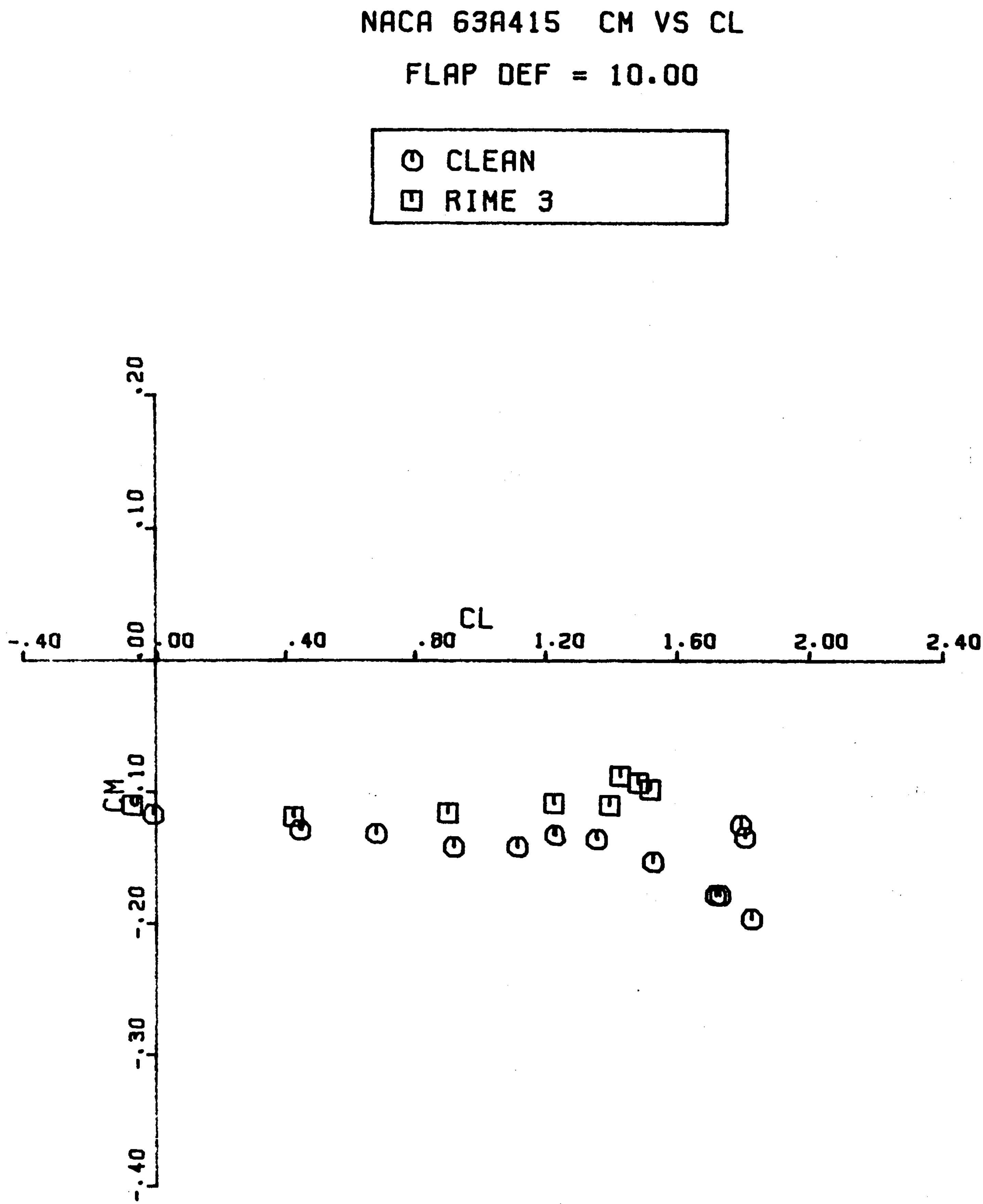
NACA 63A415 CM VS CL
FLAP DEF = 10.00
CLEAN
RIME 3
CL
CM
-.40
.00
.40
.80
1.20
1.60
2.00
2.40
.20
.10
0.0
-.10
-.20
-.30
-.40

NACA 63A415 CM VS CL

FLAP DEF = 20.00

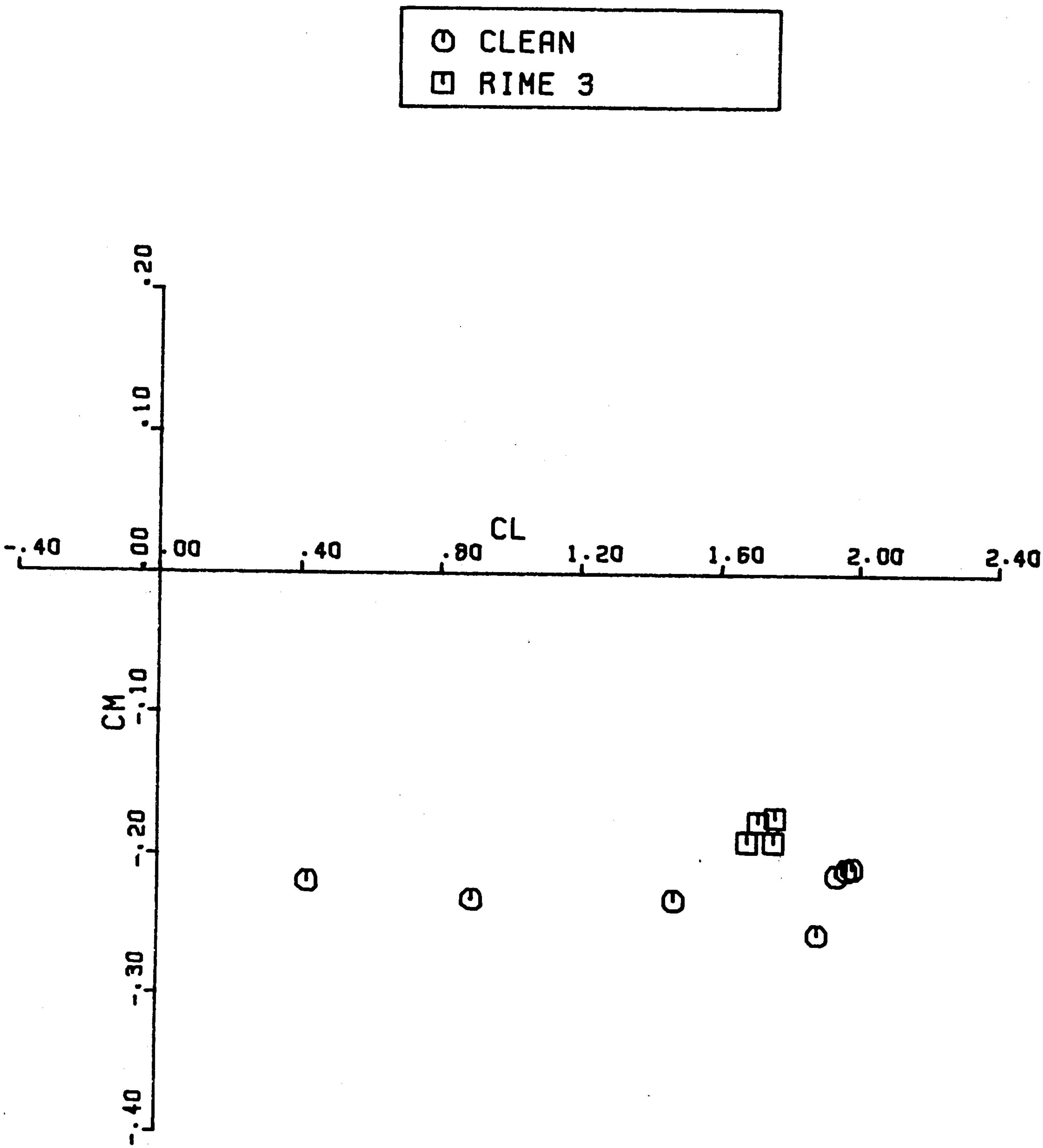

NACA 63A415 CM VS CL

FLAP DEF = 30.00

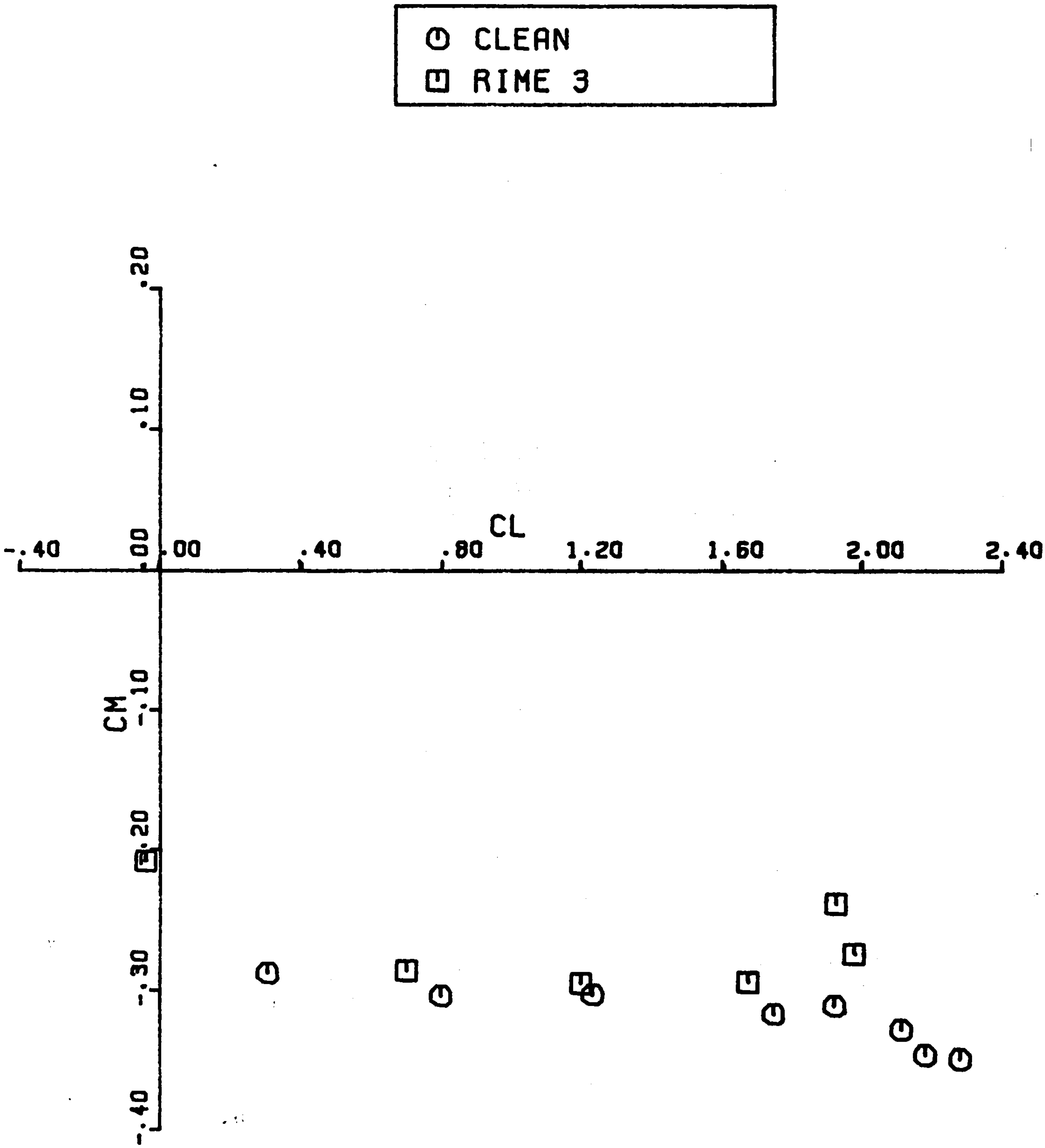

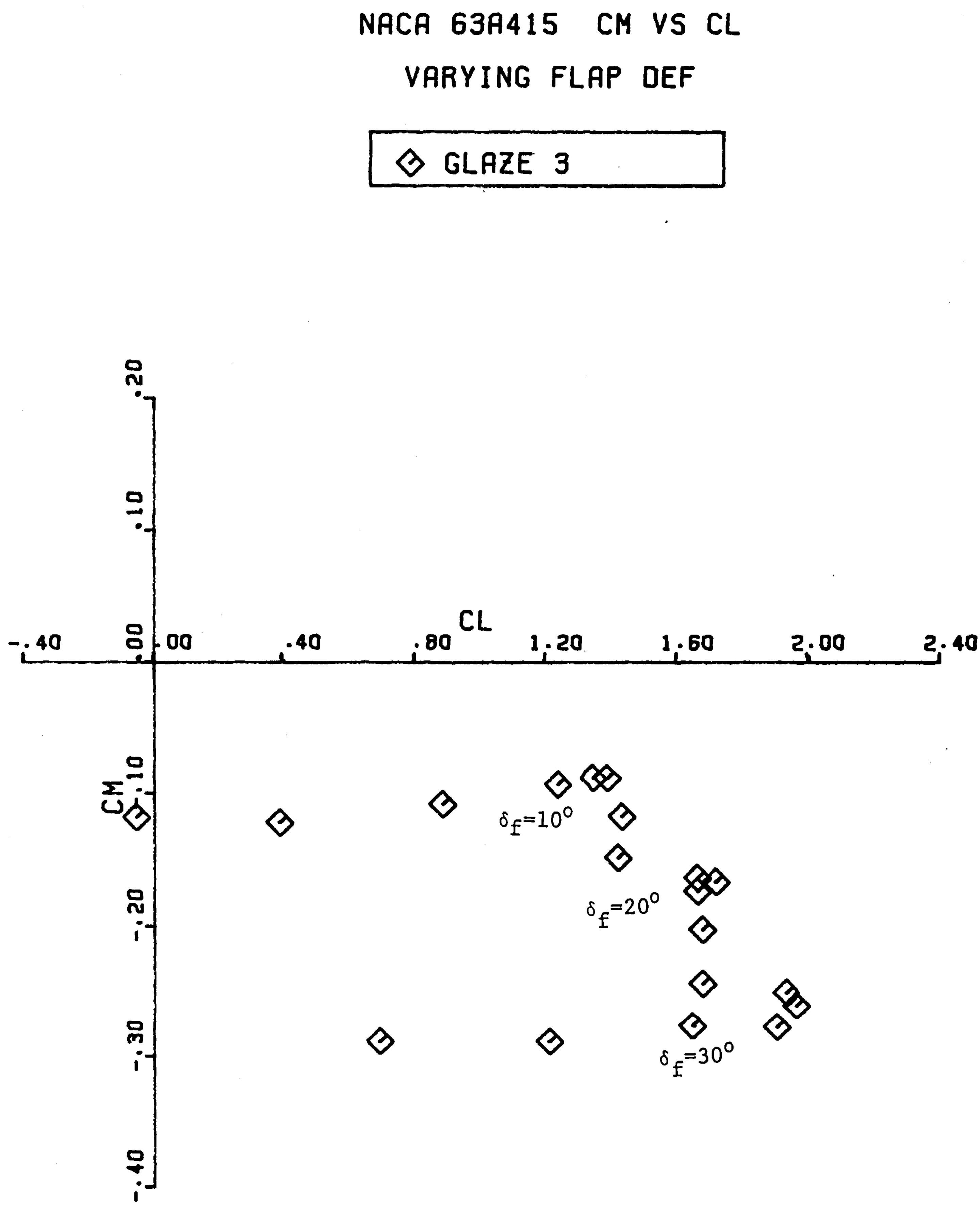
NACA 63A415 CM VS CL
VARYING FLAP DEF
GLAZE 3
CL
CM
-.40
.00
.40
.80
1.20
1.60
2.00
2.40
.20
.10
0.00
-.10
-.20
-.30
-.40
δ_f=10°
δ_f=20°
δ_f=30°

NACA 63A415 CM VS CL

FLAP DEF = 0.00

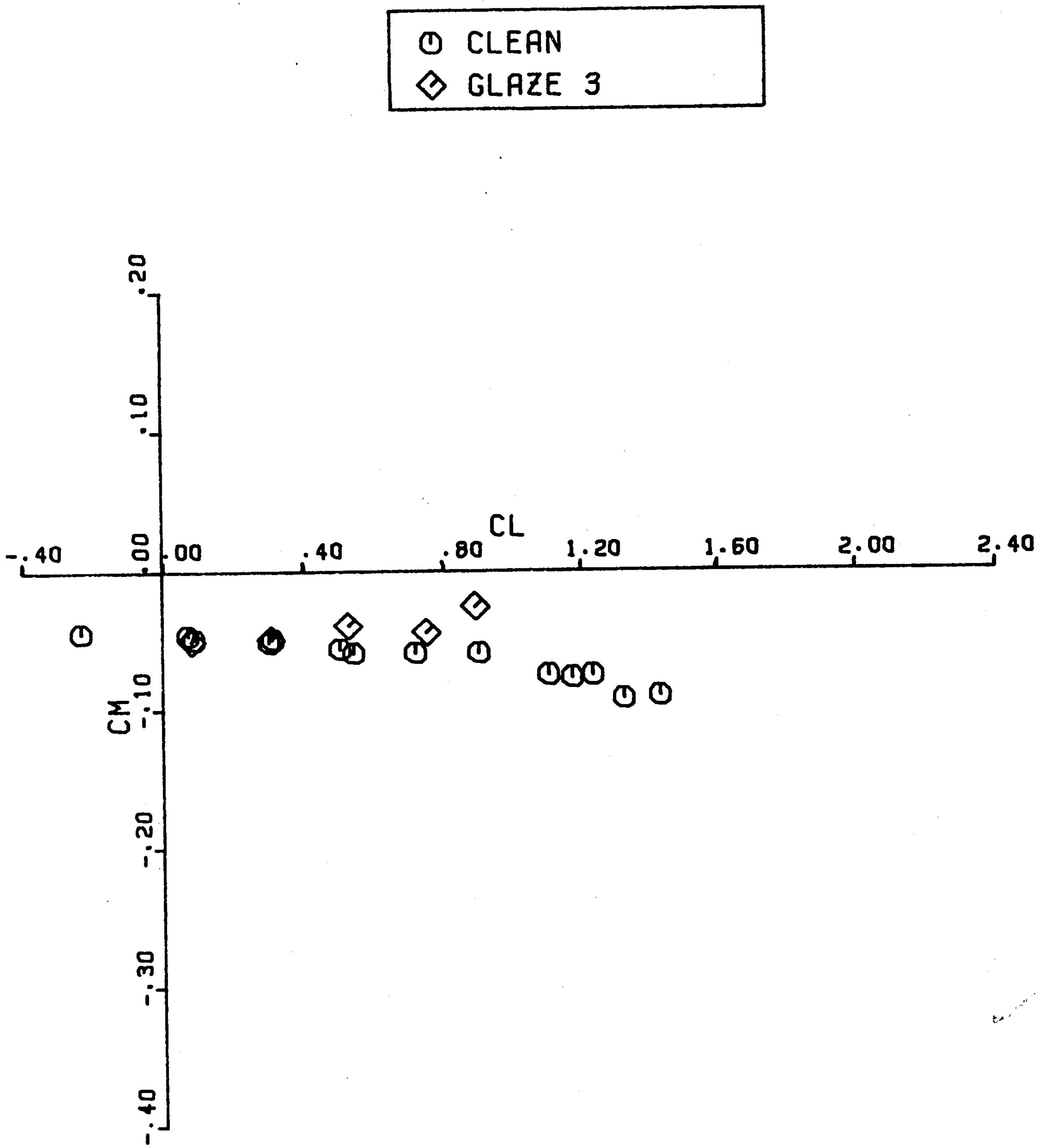

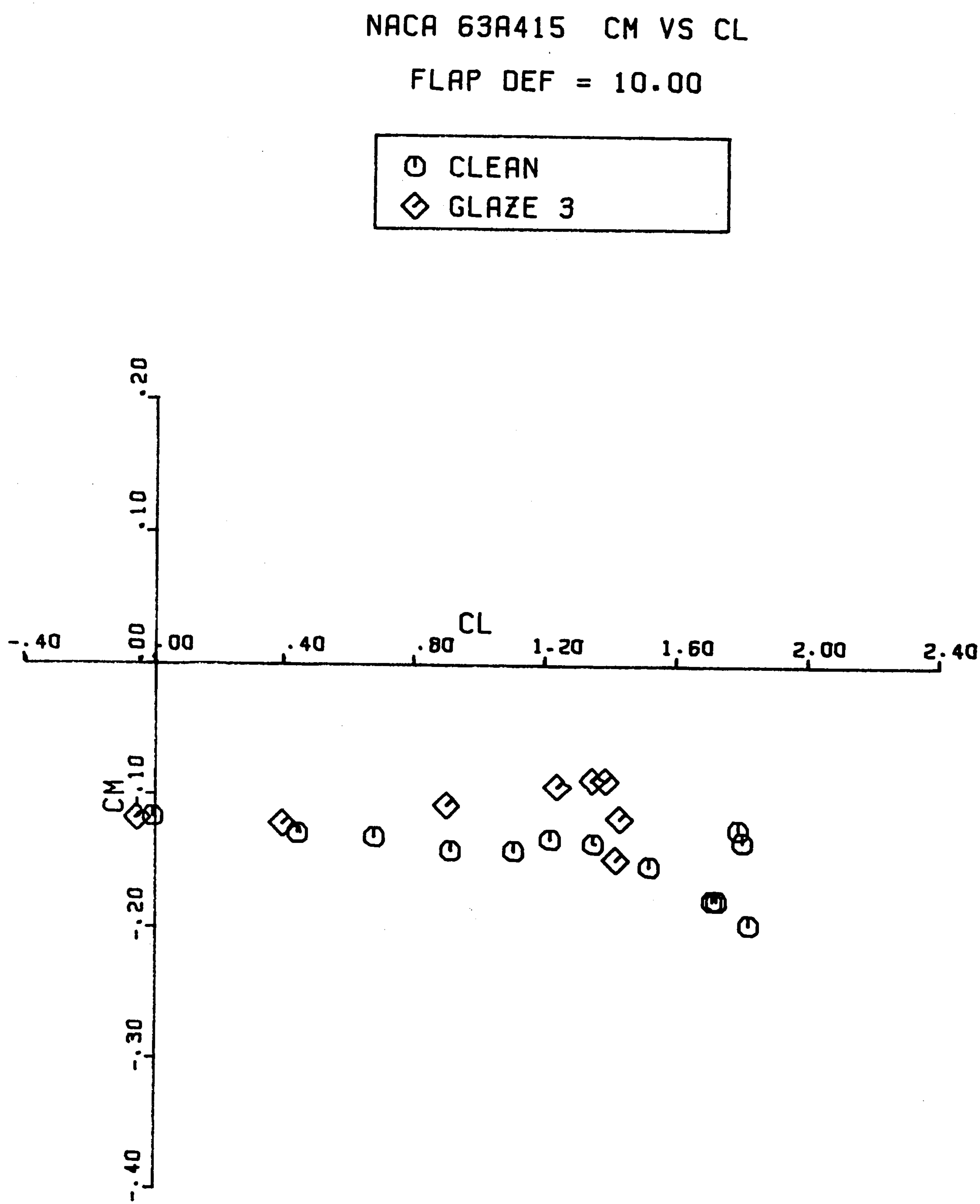

NACA 63A415 CM VS CL
FLAP DEF = 10.00
CLEAN
GLAZE 3
CL
CM
-.40
.00
.40
.80
1.20
1.60
2.00
2.40
.20
.10
-.10
-.20
-.30
-.40

NACA 63A415 CM VS CL

FLAP DEF = 20.00

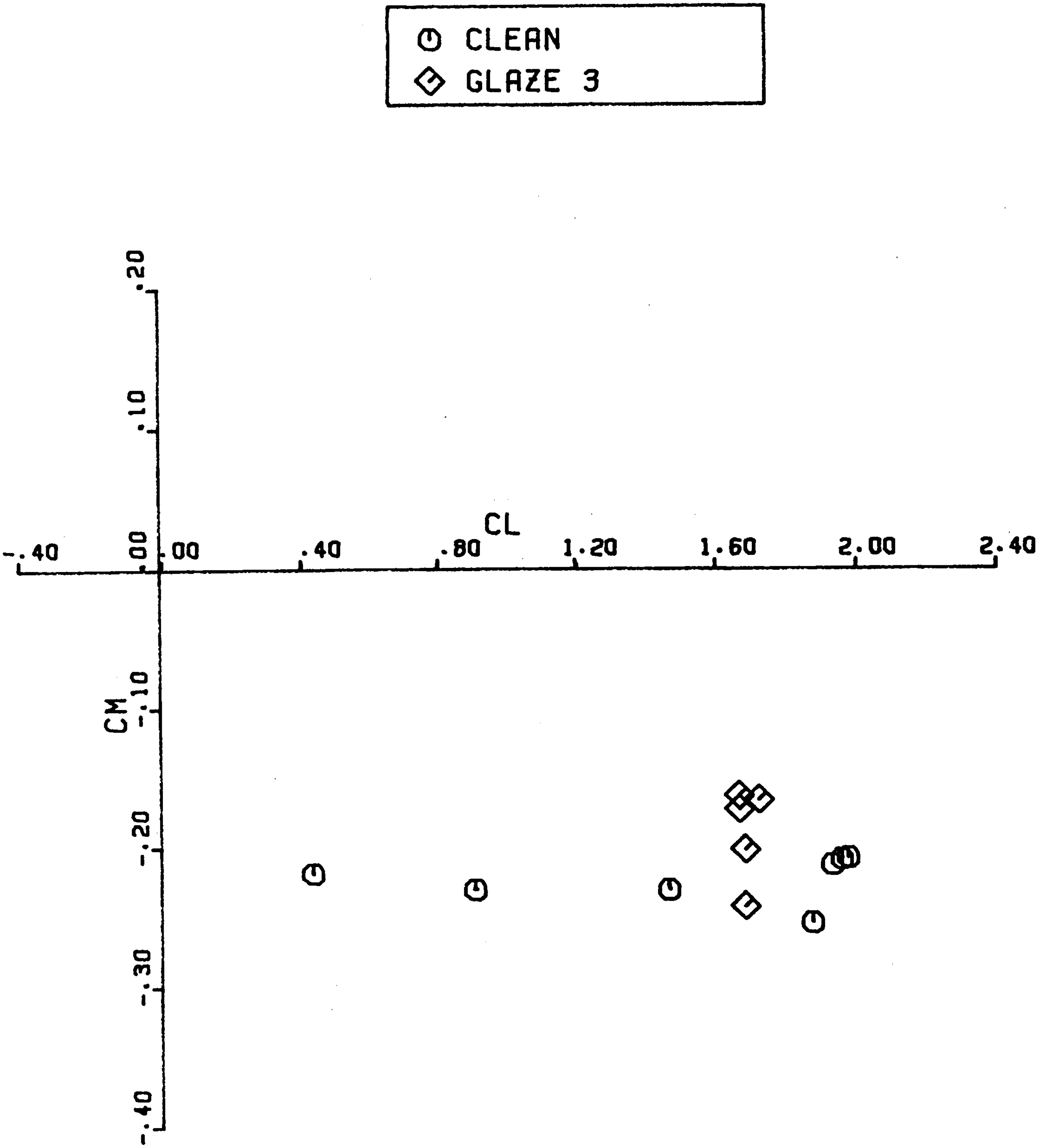

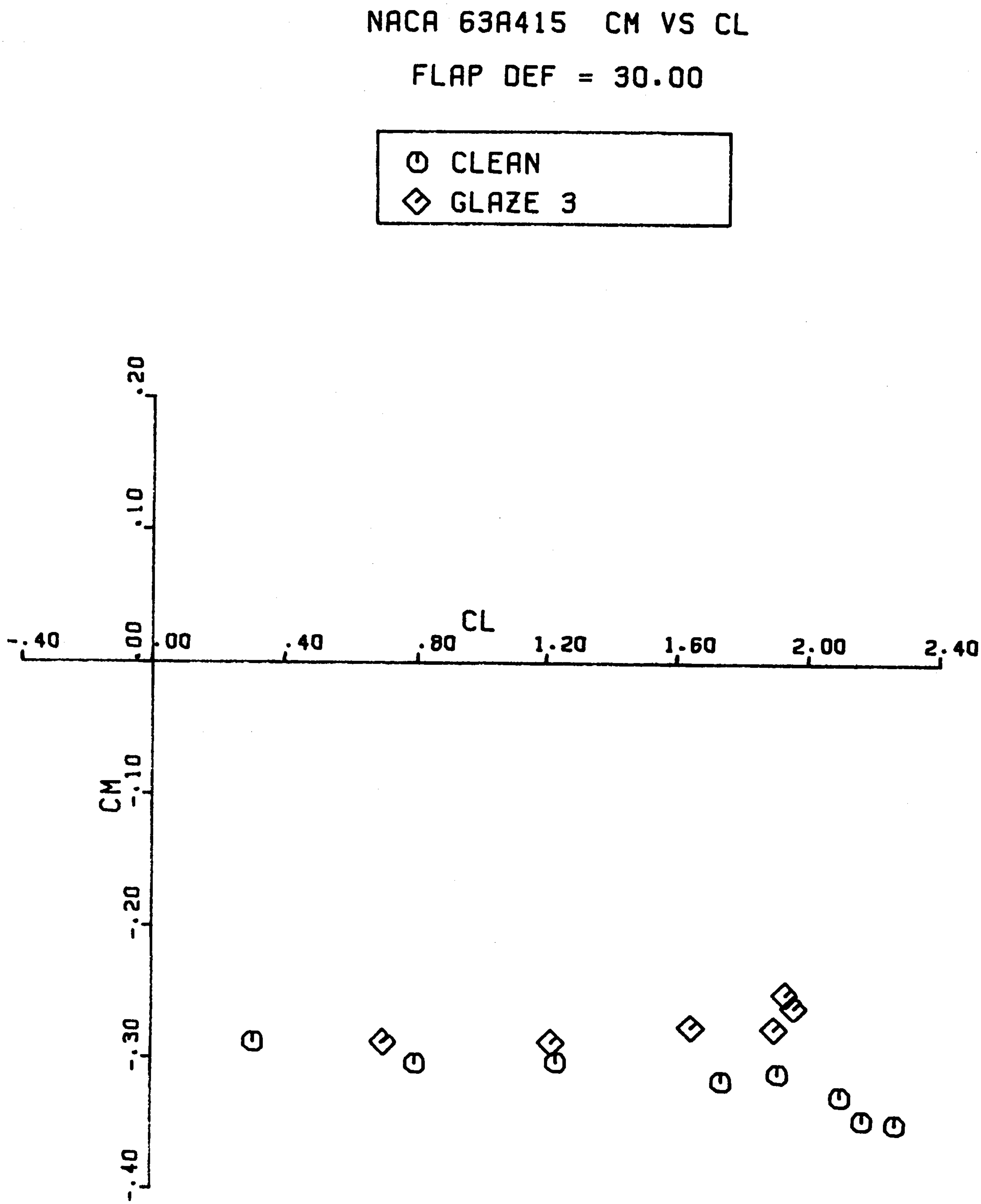
NACA 63A415 CM VS CL
FLAP DEF = 30.00
CLEAN
GLAZE 3
CL
-.40
.00
.40
.80
1.20
1.60
2.00
2.40
CM
.20
.10
.00
-.10
-.20
-.30
-.40

NACA 63A415 CM VS CL

VARYING FLAP DEF

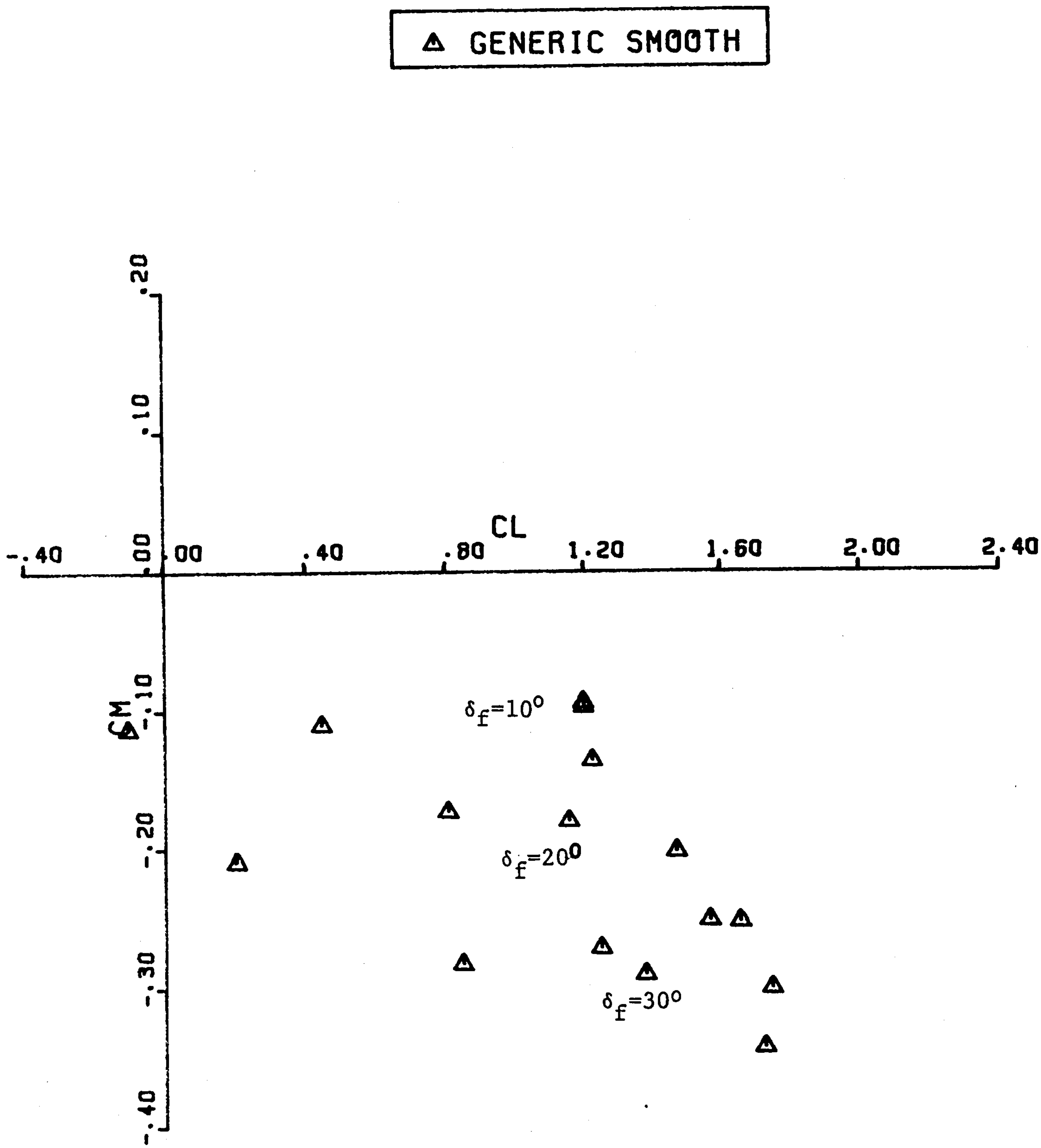

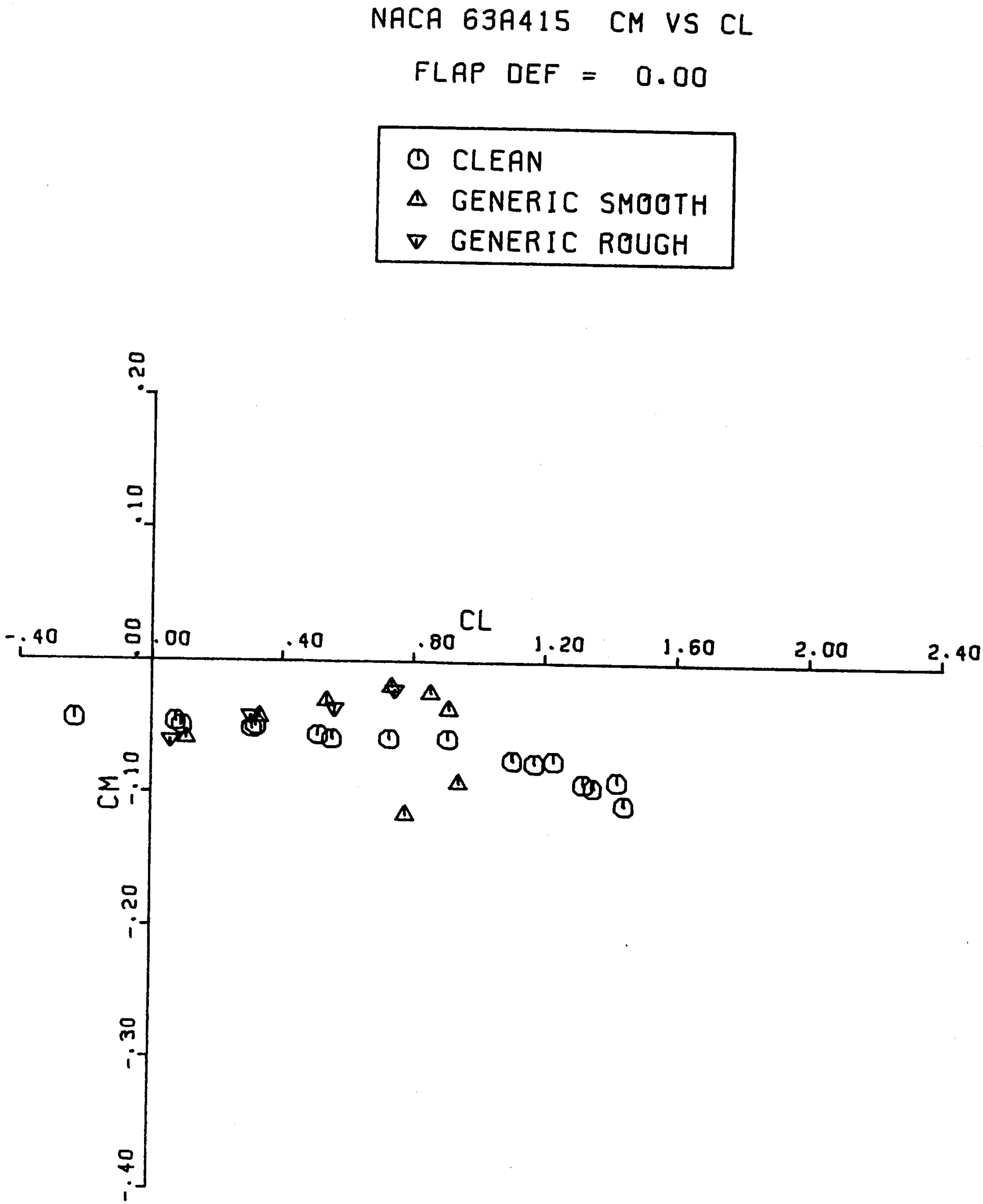
NACA 63A415 CM VS CL
FLAP DEF = 0.00
CLEAN
GENERIC SMOOTH
GENERIC ROUGH
CL
-.40
.00
.40
.80
1.20
1.60
2.00
2.40
CM
.20
.10
0.00
-.10
-.20
-.30
-.40

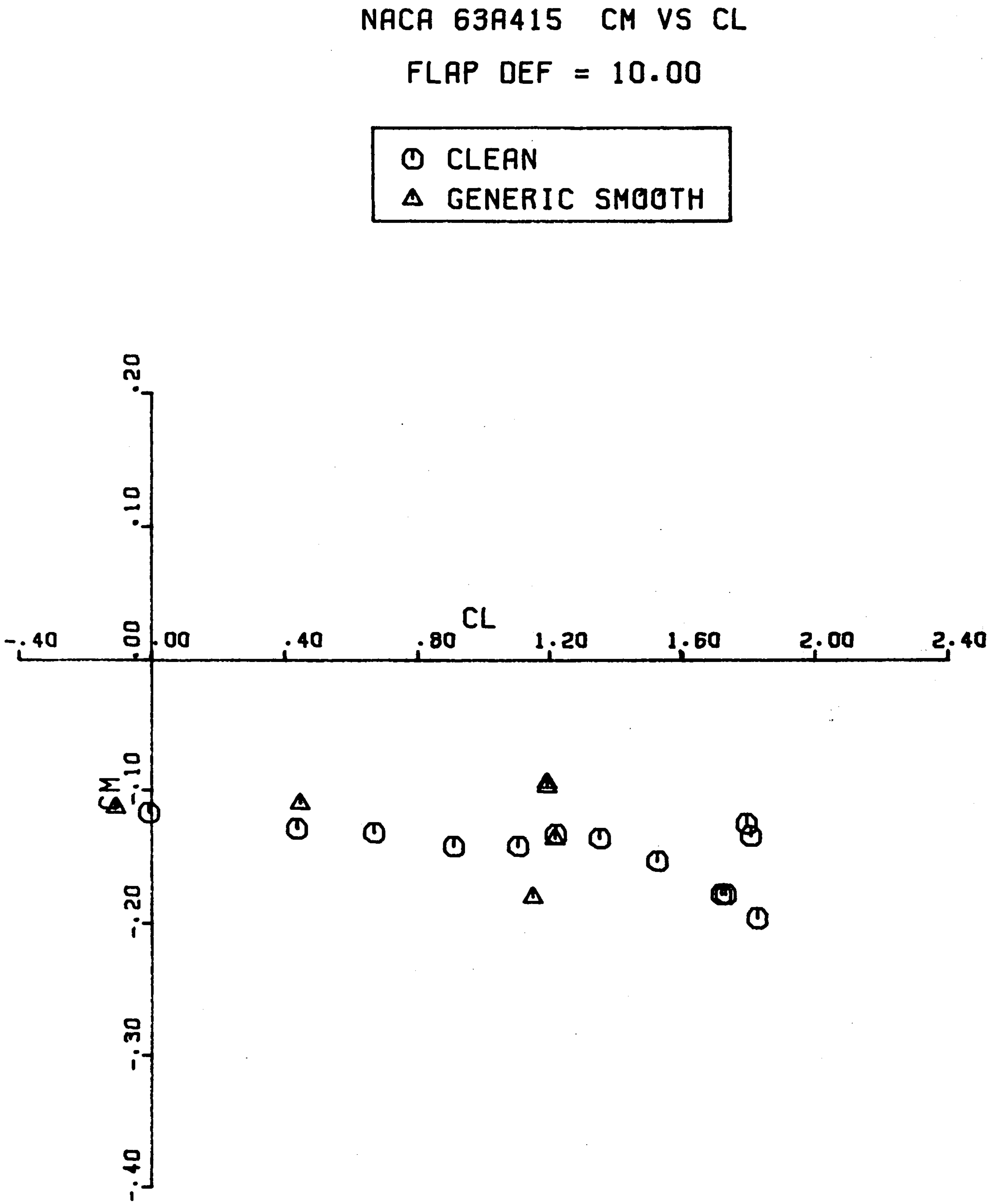

NACA 63A415 CM VS CL
FLAP DEF = 10.00
CLEAN
GENERIC SMOOTH
CL
CM
-.40
.00
.40
.80
1.20
1.60
2.00
2.40
.20
.10
.00
-.10
-.20
-.30
-.40

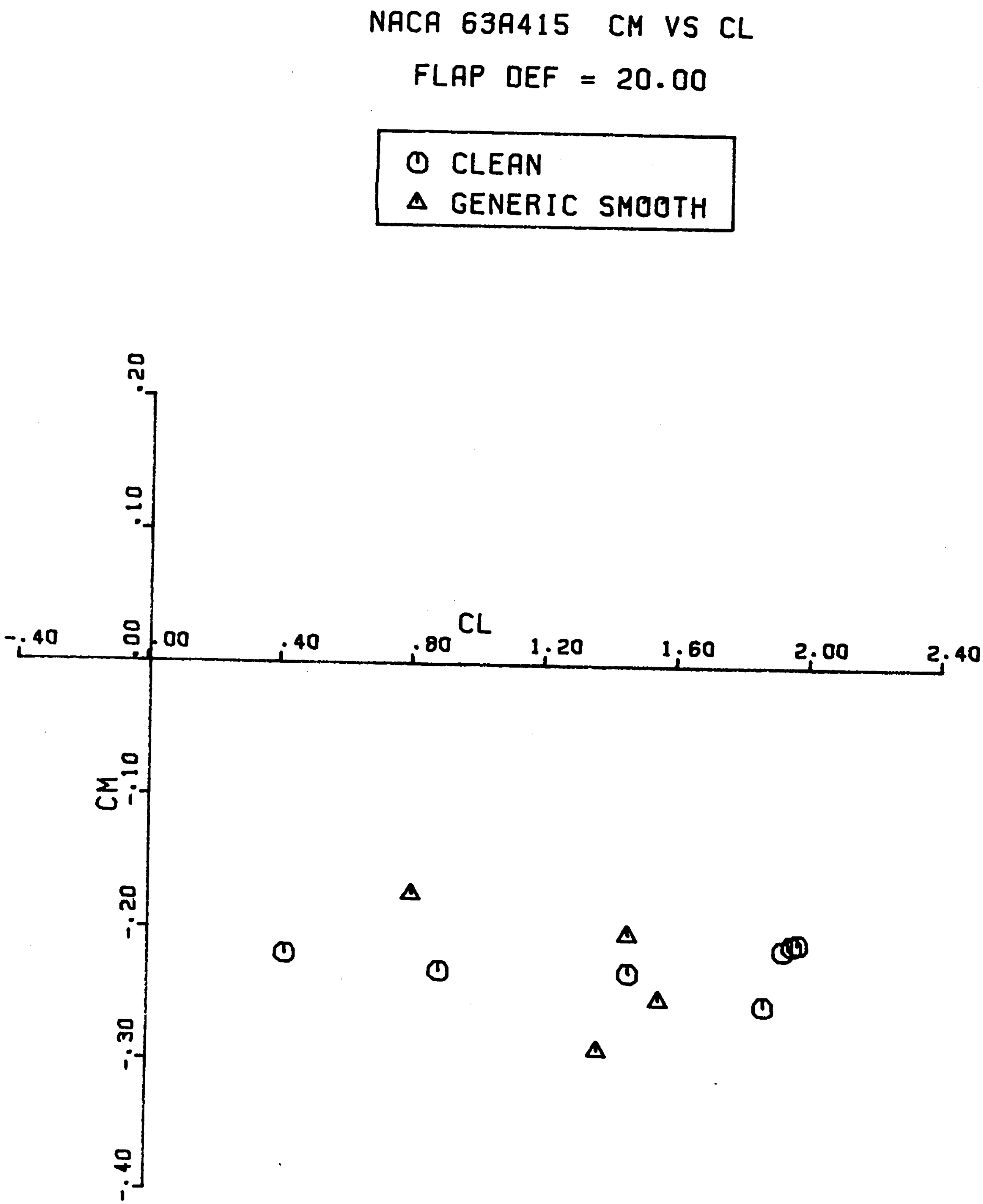

NACA 63A415 CM VS CL
FLAP DEF = 20.00
CLEAN
GENERIC SMOOTH
CL
CM
-.40
.00
.40
.80
1.20
1.60
2.00
2.40
.20
.10
0.00
-.10
-.20
-.30
-.40

NACA 63A415 CM VS CL

FLAP DEF = 30.00

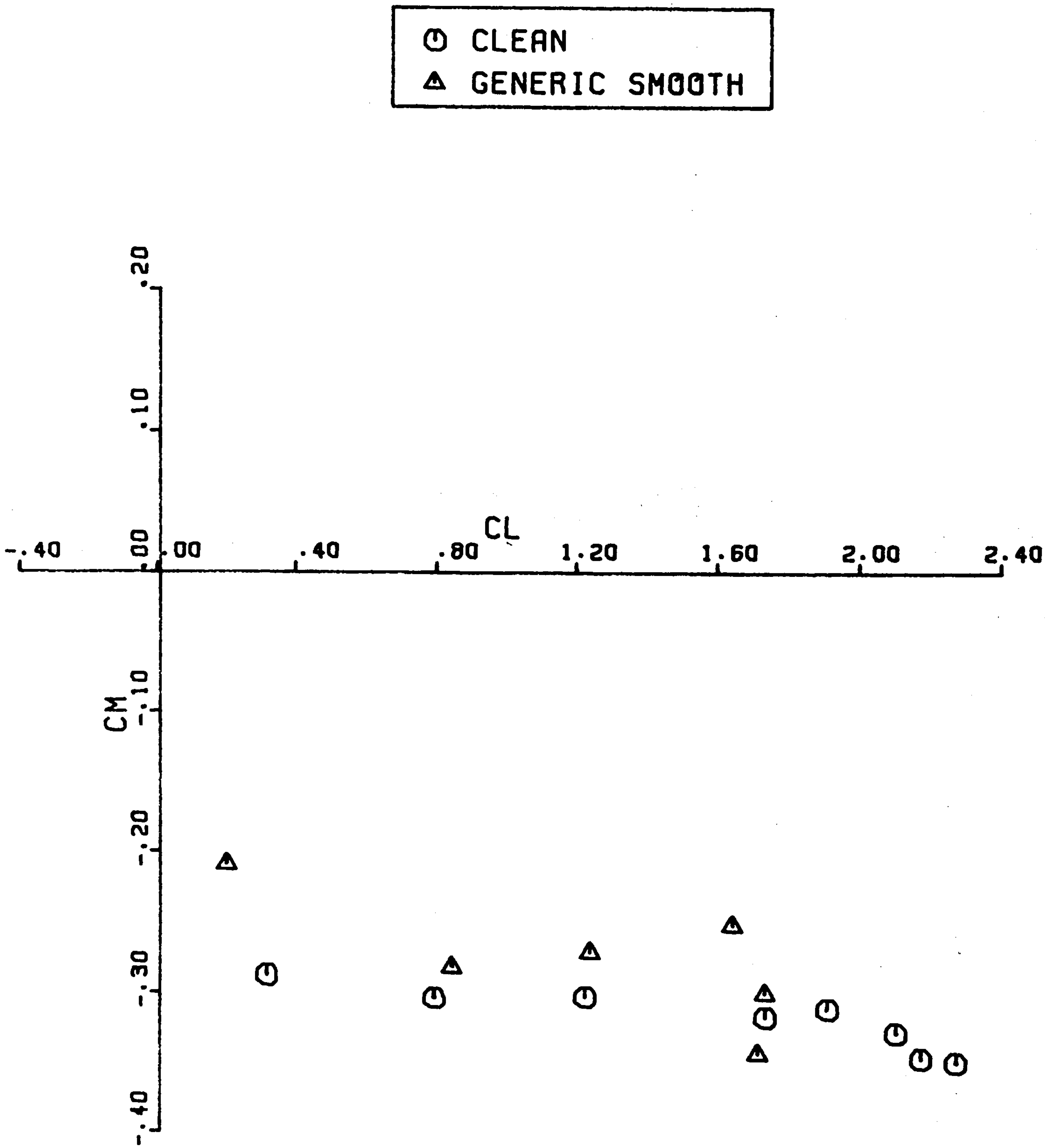

CLEAN RUN # 48

AOA = 10.60
FLAP DEF = 0.00
CL = 1.339
CM = -0.096
CD = 0.026

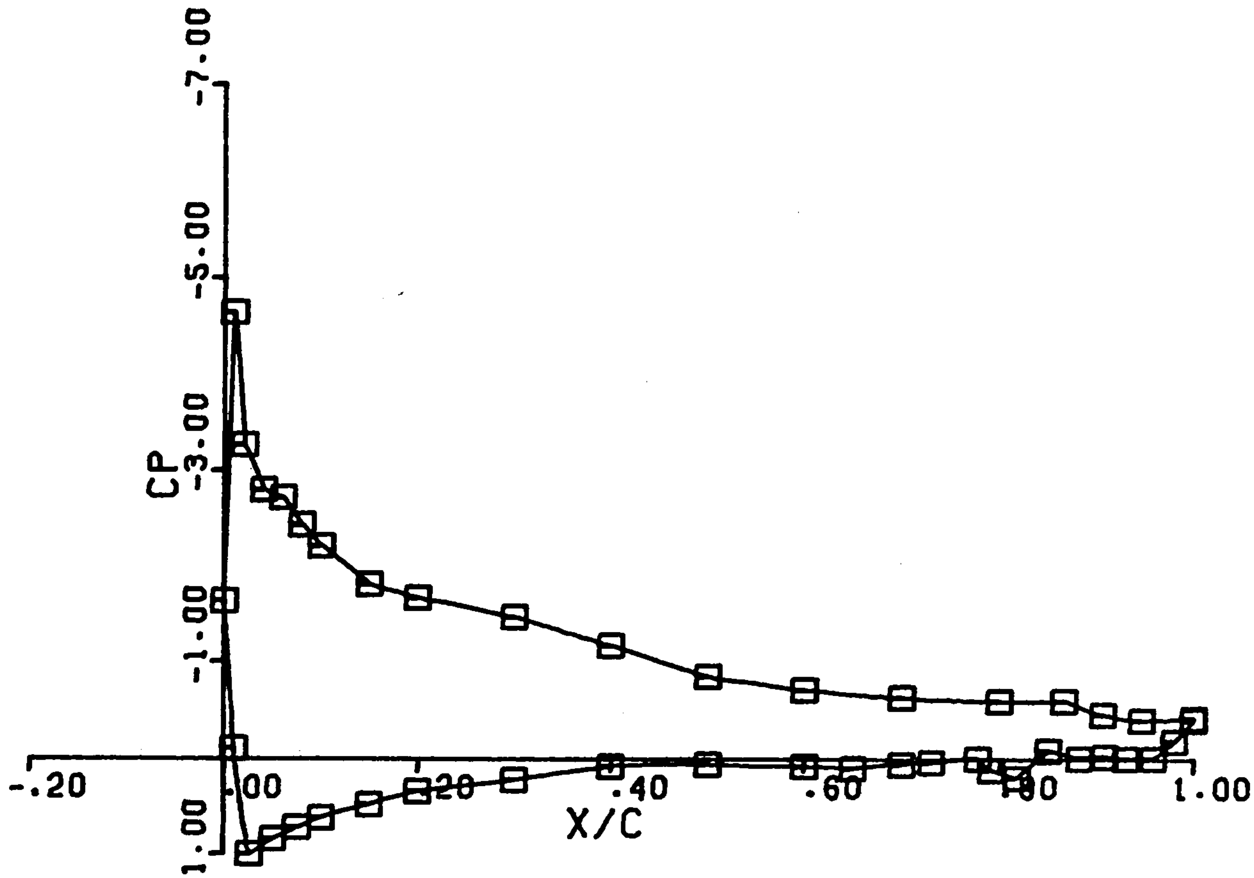

CLEAN RUN # 49

AOA = 11.60
FLAP DEF = 0.00
CL = 1.441
CM = -0.109
CD = ------

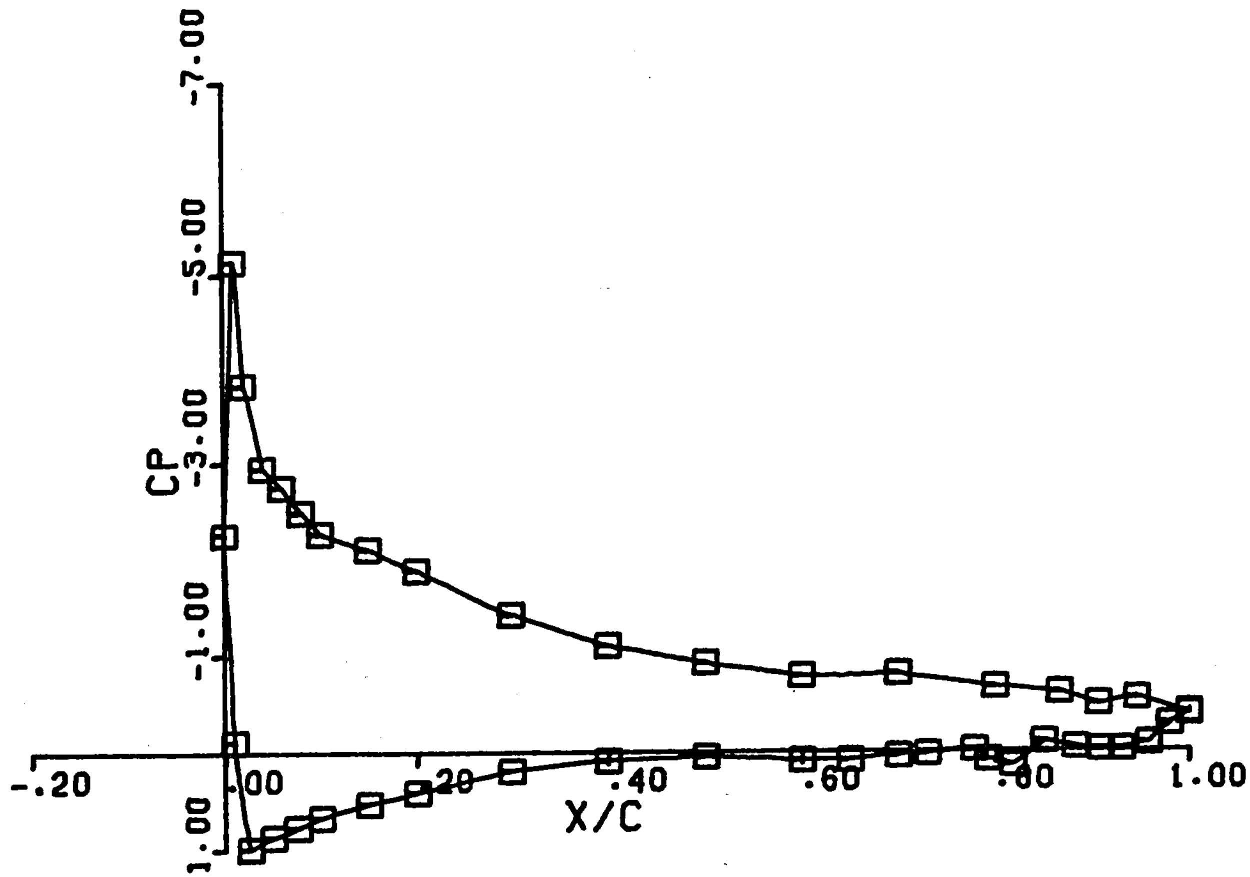

CLEAN RUN # 60

AOA = -5.40
FLAP DEF = 0.00
CL = -0.233
CM = -0.045
CD = 0.011

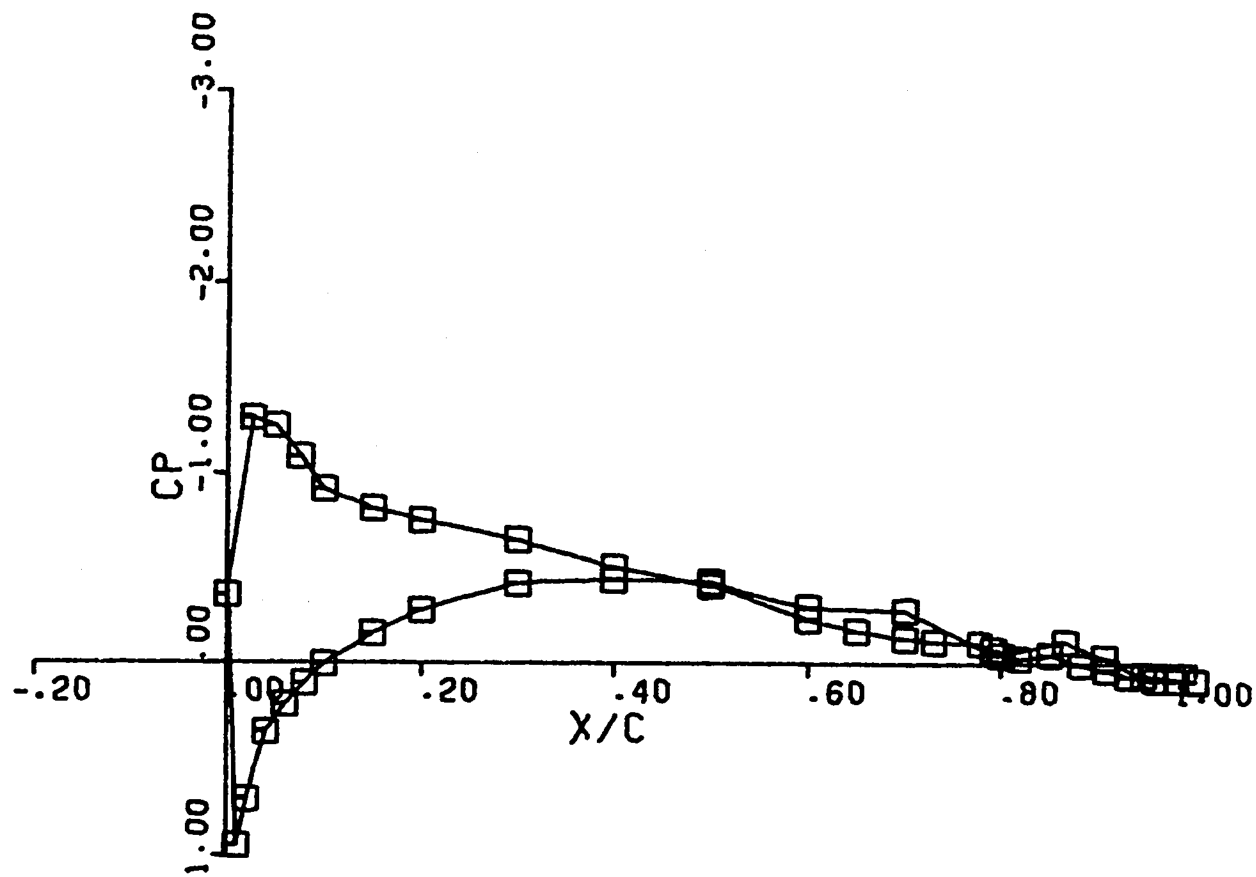

CLEAN RUN # 61

AOA = -2.40
FLAP DEF = 0.00
CL = 0.071
CM = -0.047
CD = 0.010

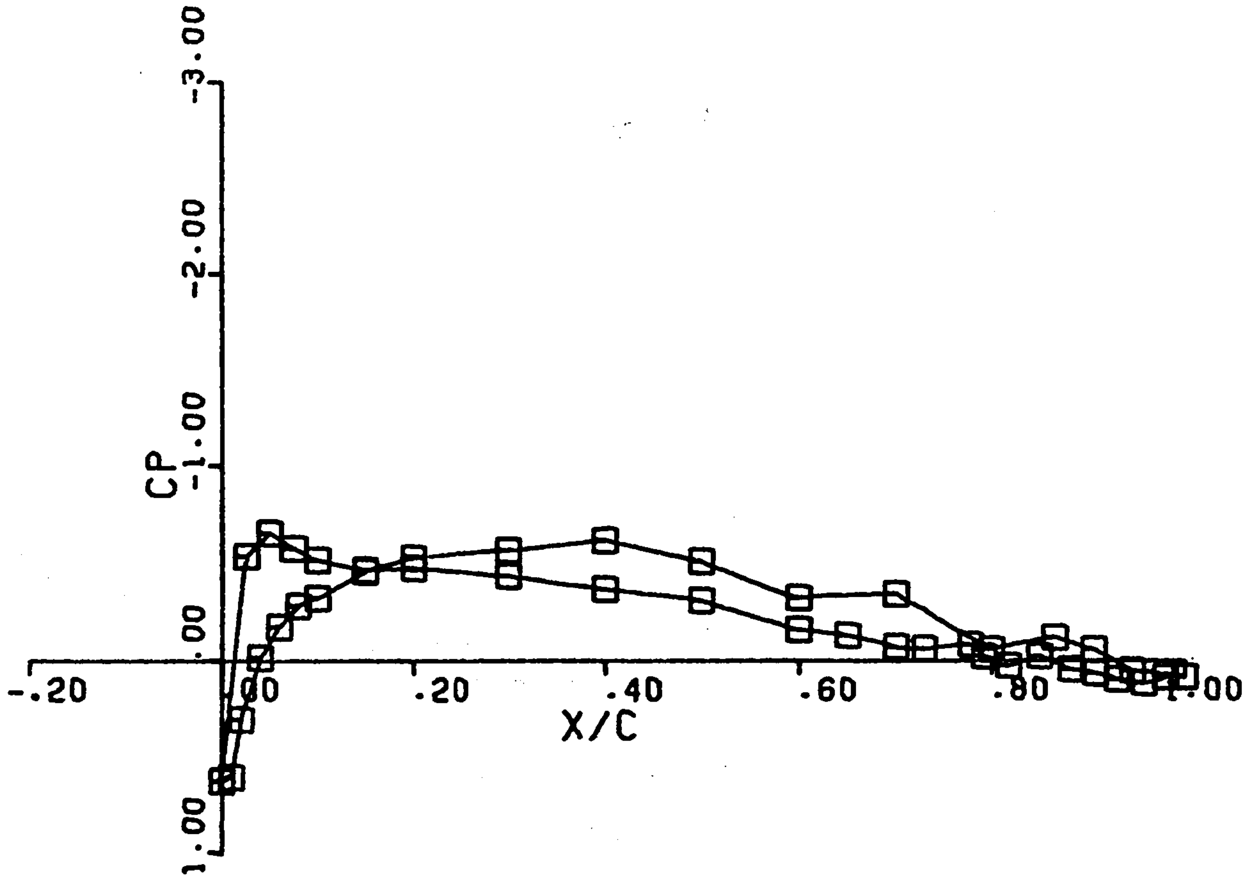

CLEAN RUN # 62

AOA = -0.40
FLAP DEF = 0.00
CL = 0.313
CM = -0.049
CD = 0.011

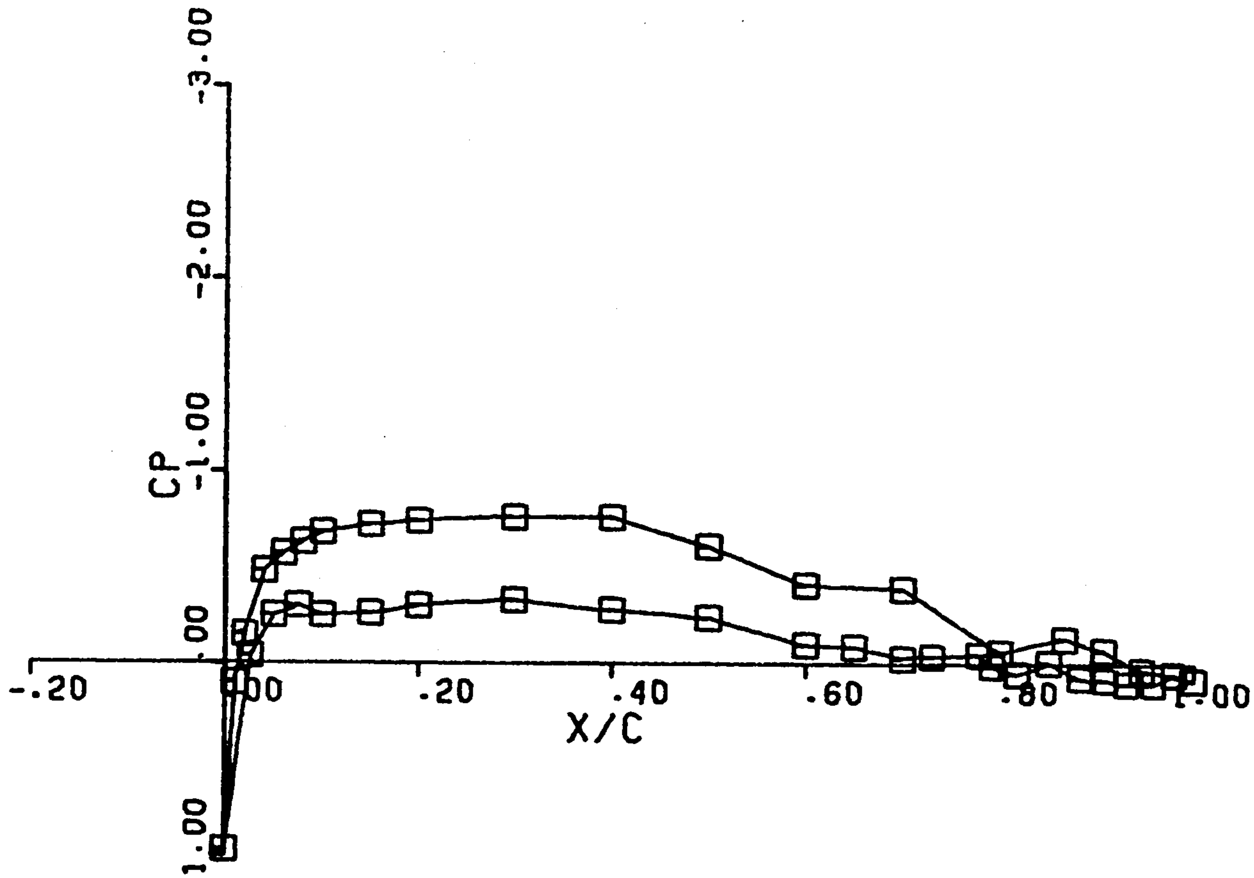

CLEAN RUN # 63

AOA = 1.60
FLAP DEF = 0.00
CL = 0.543
CM = -0.059
CD = 0.011

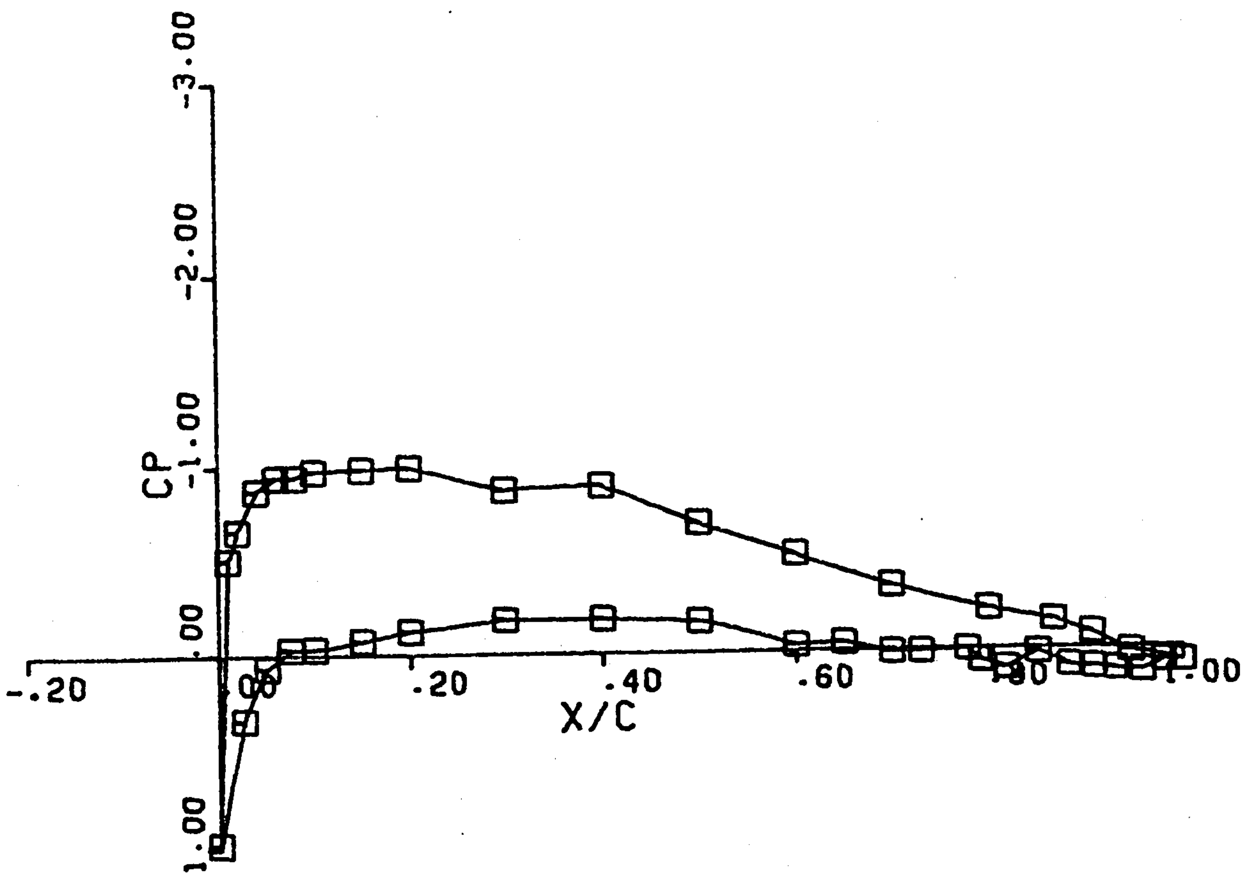

CLEAN RUN # 64

AØA = 3.60
FLAP **DEF** = 0.00
CL = 0.722
CM = -0.059
CD = 0.013

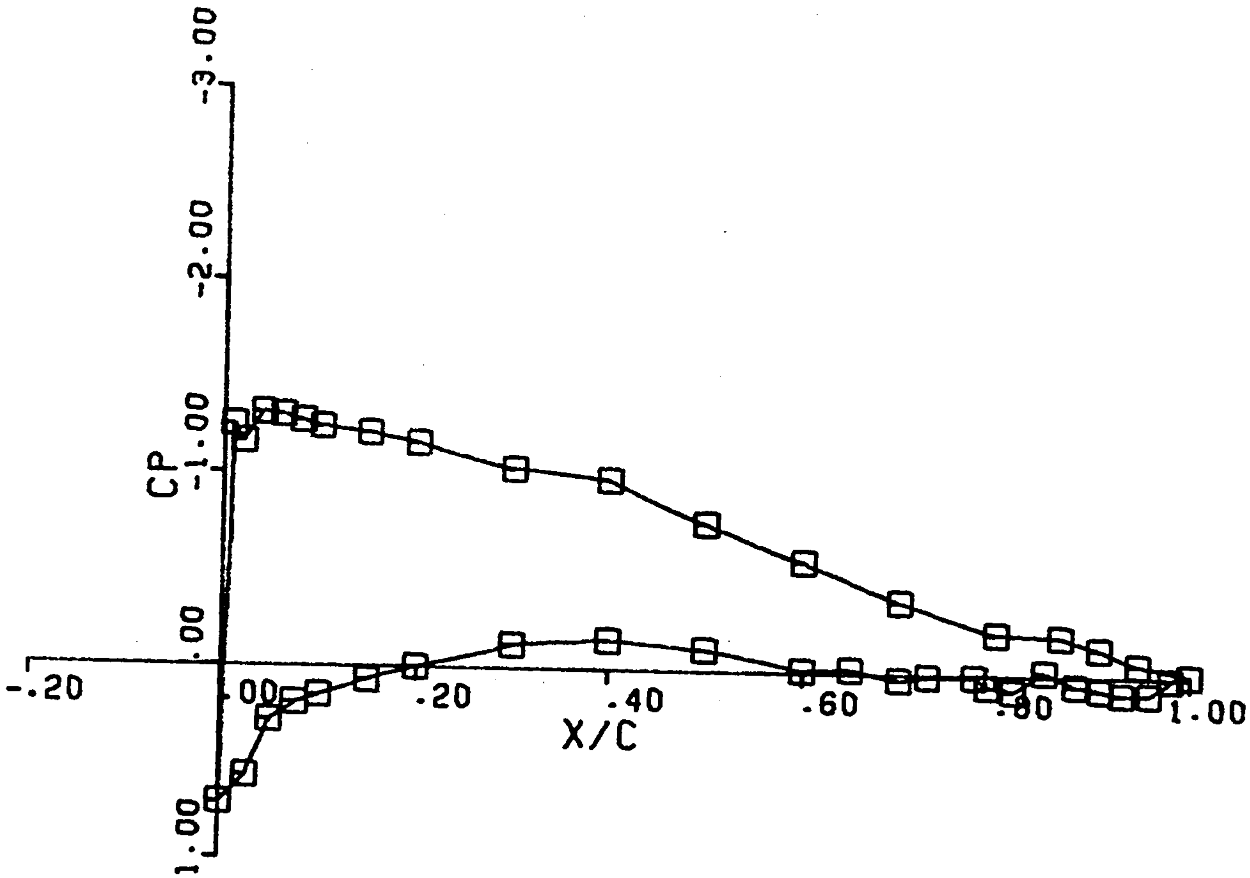

CLEAN RUN # 65

AOA = 5.60
FLAP DEF = 0.00
CL = 0.902
CM = -0.060
CD = 0.014

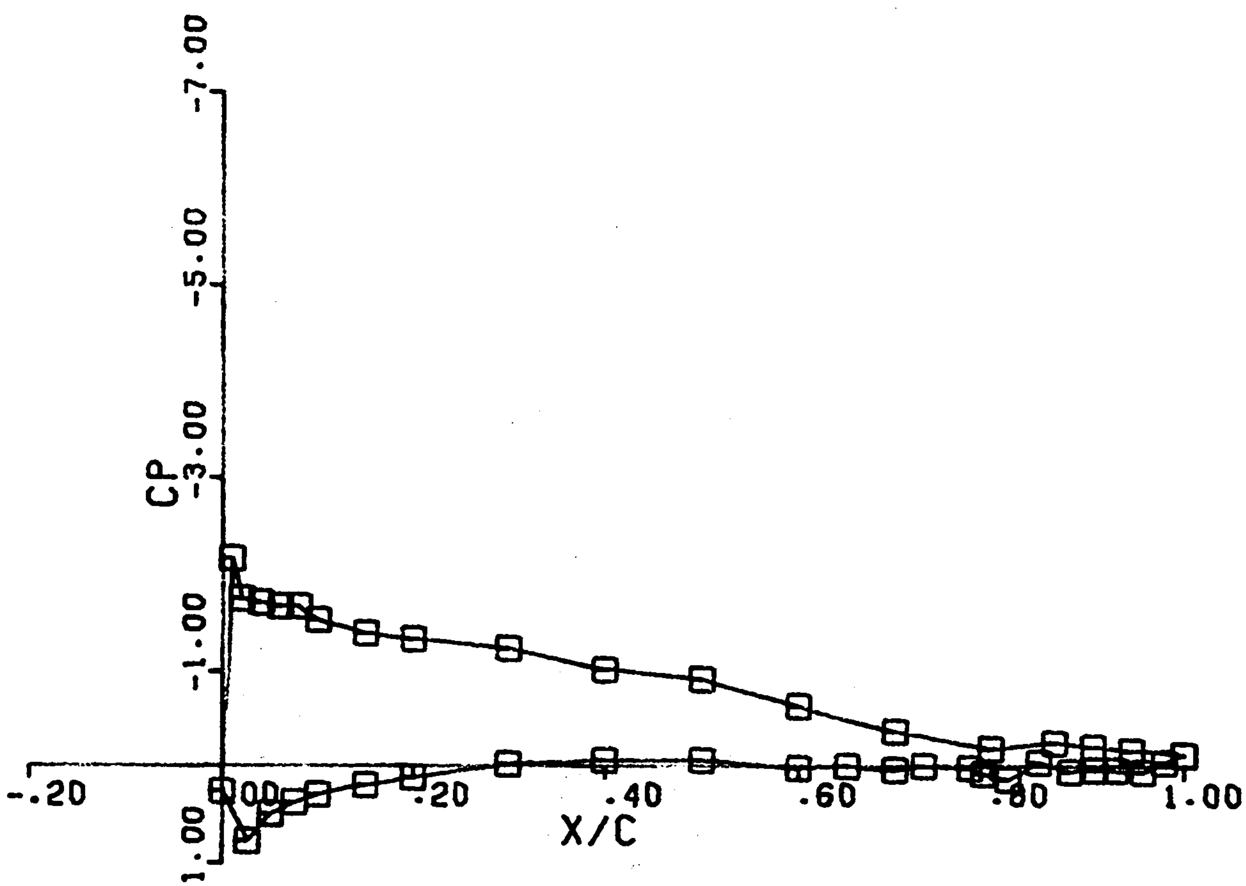

CLEAN RUN # 66

AOA = 7.60
FLAP DEF = 0.00
CL = 1.100
CM = -0.076
CD = 0.017

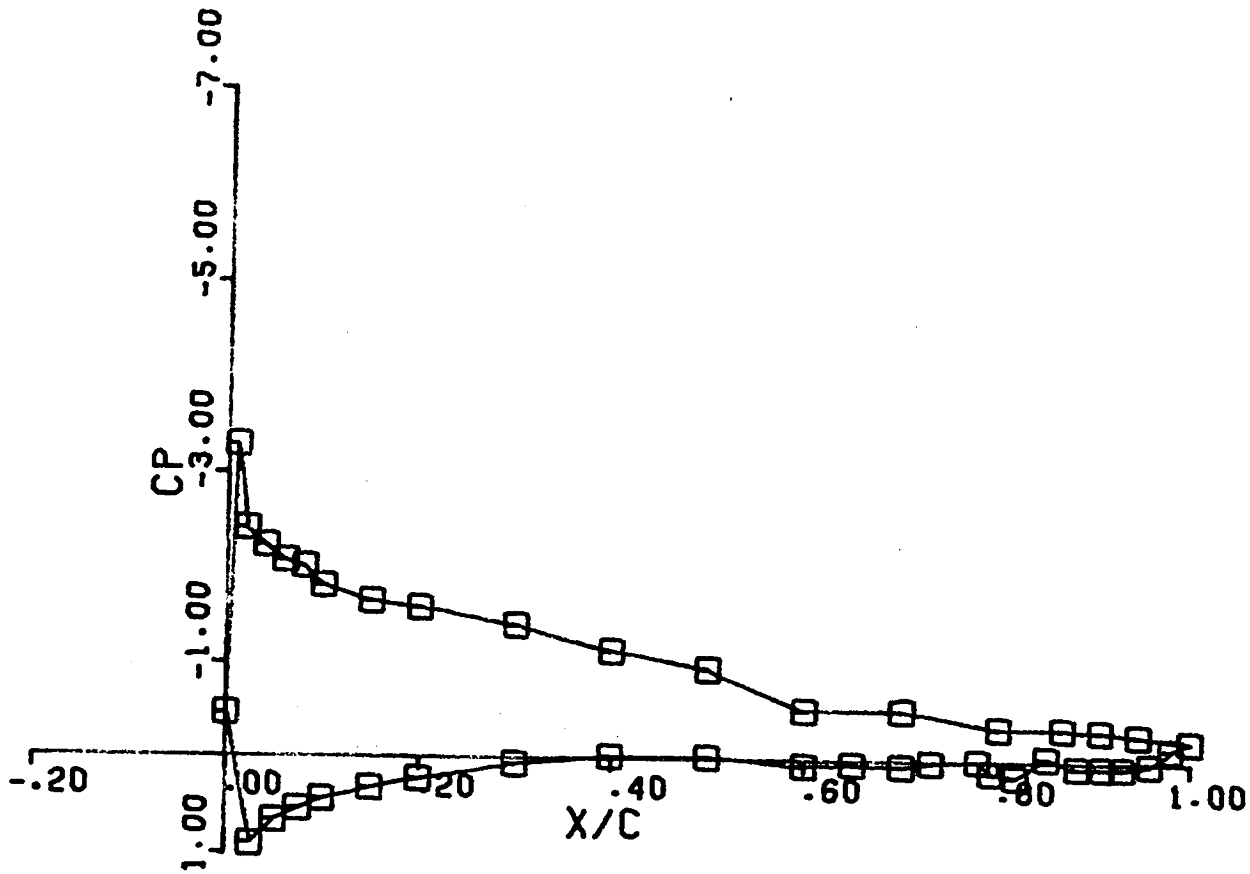

CLEAN RUN # 67

AOA = 8.60
FLAP DEF = 0.00
CL = 1.169
CM = -0.077
CD = 0.020

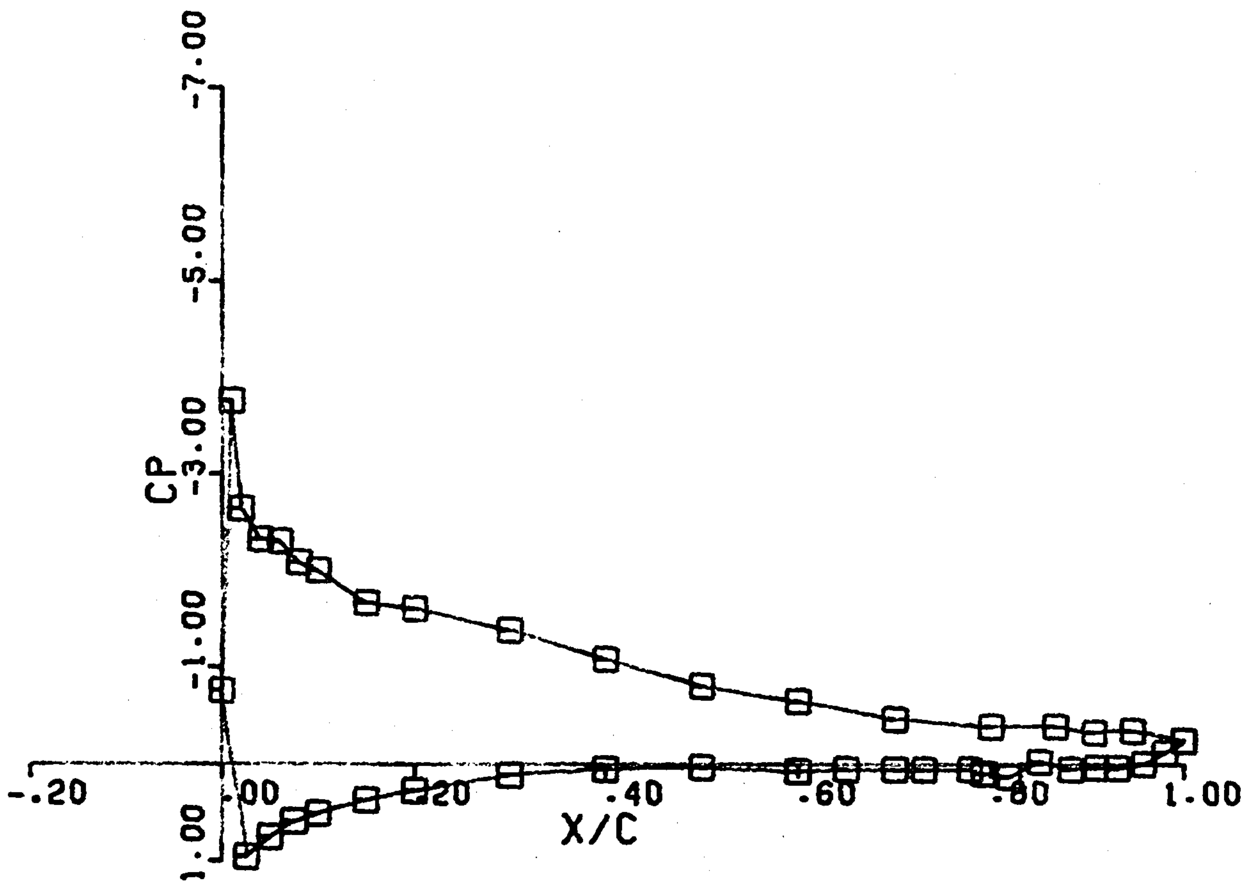

CLEAN RUN # 68

AOA = 9.60
FLAP DEF = 0.00
CL = 1.228
CM = -0.076
CD = 0.022

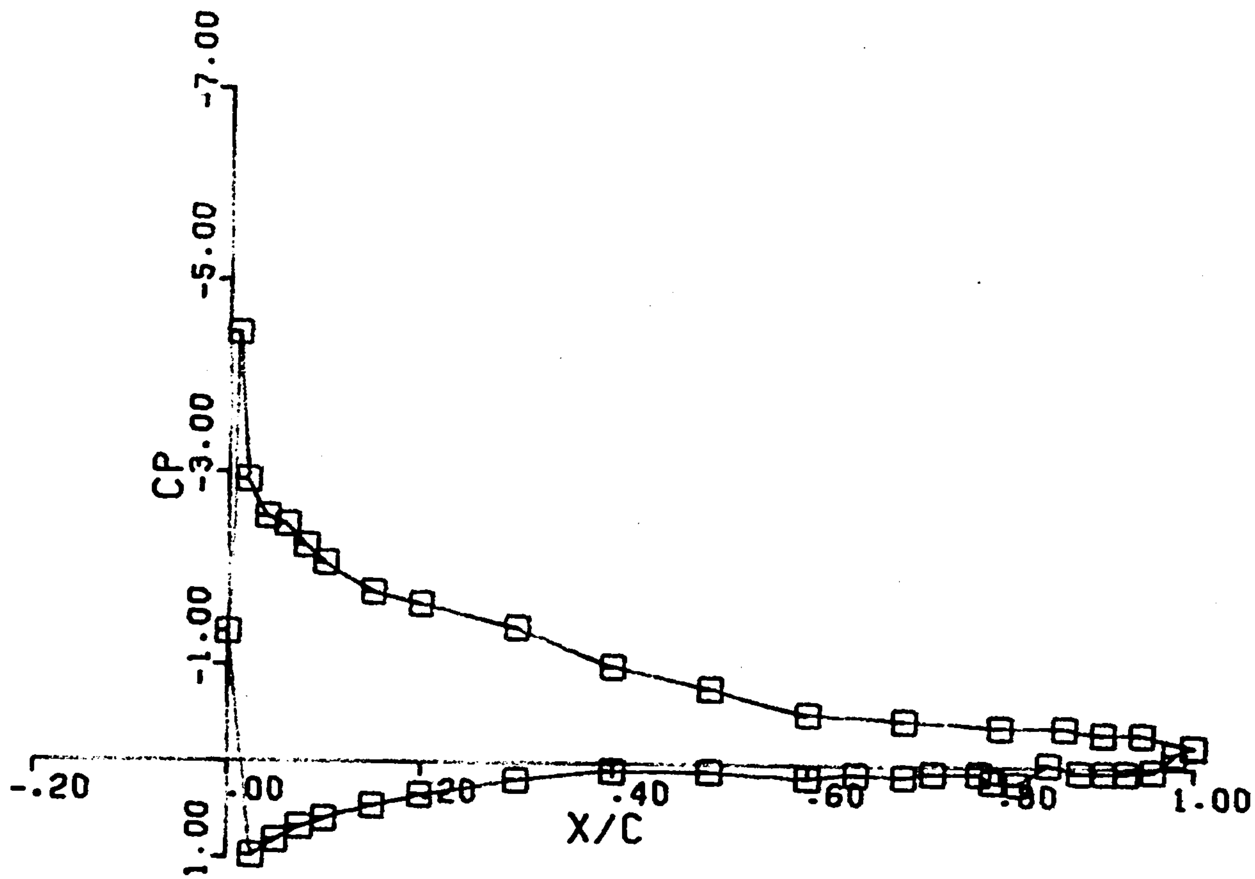

CLEAN RUN # 69

AOA = 10.60
FLAP **DEF** = 0.00
CL = 1.320
CM = -0.092
CD = 0.028

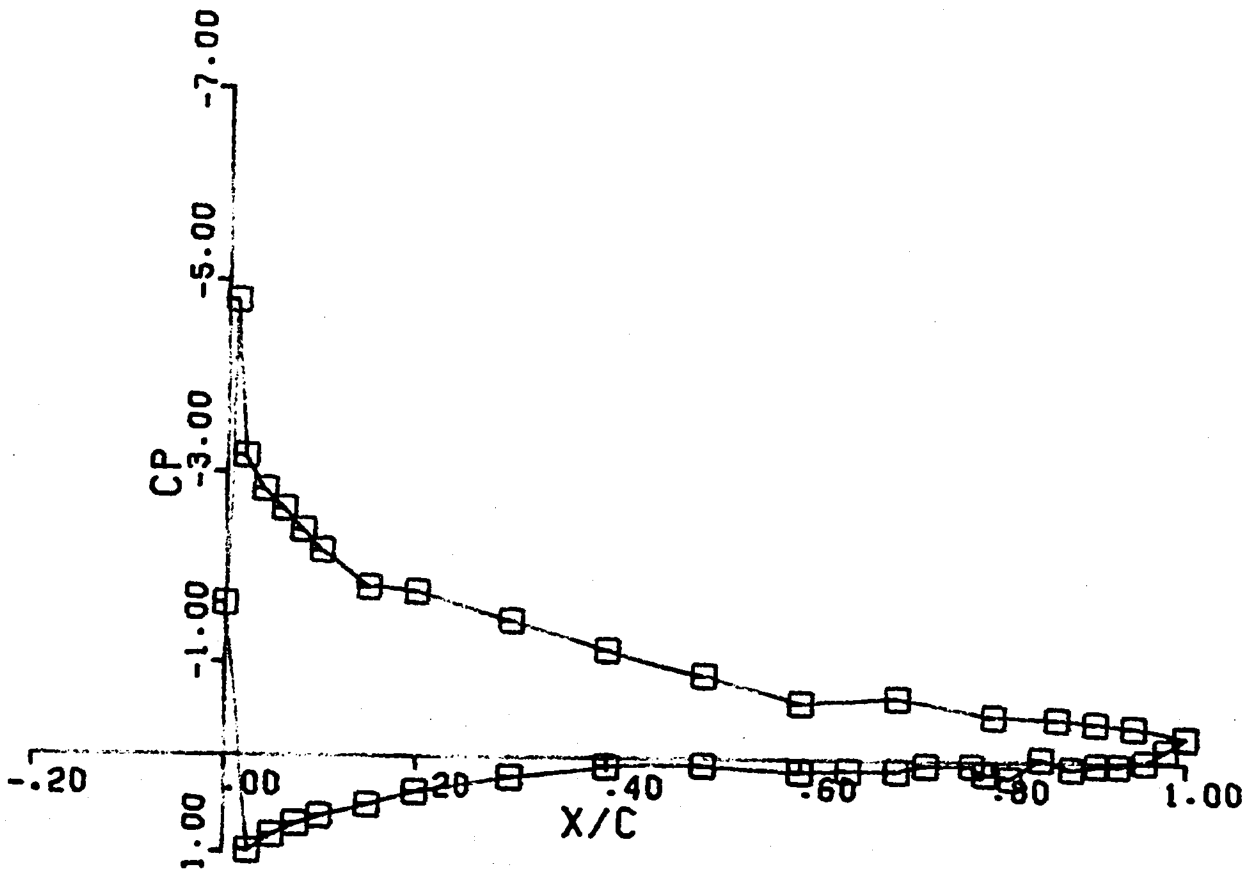

CLEAN RUN # 70

AOA = 11.60
FLAP DEF = 0.00
CL = 1.423
CM = -0.091
CD = 0.030

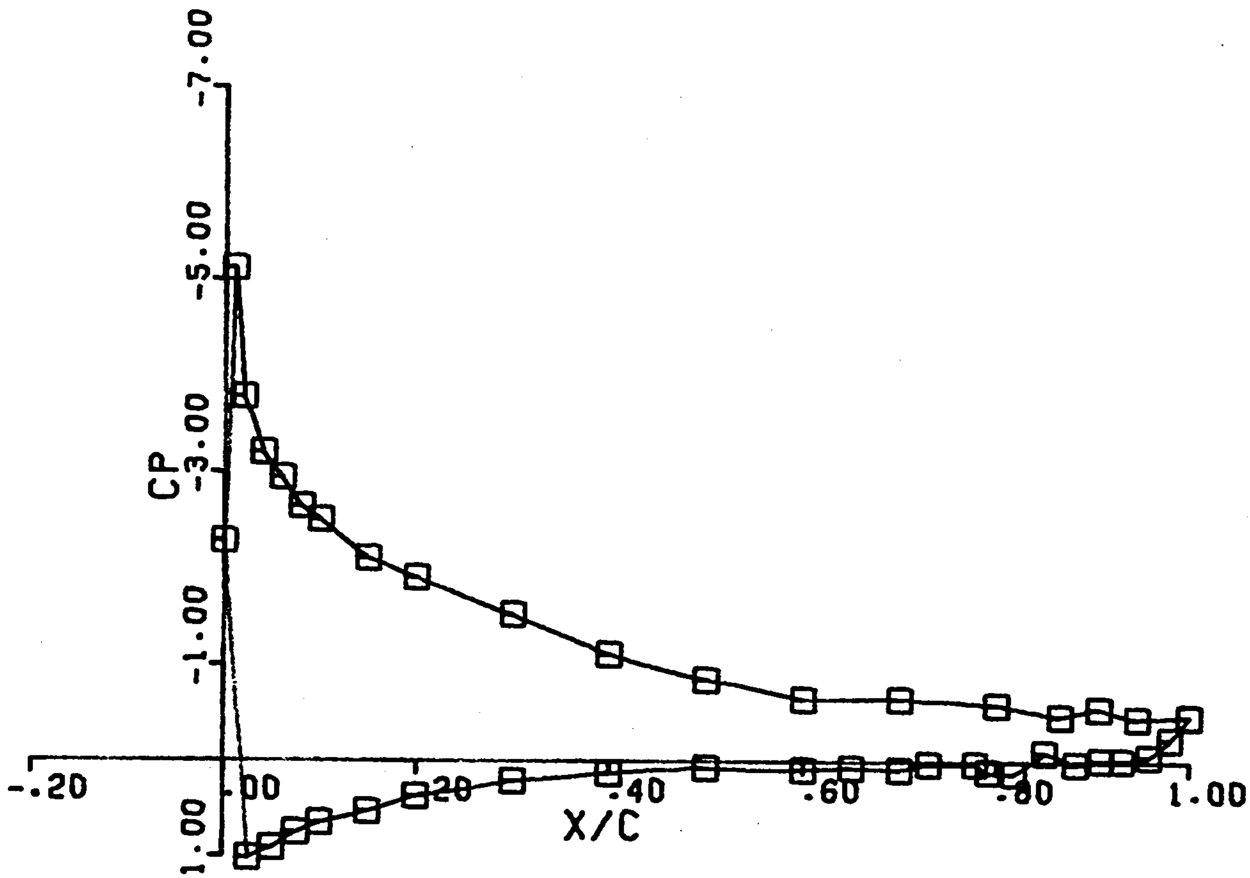

CLEAN RUN # 81

AØA = -2.40
FLAP DEF = 0.00
CL = 0.088
CM = -0.049
CD = 0.012

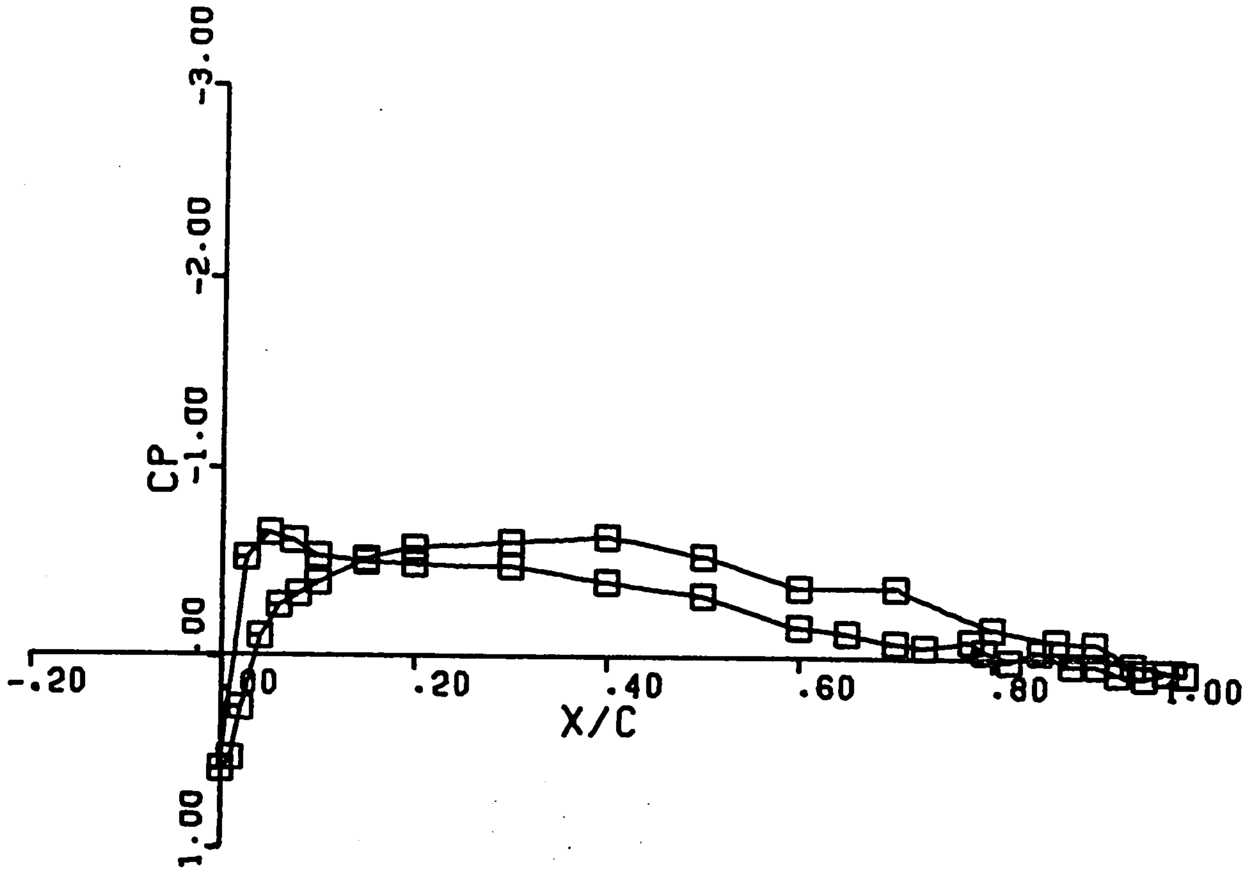

CLEAN RUN # 82

AOA = -0.40
FLAP DEF = 0.00
CL = 0.302
CM = -0.051
CD = 0.012

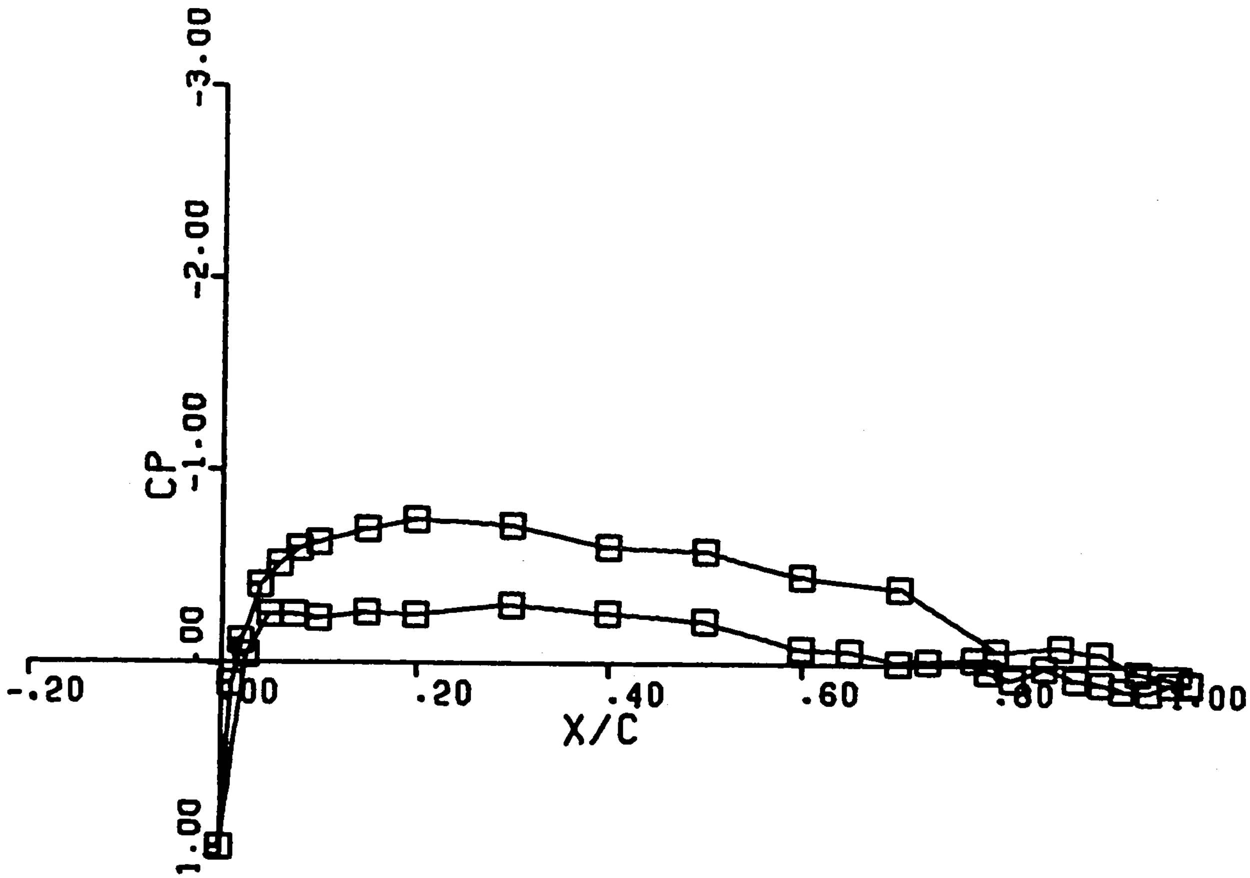

CLEAN RUN # 83

AOA = 1.60
FLAP DEF = 0.00
CL = 0.506
CM = -0.057
CD = 0.013

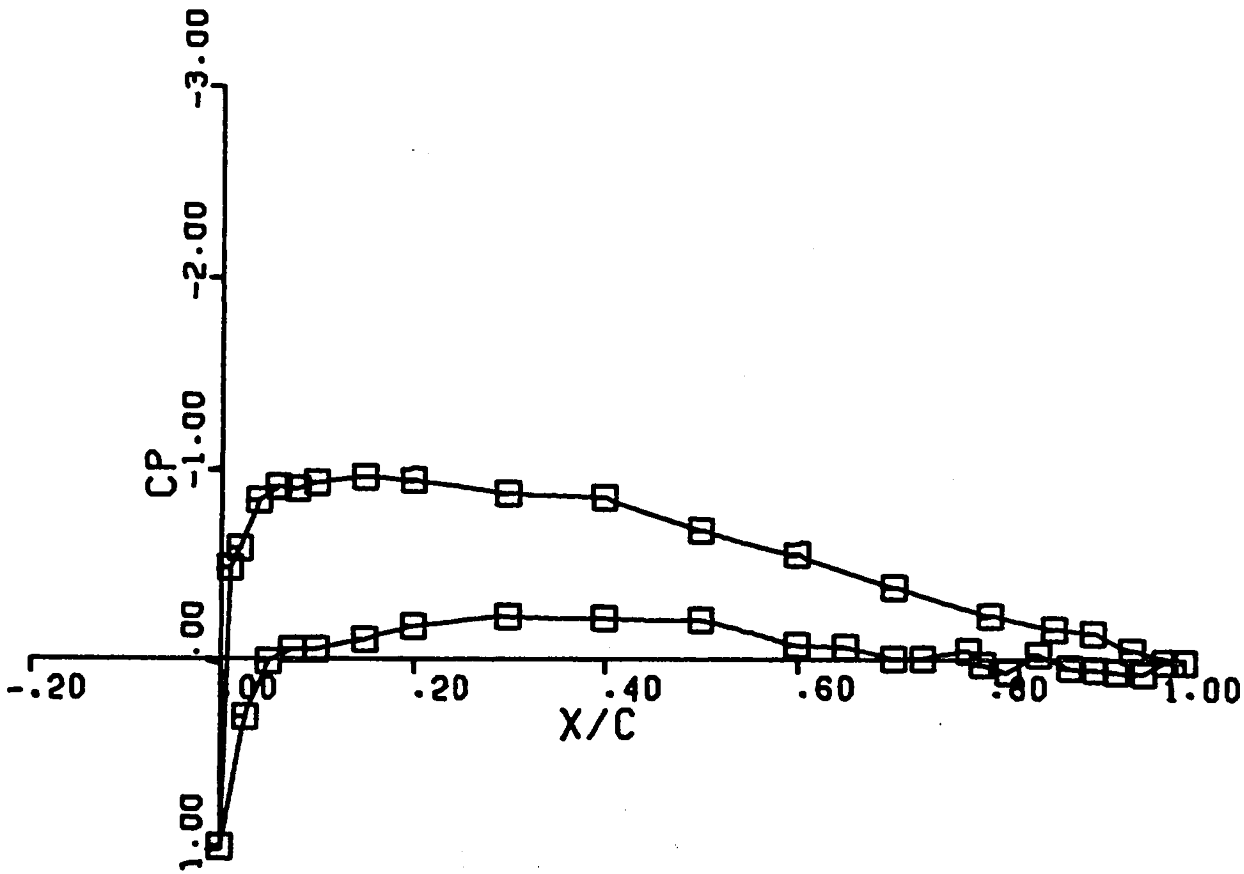

CLEAN RUN # 84

AOA = -6.40
FLAP DEF = 10.00
CL = -0.010
CM = -0.118
CD = ------

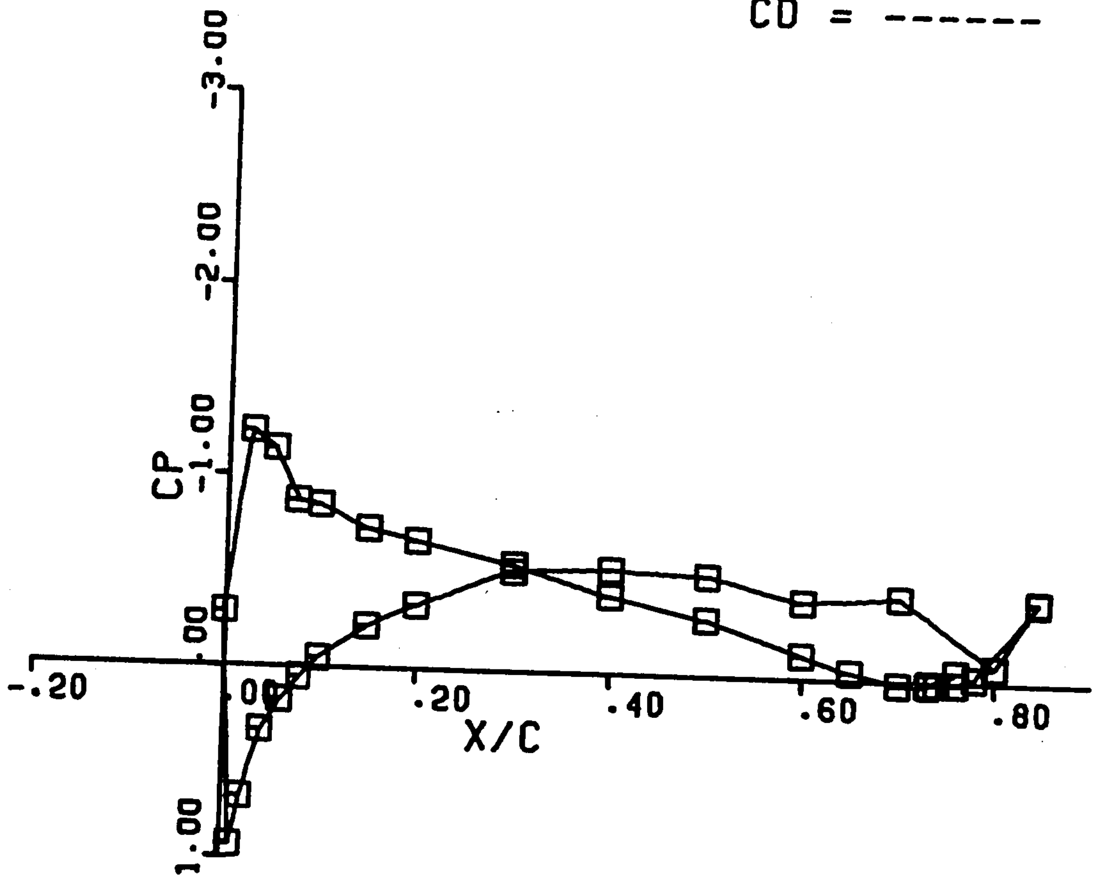

MAIN ELEMENT
CL = -0.092
CM = -0.066

FLAP
CL = 0.082
CM = -0.052

CLEAN RUN # 85

AØA = -2.40
FLAP DEF = 10.00
CL = 0.435
CM = -0.129
CD = ------

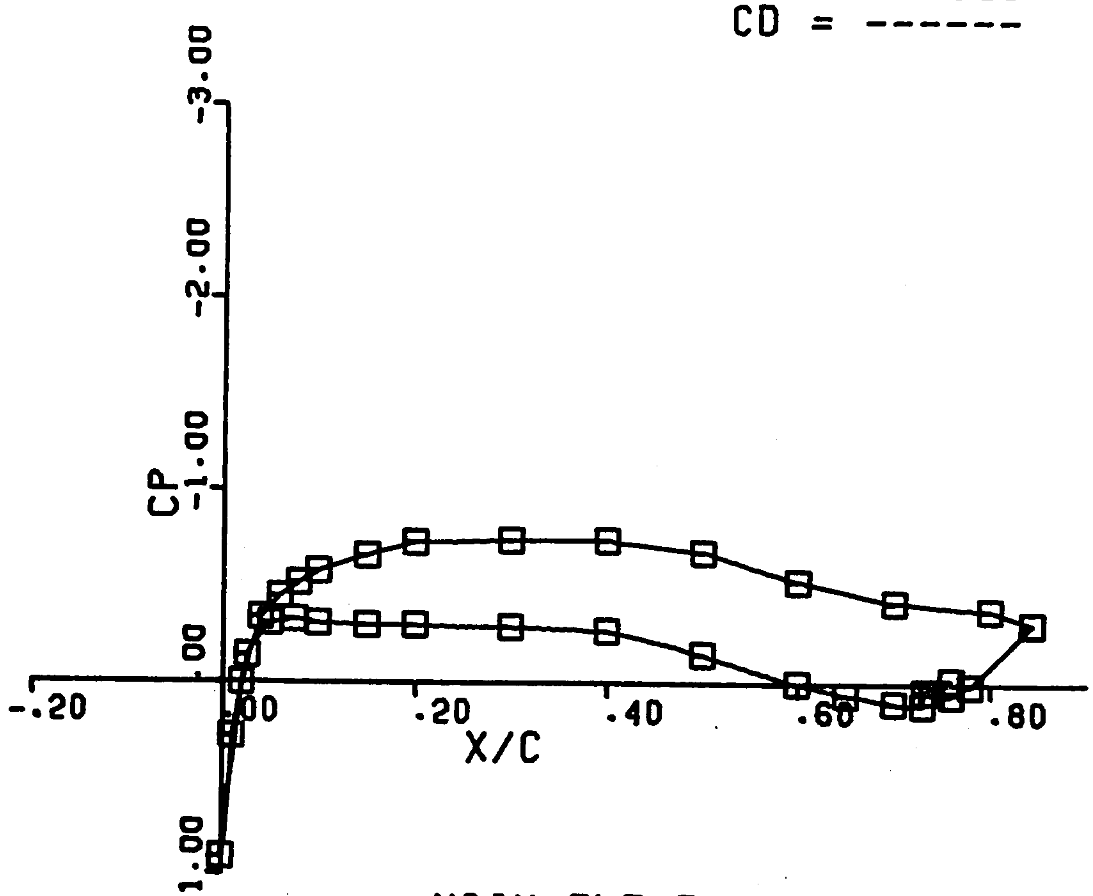

MAIN ELEMENT

CL = 0.346

CM = -0.072

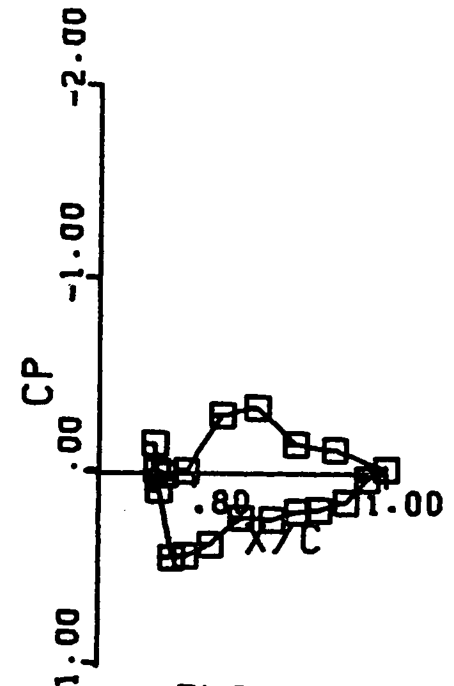

FLAP

CL = 0.090

CM = -0.057

CLEAN RUN # 86

AOA = -0.40
FLAP DEF = 10.00
CL = 0.669
CM = -0.132
CD = ------

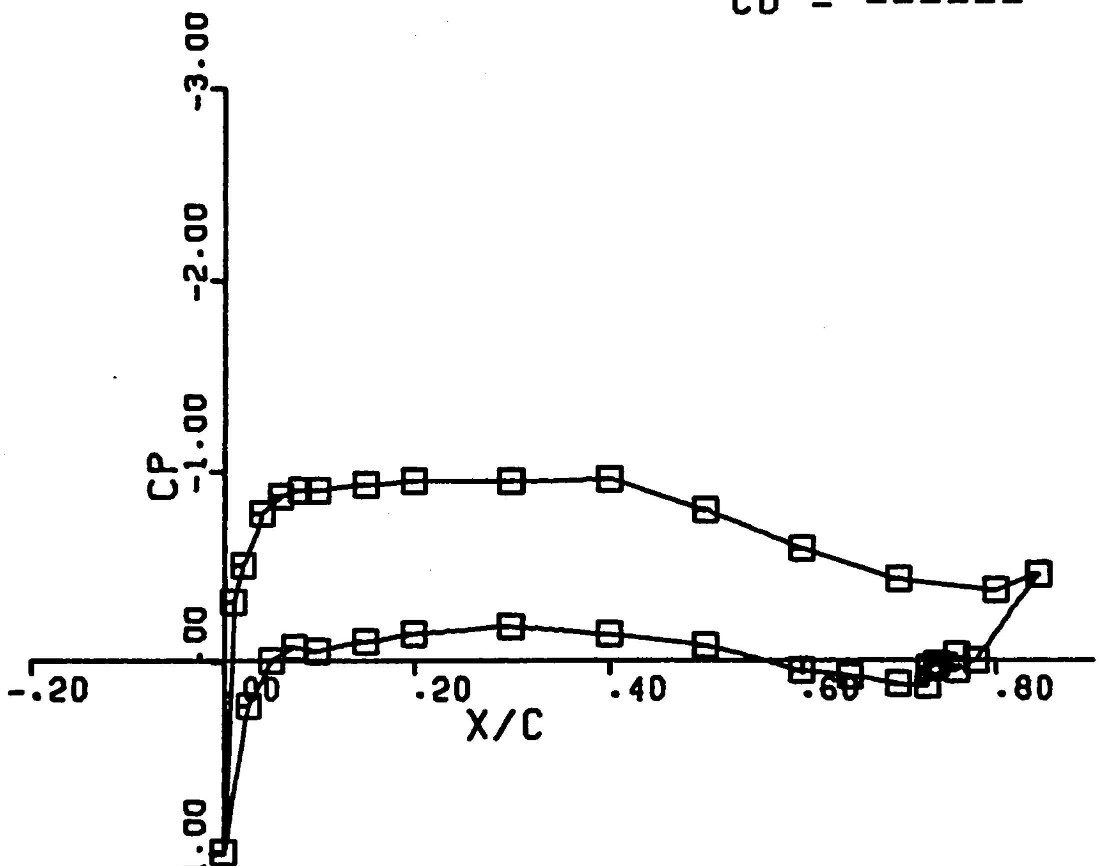

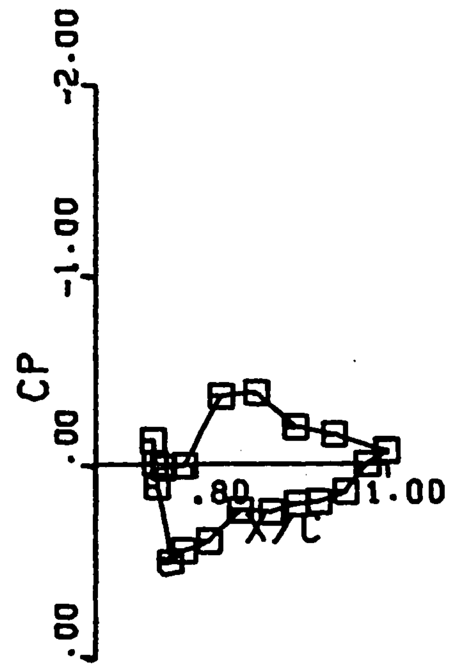

MAIN ELEMENT
CL = 0.572
CM = -0.070

FLAP
CL = 0.098
CM = -0.063

CLEAN RUN # 87

AOA = 1.60
FLAP DEF = 10.00
CL = 0.908
CM = -0.143
CD = ------

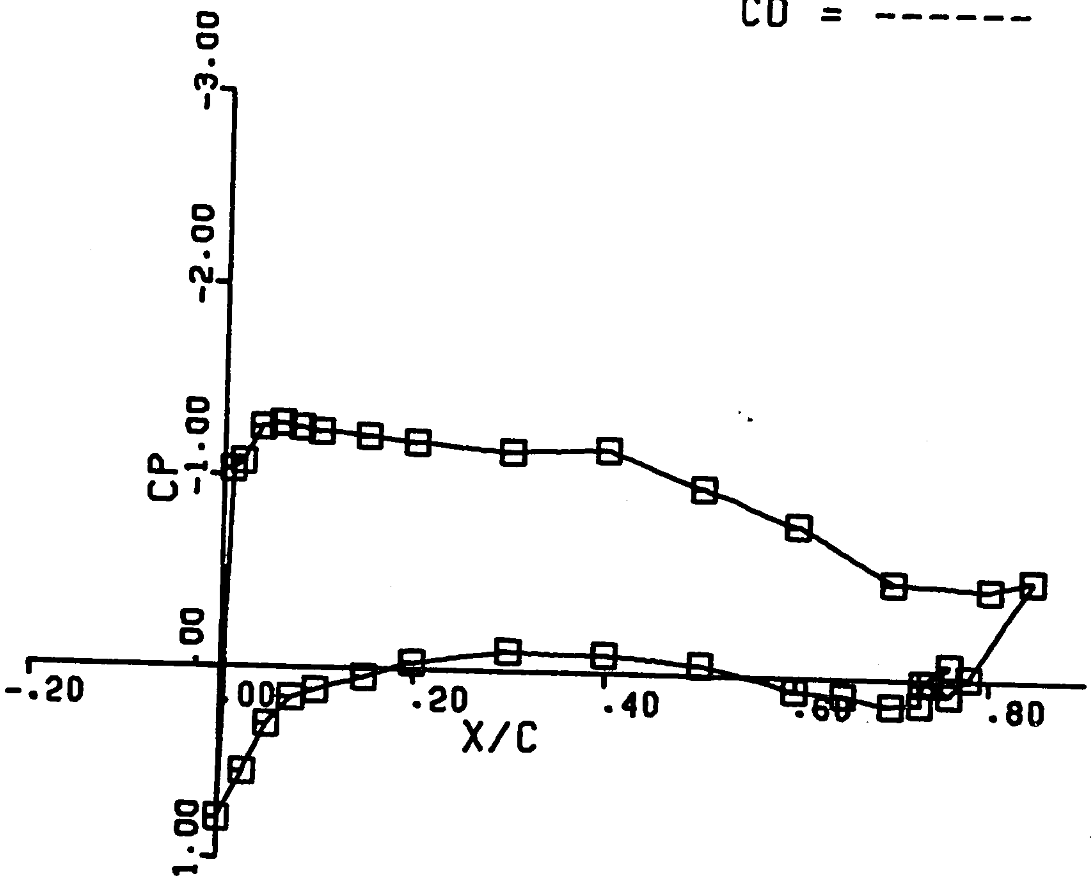

MAIN ELEMENT
CL = 0.805
CM = -0.076

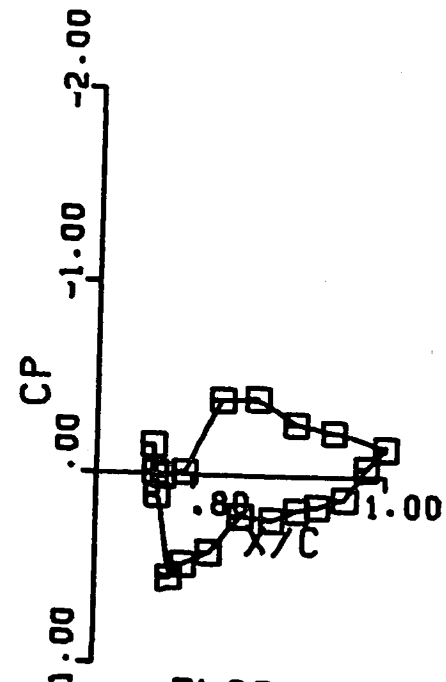

FLAP
CL = 0.102
CM = -0.066

80

CLEAN RUN # 88

AØA = 3.60
FLAP DEF = 10.00
CL = 1.106
CM = -0.142
CD = ------

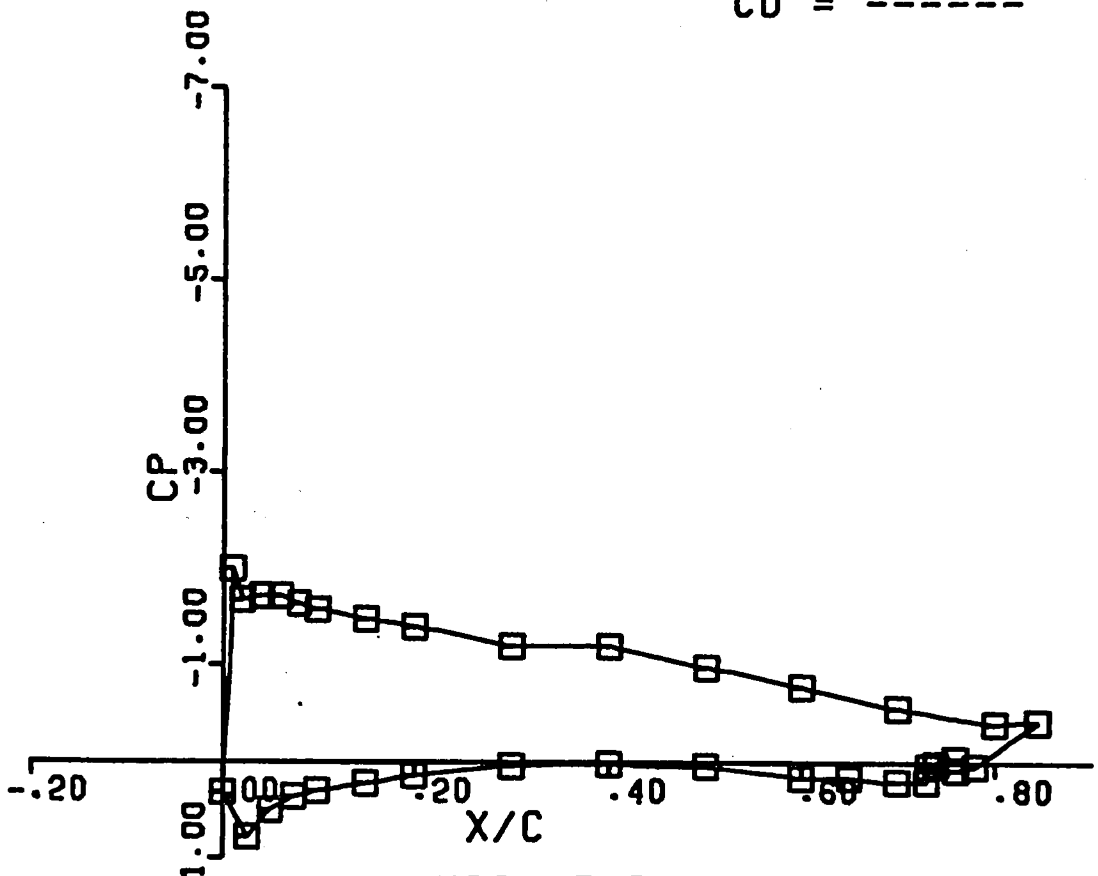

MAIN ELEMENT
CL = 1.002
CM = -0.075

FLAP
CL = 0.103
CM = -0.068

CLEAN RUN # 89

AOA = 5.60
FLAP DEF = 10.00
CL = 1.220
CM = -0.133
CD = -------

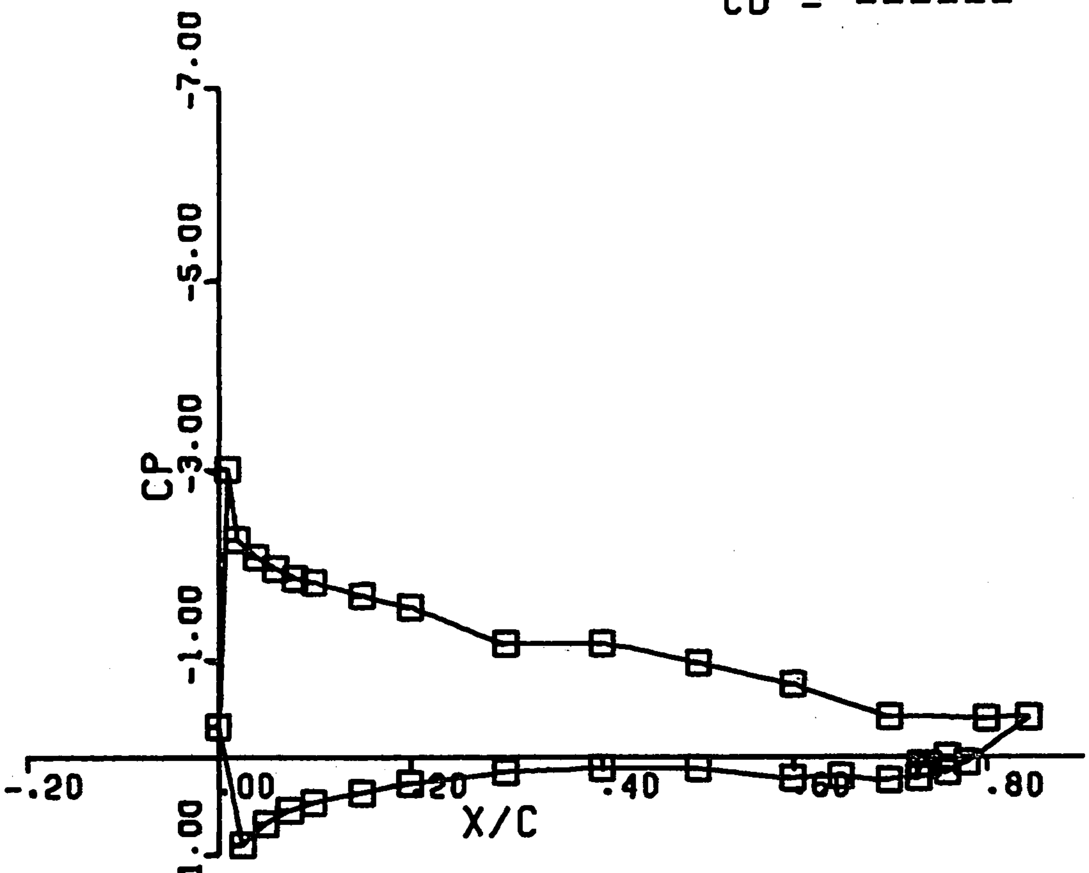

MAIN ELEMENT
CL = 1.111
CM = -0.061

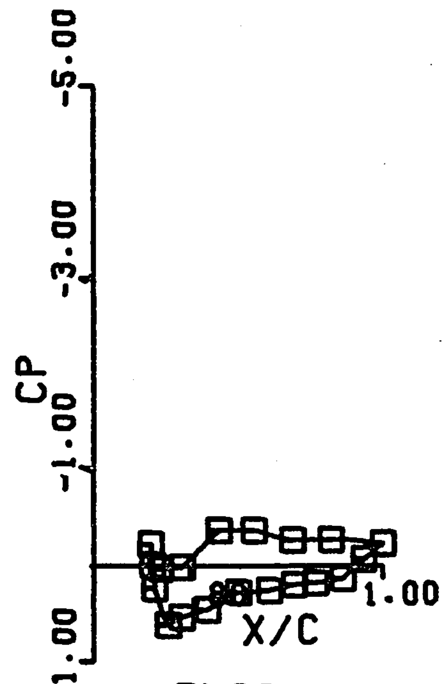

FLAP
CL = 0.109
CM = -0.072

CLEAN RUN # 90

AOA = 7.60
FLAP DEF = 10.00
CL = 1.354
CM = -0.136
CD = ------

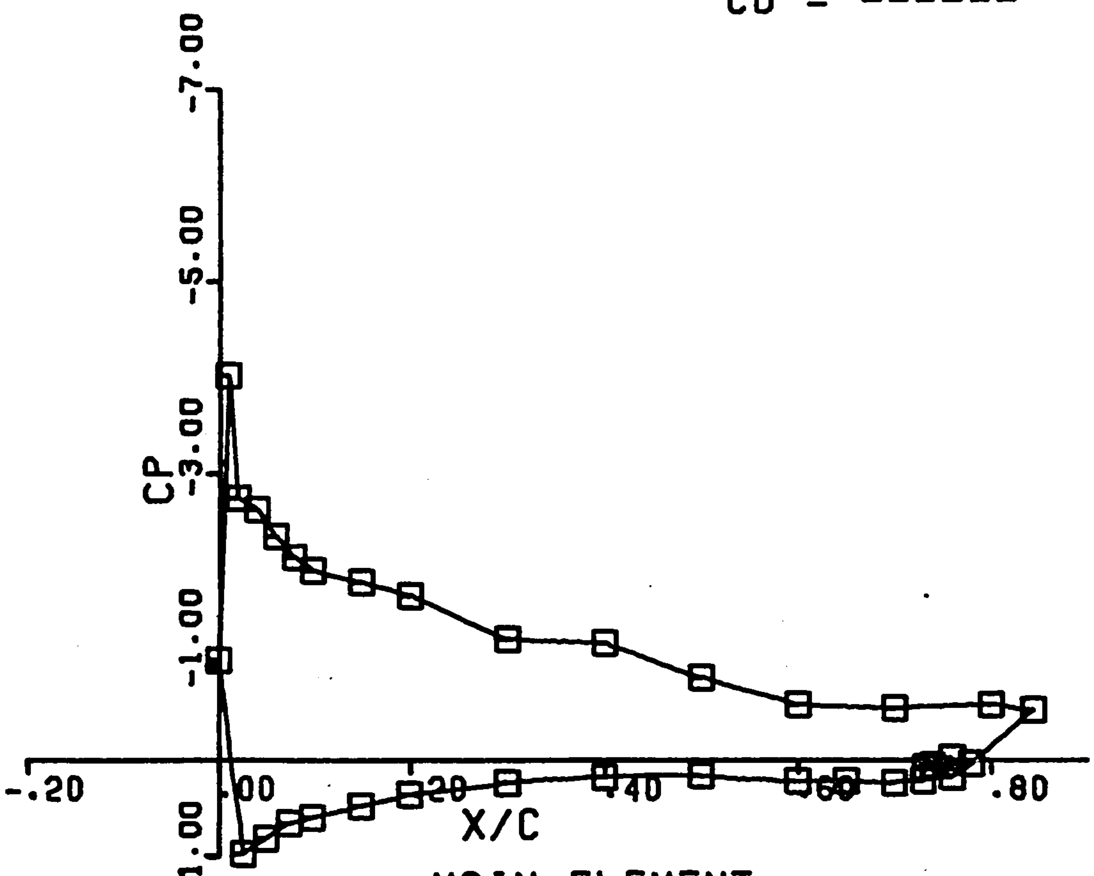

MAIN ELEMENT
CL = 1.241
CM = -0.060

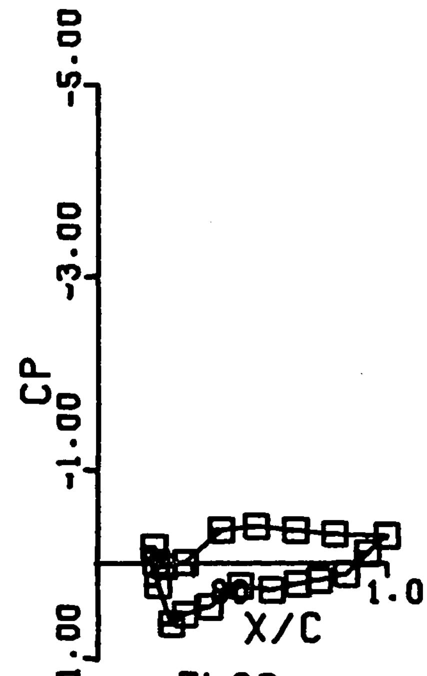

FLAP
CL = 0.113
CM = -0.077

CLEAN RUN * 91

AØA = 9.60
FLAP DEF = 10.00
CL = 1.526
CM = -0.153
CD = ------

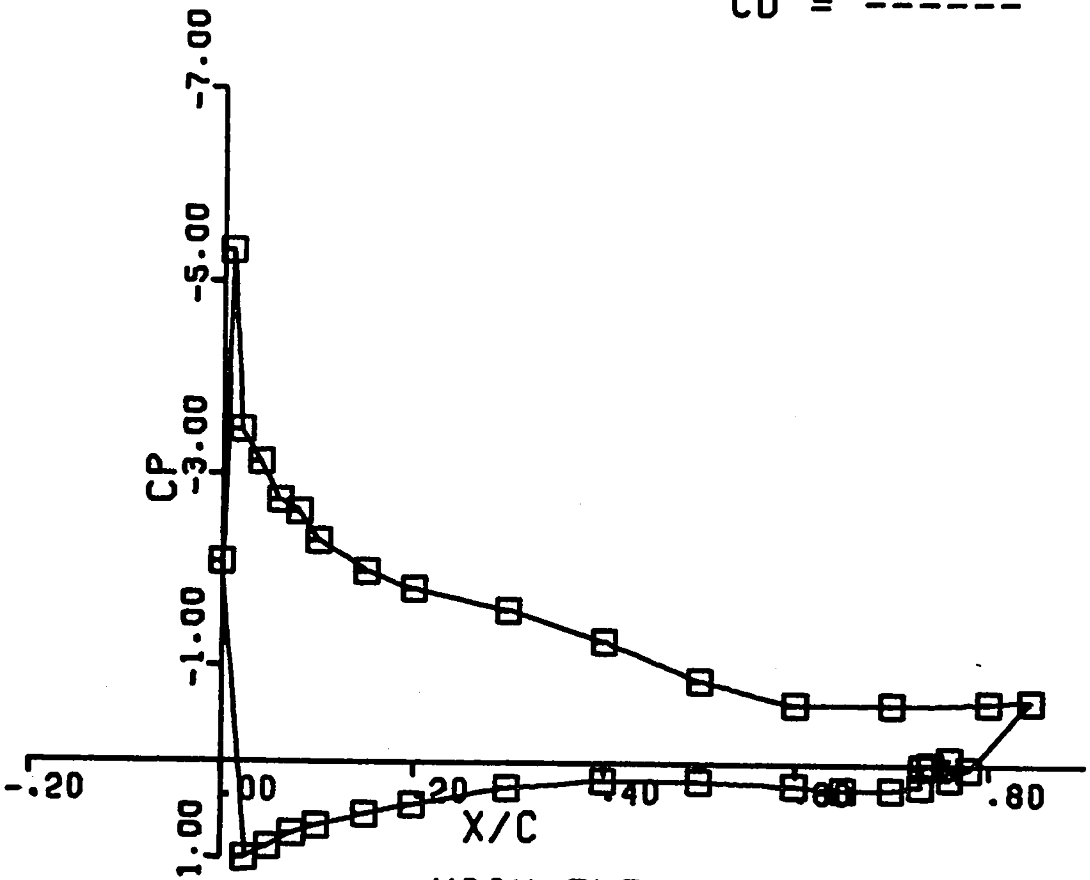

MAIN ELEMENT
CL = 1.387
CM = -0.057

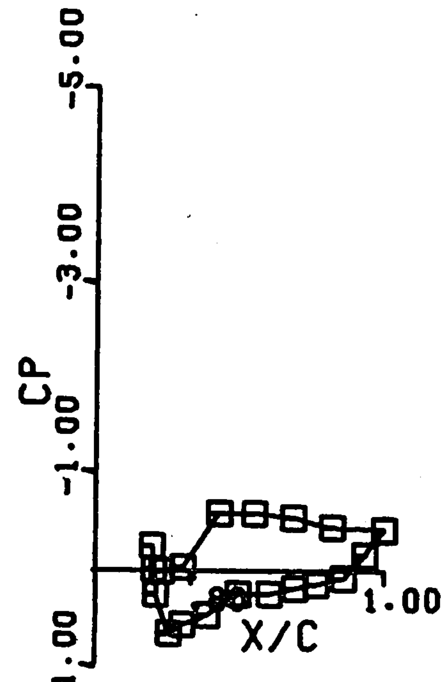

FLAP
CL = 0.138
CM = -0.096

CLEAN RUN # 92

AOA = 11.60
FLAP DEF = 10.00
CL = 1.730
CM = -0.178
CD = ------

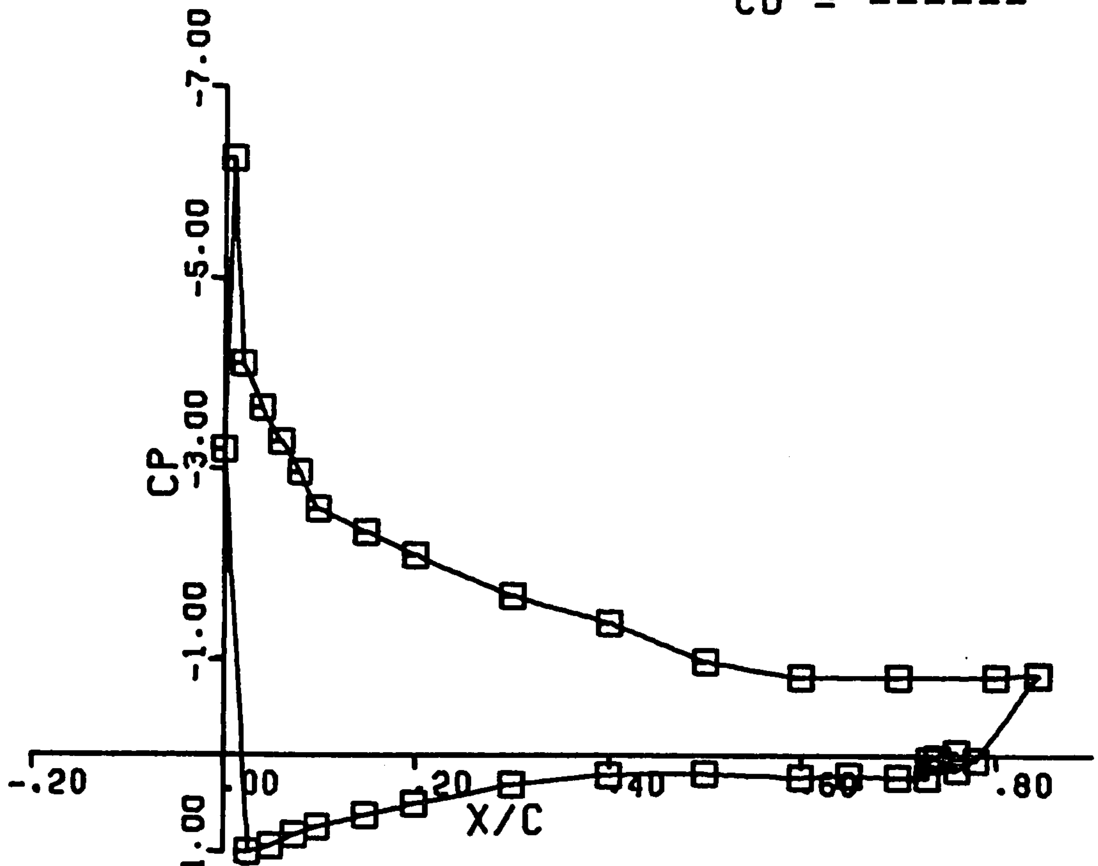

MAIN ELEMENT
CL = 1.578
CM = -0.071

FLAP
CL = 0.152
CM = -0.107

CLEAN RUN # 93

AØA = 12.60
FLAP DEF = 10.00
CL = 1.715
CM = -0.178
CD = ------

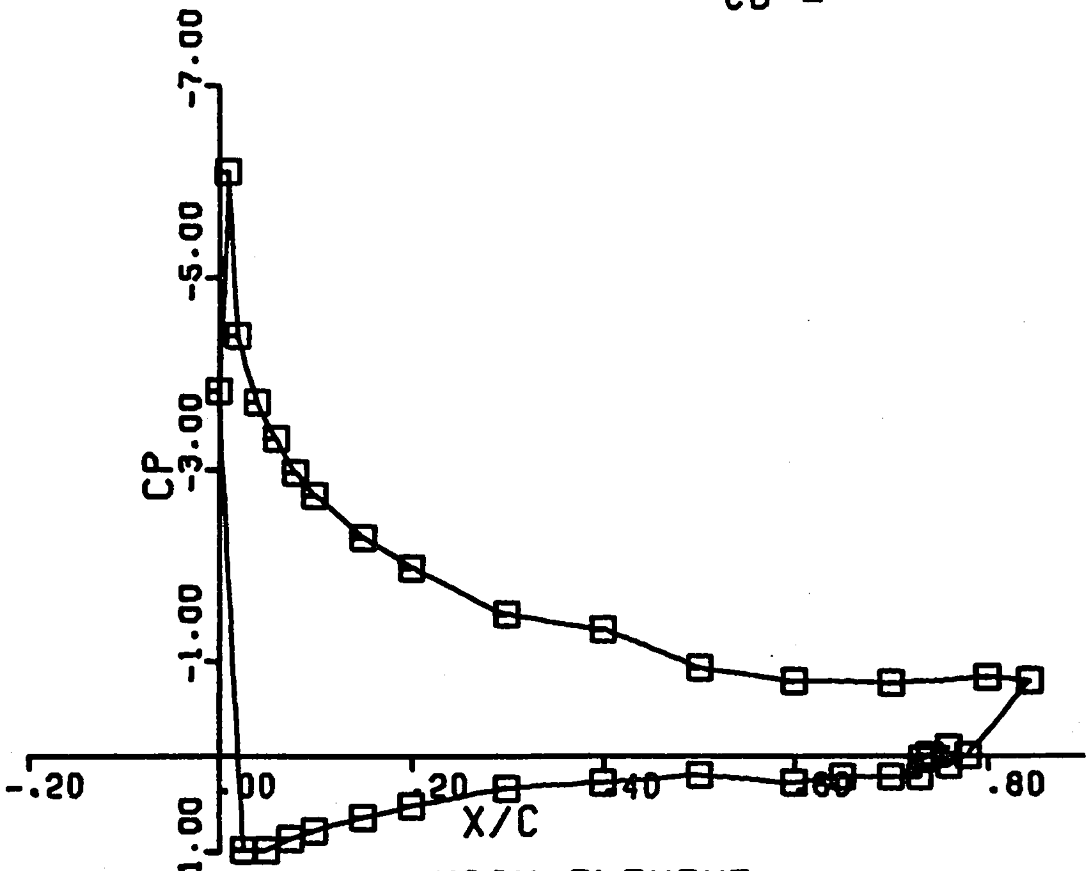

MAIN ELEMENT
CL = 1.557
CM = -0.065

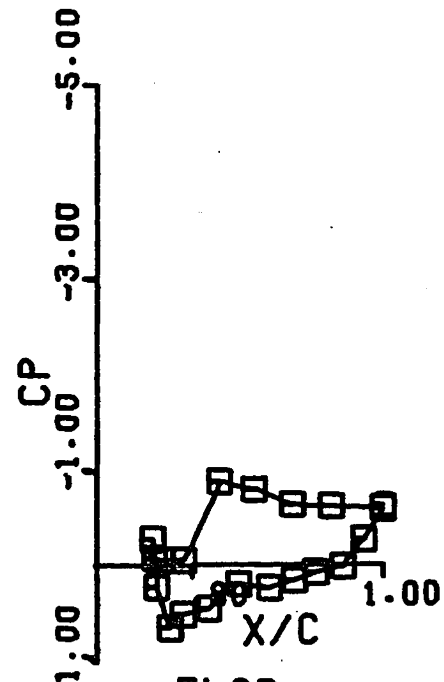

FLAP
CL = 0.158
CM = -0.113

CLEAN RUN # 94

AOA = 13.60
FLAP DEF = 10.00
CL = 1.823
CM = -0.196
CD = ------

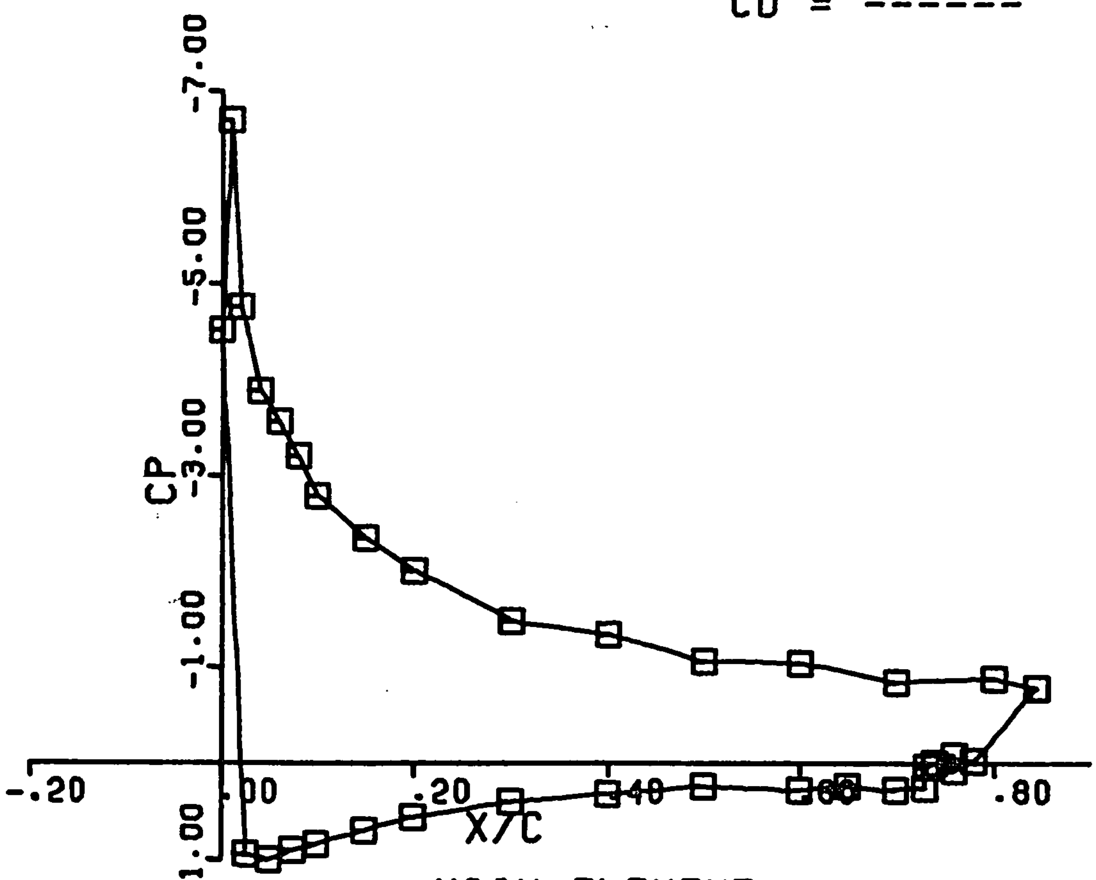

MAIN ELEMENT
CL = 1.666
CM = -0.082

FLAP
CL = 0.157
CM = -0.114

CLEAN RUN # 95

AØA = -6.40
FLAP DEF = 20.00
CL = 0.426
CM = -0.219
CD = ------

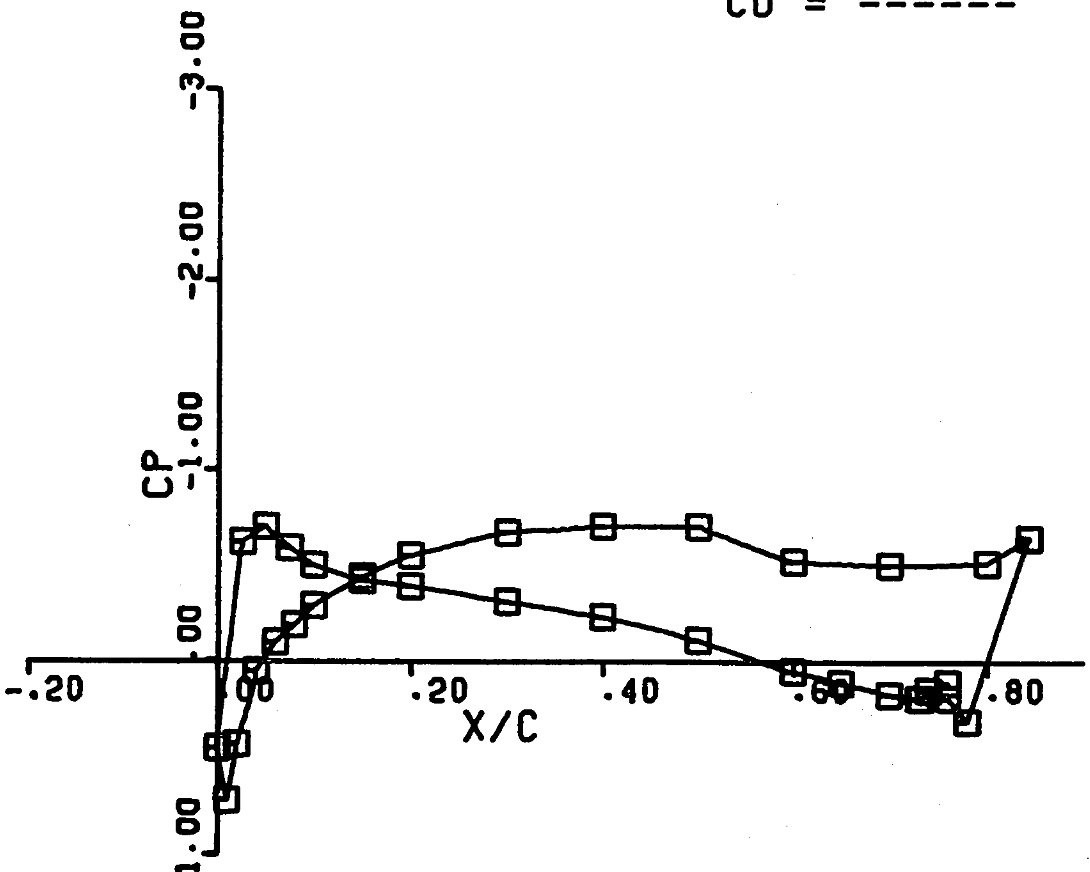

MAIN ELEMENT
CL = 0.263
CM = -0.109

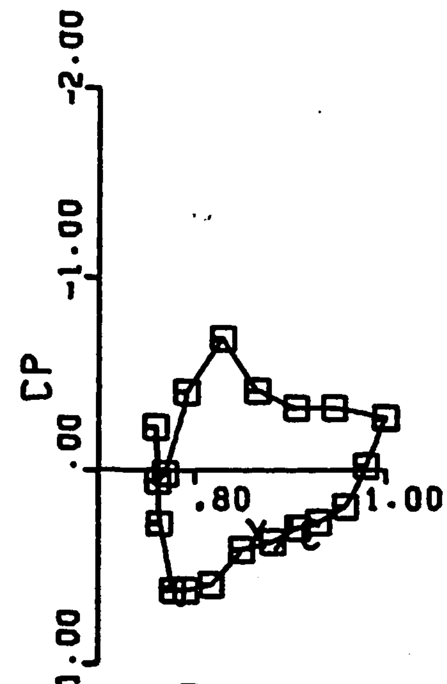

FLAP
CL = 0.163
CM = -0.110

CLEAN RUN # 96

AOA = -2.40
FLAP DEF = 20.00
CL = 0.894
CM = -0.231
CD = ------

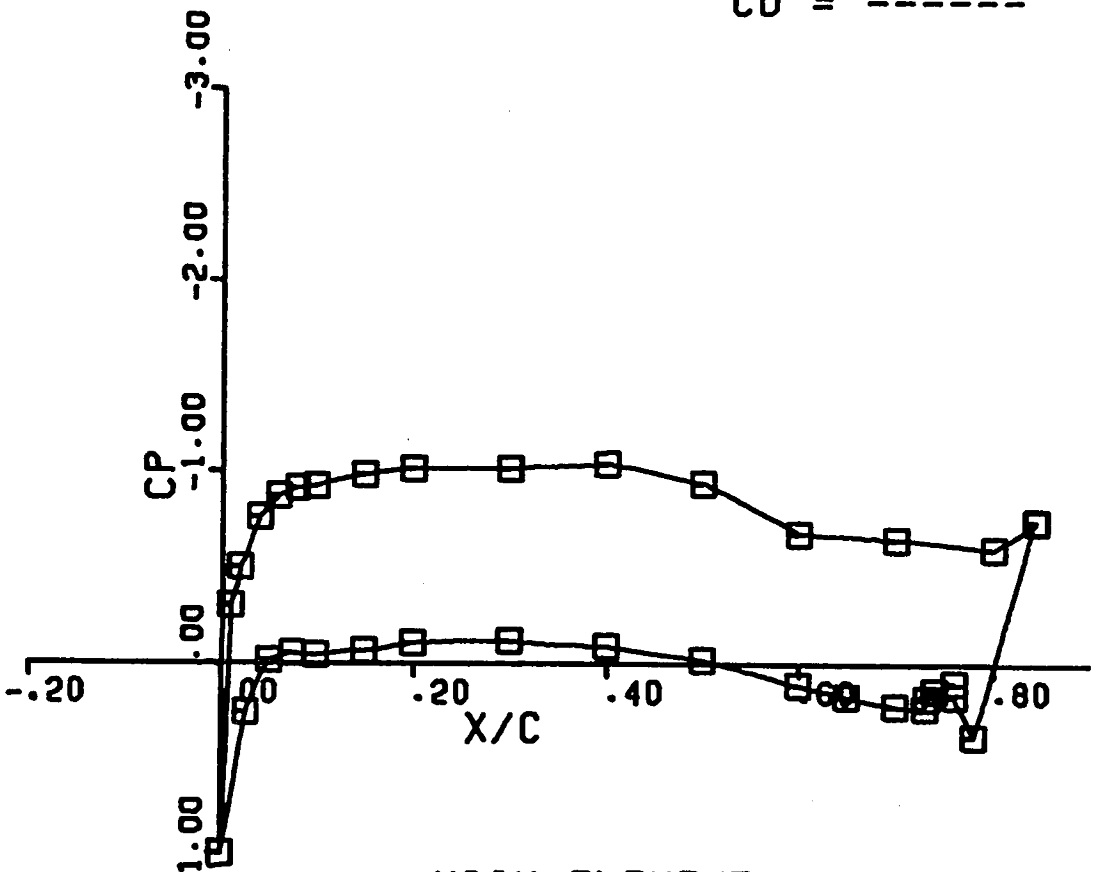

MAIN ELEMENT
CL = 0.724
CM = -0.115

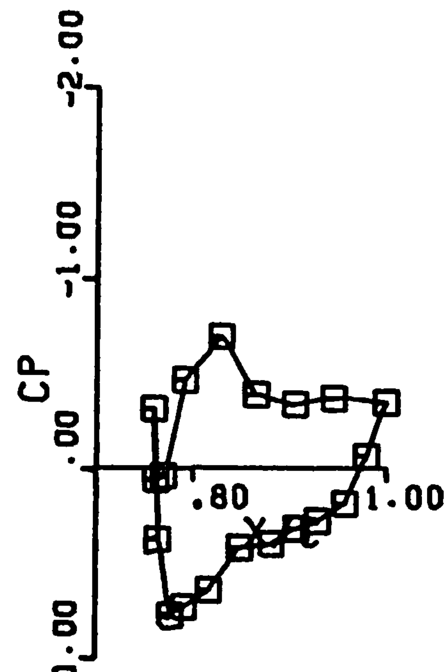

FLAP
CL = 0.169
CM = -0.117

CLEAN RUN # 98

AOA = 9.60
FLAP DEF = 20.00
CL = 1.871
CM = -0.255
CD = ------

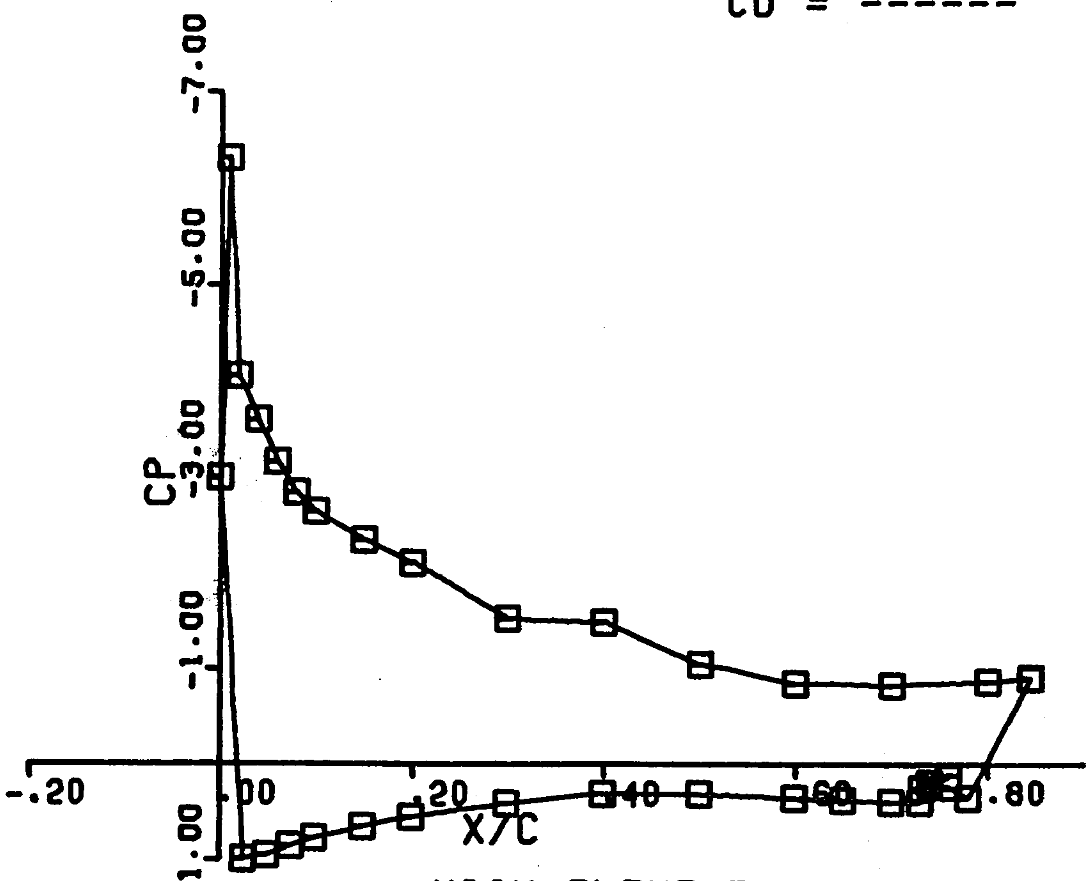

MAIN ELEMENT
CL = 1.668
CM = -0.100

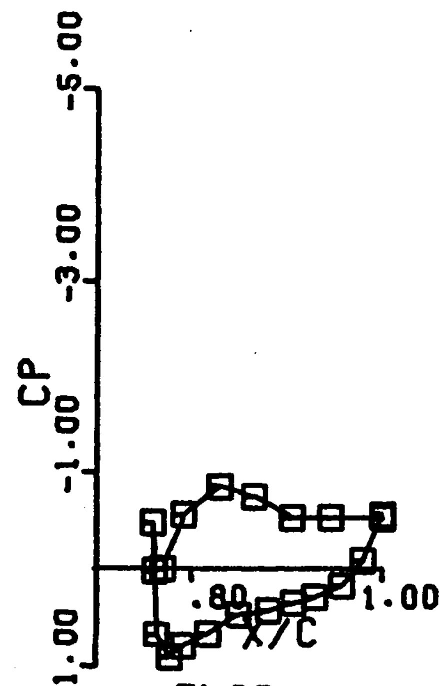

FLAP
CL = 0.203
CM = -0.155

CLEAN RUN # 99

AOA = 3.60
FLAP DEF = 20.00
CL = 1.463
CM = -0.231
CD = ------

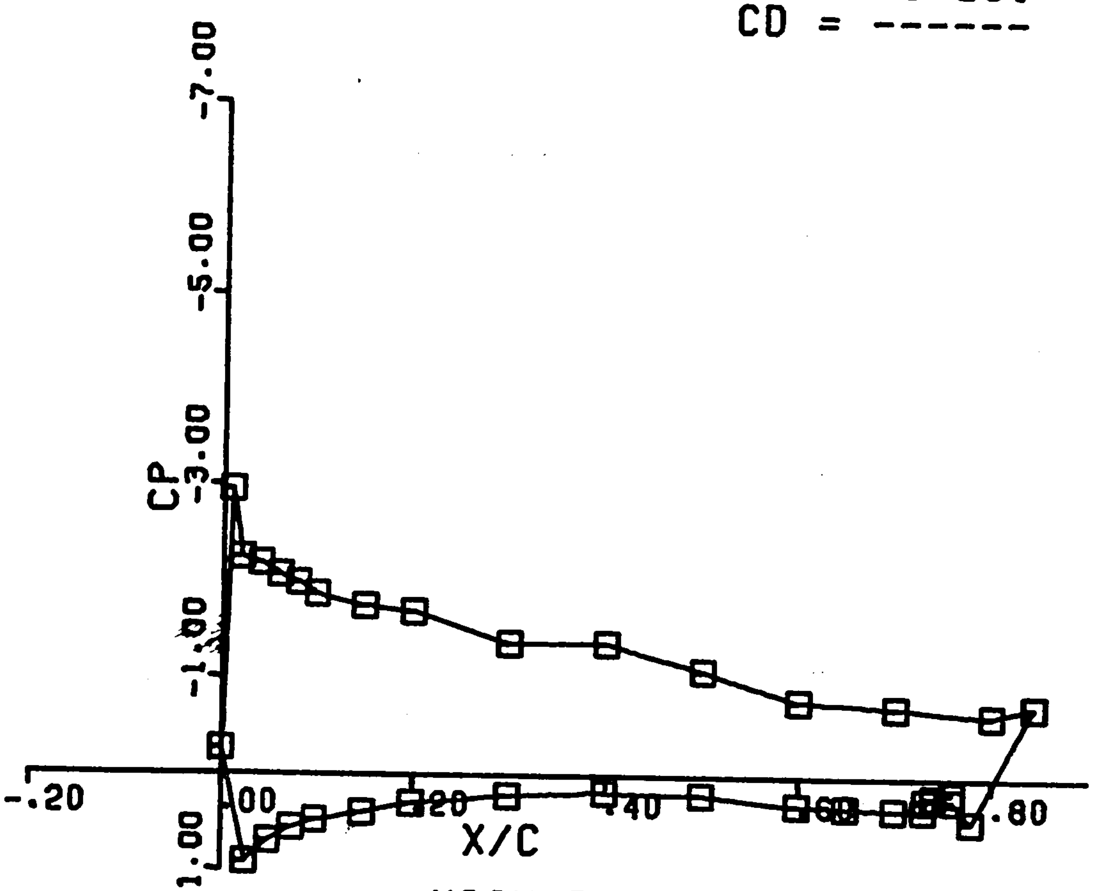

MAIN ELEMENT
CL = 1.295
CM = -0.111

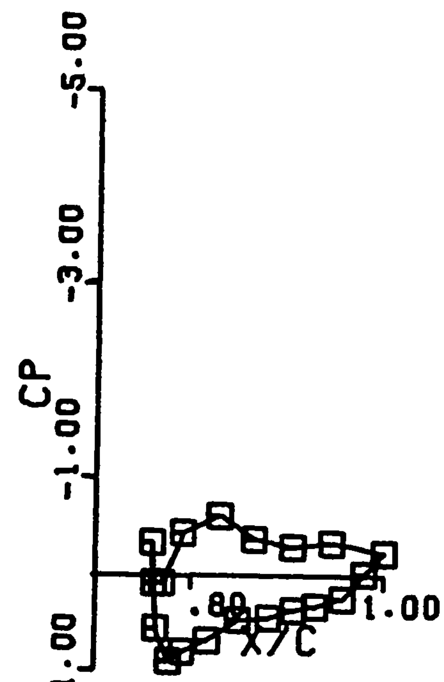

FLAP
CL = 0.168
CM = -0.120

CLEAN RUN # 100

AOA =-10.40
FLAP DEF = 30.00
CL = 0.308
CM = -0.288
CD = ------

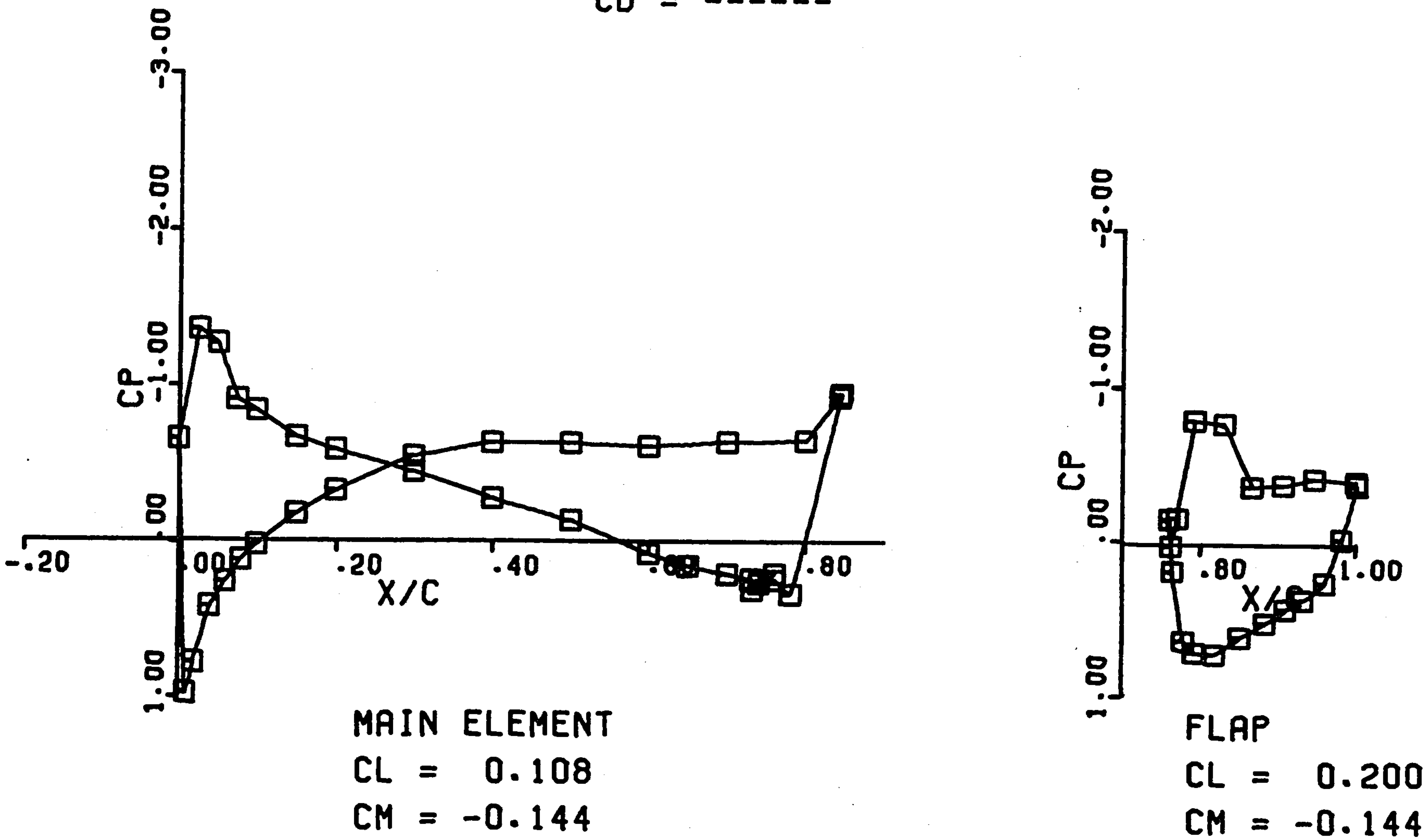

CLEAN RUN # 101

AOA = -6.40
FLAP DEF = 30.00
CL = 0.797
CM = -0.305
CD = ------

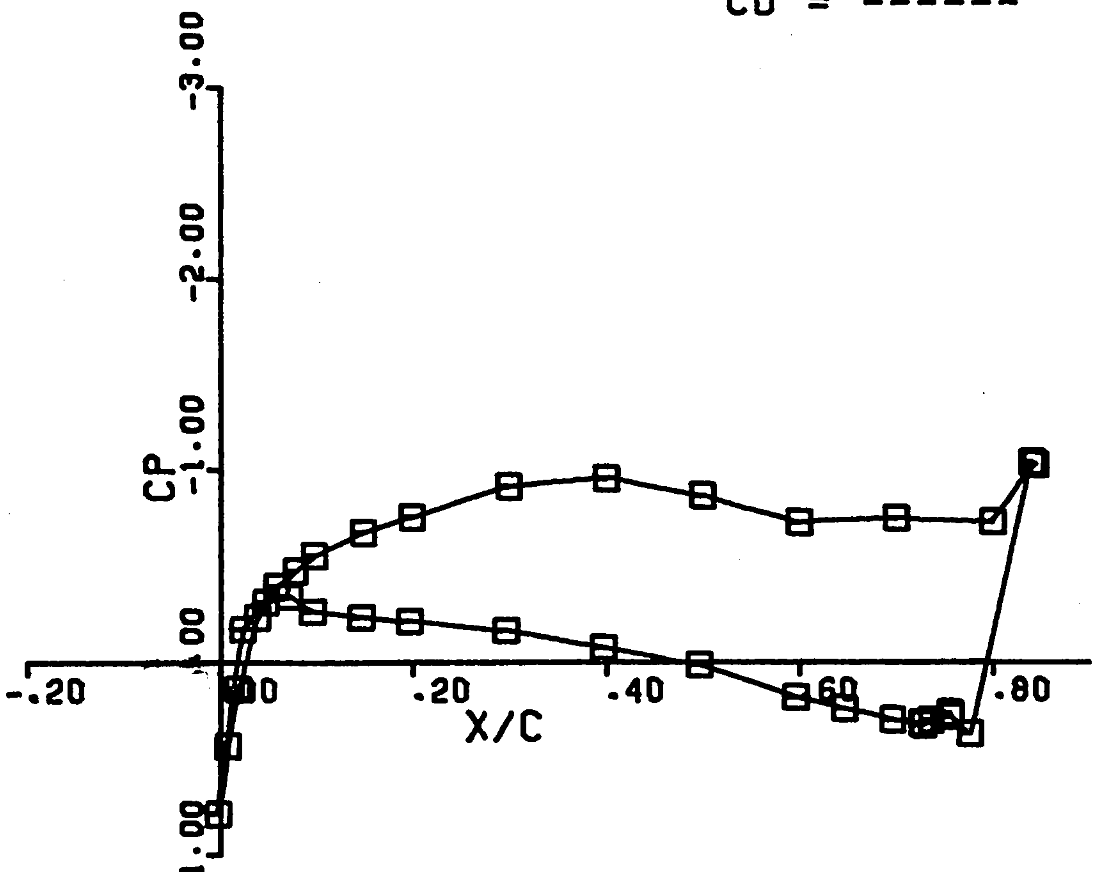

MAIN ELEMENT
CL = 0.580
CM = -0.146

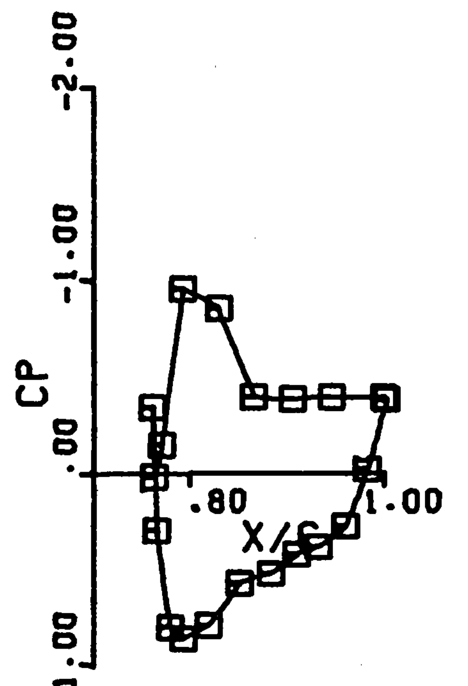

FLAP
CL = 0.218
CM = -0.159

CLEAN RUN # 102

AOA = -2.40
FLAP DEF = 30.00
CL = 1.229
CM = -0.304
CD = ------

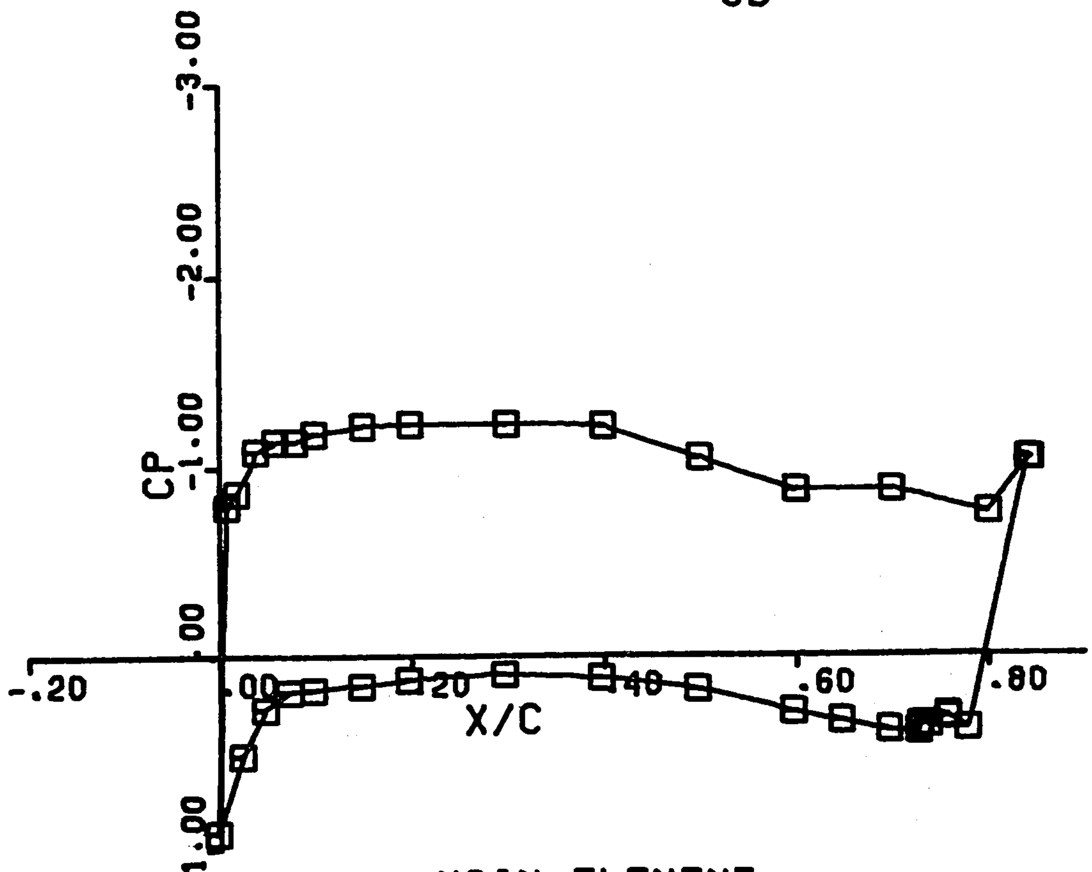

MAIN ELEMENT
CL = 1.025
CM = -0.150

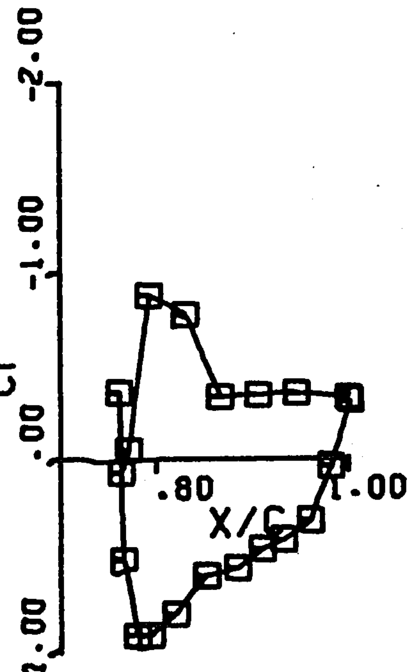

FLAP
CL = 0.204
CM = -0.153

CLEAN RUN # 103

AOA = 1.60
FLAP DEF = 30.00
CL = 1.741
CM = -0.318
CD = ------

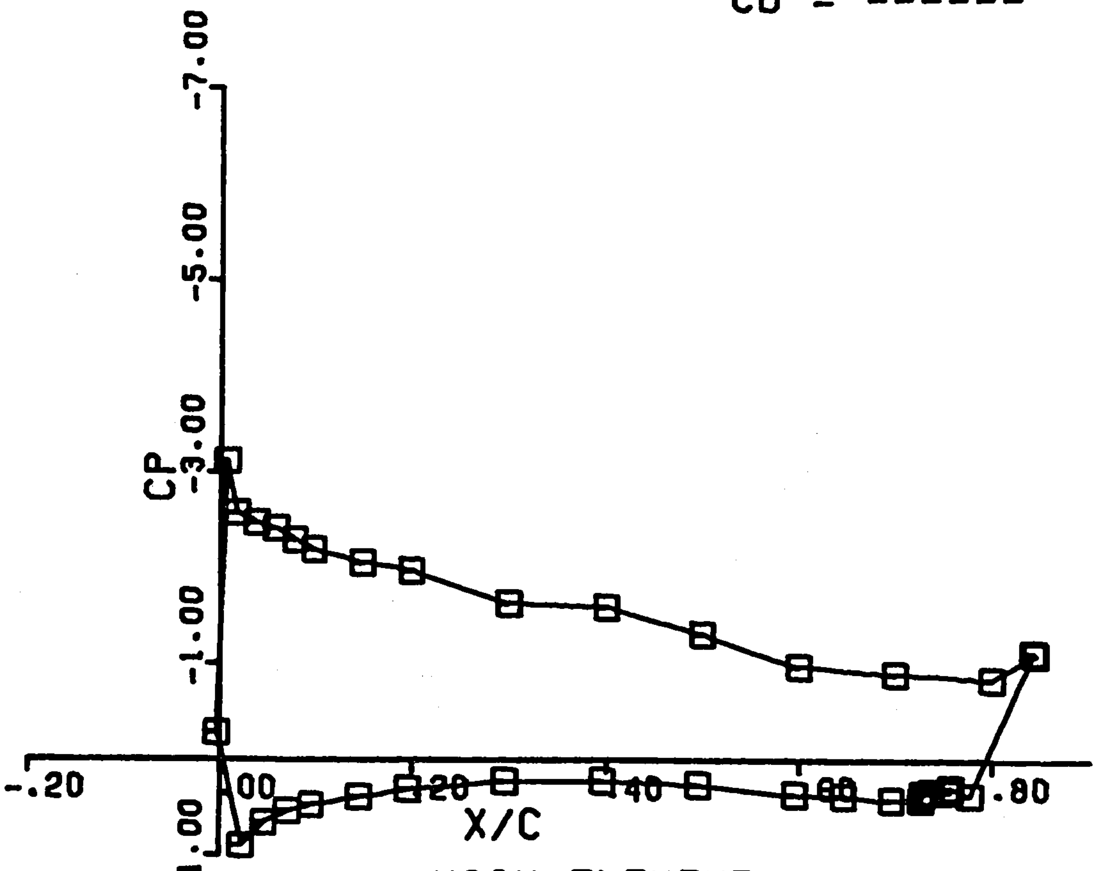

MAIN ELEMENT
CL = 1.513
CM = -0.142

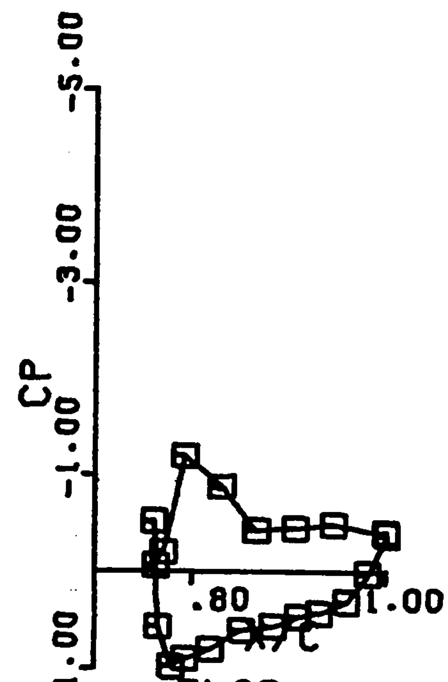

FLAP
CL = 0.228
CM = -0.176

CLEAN RUN # 104

AOA = 5.60
FLAP DEF = 30.00
CL = 1.917
CM = -0.311
CD = ------

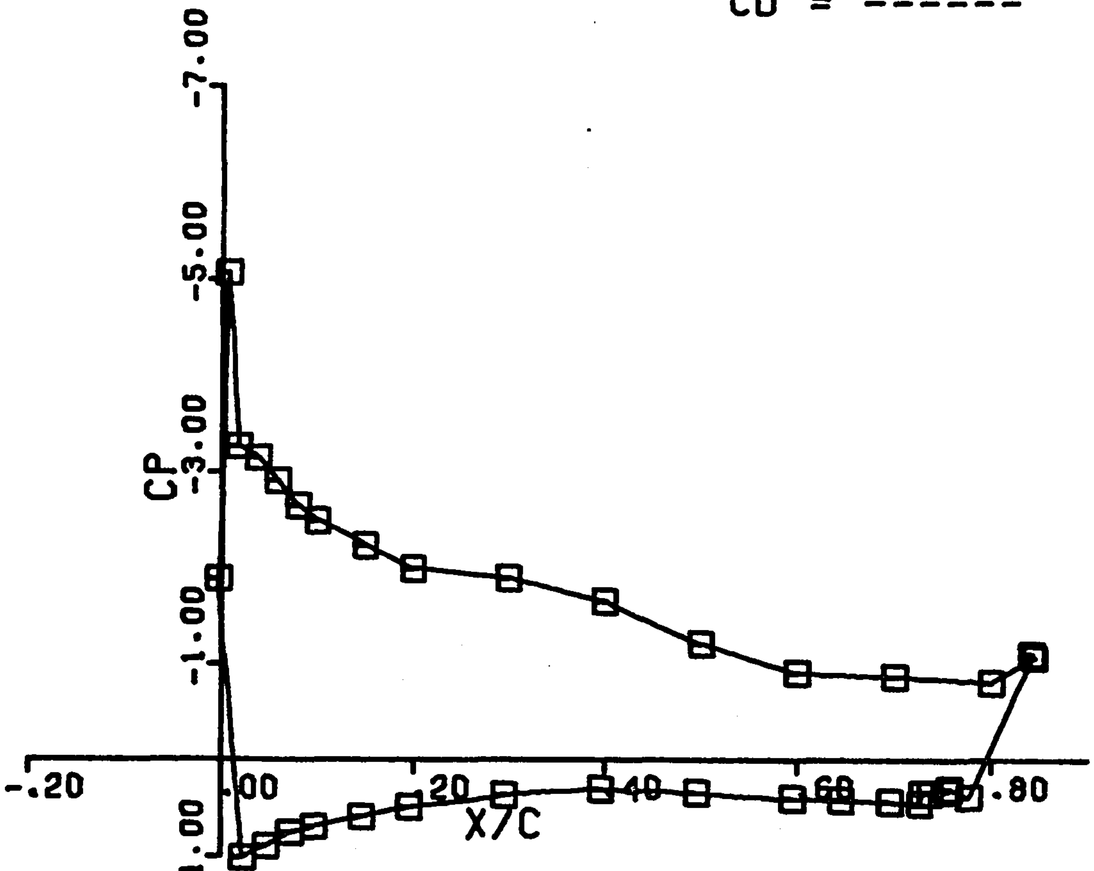

MAIN ELEMENT
CL = 1.695
CM = -0.130

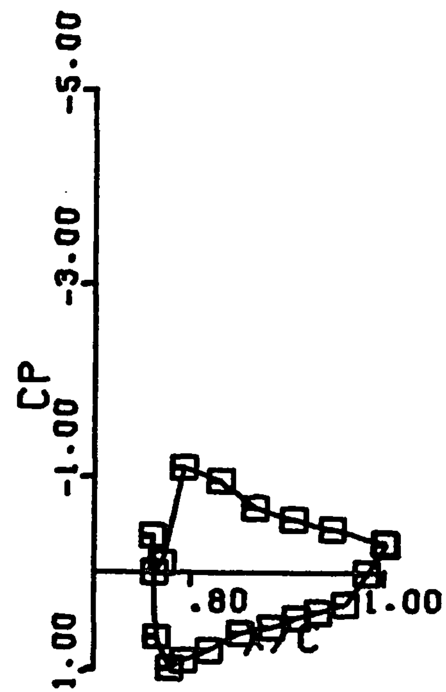

FLAP
CL = 0.222
CM = -0.182

CLEAN RUN * 105

AOA = 9.60
FLAP DEF = 30.00
CL = 2.107
CM = -0.328
CD = ------

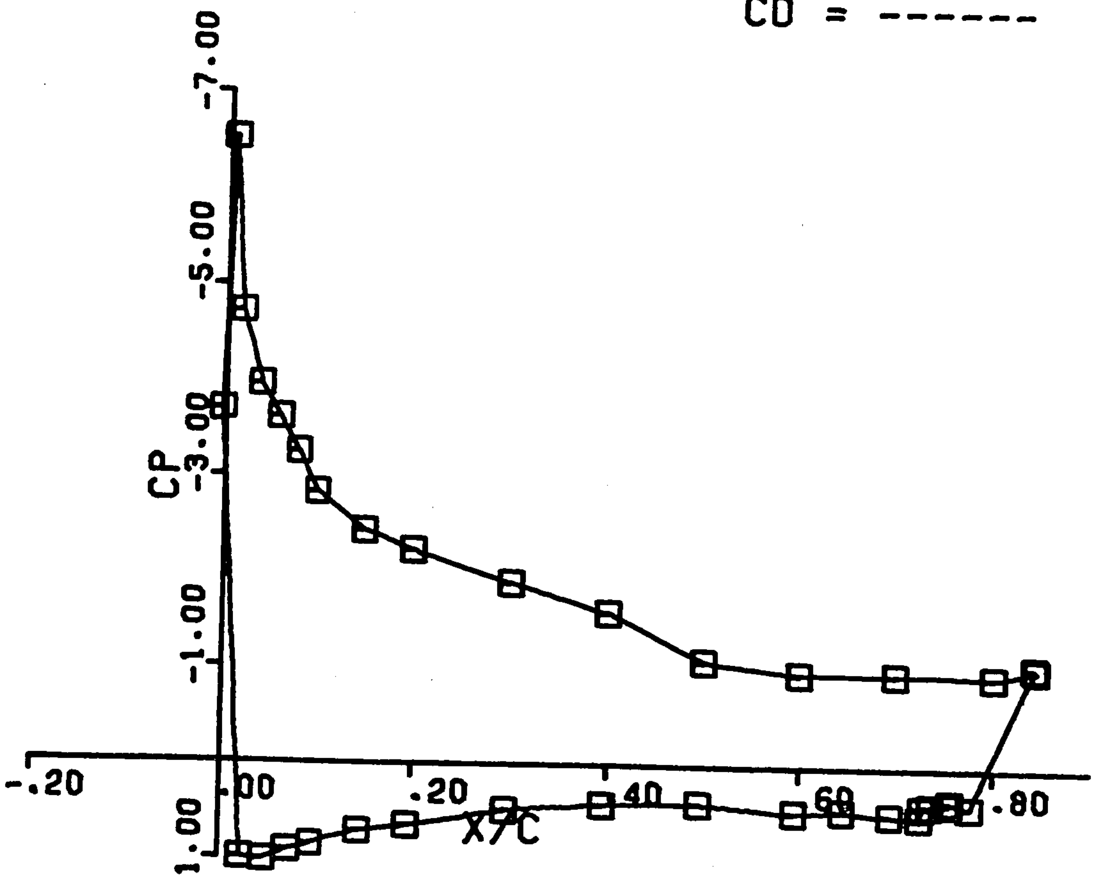

MAIN ELEMENT
CL = 1.879
CM = -0.127

FLAP
CL = 0.228
CM = -0.201

CLEAN RUN # 106

AOA = 10.60
FLAP DEF = 30.00
CL = 2.276
CM = -0.350
CD = ------

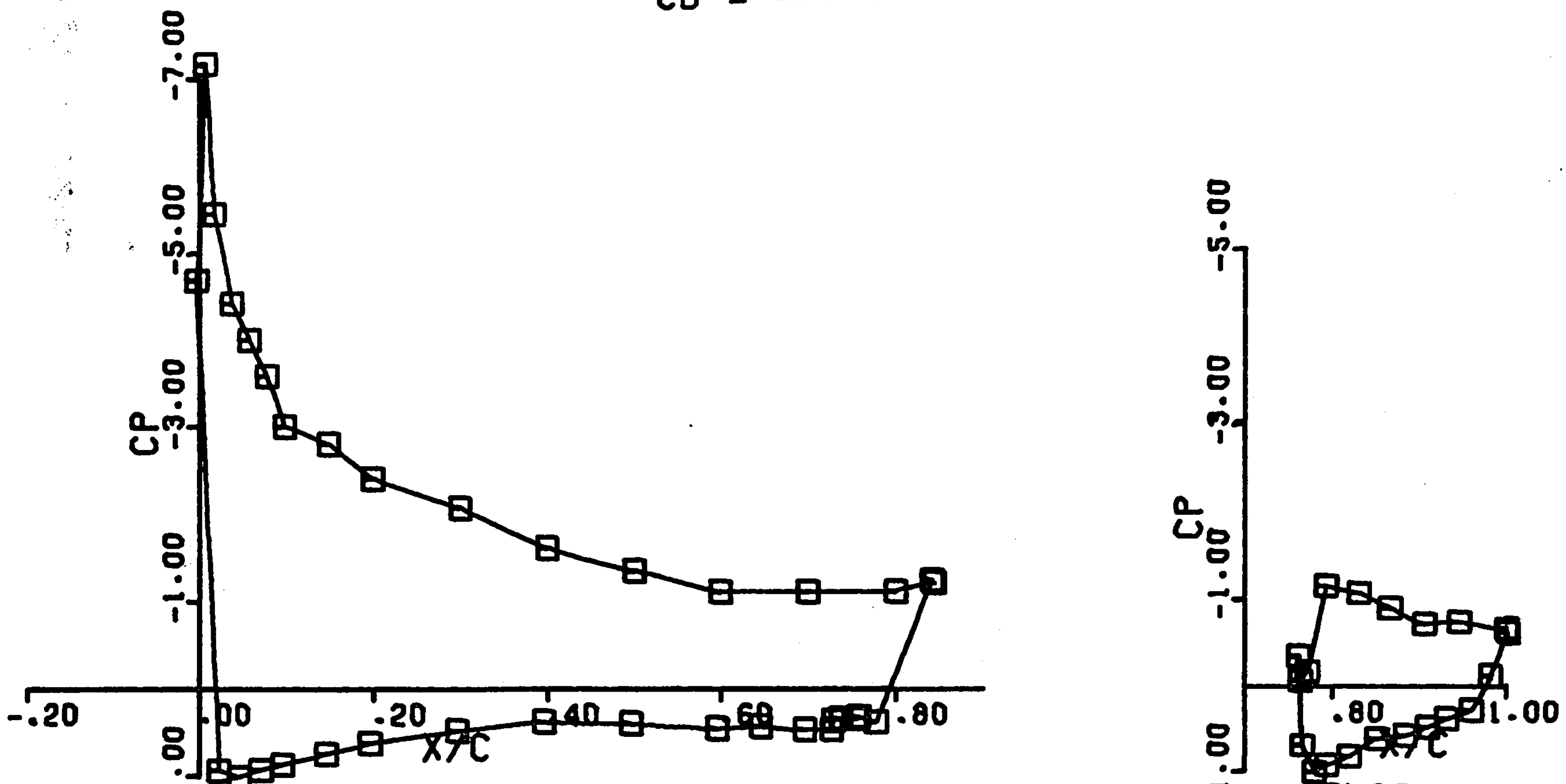

MAIN ELEMENT
CL = 2.043
CM = -0.140

FLAP
CL = 0.233
CM = -0.209

CLEAN RUN # 107

AOA = 11.60
FLAP DEF = 30.00
CL = 2.174
CM = -0.347
CD = ------

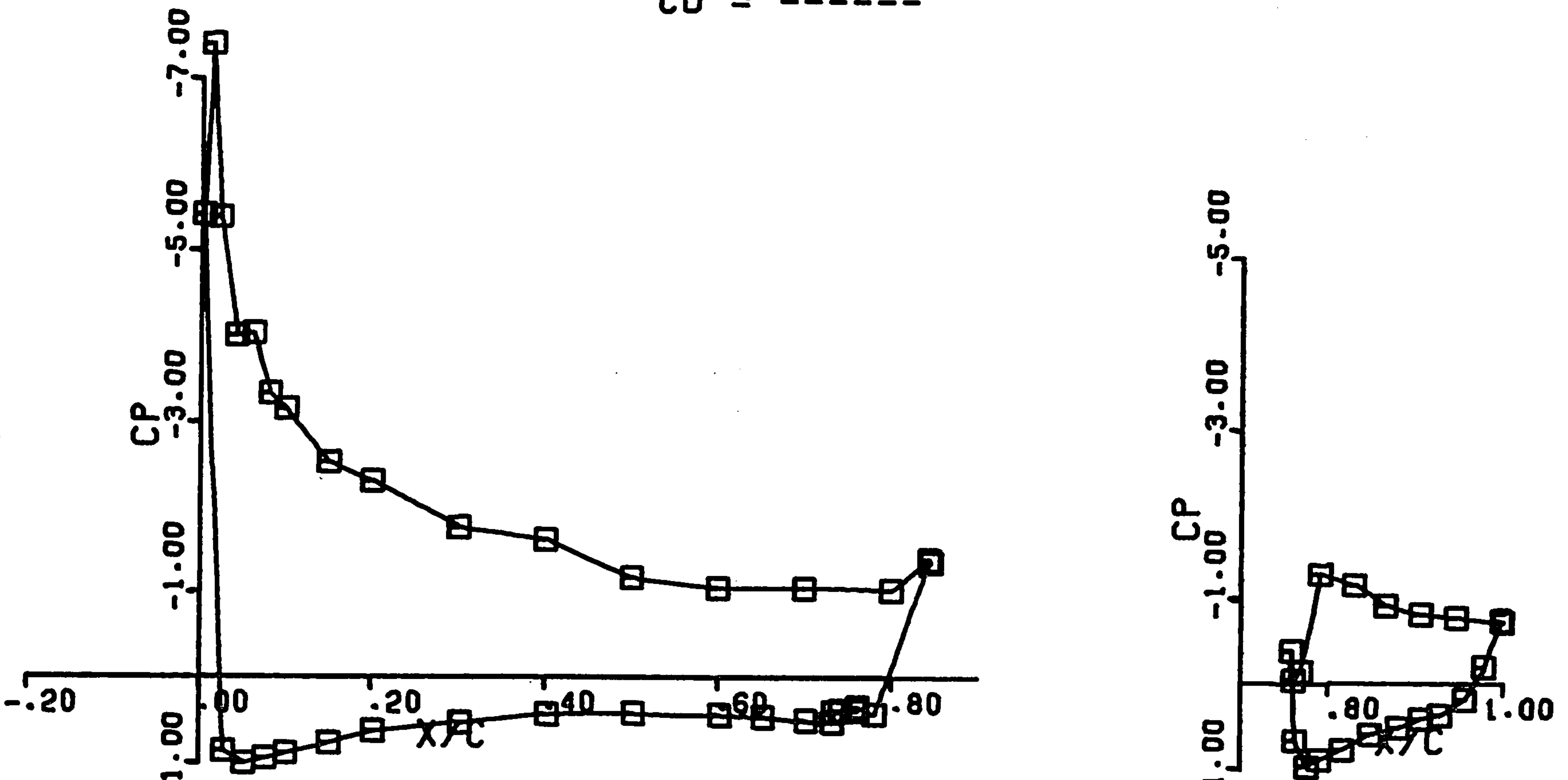

MAIN ELEMENT
CL = 1.935
CM = -0.128

FLAP
CL = 0.239
CM = -0.219

CLEAN RUN # 135

AOA = 13.60
FLAP DEF = 10.00
CL = 1.791
CM = -0.125
CD = ------

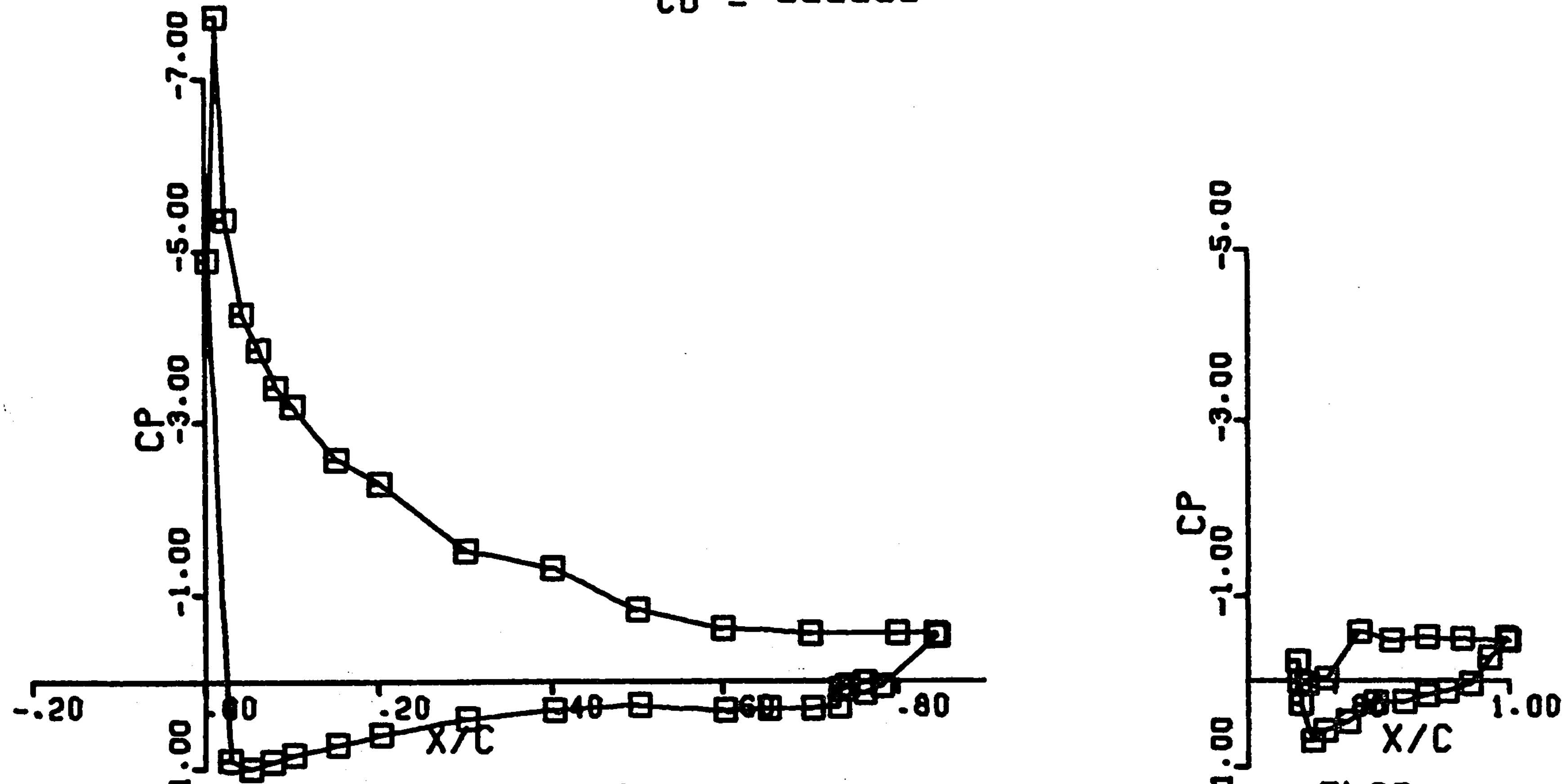

MAIN ELEMENT
CL = 1.662
CM = -0.033

FLAP
CL = 0.129
CM = -0.092

CLEAN RUN # 136

AOA = 14.60
FLAP DEF = 10.00
CL = 1.802
CM = -0.134
CD = ------

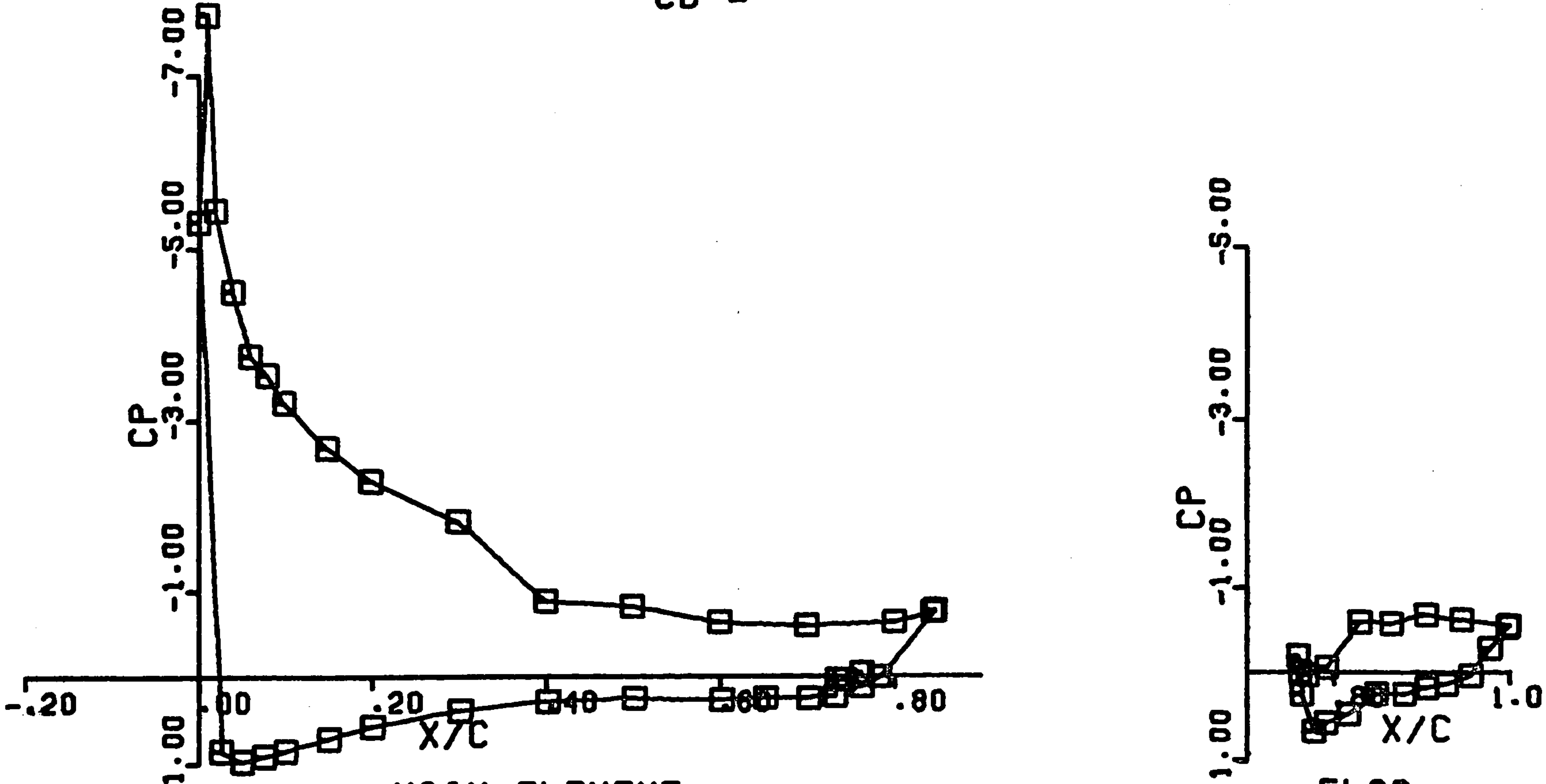

MAIN ELEMENT
CL = 1.661
CM = -0.031

FLAP
CL = 0.141
CM = -0.103

CLEAN RUN # 137

AOA = 11.60
FLAP DEF = 20.00
CL = 1.955
CM = -0.209
CD = ------

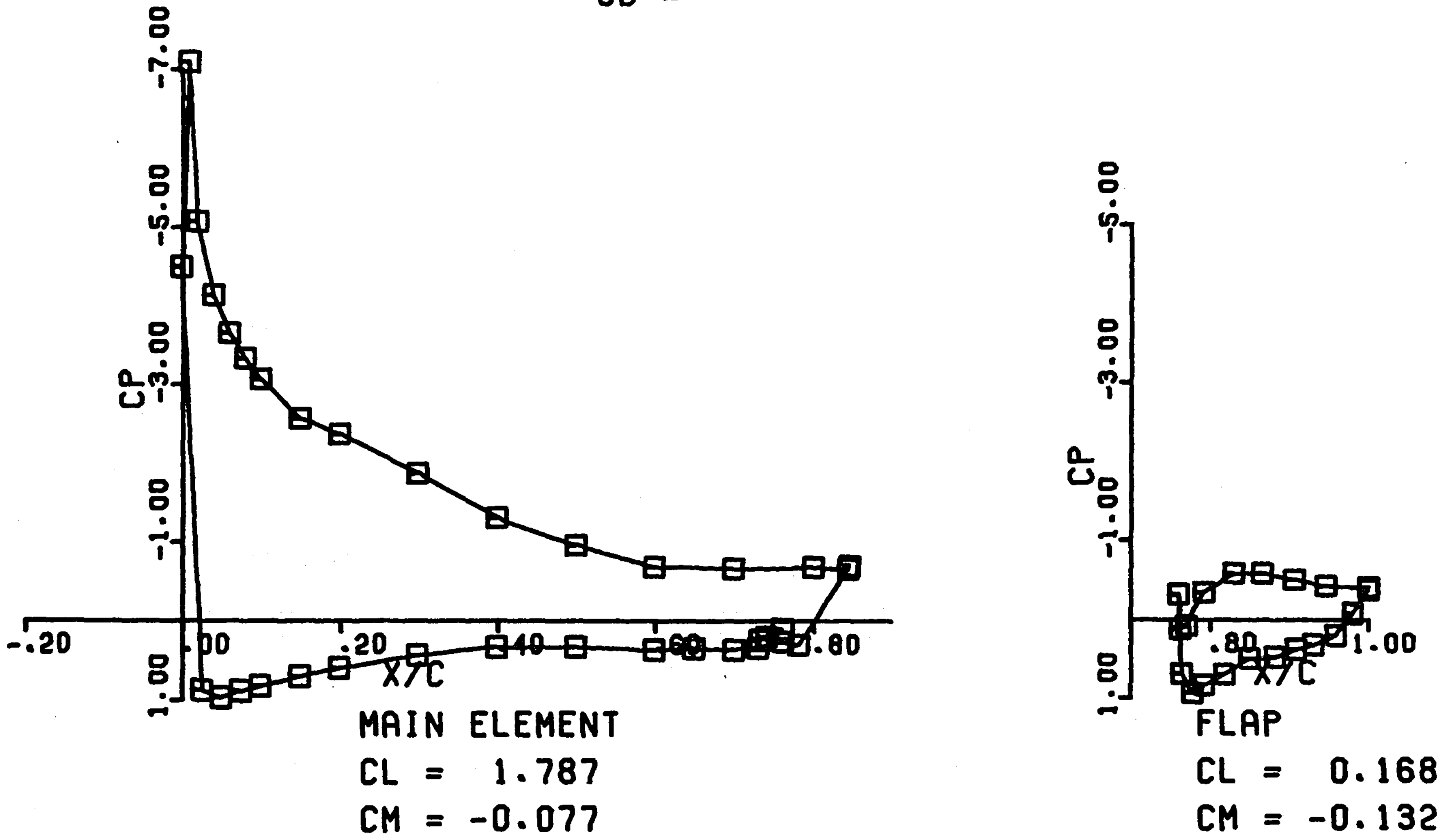

CLEAN RUN # 138

AOA = 12.60
FLAP DEF = 20.00
CL = 1.972
CM = -0.208
CD = ------

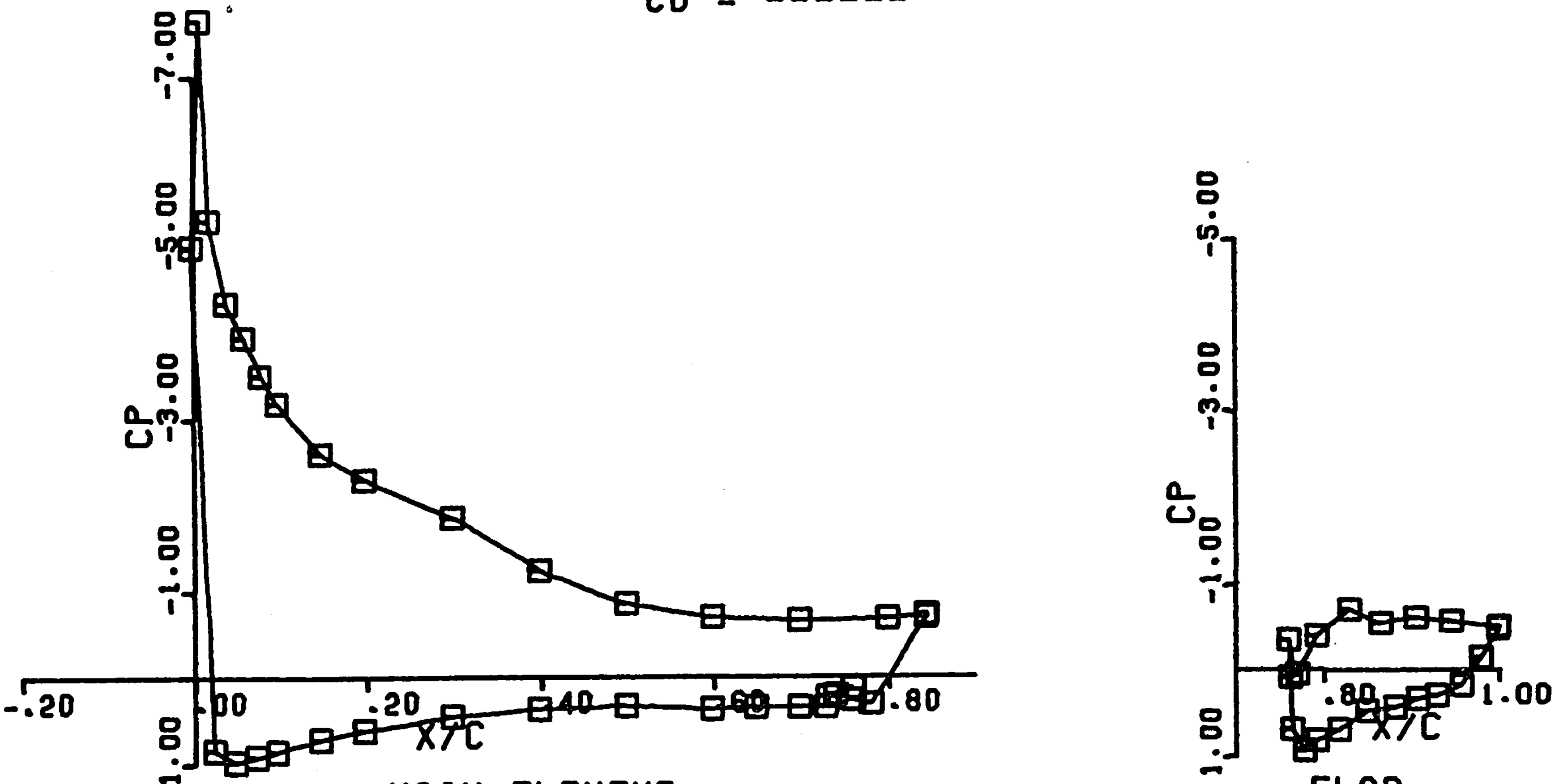

MAIN ELEMENT
CL = 1.796
CM = -0.067

FLAP
CL = 0.176
CM = -0.141

CLEAN RUN # 139

AOA = 13.60
FLAP DEF = 20.00
CL = 1.928
CM = -0.213
CD = ------

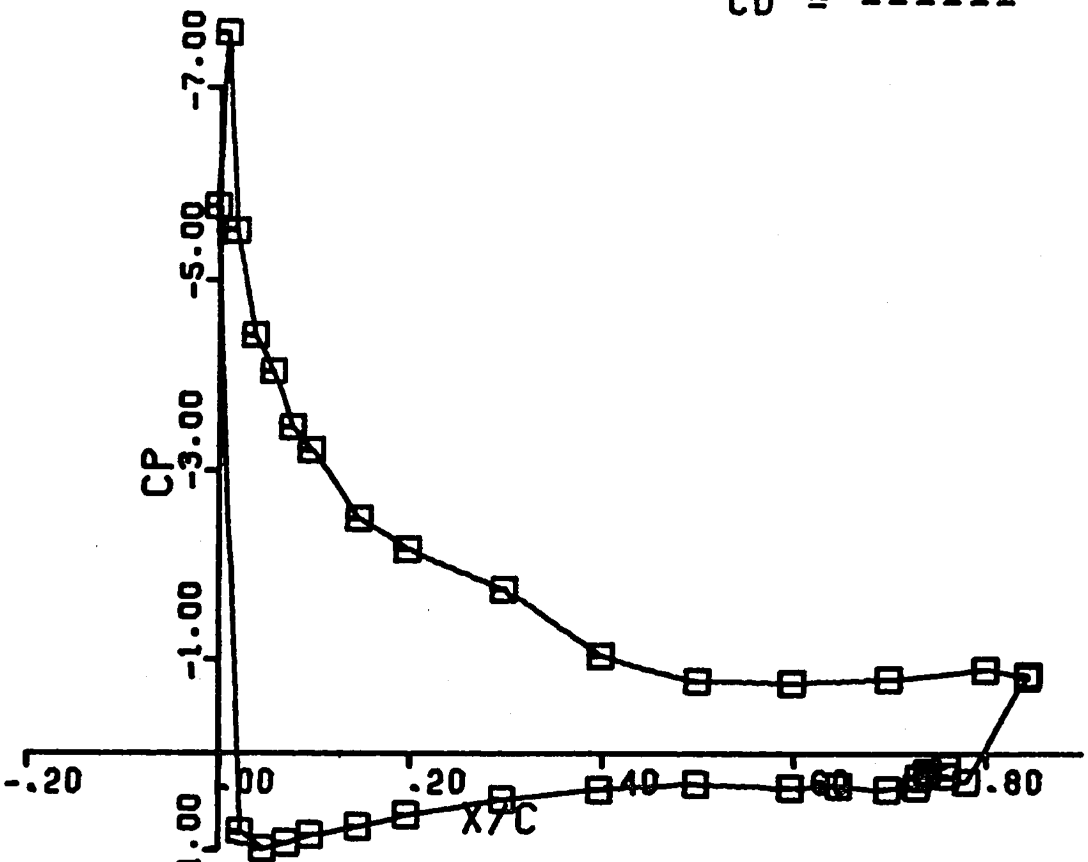

MAIN ELEMENT
CL = 1.755
CM = -0.073

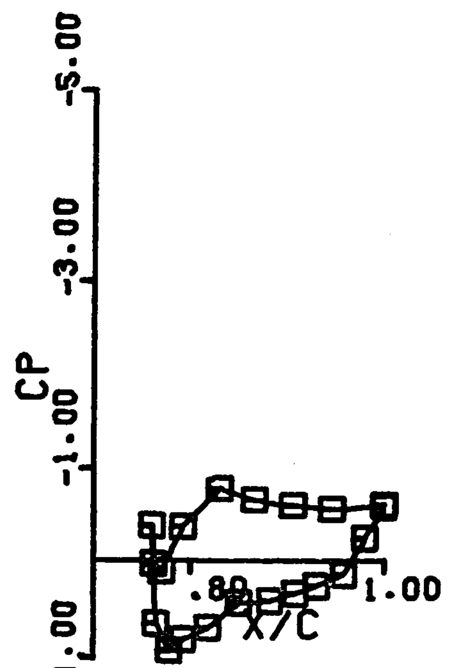

FLAP
CL = 0.173
CM = -0.140

RIME 3 ROUGH RUN # 76

AOA = -2.40
FLAP DEF = 0.00
CL = 0.054
CM = -0.054
CD = 0.016

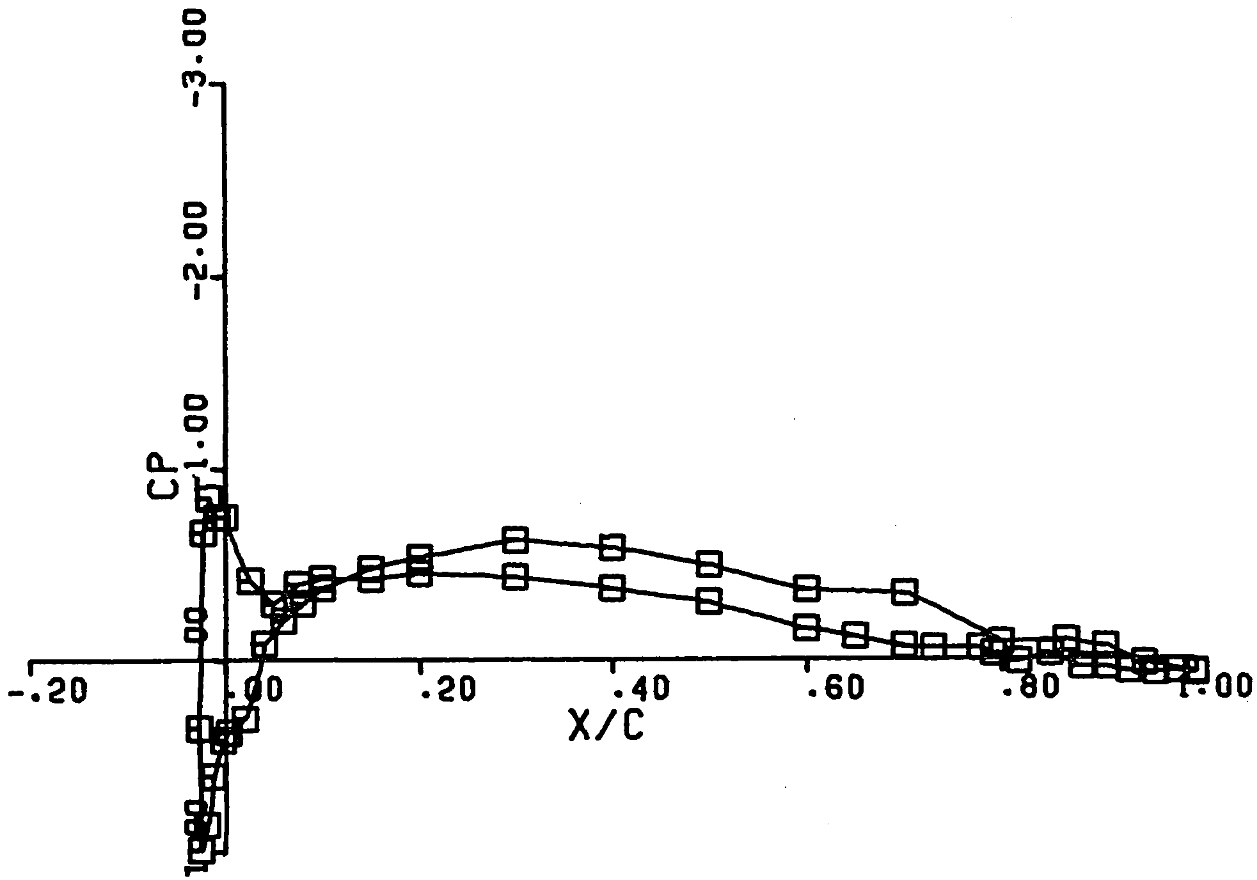

RIME 3 RØUGH RUN # 77

AØA = -0.40
FLAP DEF = 0.00
CL = 0.346
CM = -0.059
CD = 0.014

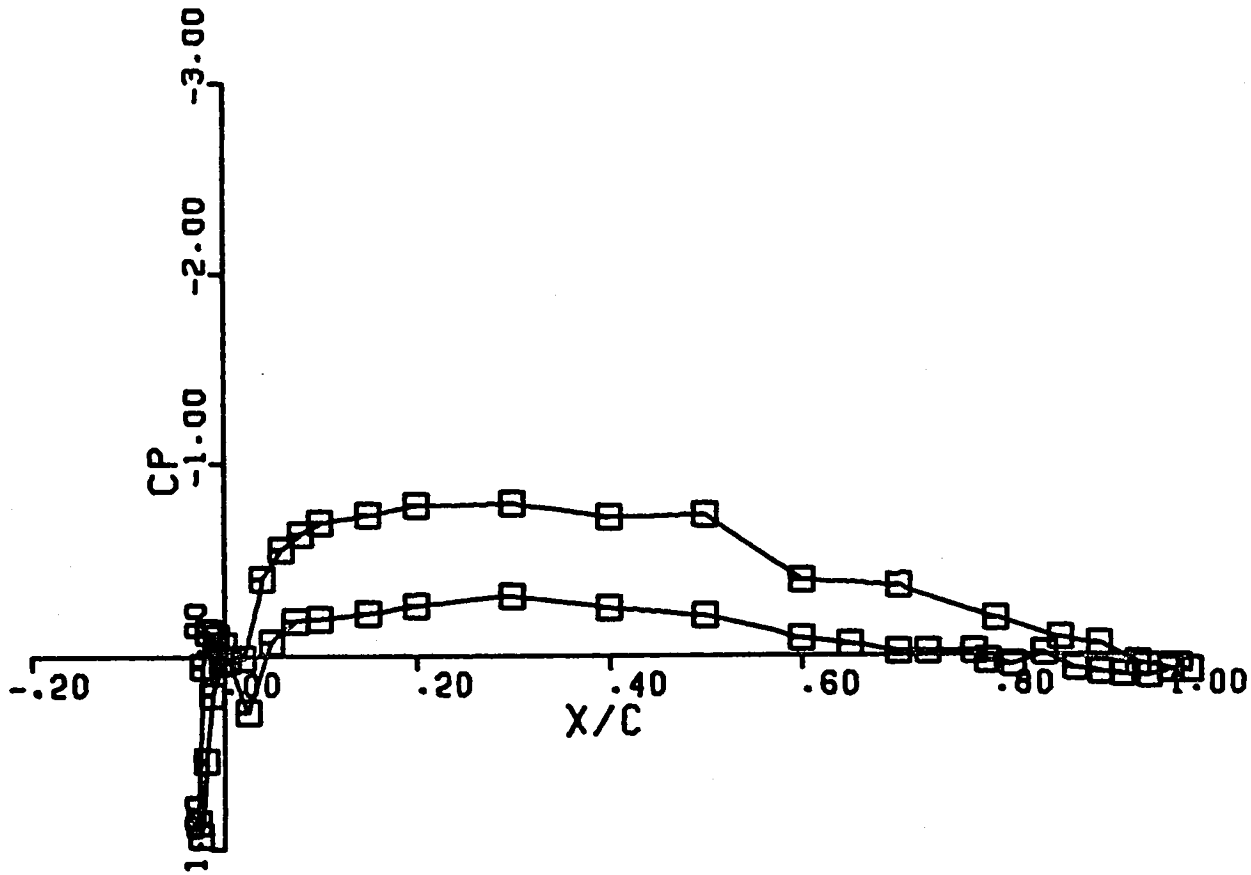

RIME 3 ROUGH RUN * 78

AOA = 1.60
FLAP DEF = 0.00
CL = 0.521
CM = -0.049
CD = 0.015

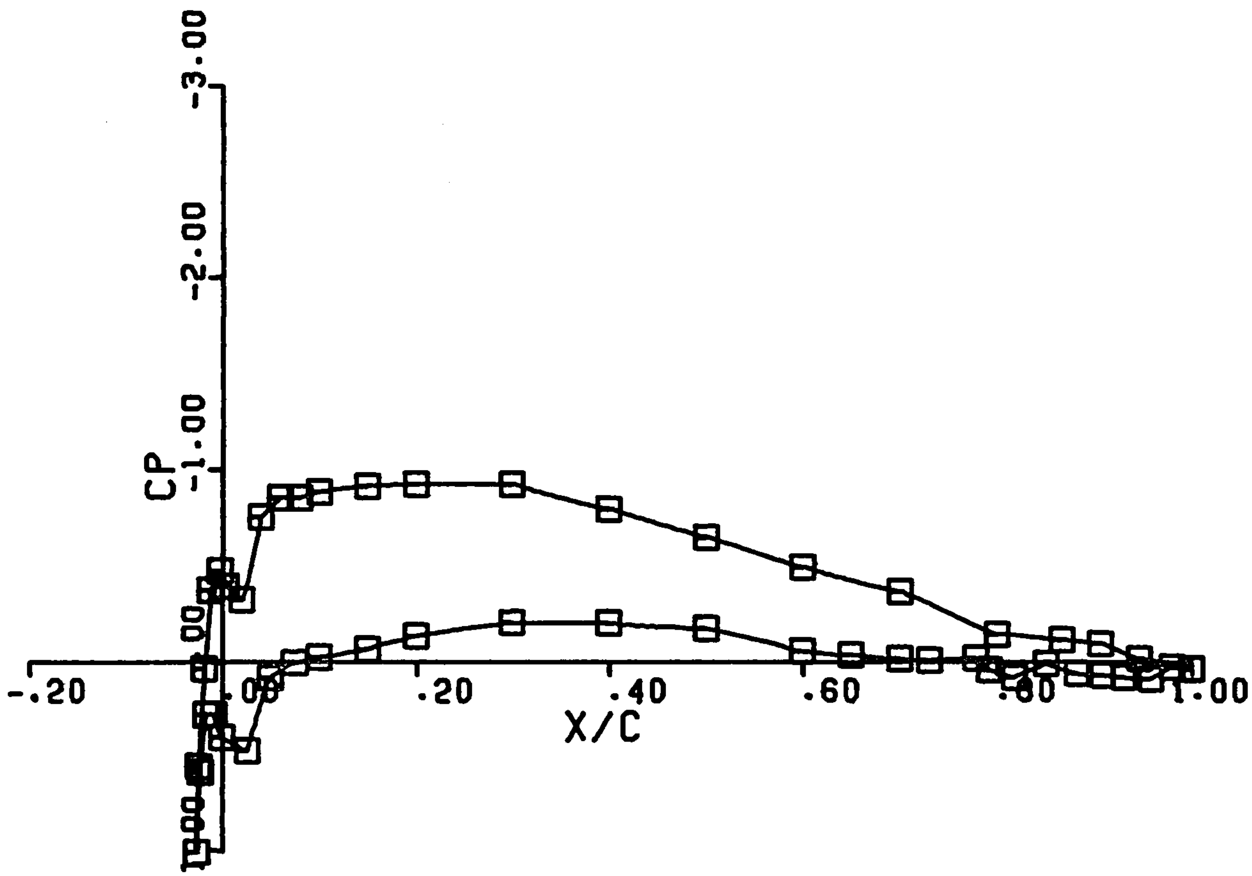

RIME 3 ROUGH RUN * 79

AOA = 3.60
FLAP DEF = 0.00
CL = 0.747
CM = -0.049
CD = 0.017

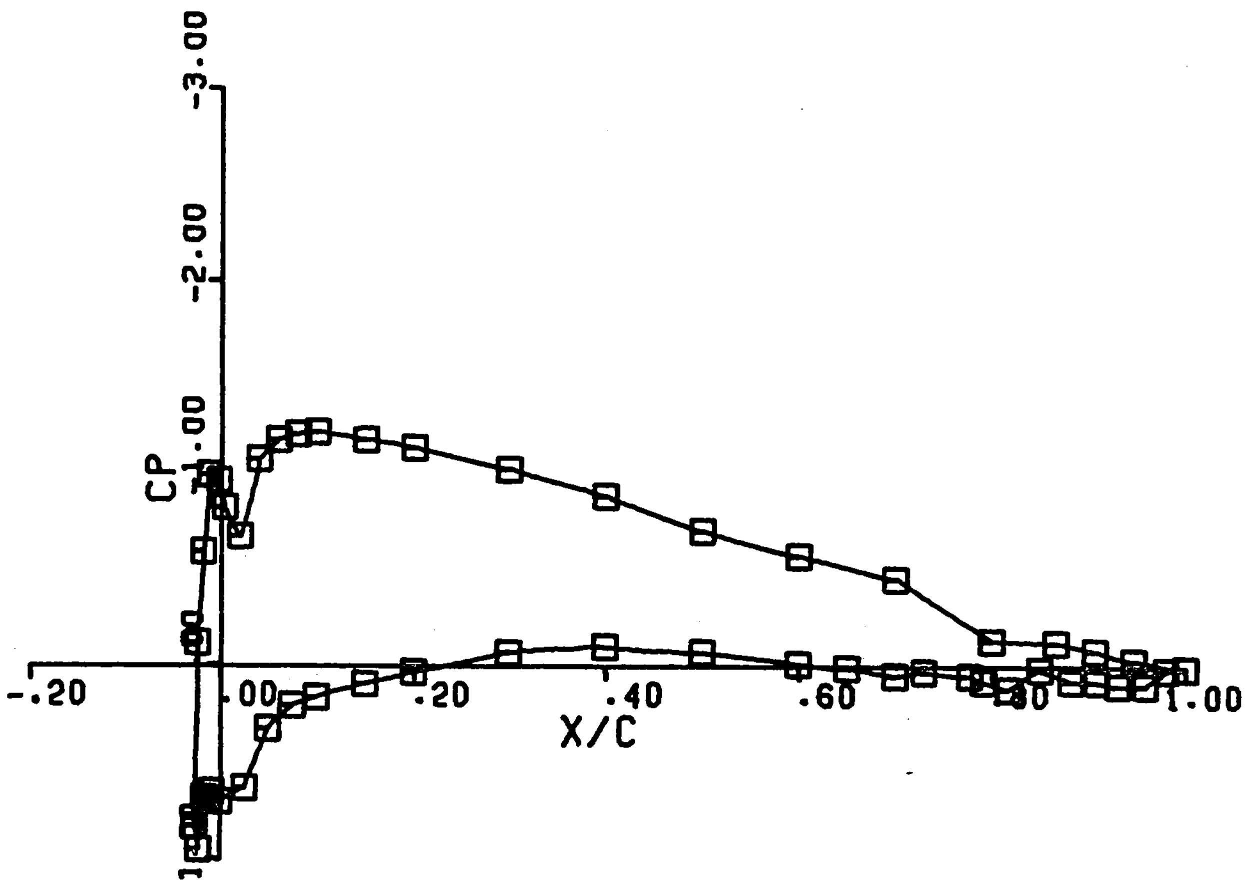

RIME 3 ROUGH RUN # 80

AOA = 5.60
FLAP DEF = 0.00
CL = 0.933
CM = -0.046
CD = 0.021

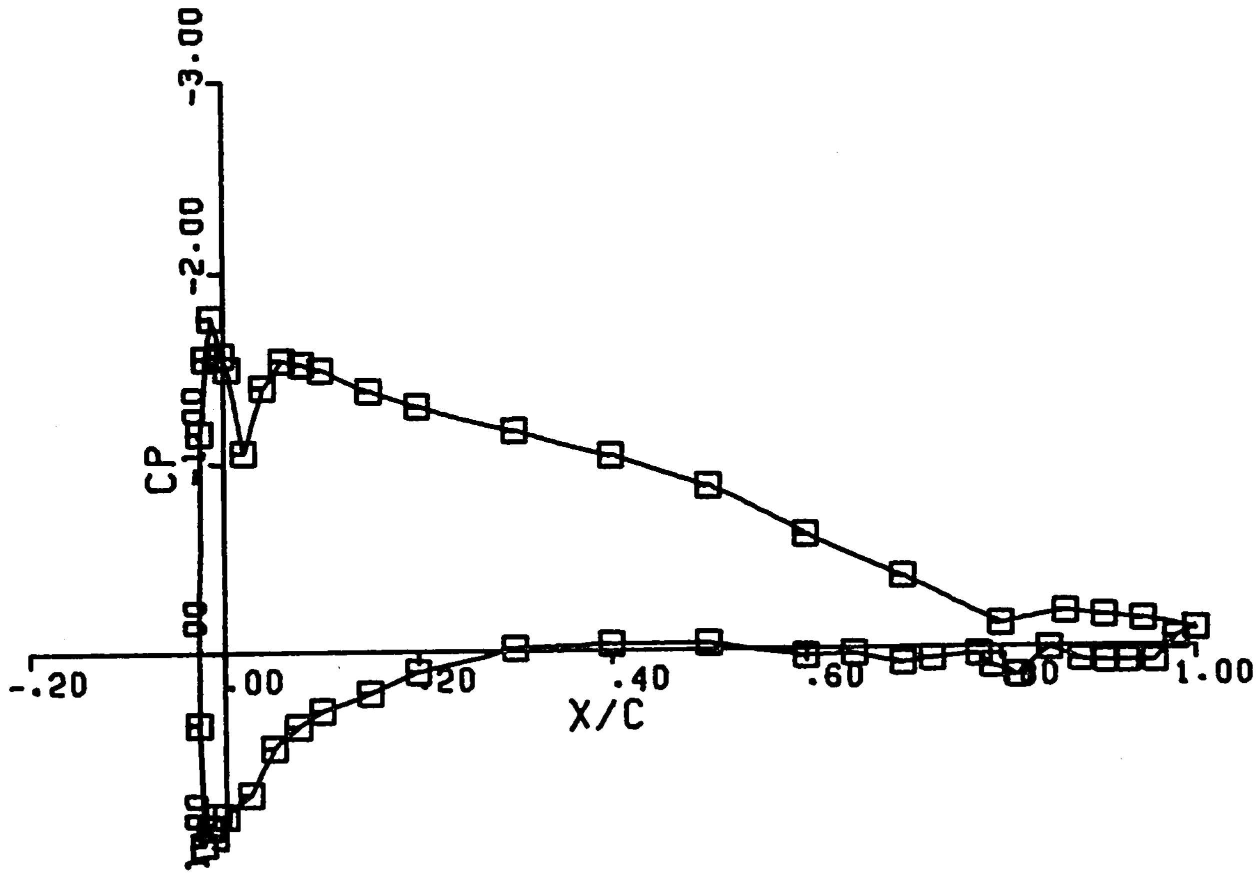

RIME 3 ROUGH RUN # 159

AOA =-10.40
FLAP DEF = 30.00
CL = -0.037
CM = -0.209
CD = ------

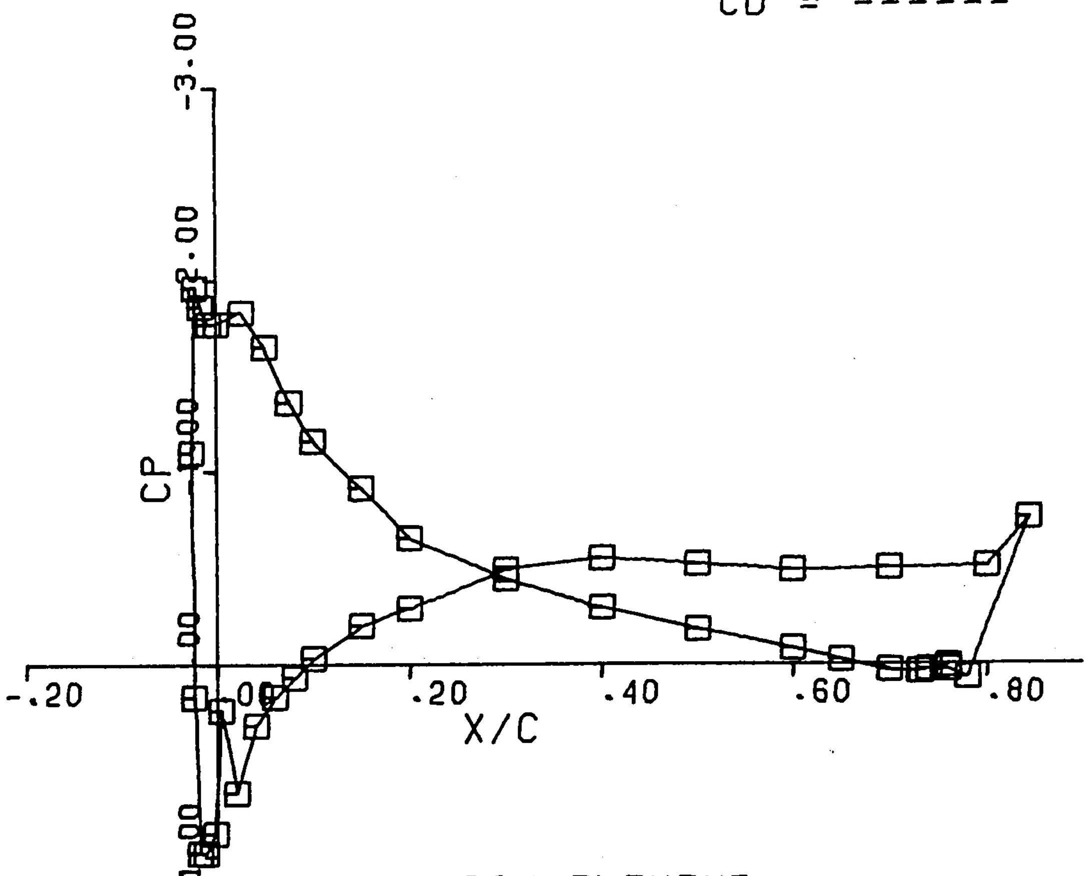

MAIN ELEMENT
CL = -0.151
CM = -0.128

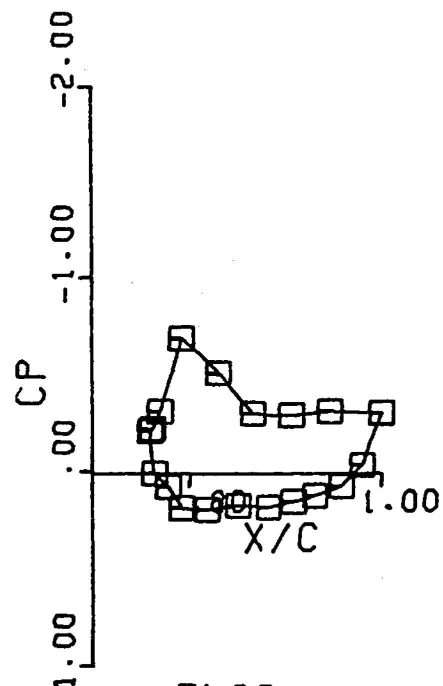

FLAP
CL = 0.114
CM = -0.081

RIME 3 ROUGH RUN # 160

AOA = -6.40
FLAP DEF = 30.00
CL = 0.700
CM = -0.287
CD = ------

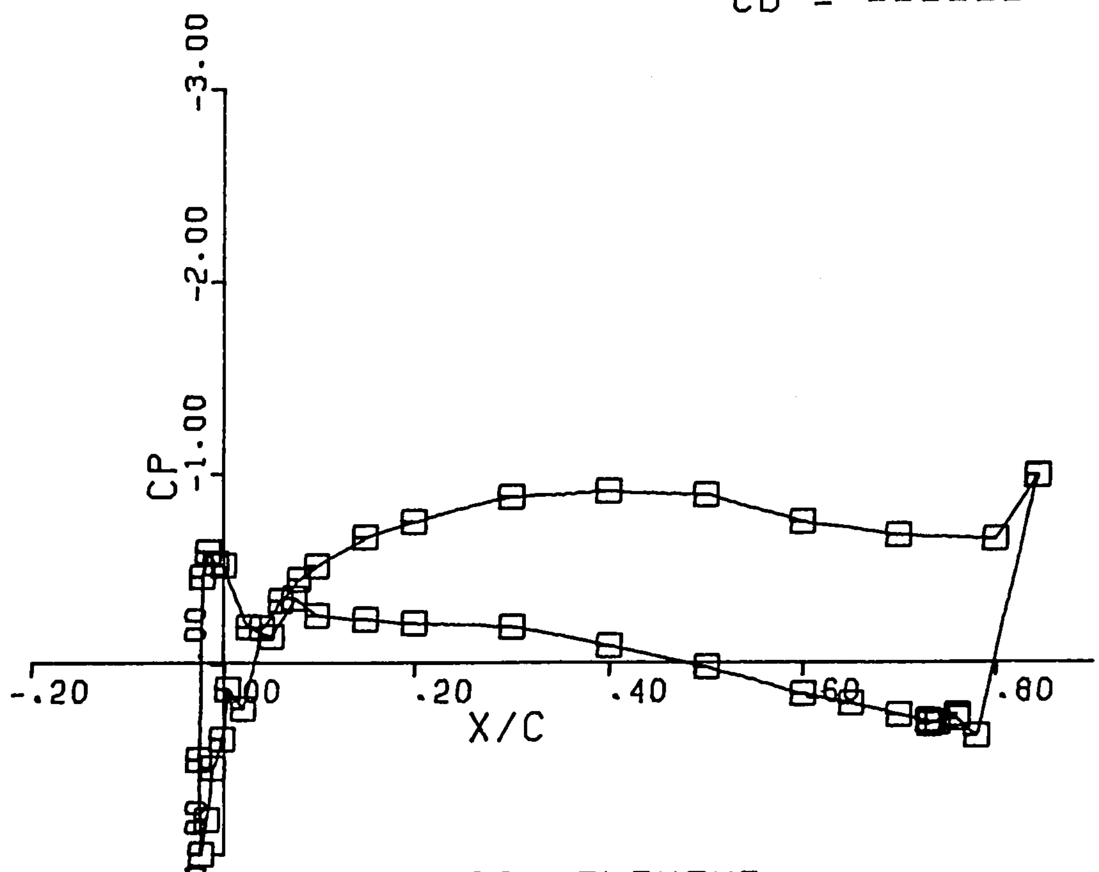

MAIN ELEMENT
CL = 0.511
CM = -0.148

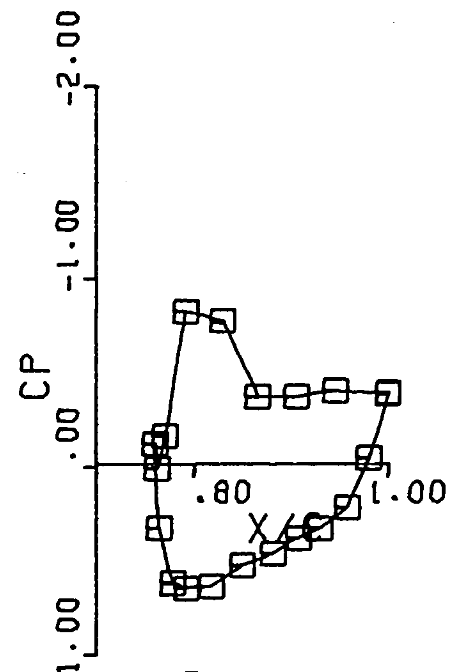

FLAP
CL = 0.189
CM = -0.139

RIME 3 ROUGH RUN # 161

AOA = -2.40
FLAP DEF = 30.00
CL = 1.194
CM = -0.296
CD = -------

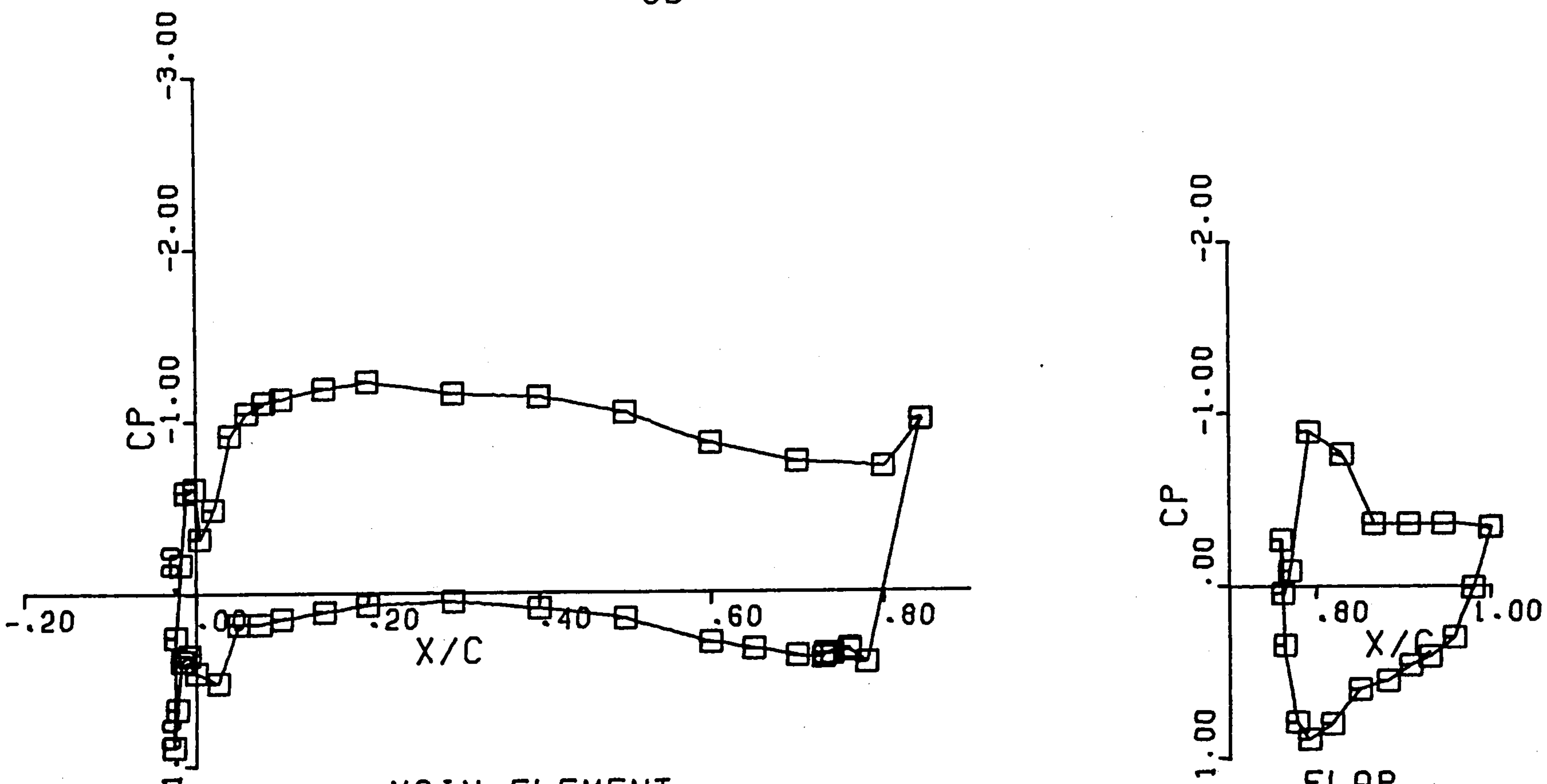

MAIN ELEMENT
CL = 0.988
CM = -0.141

FLAP
CL = 0.206
CM = -0.155

RIME 3 ROUGH RUN # 162

AOA = 1.60
FLAP DEF = 30.00
CL = 1.669
CM = -0.295
CD = ------

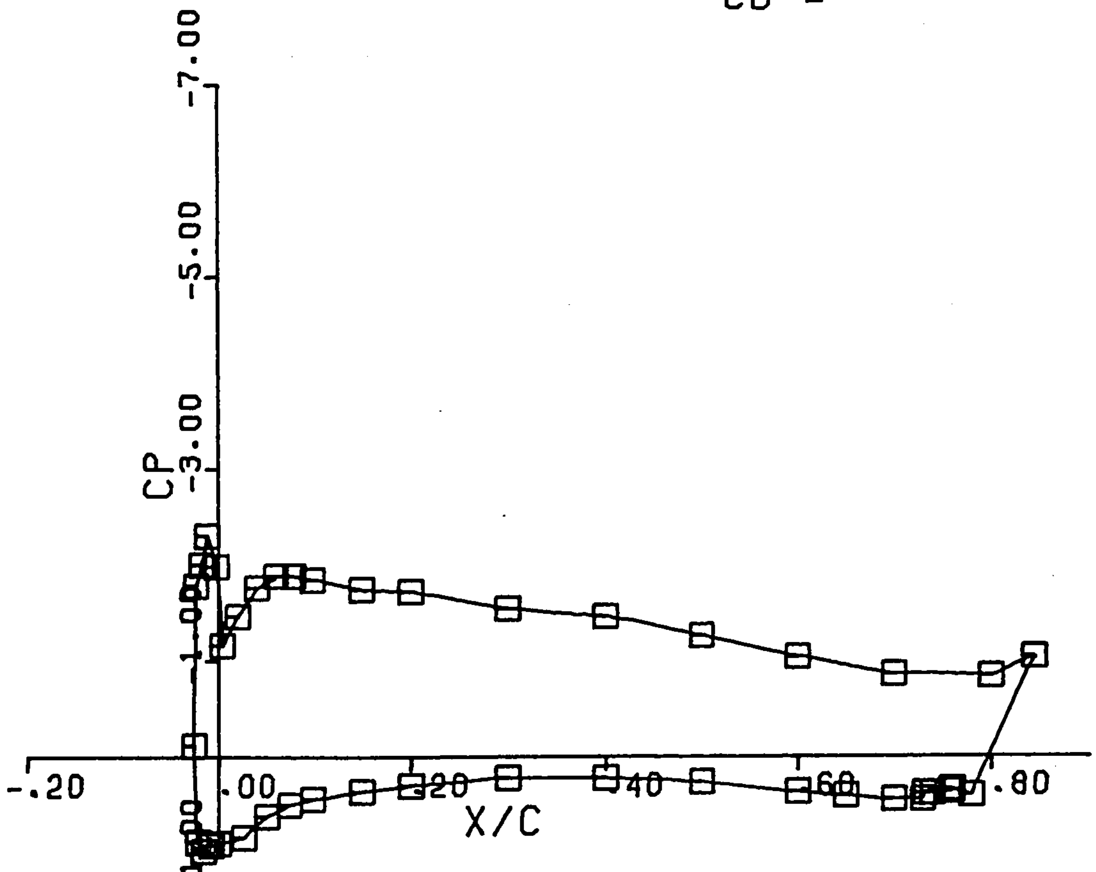

MAIN ELEMENT
CL = 1.463
CM = -0.133

FLAP
CL = 0.206
CM = -0.161

RIME 3 ROUGH RUN # 163

AOA = 5.60
FLAP DEF = 30.00
CL = 1.971
CM = -0.274
CD = -------

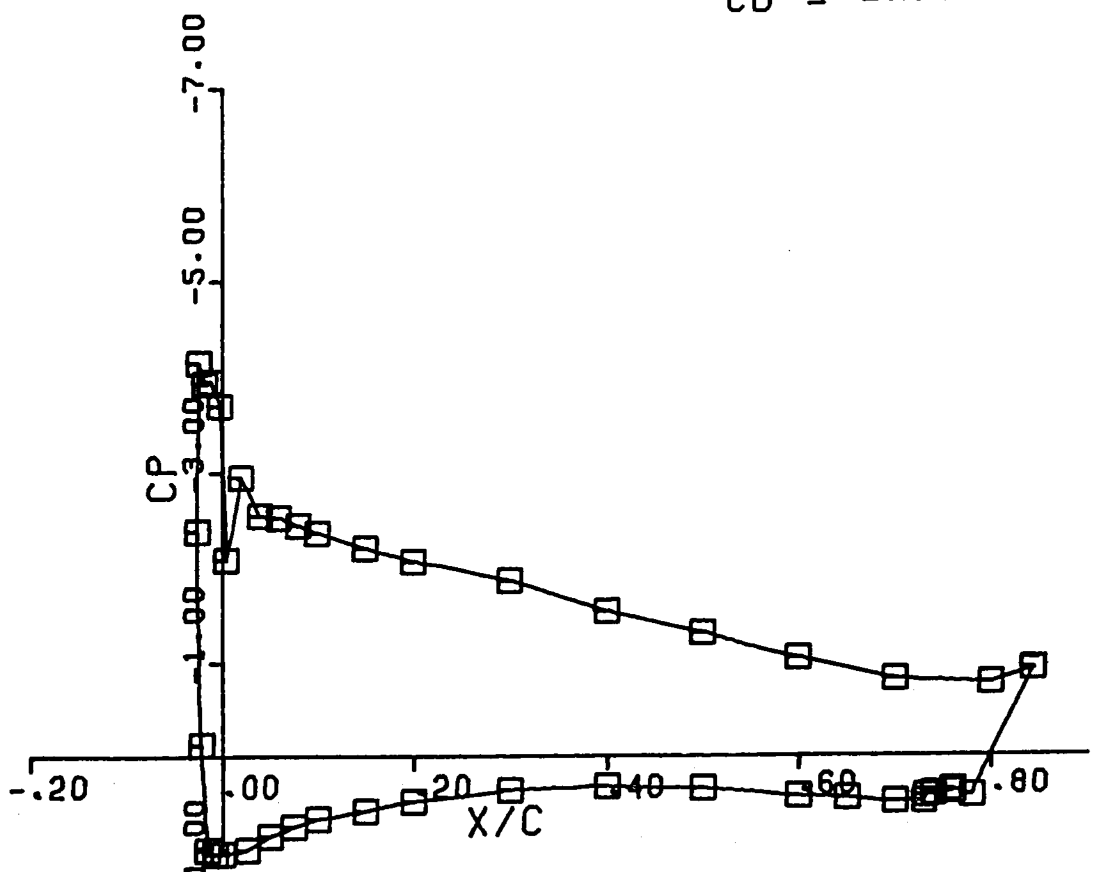

MAIN ELEMENT
CL = 1.768
CM = -0.106

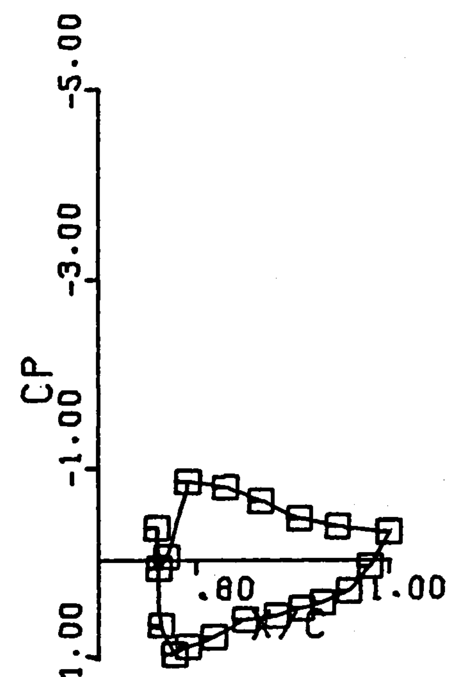

FLAP
CL = 0.204
CM = -0.168

RIME 3 ROUGH RUN # 164

AØA = 7.60
FLAP DEF = 30.00
CL = 1.921
CM = -0.239
CD = ------

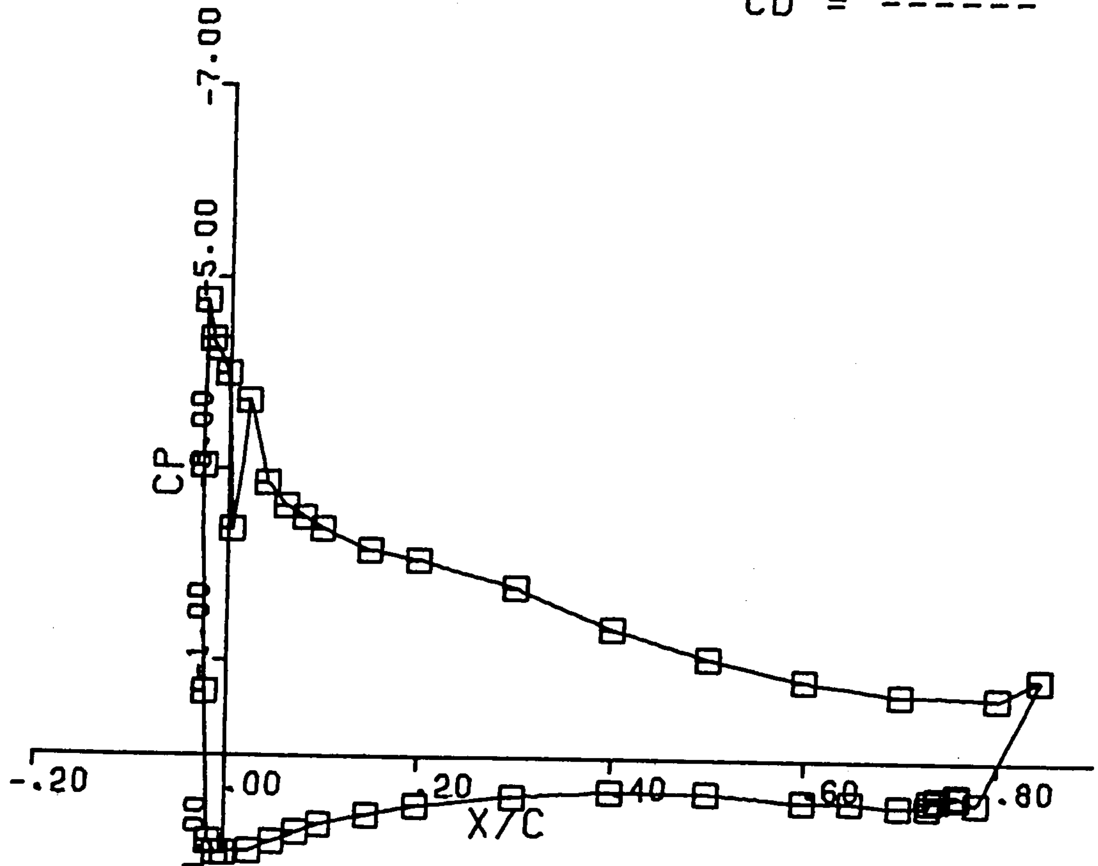

MAIN ELEMENT
CL = 1.728
CM = -0.071

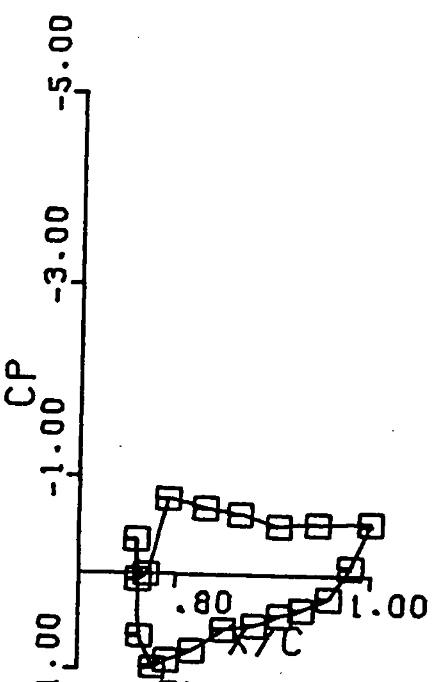

FLAP
CL = 0.193
CM = -0.168

RIME 3 ROUGH RUN # 165

AOA = 7.60
FLAP DEF = 20.00
CL = 1.750
CM = -0.190
CD = ------

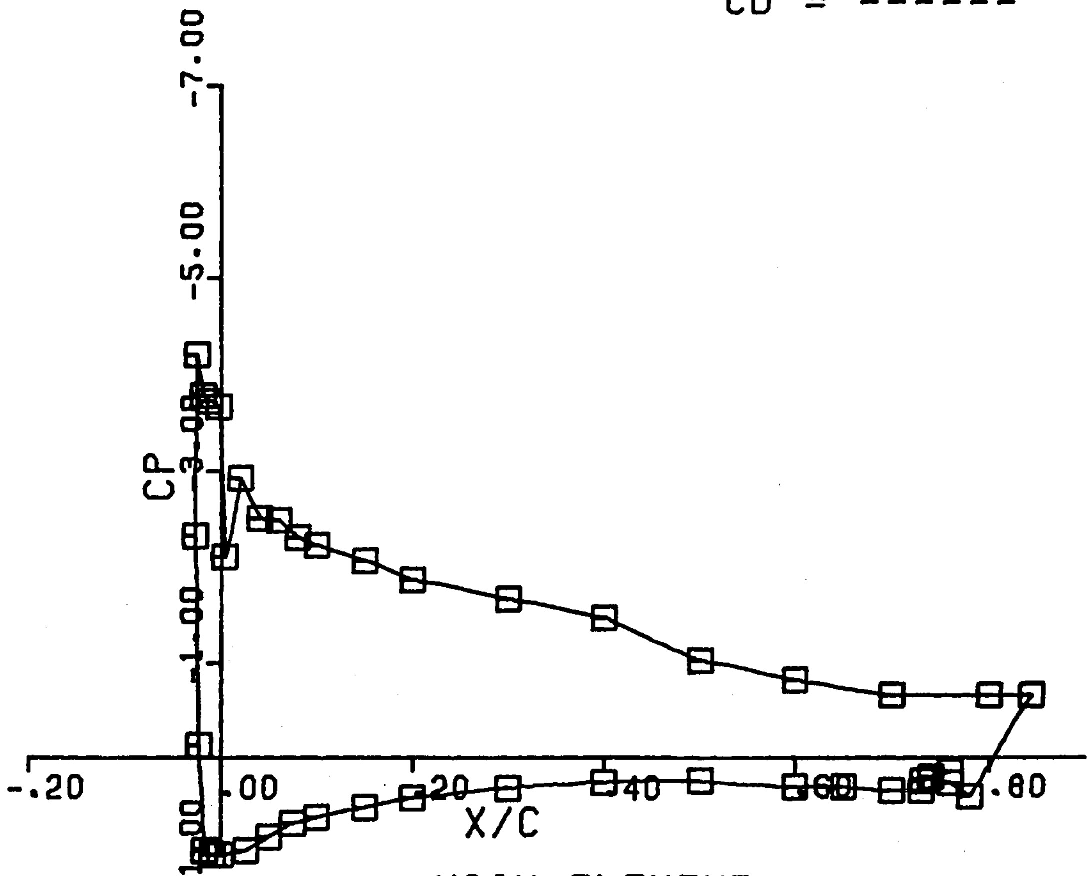

MAIN ELEMENT
CL = 1.592
CM = -0.068

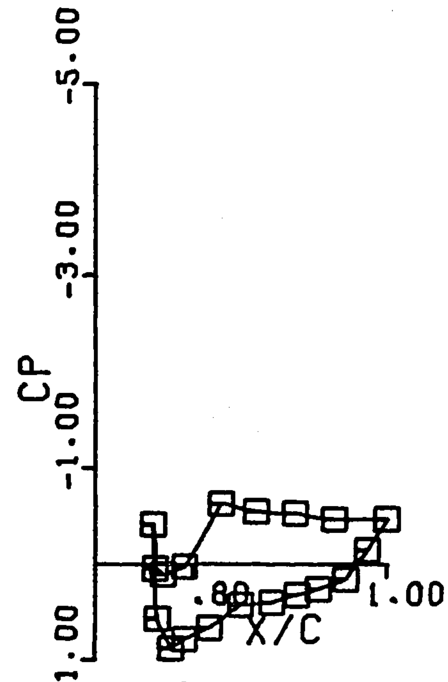

FLAP
CL = 0.158
CM = -0.122

RIME 3 ROUGH RUN # 166

AOA = 9.60
FLAP DEF = 20.00
CL = 1.752
CM = -0.173
CD = ------

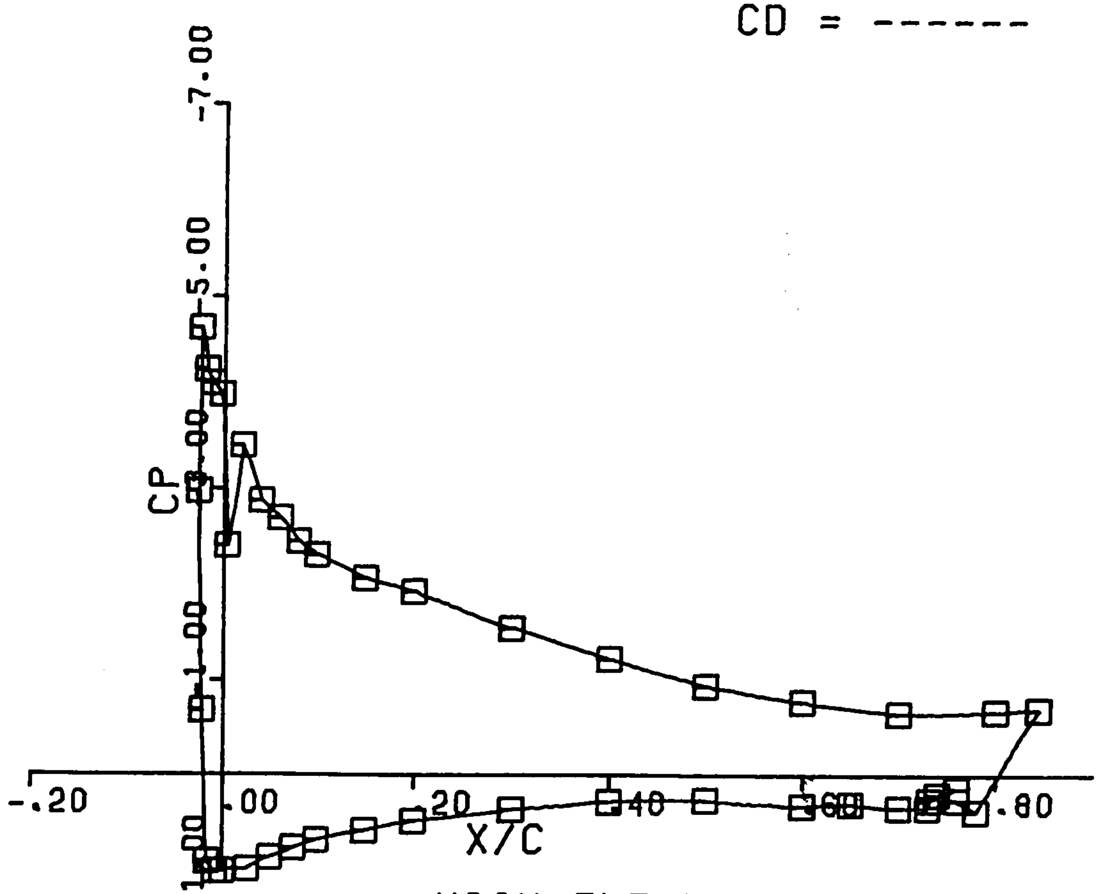

MAIN ELEMENT
CL = 1.596
CM = -0.051

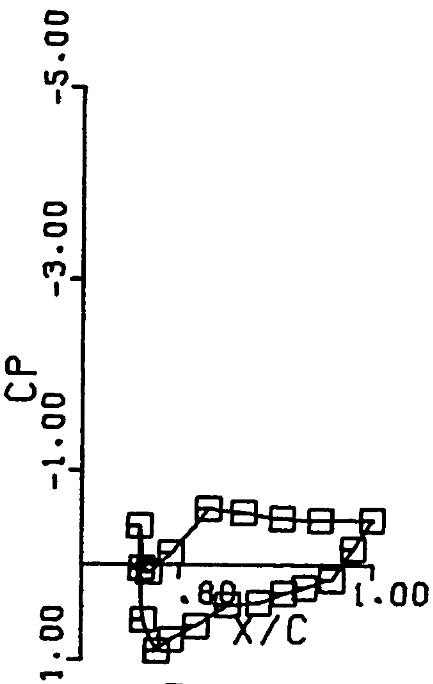

FLAP
CL = 0.156
CM = -0.122

RIME 3 ROUGH RUN # 167

AOA = 8.60
FLAP DEF = 20.00
CL = 1.704
CM = -0.176
CD = -------

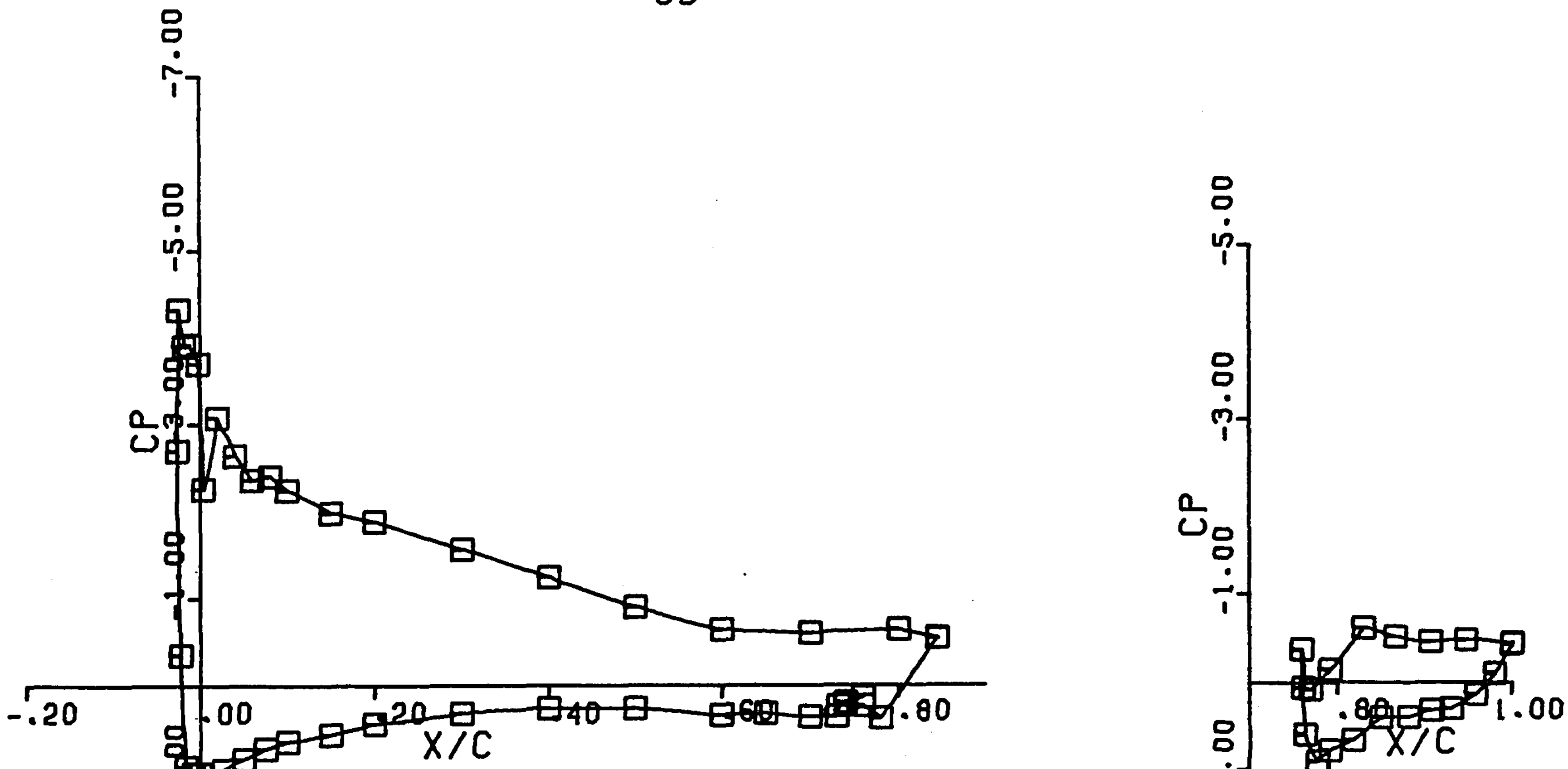

MAIN ELEMENT
CL = 1.543
CM = -0.052

FLAP
CL = 0.161
CM = -0.124

RIME 3 ROUGH RUN # 168

AOA = 6.60
FLAP DEF = 20.00
CL = 1.670
CM = -0.190
CD = ------

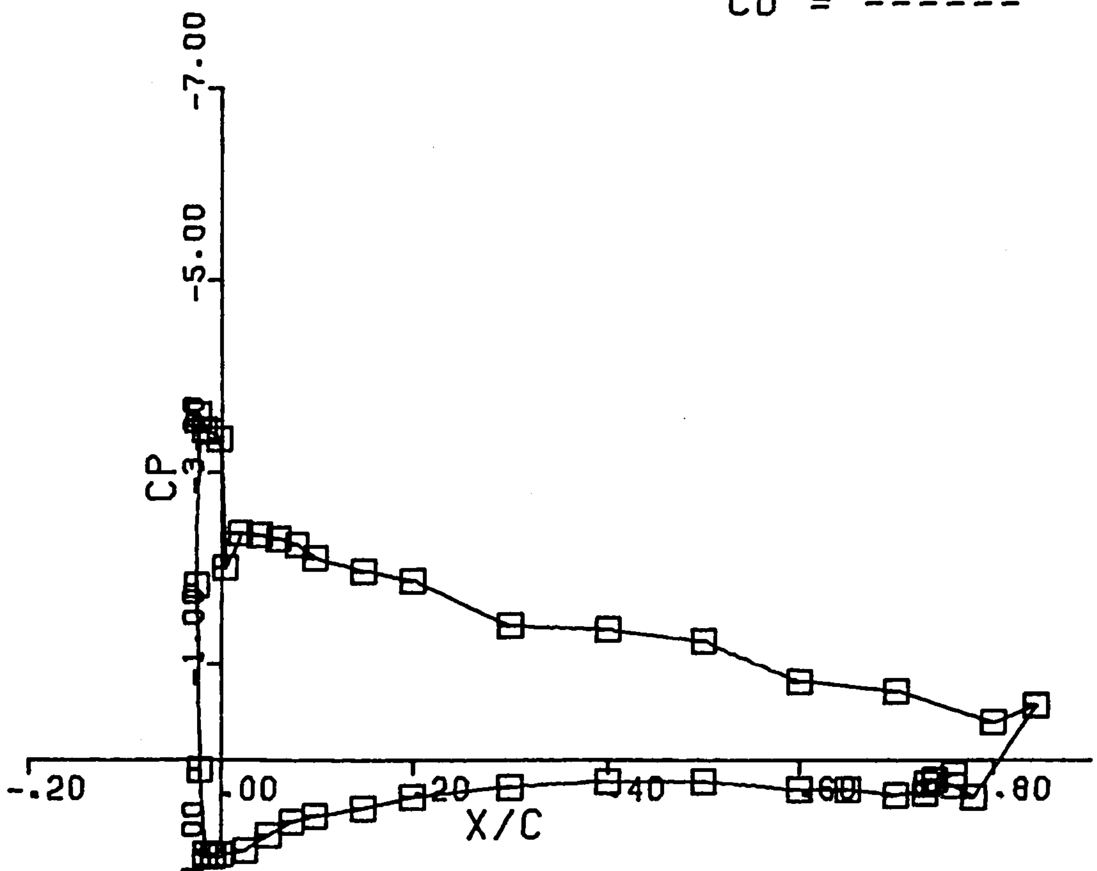

MAIN ELEMENT
CL = 1.510
CM = -0.071

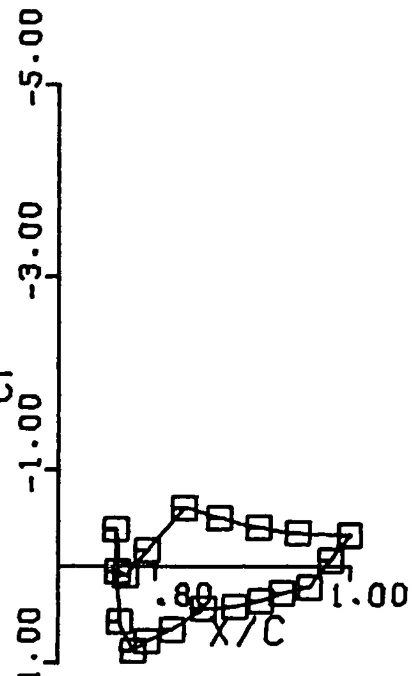

FLAP
CL = 0.160
CM = -0.120

RIME 3 RØUGH RUN # 169

AØA = -6.40
FLAP DEF = 10.00
CL = -0.073
CM = -0.110
CD = ------

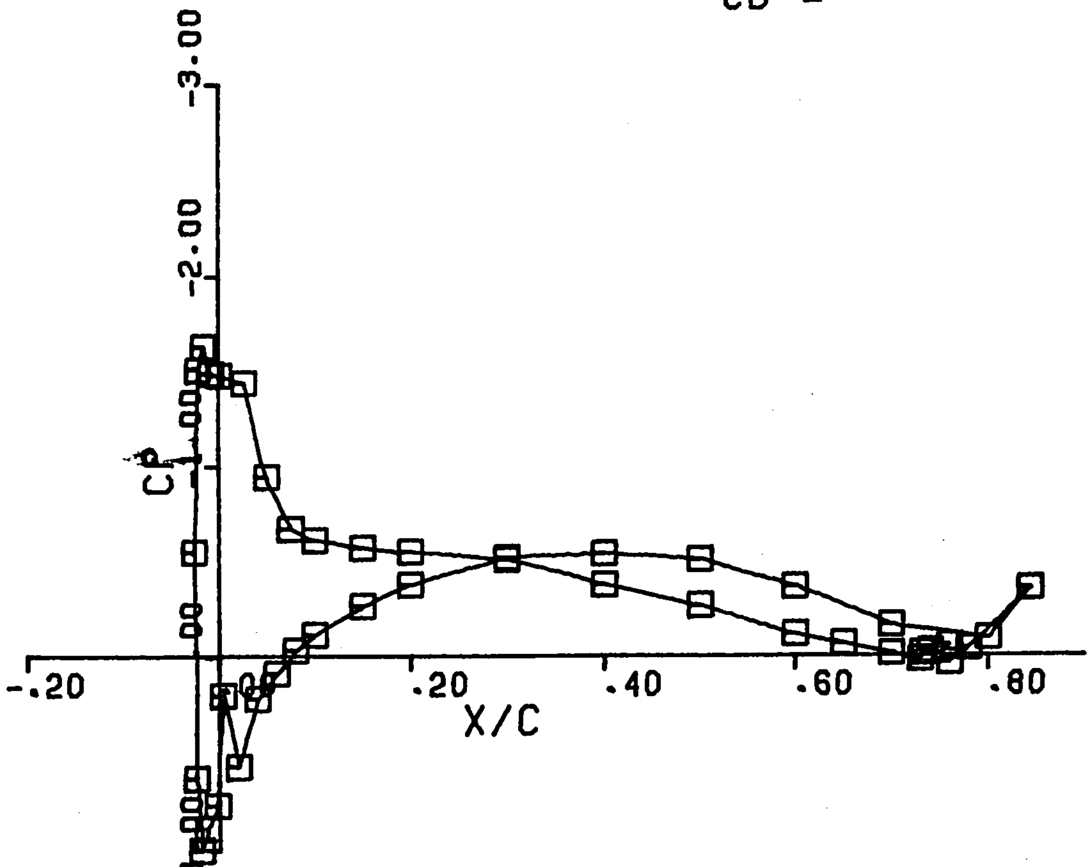

MAIN ELEMENT
CL = -0.142
CM = -0.066

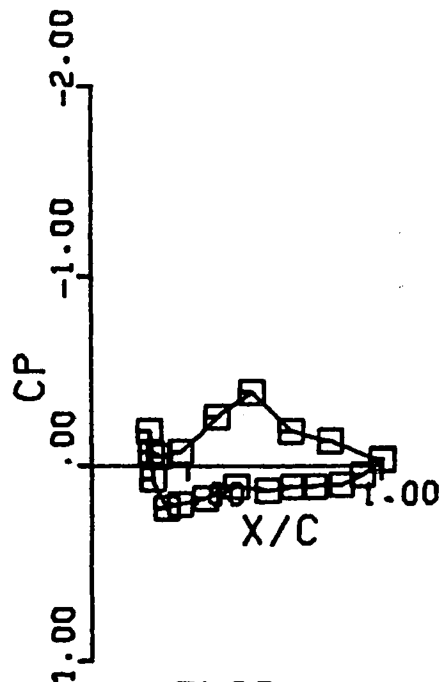

FLAP
CL = 0.069
CM = -0.044

RIME 3 RØUGH RUN # 170

AØA = -2.40
FLAP DEF = 10.00
CL = 0.418
CM = -0.120
CD = ------

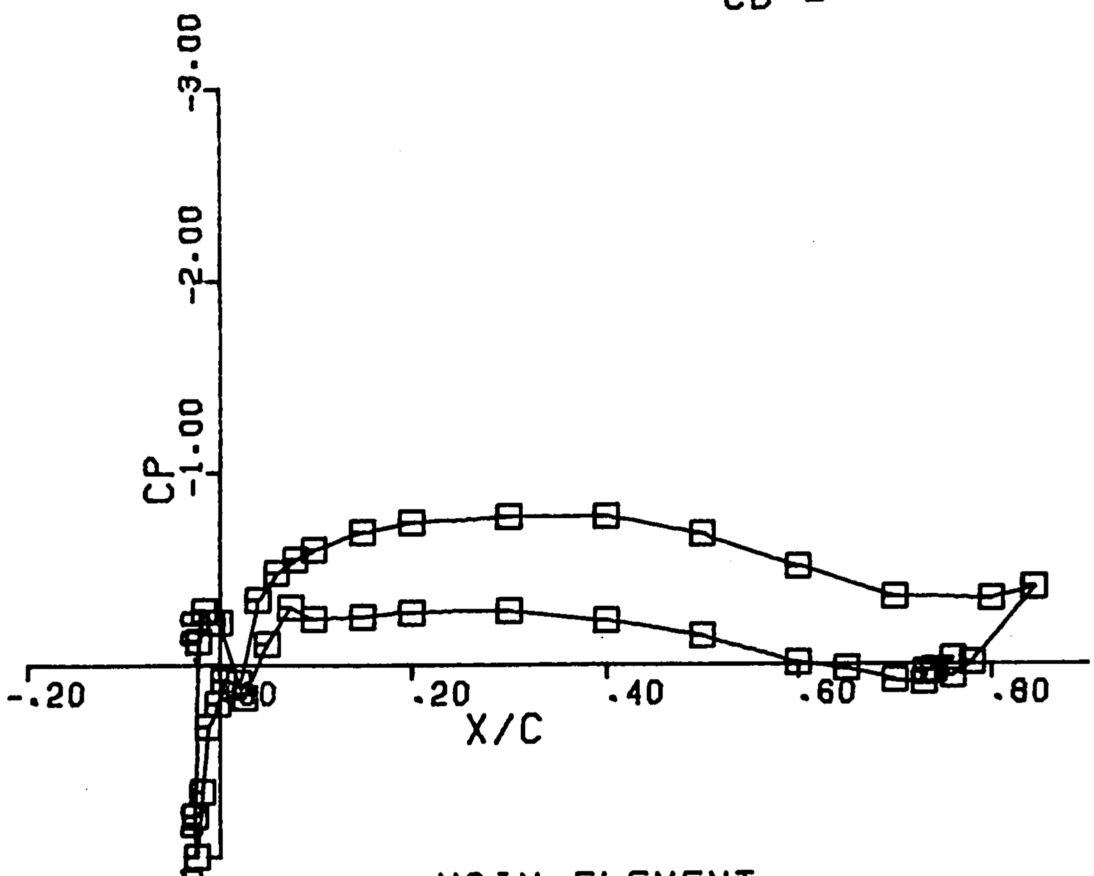

MAIN ELEMENT
CL = 0.337
CM = -0.068

FLAP
CL = 0.081
CM = -0.052

RIME 3 ROUGH RUN # 171

AOA = 1.60
FLAP DEF = 10.00
CL = 0.890
CM = -0.116
CD = ------

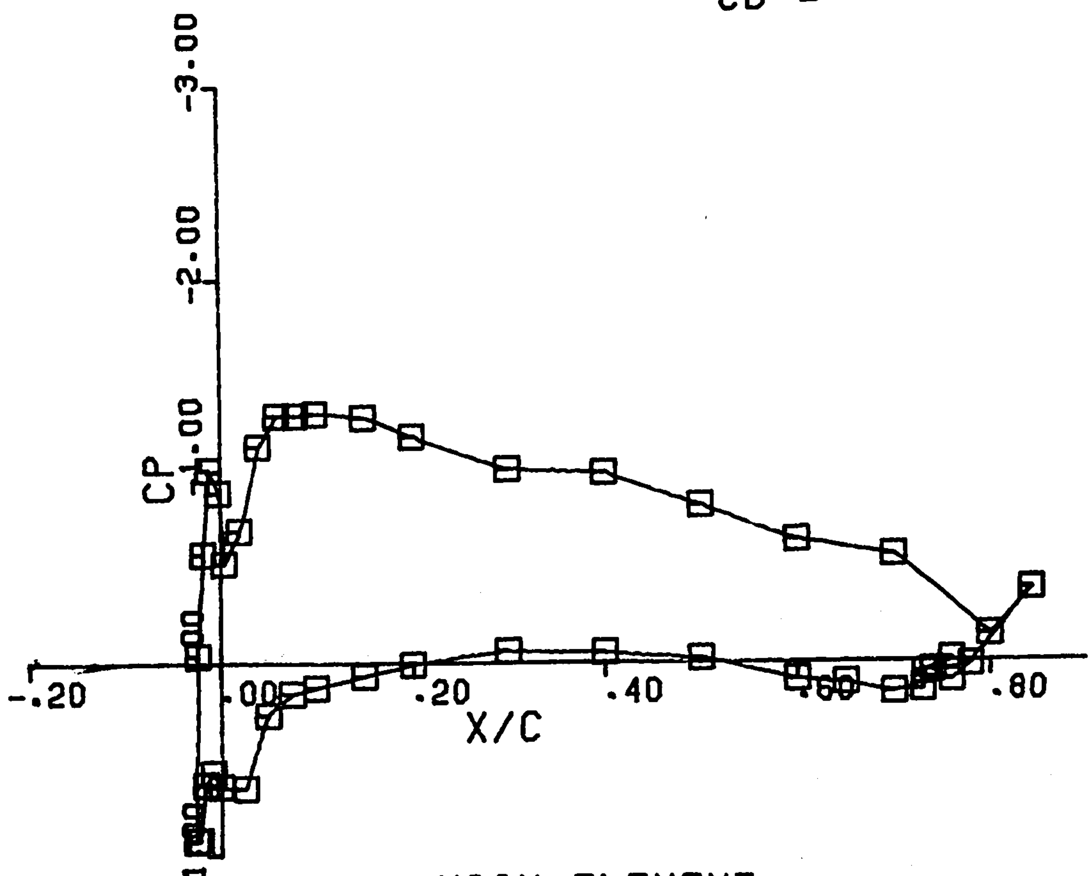

MAIN ELEMENT
CL = 0.791
CM = -0.052

FLAP
CL = 0.099
CM = -0.064

RIME 3 ROUGH RUN # 172

AOA = 5.60
FLAP DEF = 10.00
CL = 1.216
CM = -0.109
CD = ------

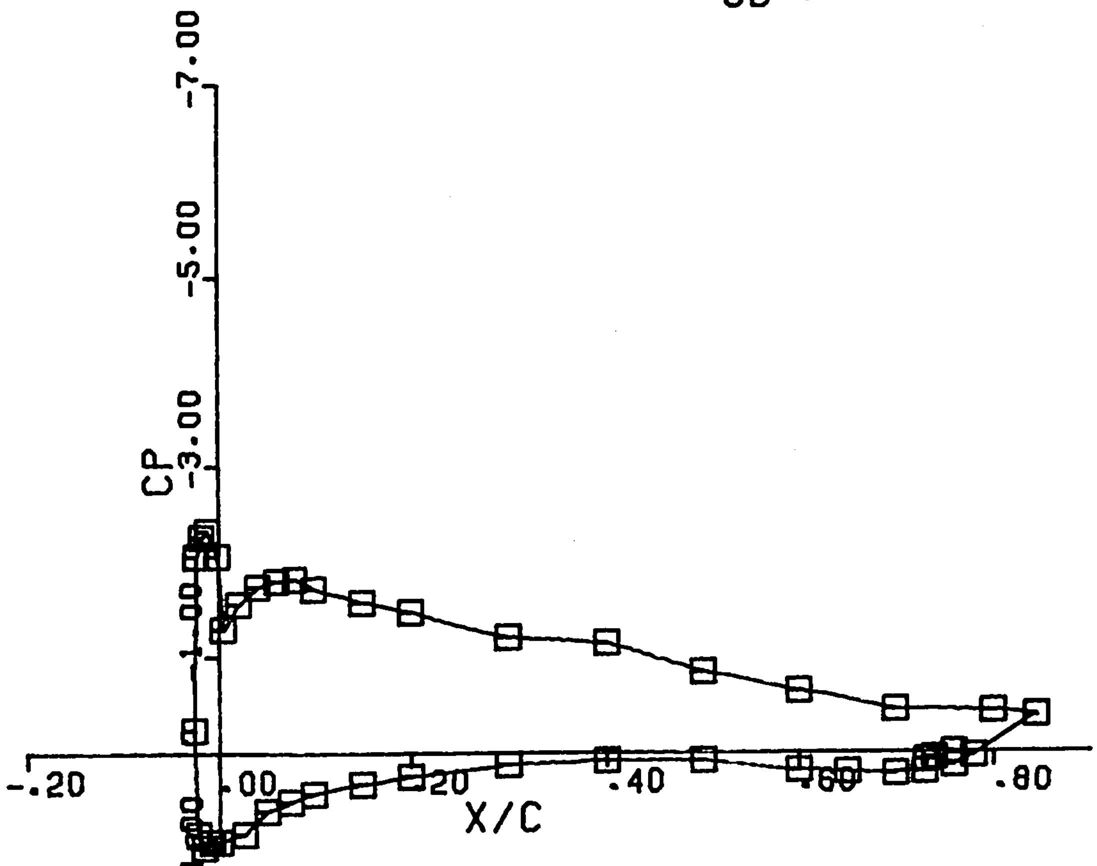

MAIN ELEMENT
CL = 1.112
CM = -0.040

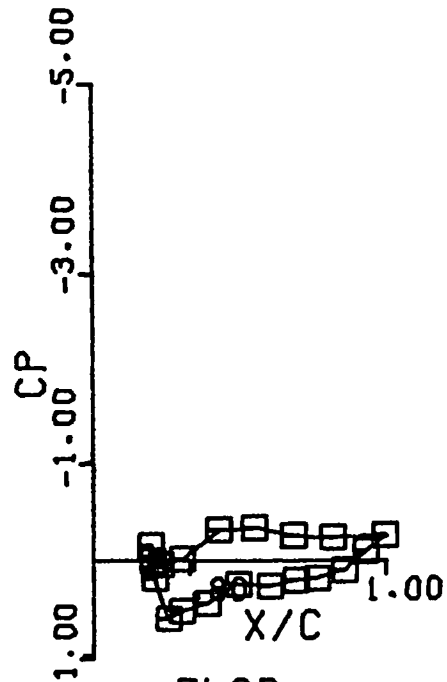

FLAP
CL = 0.104
CM = -0.069

RIME 3 ROUGH RUN # 173

AOA = 7.60
FLAP DEF = 10.00
CL = 1.393
CM = -0.111
CD = -------

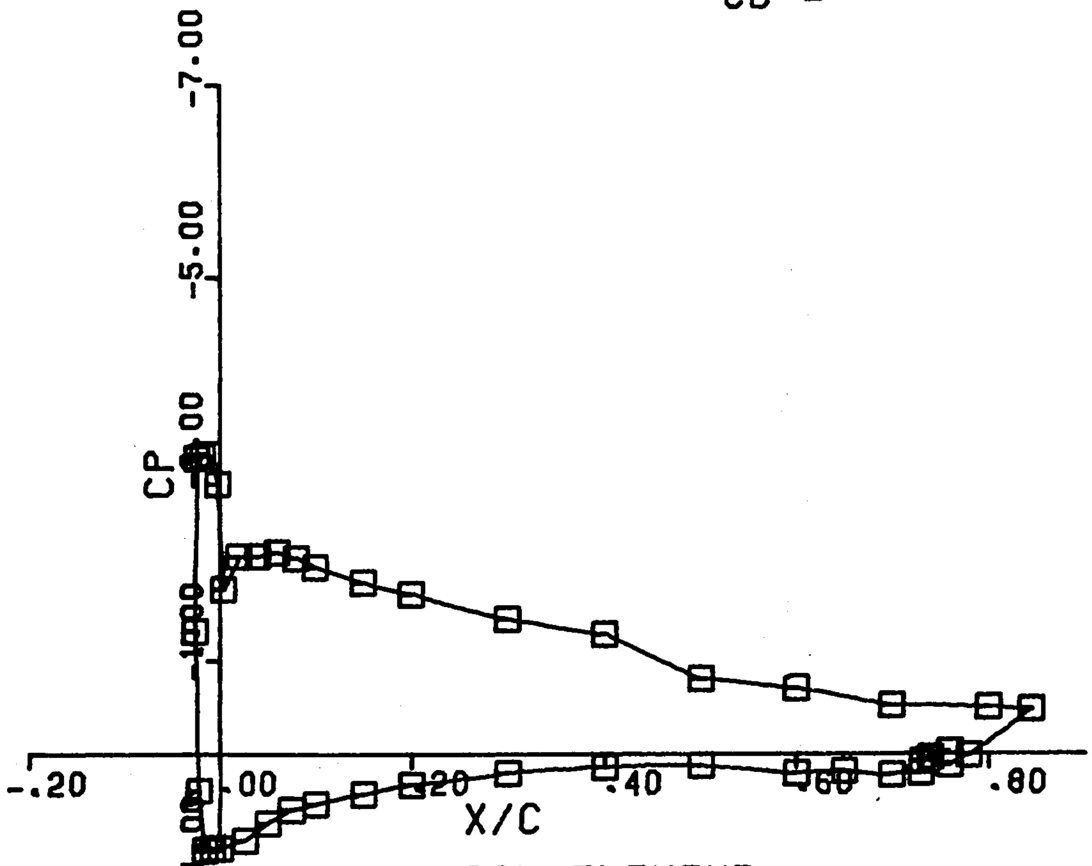

MAIN ELEMENT
CL = 1.277
CM = -0.032

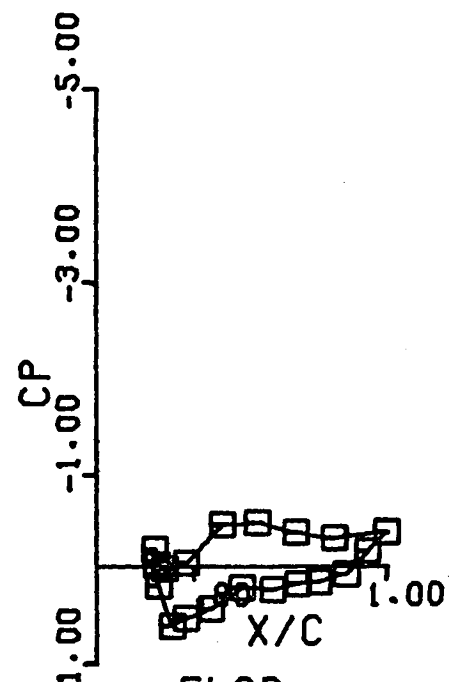

FLAP
CL = 0.116
CM = -0.078

RIME 3 ROUGH RUN # 174

AOA = 9.60
FLAP DEF = 10.00
CL = 1.424
CM = -0.088
CD = ------

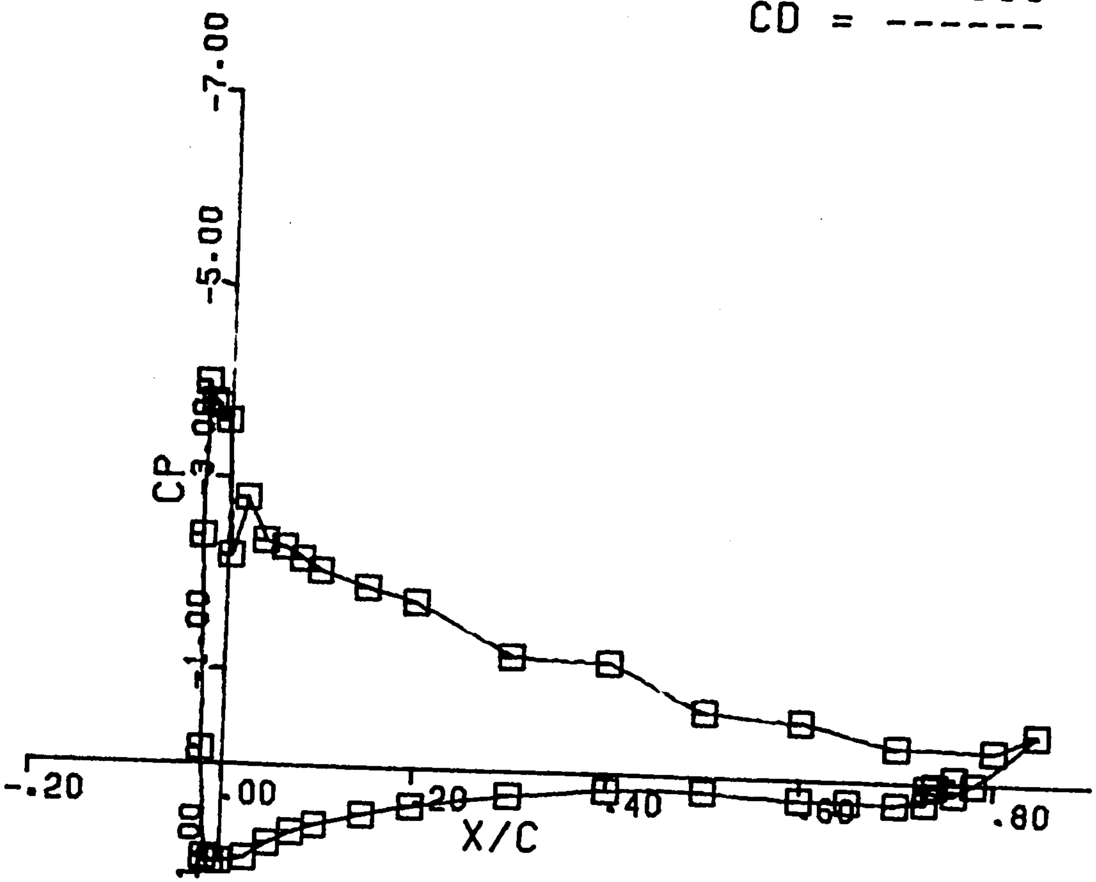

MAIN ELEMENT
CL = 1.299
CM = -0.002

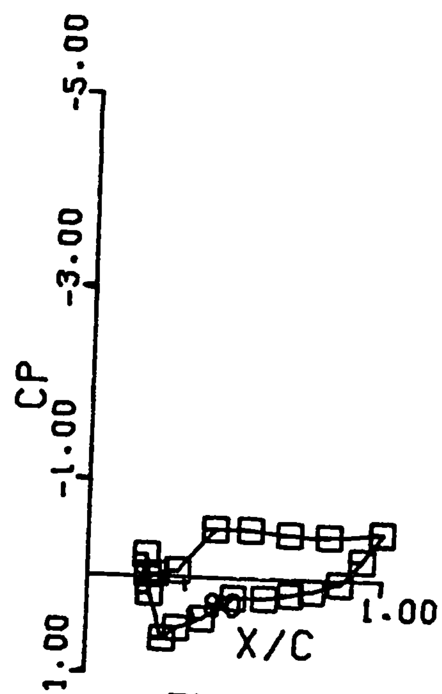

FLAP
CL = 0.125
CM = -0.087

RIME 3 RØUGH RUN # 175

AØA = 10.60
FLAP DEF = 10.00
CL = 1.516
CM = -0.098
CD = ------

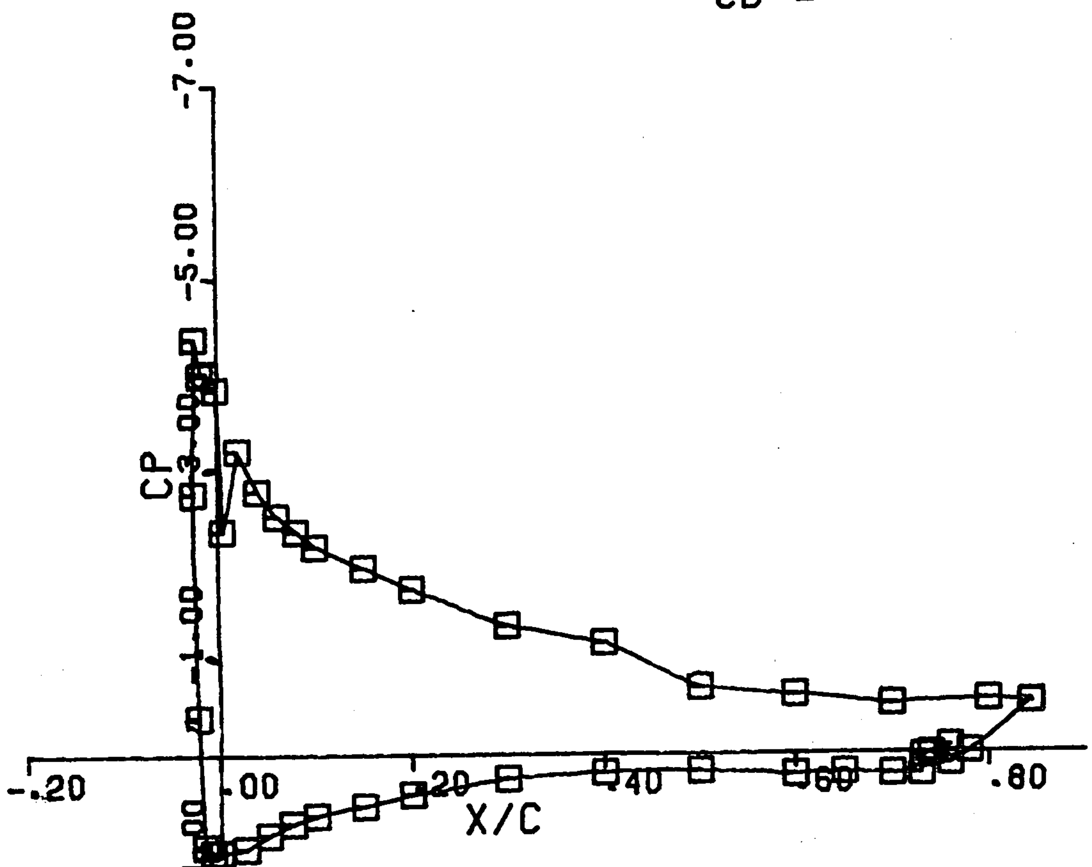

MAIN ELEMENT
CL = 1.392
CM = -0.011

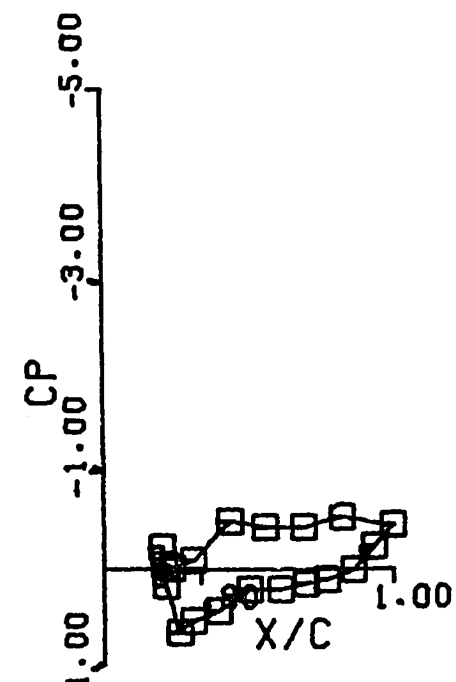

FLAP
CL = 0.125
CM = -0.087

RIME 3 RØUGH RUN # 176

AØA = 11.60
FLAP DEF = 10.00
CL = 1.480
CM = -0.093
CD = ------

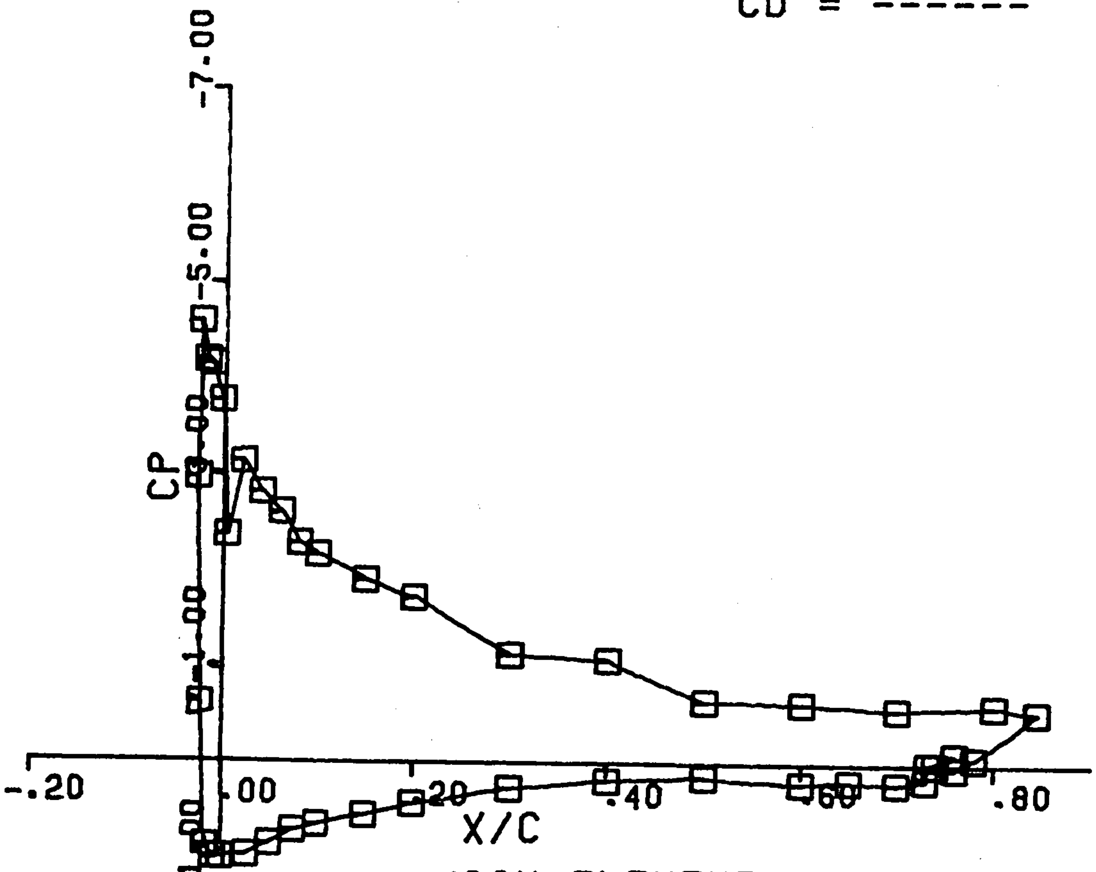

MAIN ELEMENT
CL = 1.355
CM = -0.005

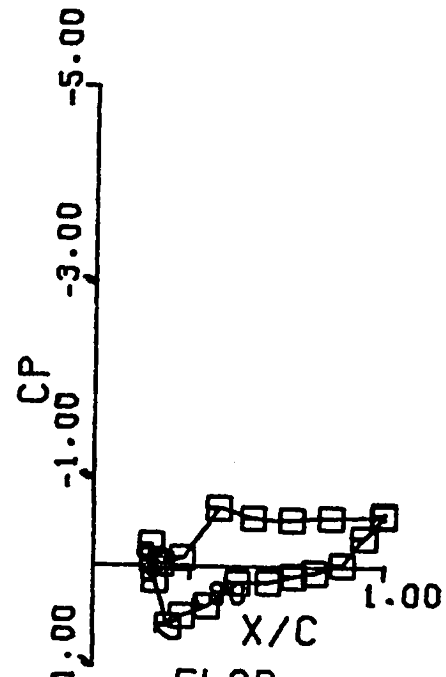

FLAP
CL = 0.125
CM = -0.088

GLAZE 3 ROUGH RUN # 71

AOA = -2.40
FLAP DEF = 0.00
CL = 0.082
CM = -0.050
CD = 0.016

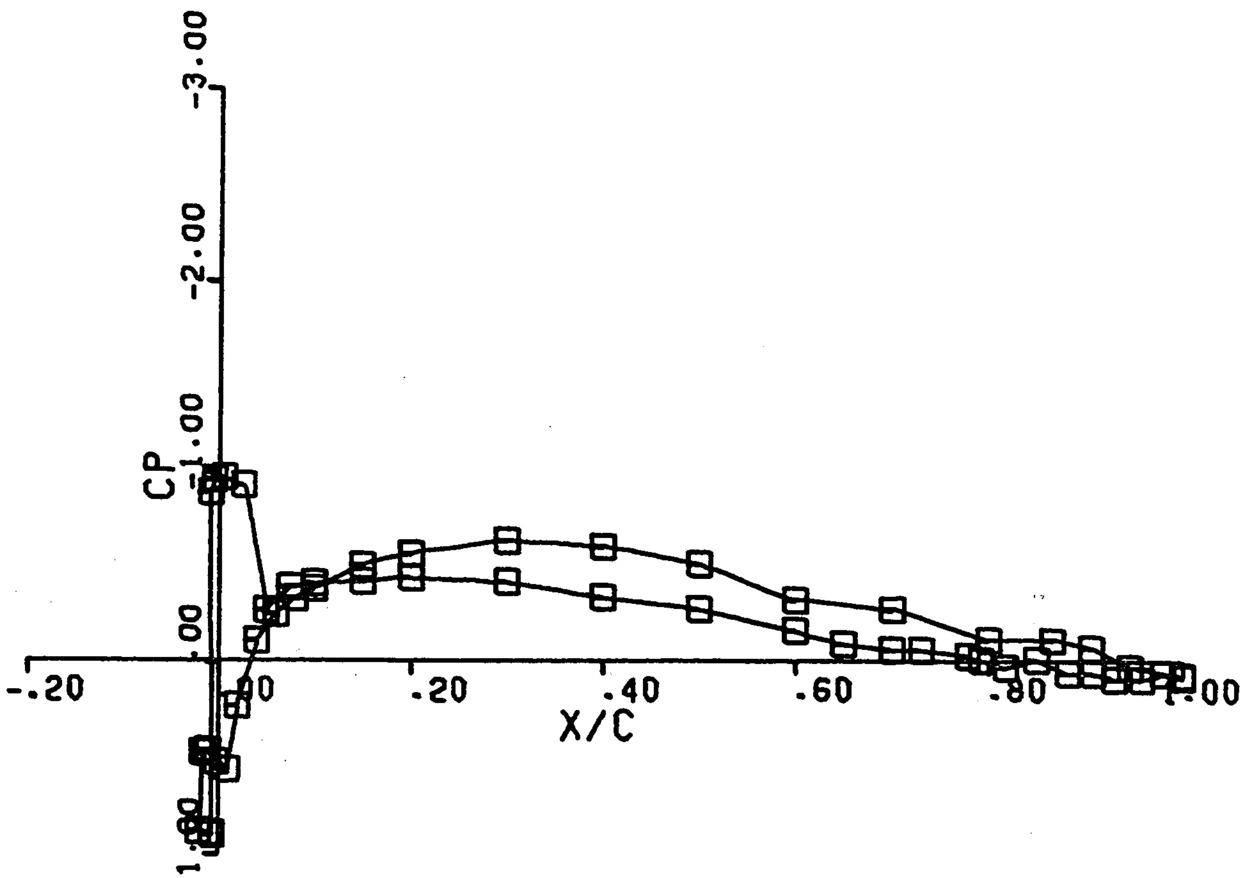

GLAZE 3 ROUGH RUN # 72

AOA = -0.40
FLAP DEF = 0.00
CL = 0.306
CM = -0.050
CD = 0.015

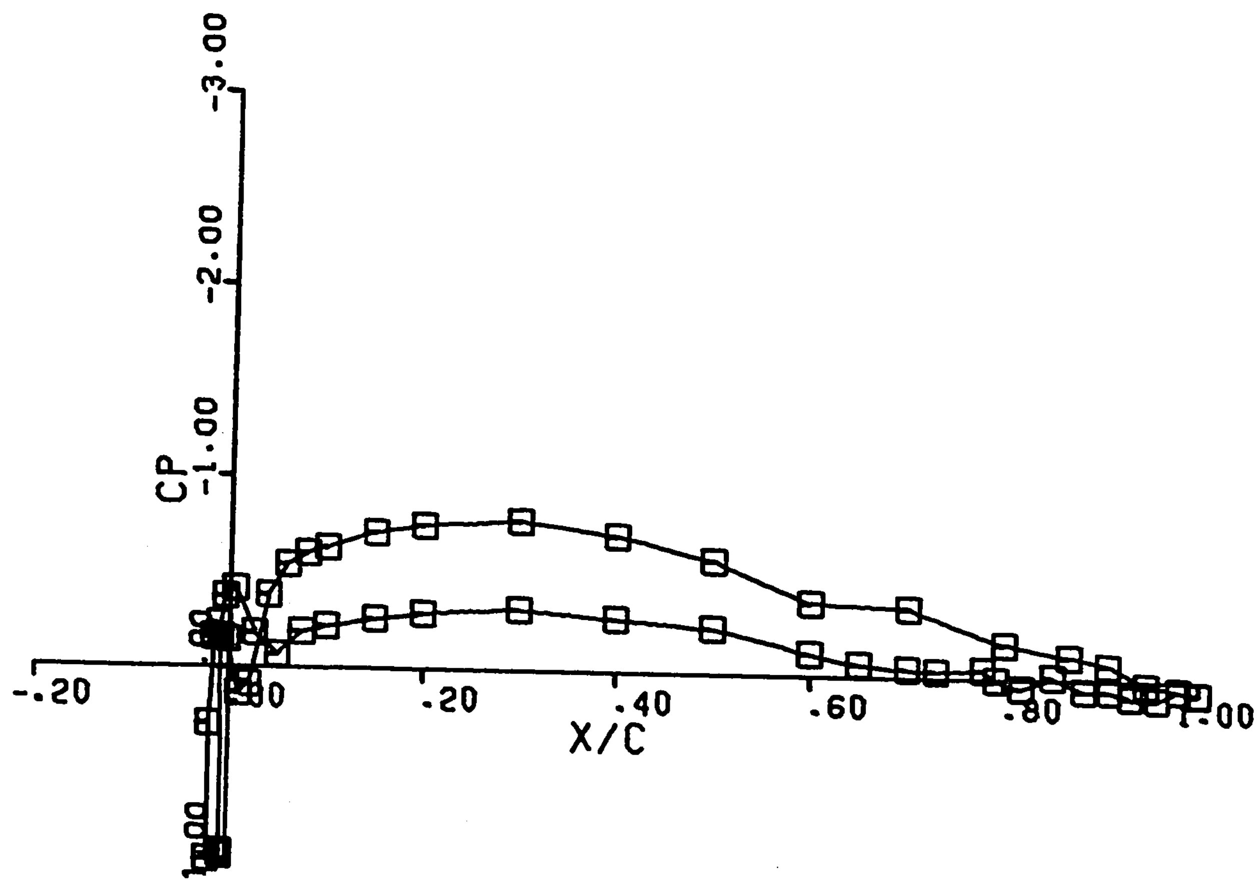

GLAZE 3 ROUGH RUN # 73

AOA = 1.60
FLAP DEF = 0.00
CL = 0.528
CM = -0.040
CD = 0.016

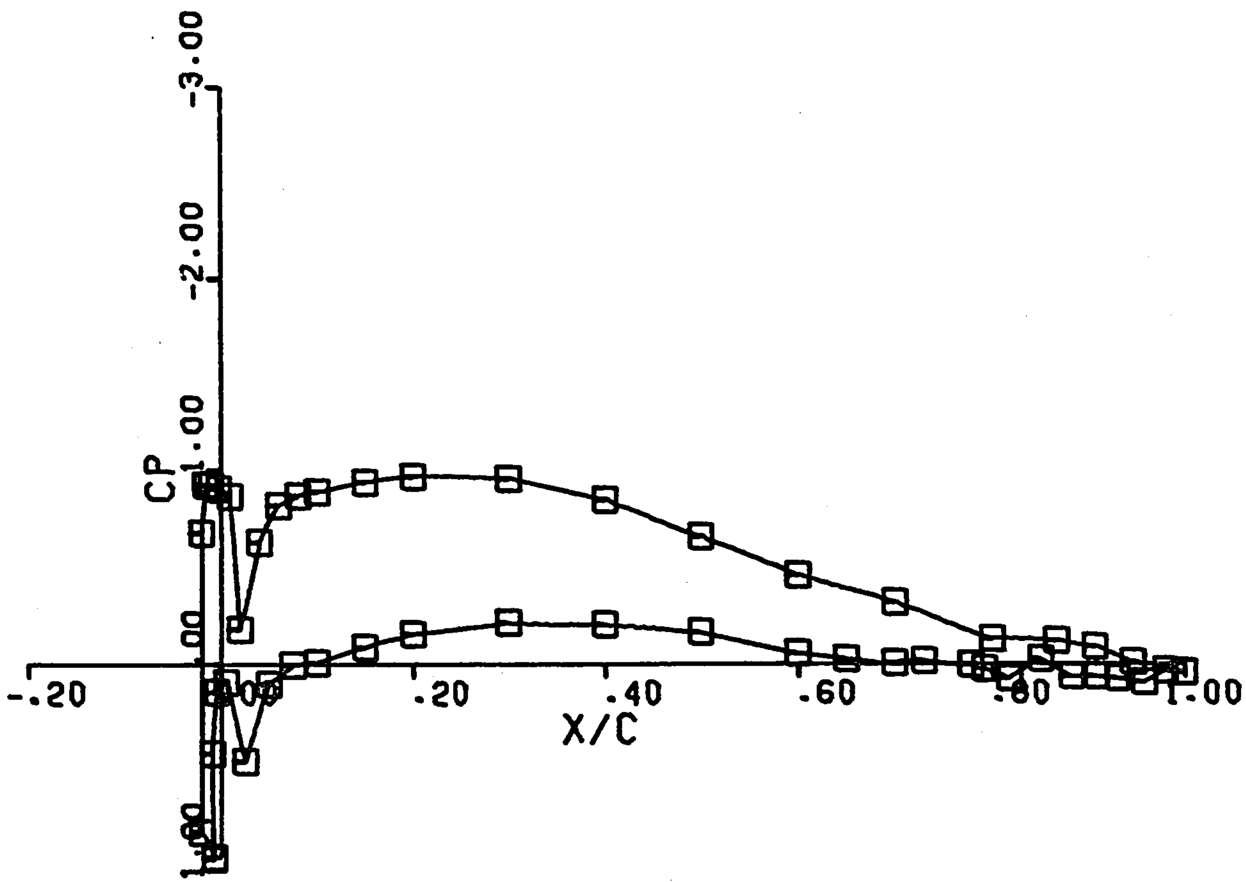

GLAZE 3 ROUGH RUN # 74

AOA = 3.60
FLAP DEF = 0.00
CL = 0.752
CM = -0.044
CD = 0.023

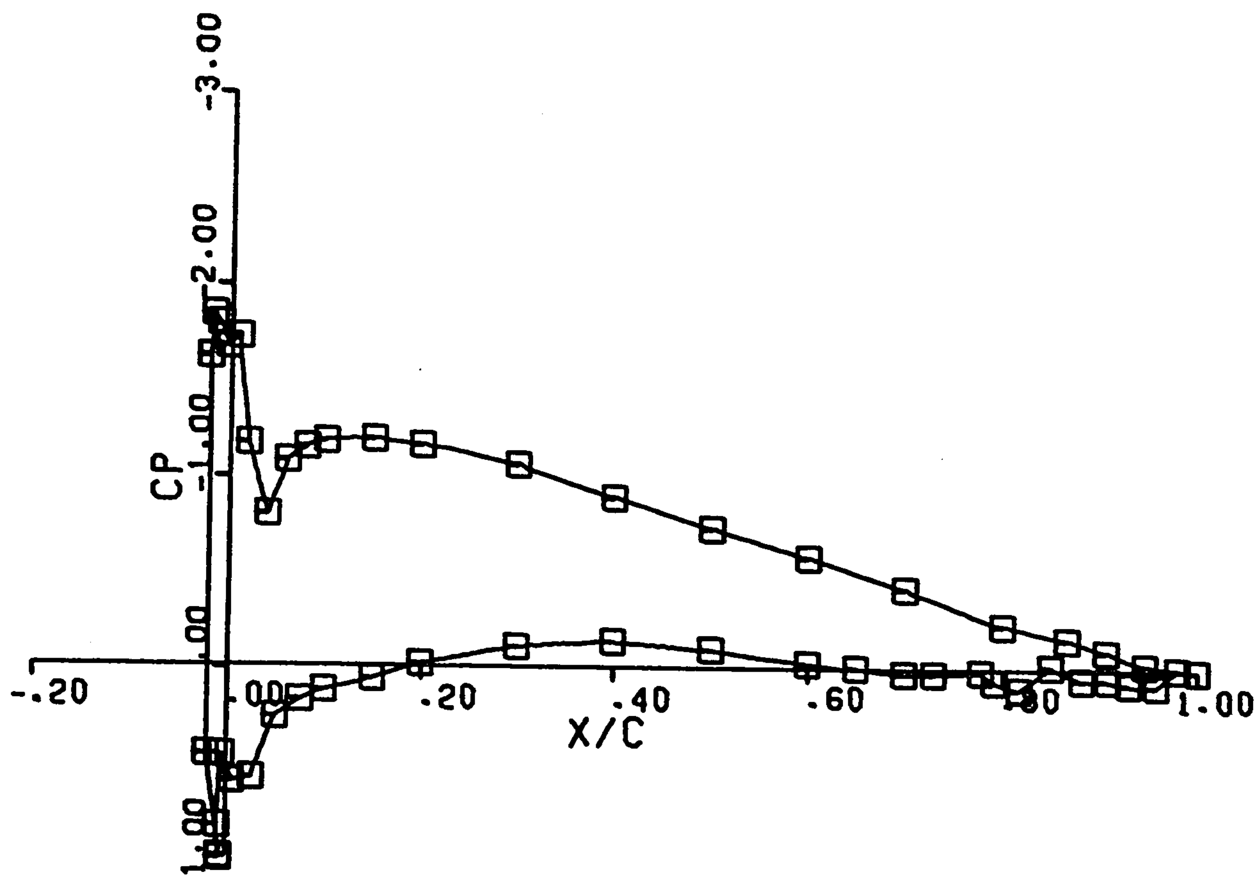

GLAZE 3 ROUGH RUN # 75

AOA = 5.60
FLAP DEF = 0.00
CL = 0.893
CM = -0.025
CD = 0.032

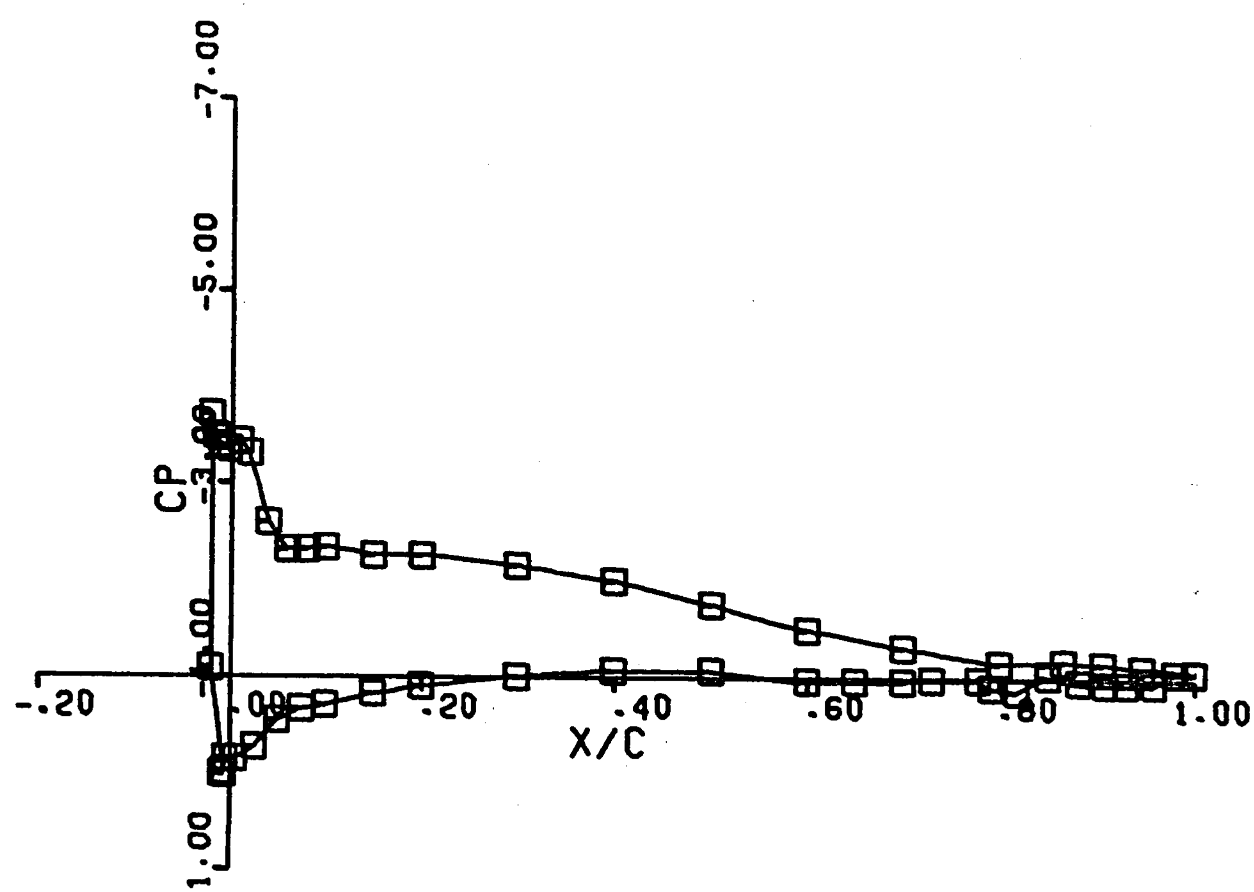

GLAZE 3 ROUGH RUN # 140

AOA = -6.40
FLAP DEF = 10.00
CL = -0.055
CM = -0.118
CD = ------

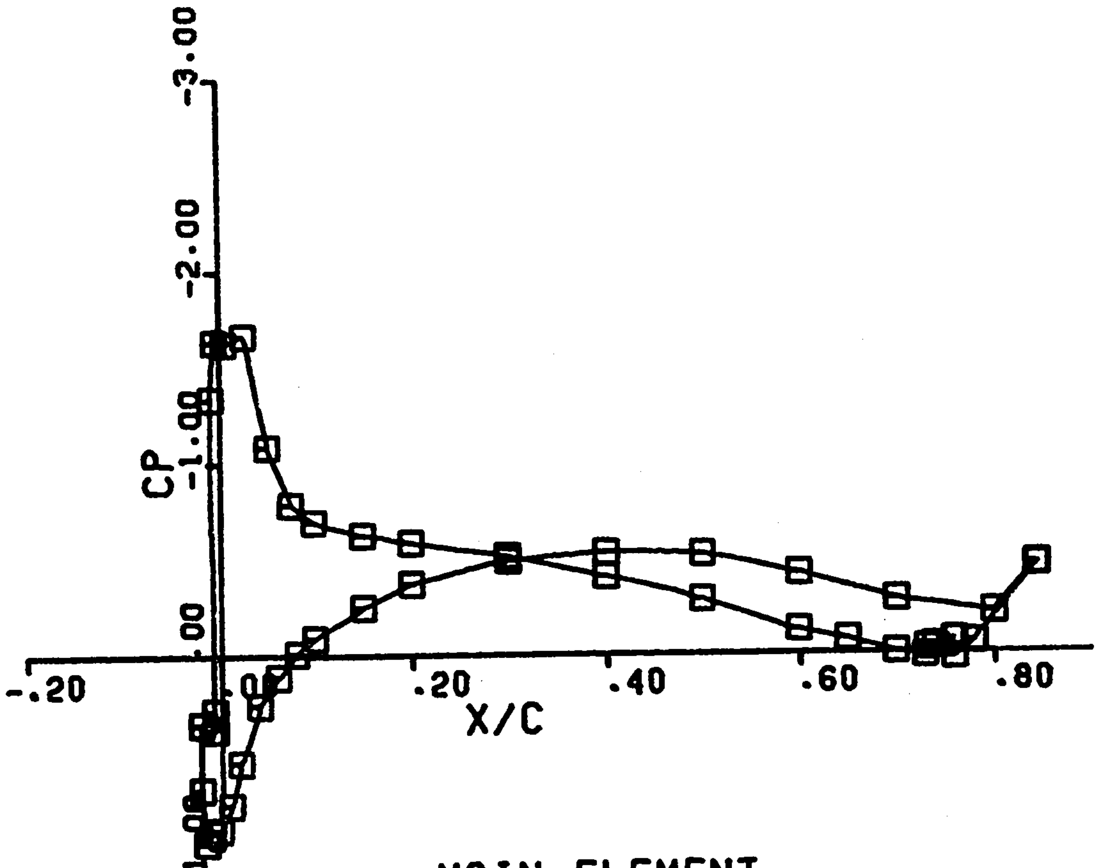

MAIN ELEMENT
CL = -0.126
CM = -0.073

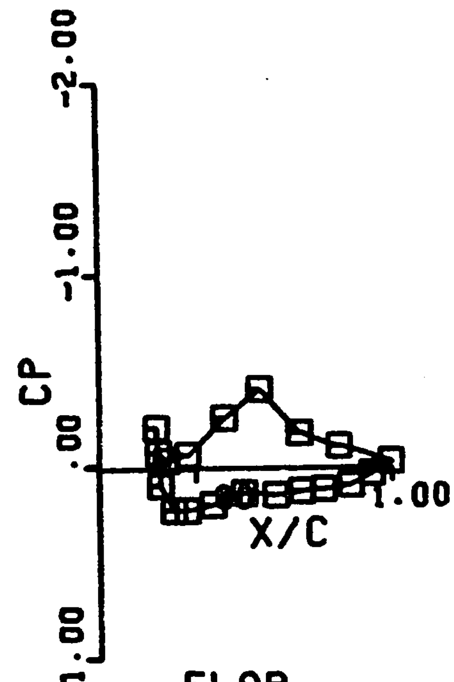

FLAP
CL = 0.071
CM = -0.045

GLAZE 3 ROUGH RUN # 141

AOA = -2.40
FLAP DEF = 10.00
CL = 0.388
CM = -0.123
CD = ------

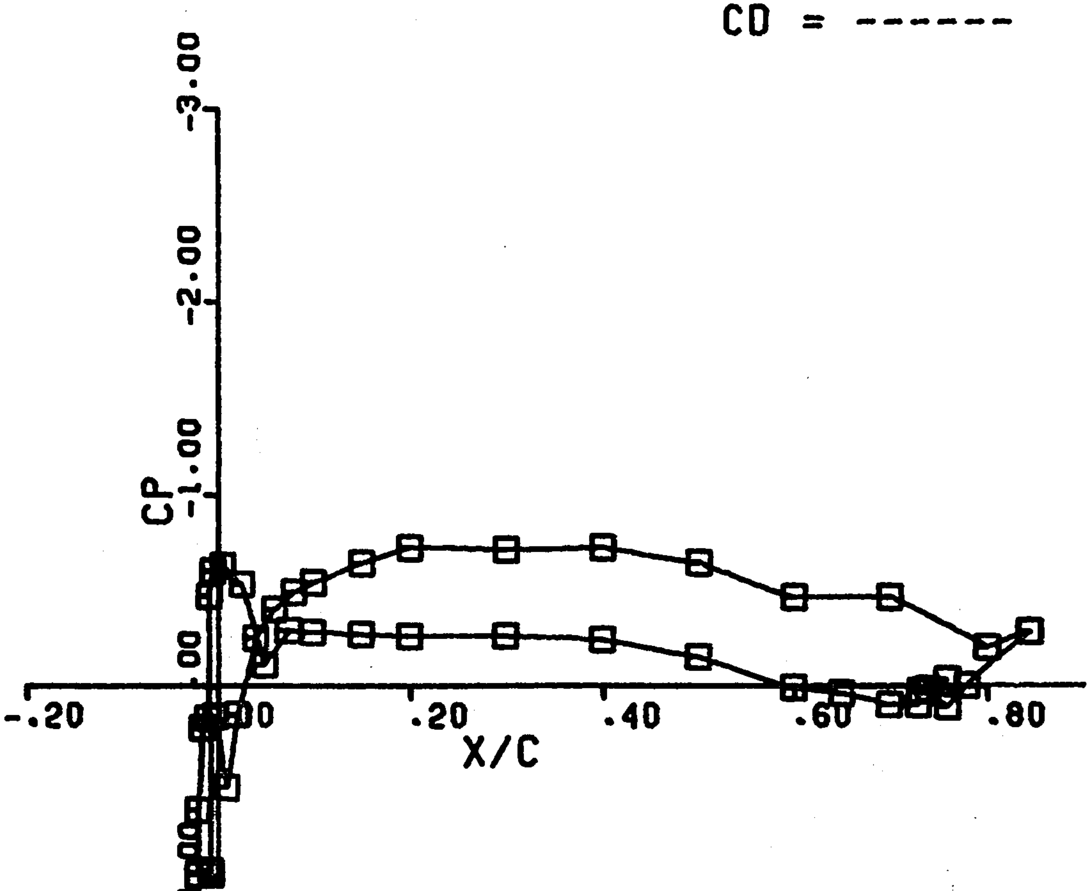

MAIN ELEMENT
CL = 0.303
CM = -0.069

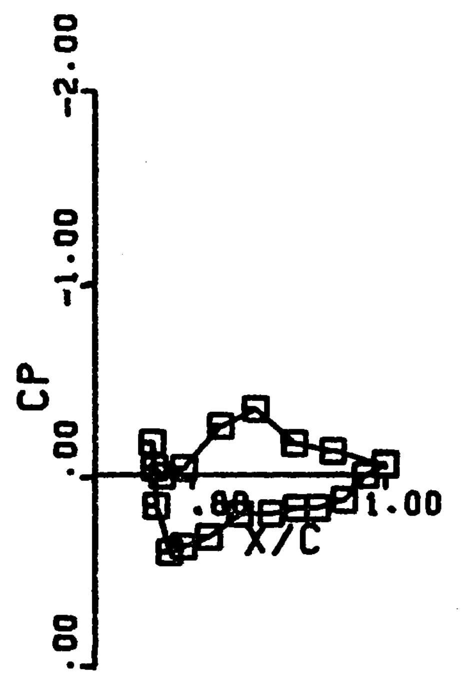

FLAP
CL = 0.085
CM = -0.054

GLAZE 3 ROUGH RUN # 142

AOA = 1.60
FLAP DEF = 10.00
CL = 0.891
CM = -0.108
CD = ------

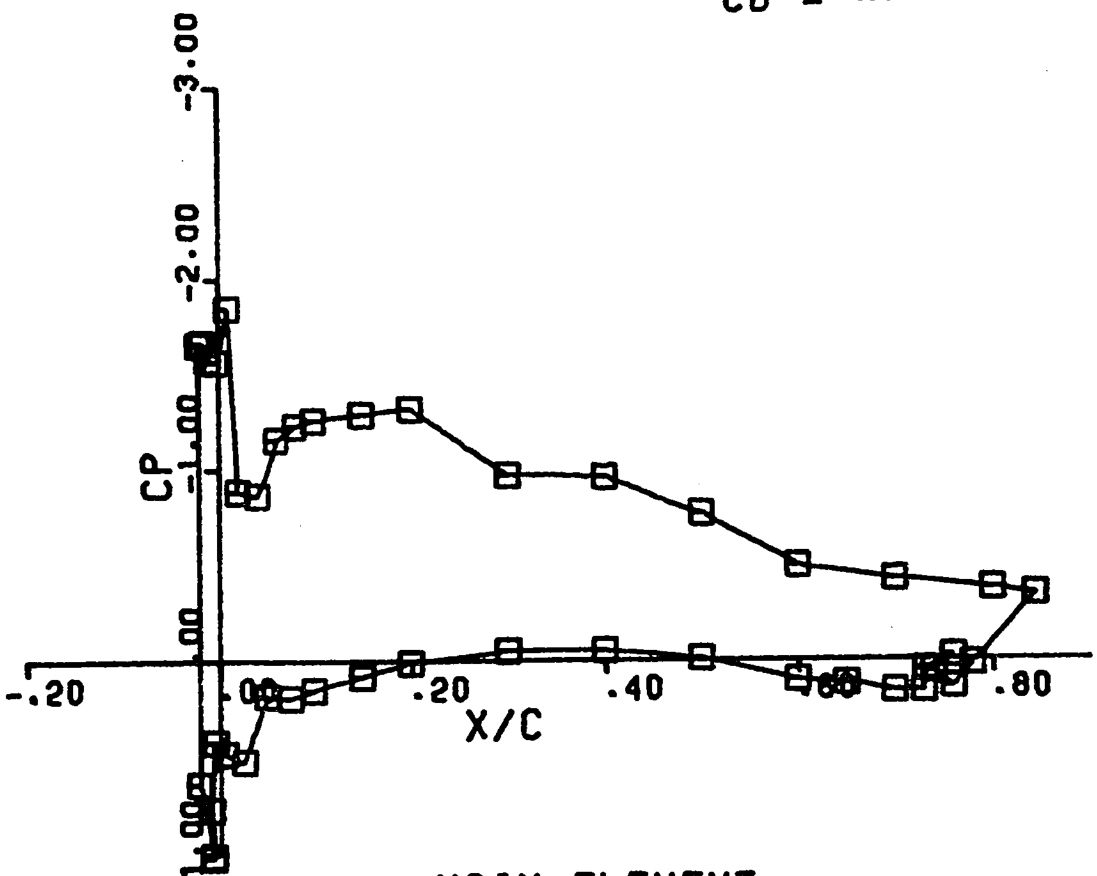

MAIN ELEMENT
CL = 0.791
CM = -0.045

FLAP
CL = 0.099
CM = -0.063

GLAZE 3 ROUGH RUN # 143

AOA = 5.60
FLAP DEF = 10.00
CL = 1.235
CM = -0.094
CD = ------

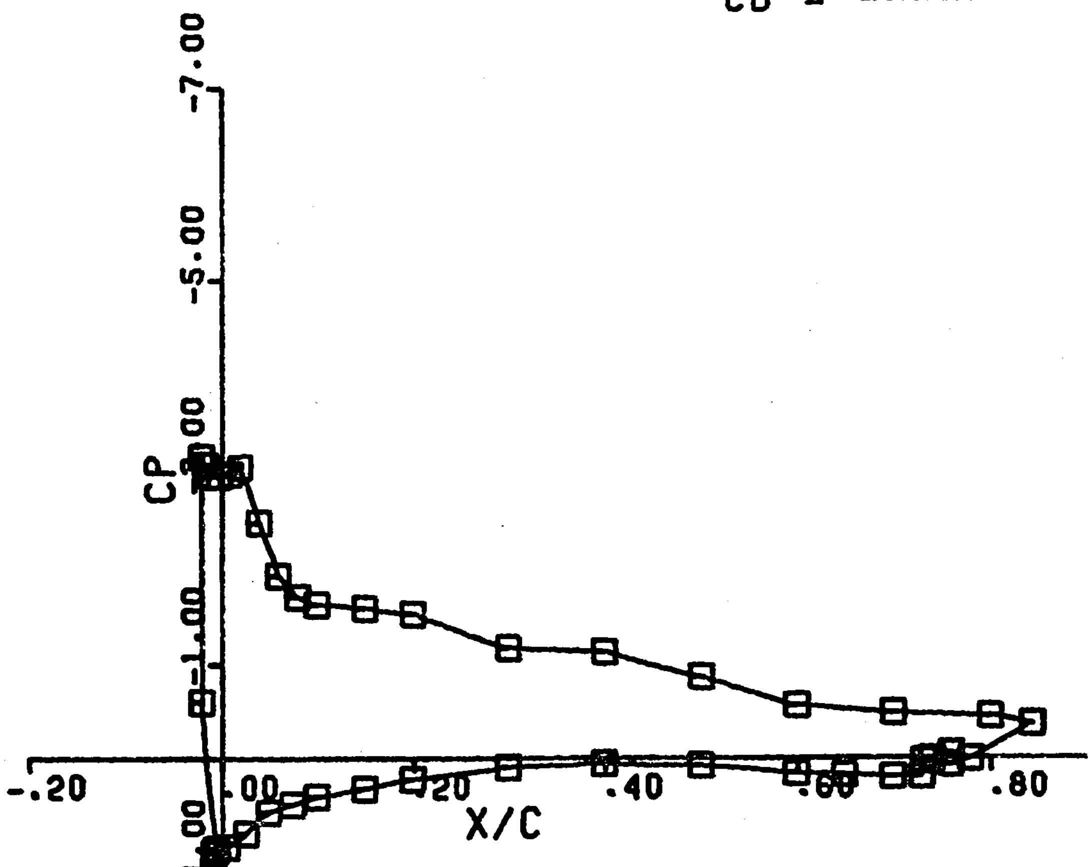

MAIN ELEMENT
CL = 1.131
CM = -0.025

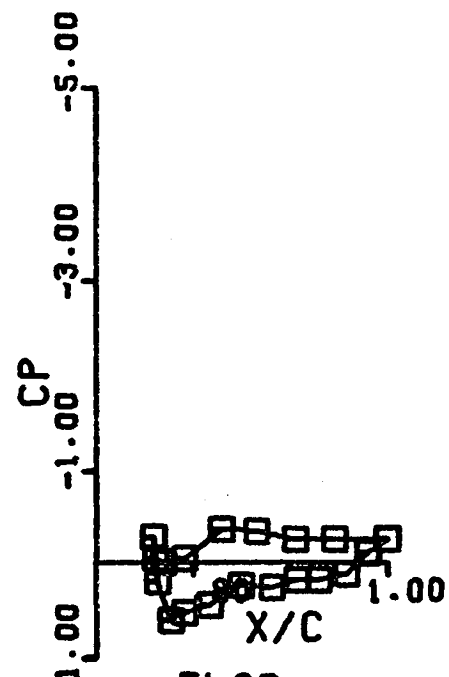

FLAP
CL = 0.104
CM = -0.069

GLAZE 3 ROUGH RUN # 144

AOA = 7.60
FLAP DEF = 10.00
CL = 1.346
CM = -0.089
CD = -------

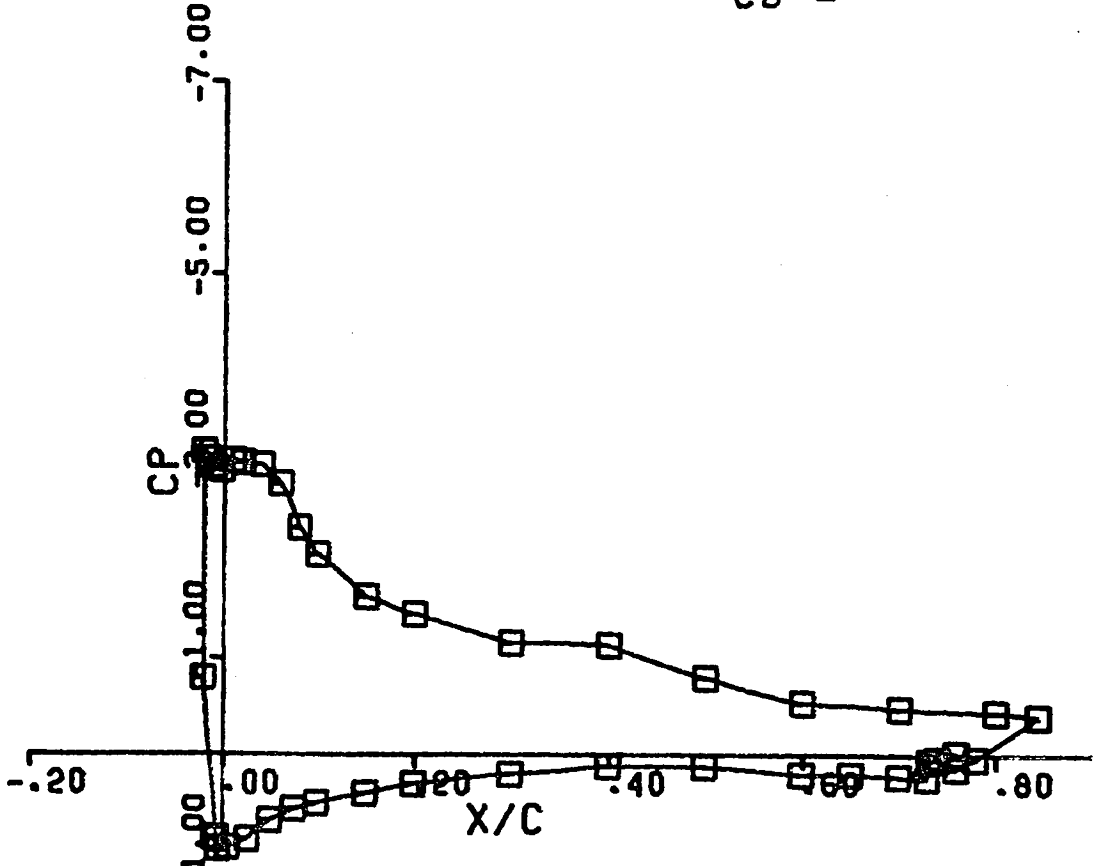

MAIN ELEMENT
CL = 1.241
CM = -0.018

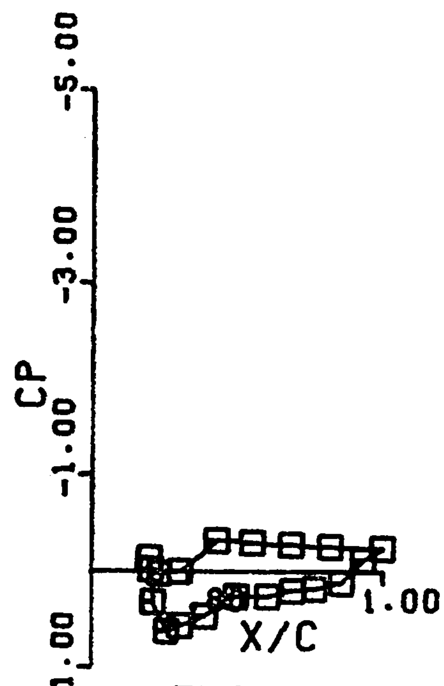

FLAP
CL = 0.105
CM = -0.070

GLAZE 3 ROUGH RUN = 145

AOA = 9.60
FLAP DEF = 10.00
CL = 1.389
CM = -0.089
CD = ------

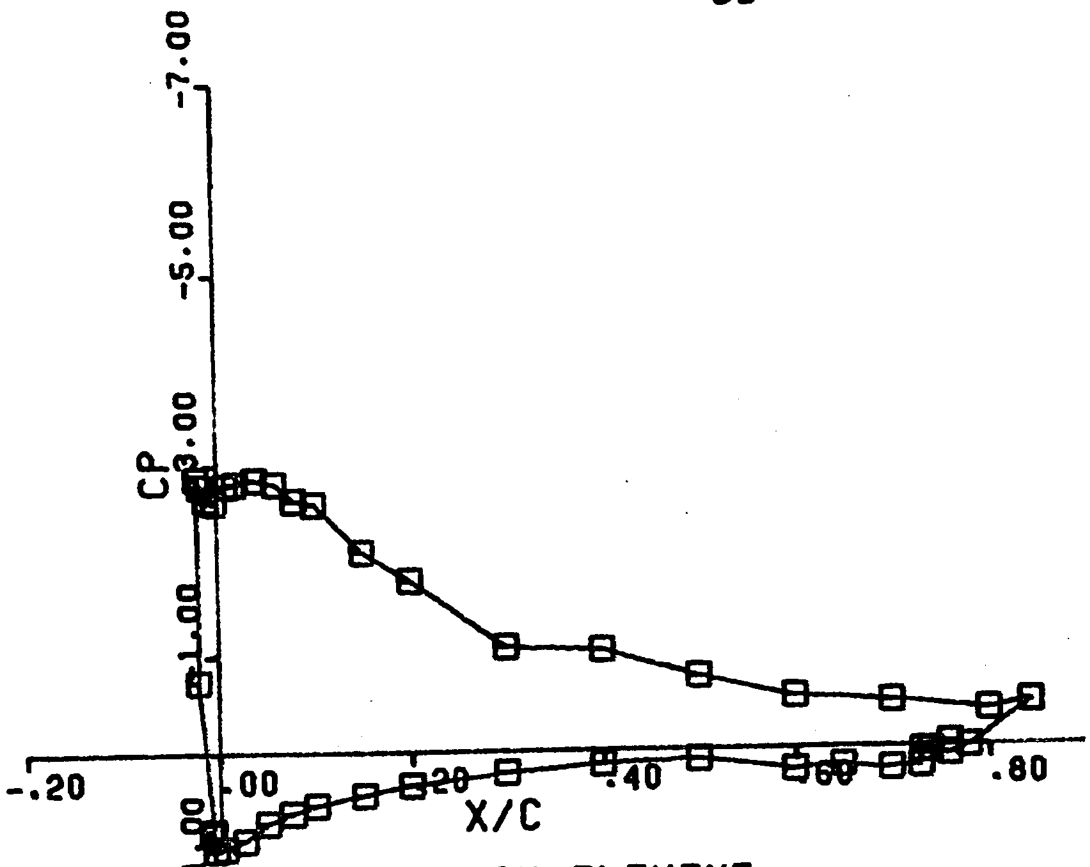

MAIN ELEMENT
CL = 1.275
CM = -0.010

FLAP
CL = 0.114
CM = -0.078

GLAZE 3 ROUGH RUN # 146

AOA = 10.60
FLAP DEF = 10.00
CL = 1.431
CM = -0.117
CD = ------

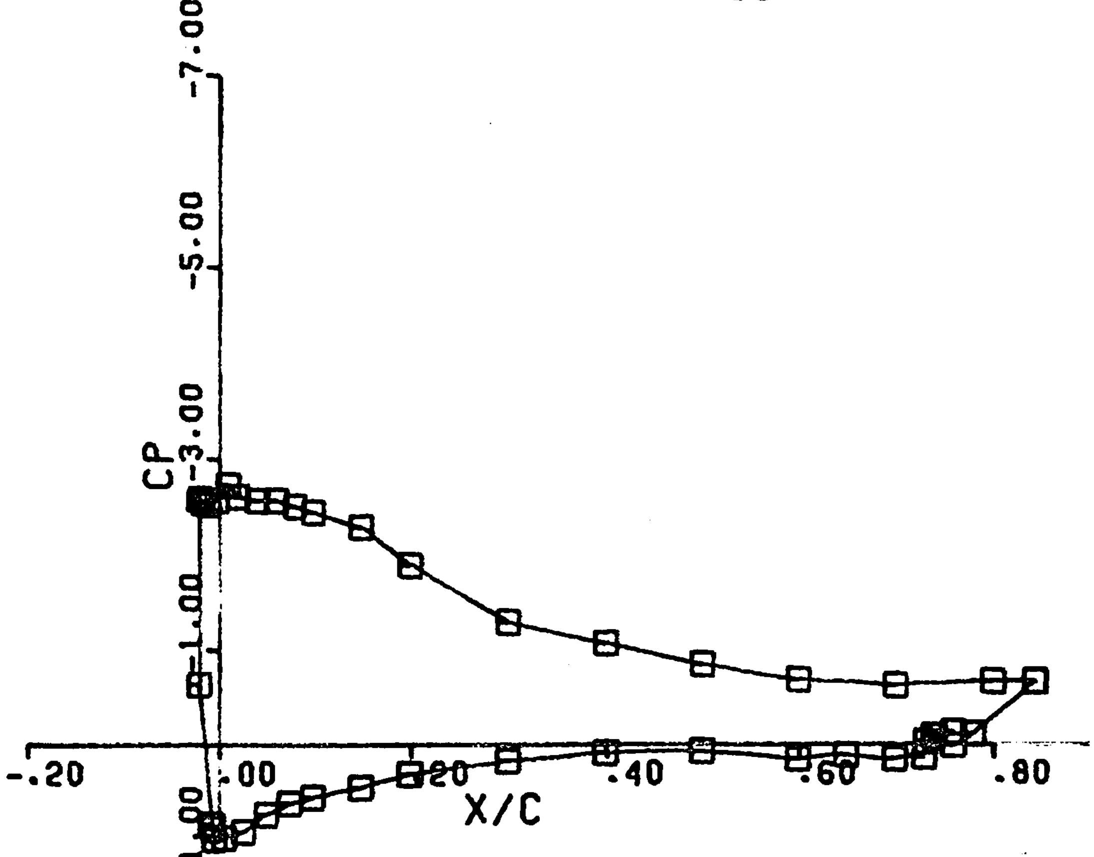

MAIN ELEMENT
CL = 1.300
CM = -0.026

FLAP
CL = 0.132
CM = -0.092

GLAZE 3 ROUGH RUN # 147

AOA = 11.60
FLAP DEF = 10.00
CL = 1.419
CM = -0.148
CD = ------

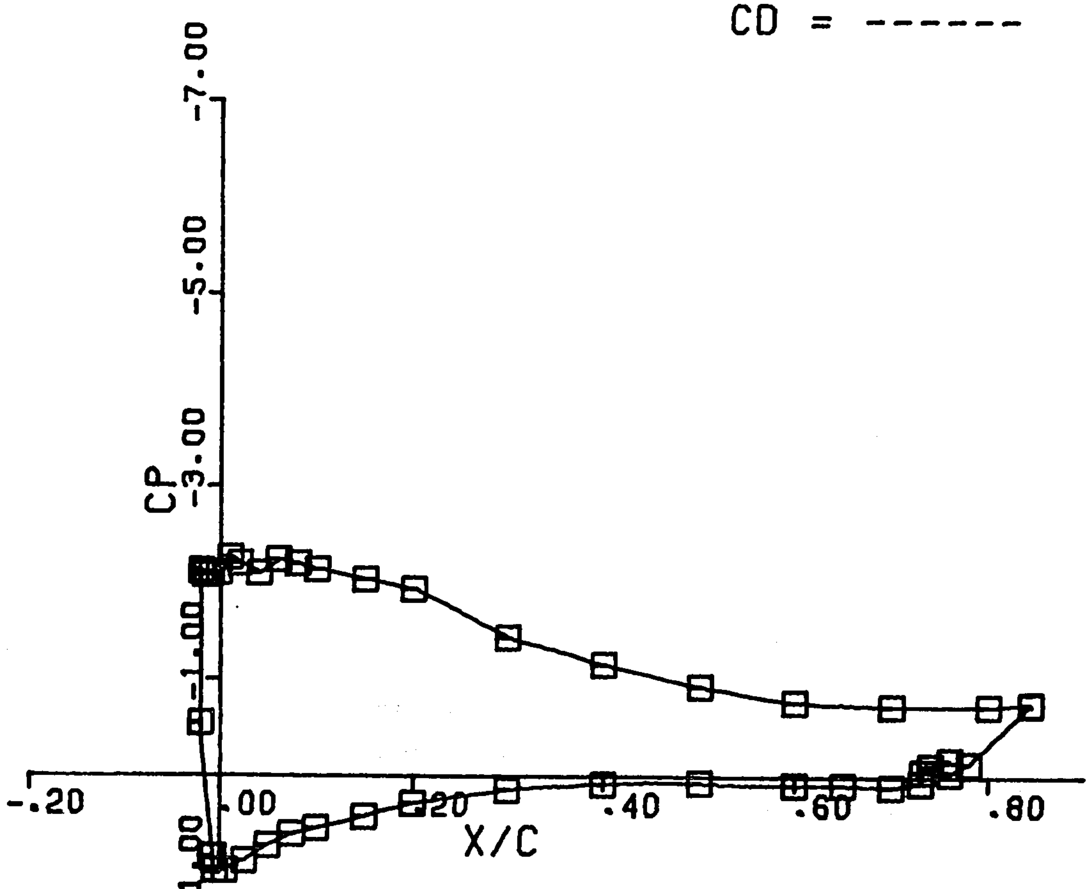

MAIN ELEMENT
CL = 1.276
CM = -0.047

FLAP
CL = 0.143
CM = -0.101

GLAZE 3 RØUGH RUN # 148

AØA = 7.60
FLAP DEF = 20.00
CL = 1.720
CM = -0.167
CD = ------

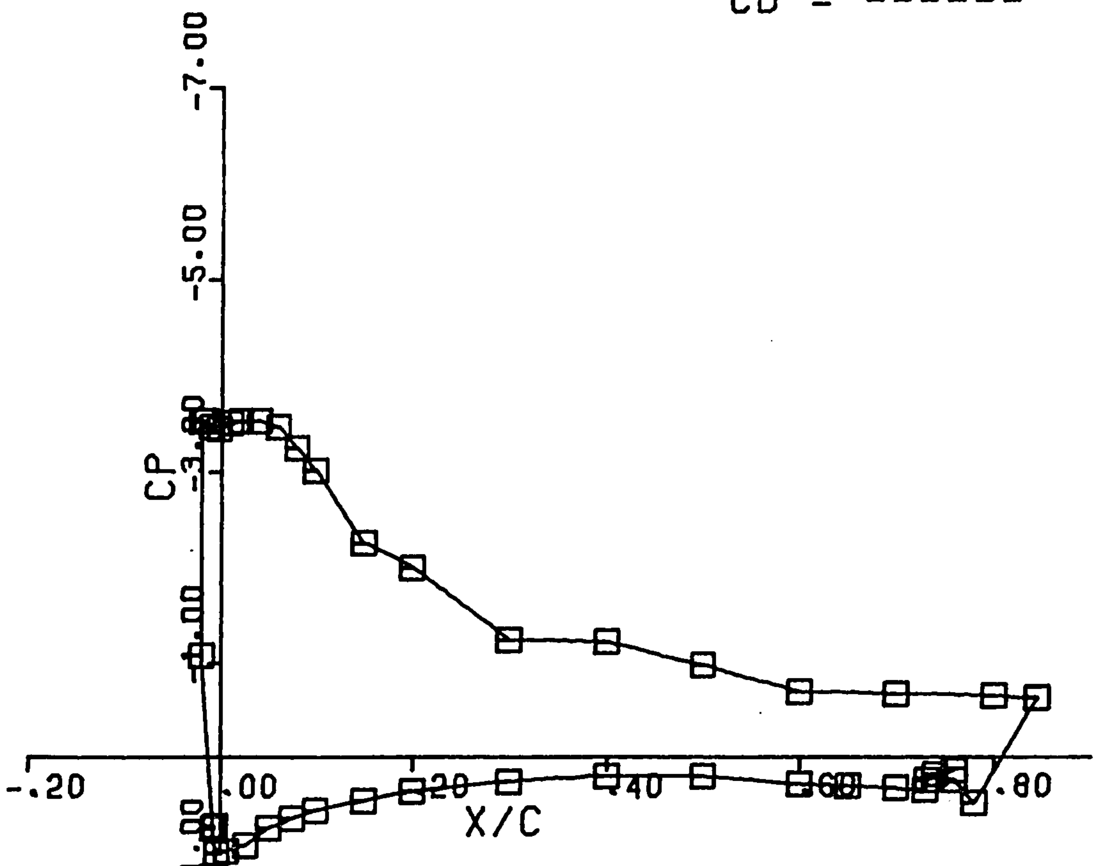

MAIN ELEMENT
CL = 1.559
CM = -0.046

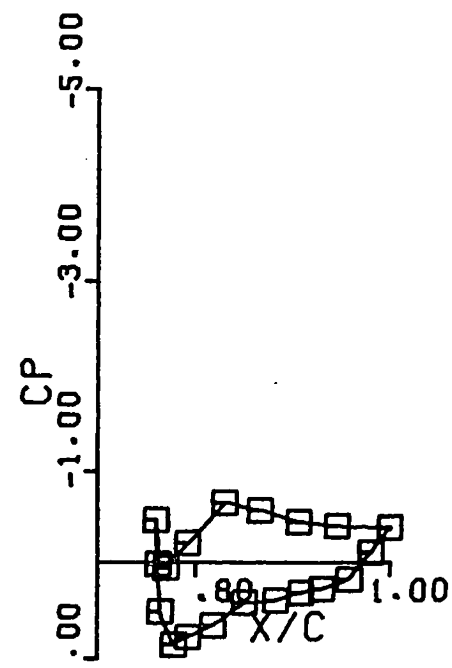

FLAP
CL = 0.160
CM = -0.121

GLAZE 3 ROUGH RUN # 149

AOA = 9.60
FLAP DEF = 20.00
CL = 1.681
CM = -0.203
CD = ------

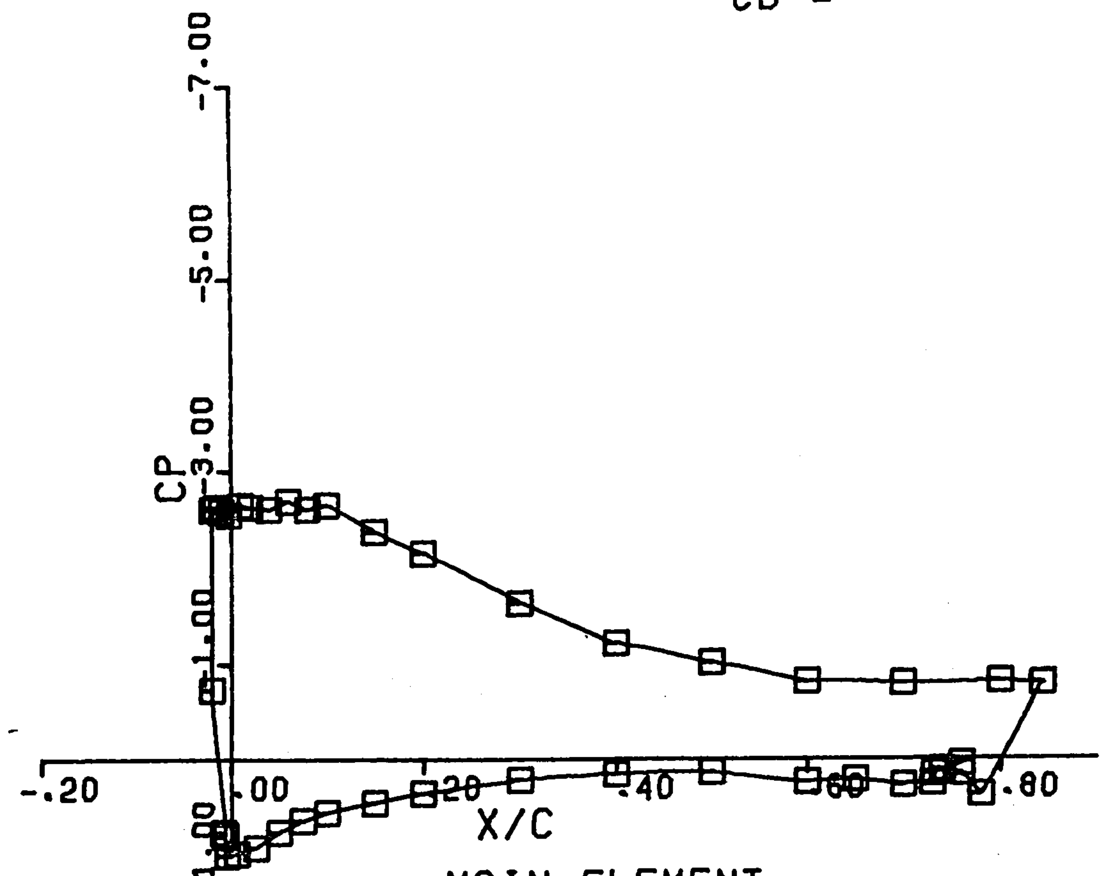

MAIN ELEMENT
CL = 1.516
CM = -0.072

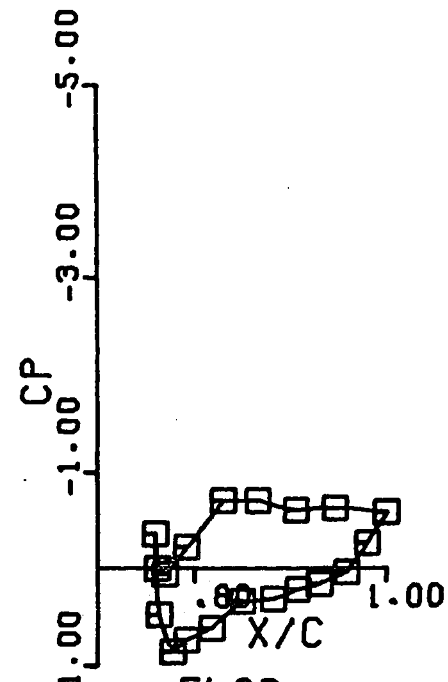

FLAP
CL = 0.165
CM = -0.131

GLAZE 3 ROUGH RUN # 150

AOA = 8.60
FLAP DEF = 20.00
CL = 1.664
CM = -0.174
CD = ------

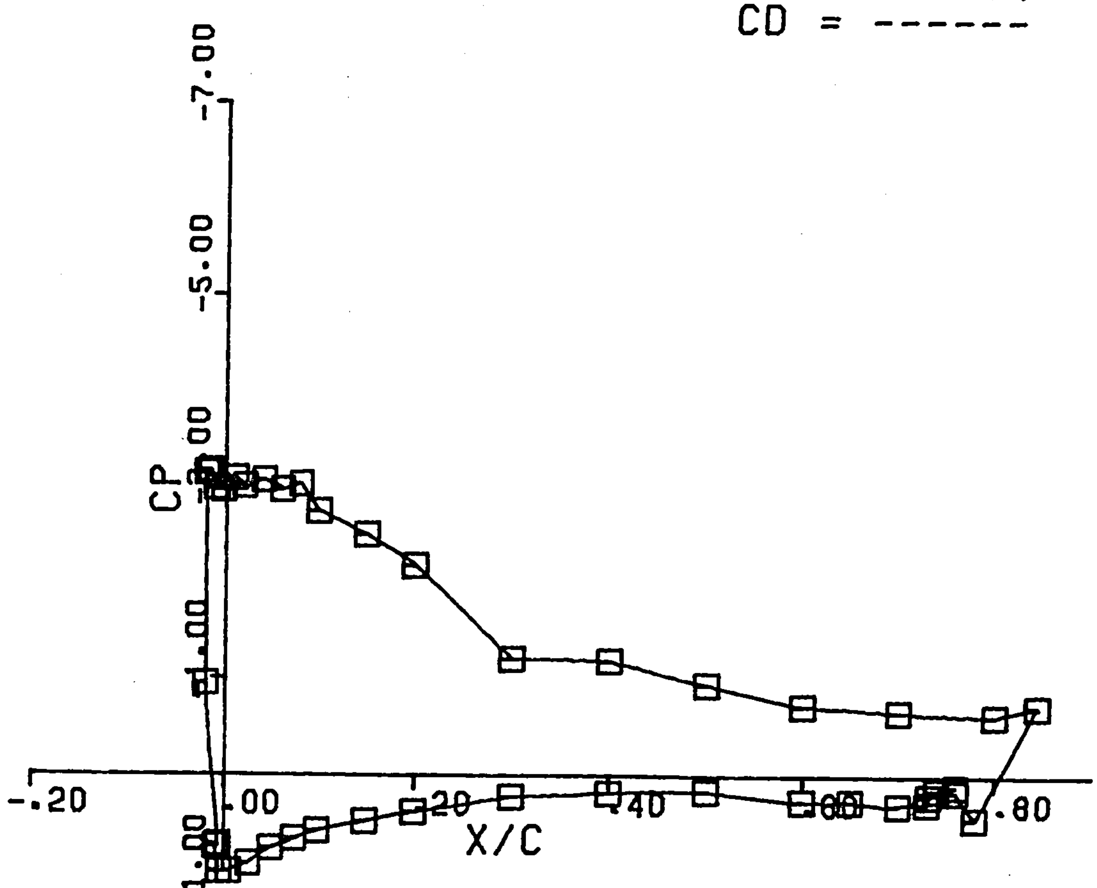

MAIN ELEMENT
CL = 1.504
CM = -0.049

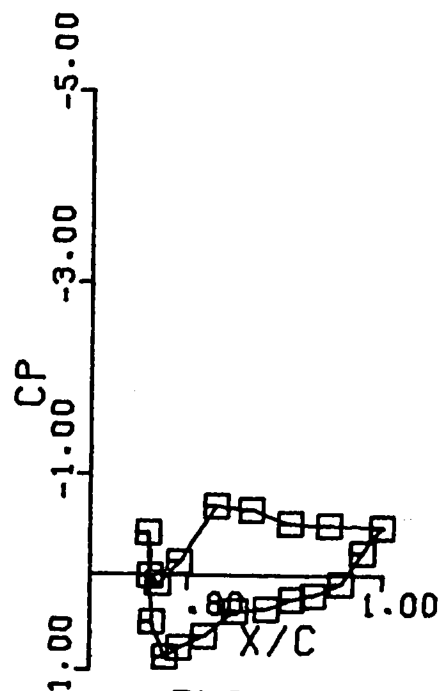

FLAP
CL = 0.160
CM = -0.125

GLAZE 3 ROUGH RUN # 151

AOA = 10.60
FLAP DEF = 20.00
CL = 1.681
CM = -0.244
CD = ------

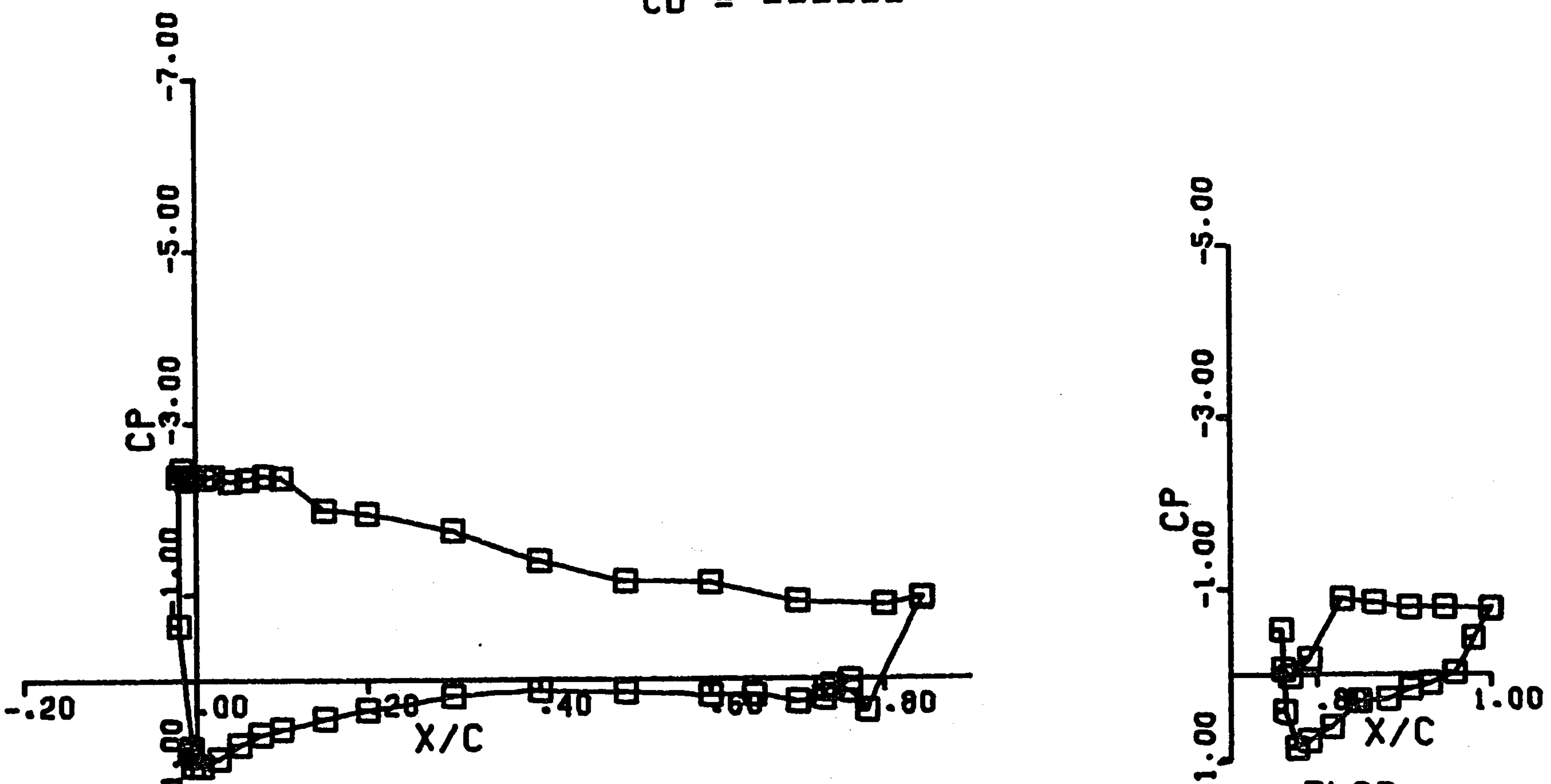

MAIN ELEMENT
CL = 1.504
CM = -0.100

FLAP
CL = 0.177
CM = -0.143

GLAZE 3 ROUGH RUN # 152

AOA = 6.60
FLAP DEF = 20.00
CL = 1.665
CM = -0.163
CD = ------

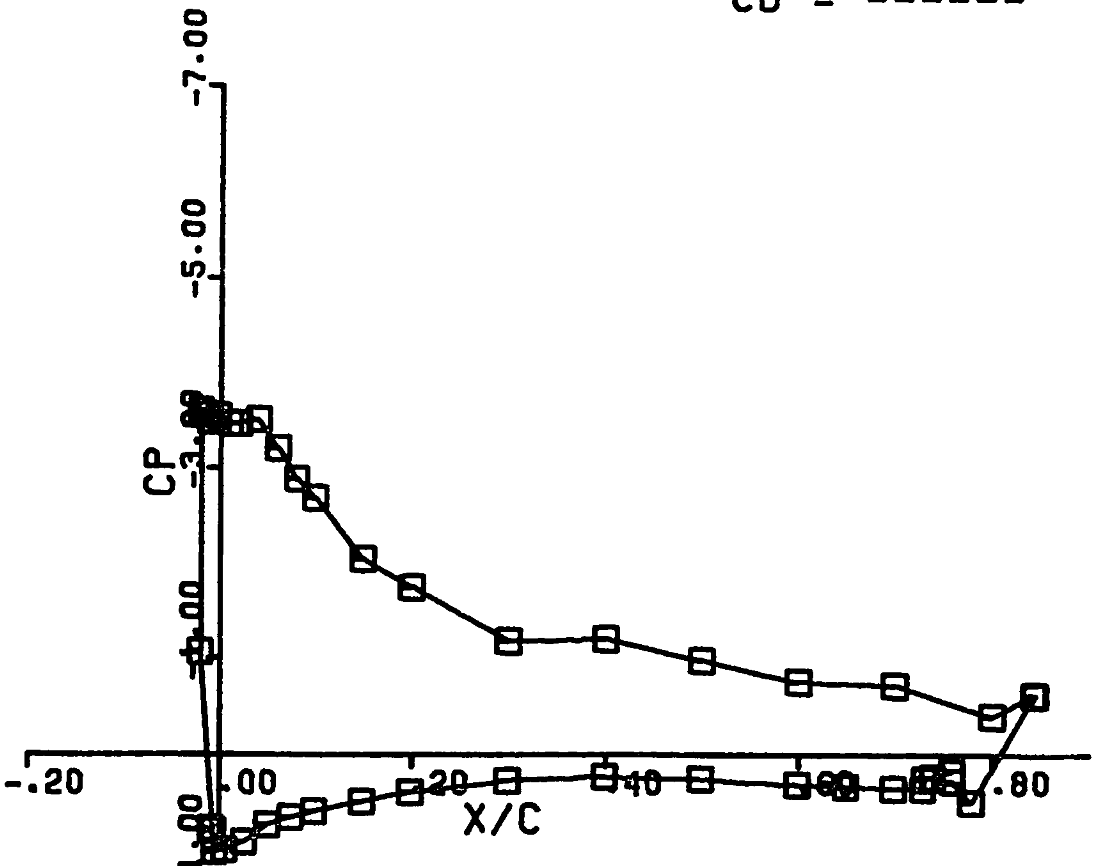

MAIN ELEMENT
CL = 1.513
CM = -0.050

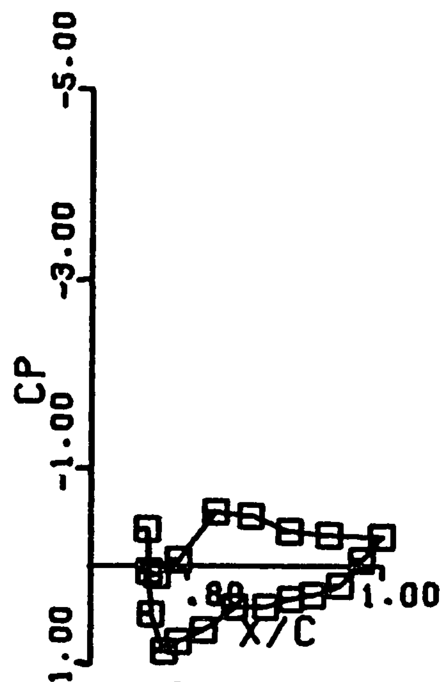

FLAP
CL = 0.151
CM = -0.113

GLAZE 3 ROUGH RUN # 153

AOA = -6.40
FLAP DEF = 30.00
CL = 0.696
CM = -0.288
CD = ------

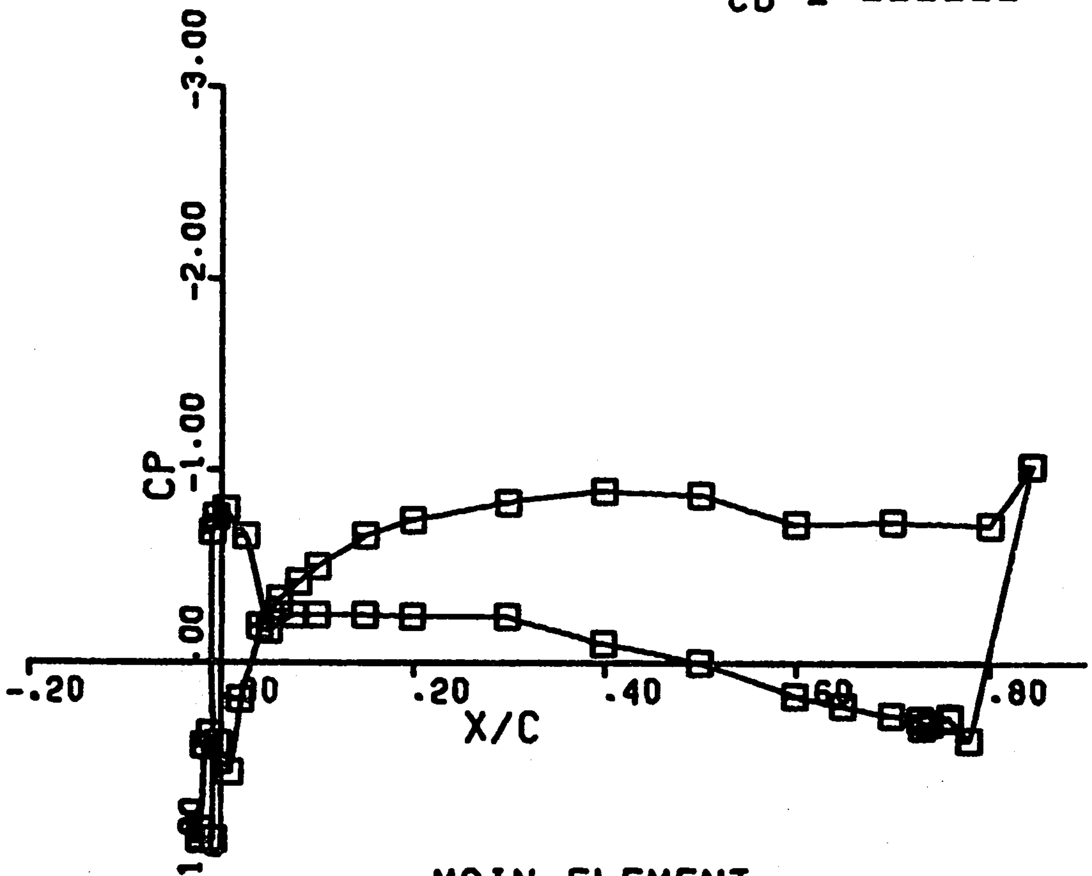

MAIN ELEMENT
CL = 0.509
CM = -0.148

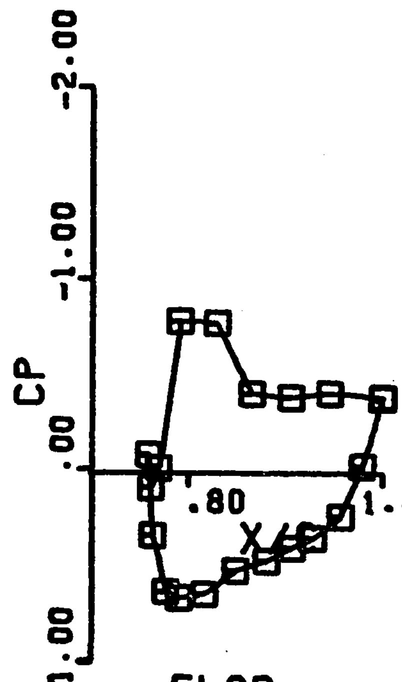

FLAP
CL = 0.187
CM = -0.140

GLAZE 3 ROUGH RUN # 154

AOA = -2.40
FLAP DEF = 30.00
CL = 1.212
CM = -0.289
CD = ------

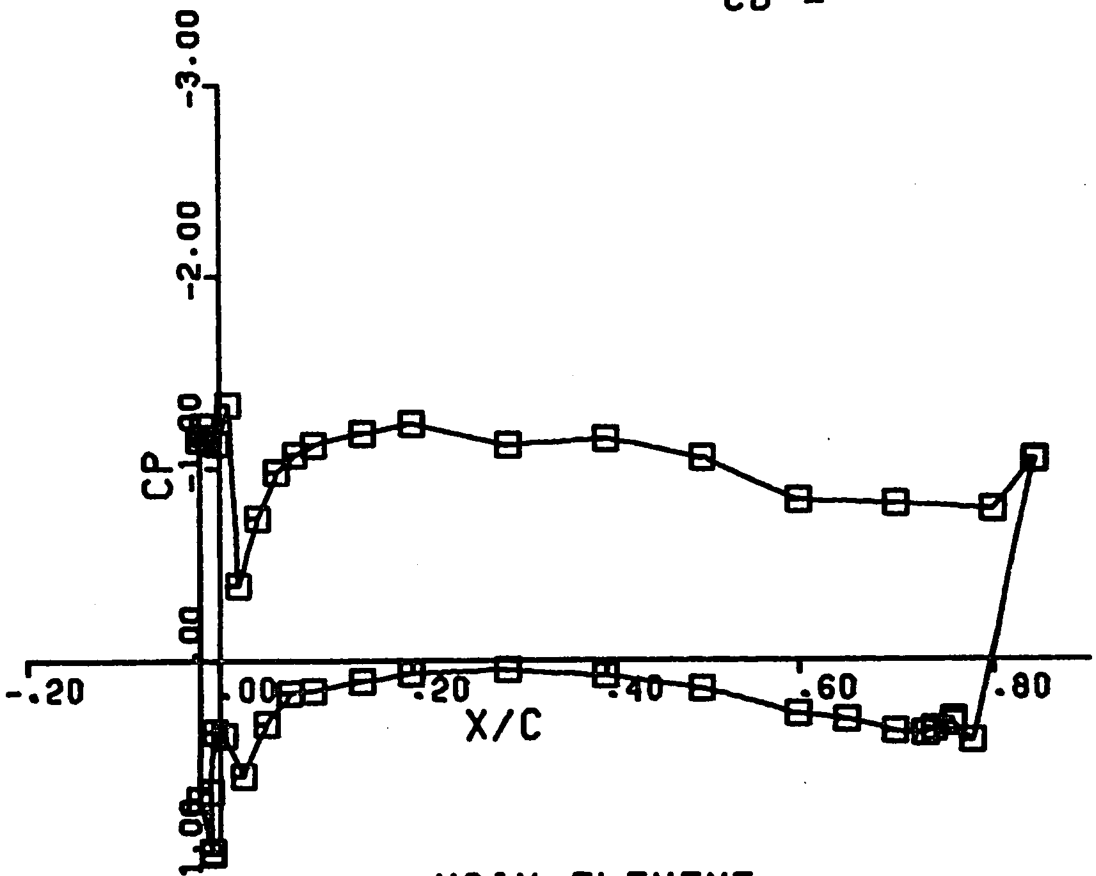

MAIN ELEMENT
CL = 1.012
CM = -0.136

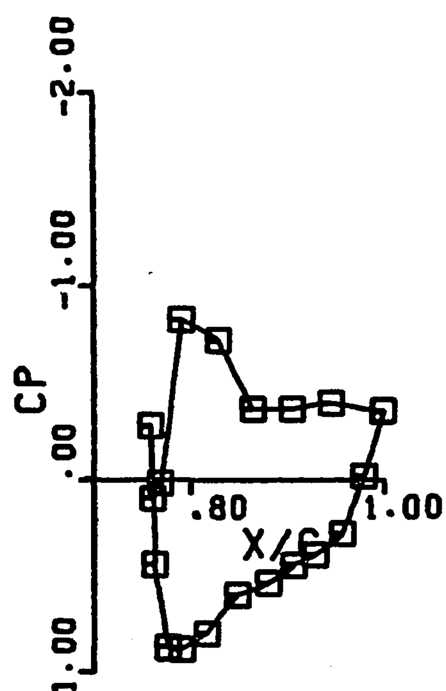

FLAP
CL = 0.200
CM = -0.153

GLAZE 3 ROUGH RUN # 155

AOA = 1.60
FLAP DEF = 30.00
CL = 1.648
CM = -0.277
CD = ------

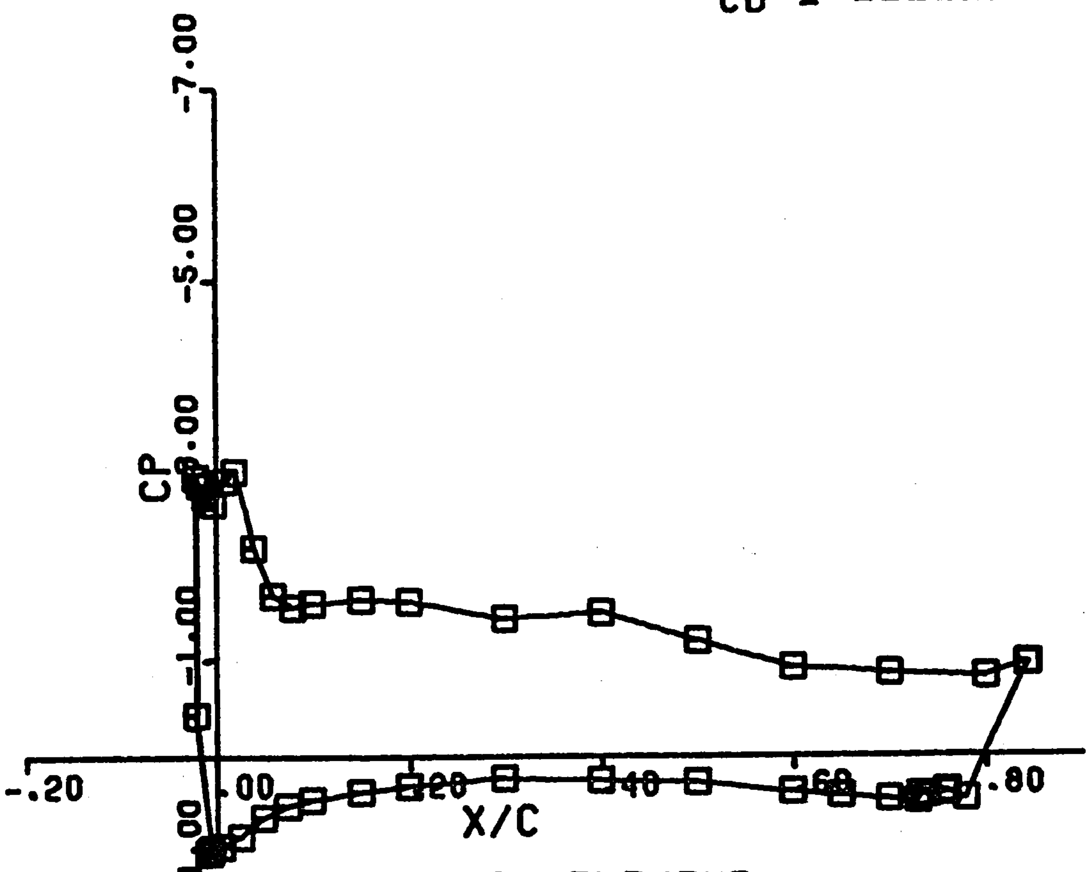

MAIN ELEMENT
CL = 1.456
CM = -0.125

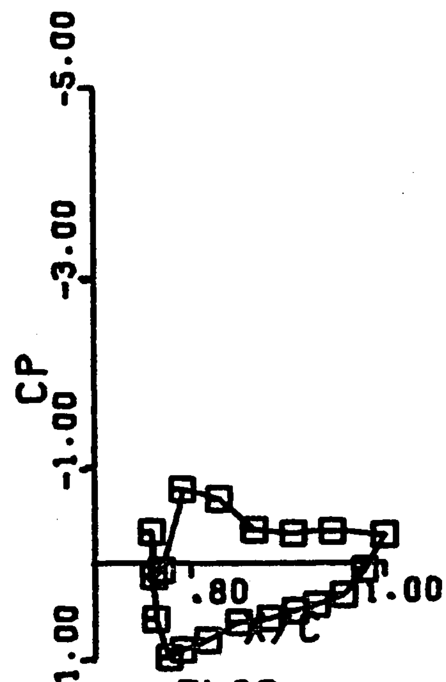

FLAP
CL = 0.192
CM = -0.152

GLAZE 3 ROUGH RUN * 156

AOA = 5.60
FLAP DEF = 30.00
CL = 1.934
CM = -0.250
CD = ------

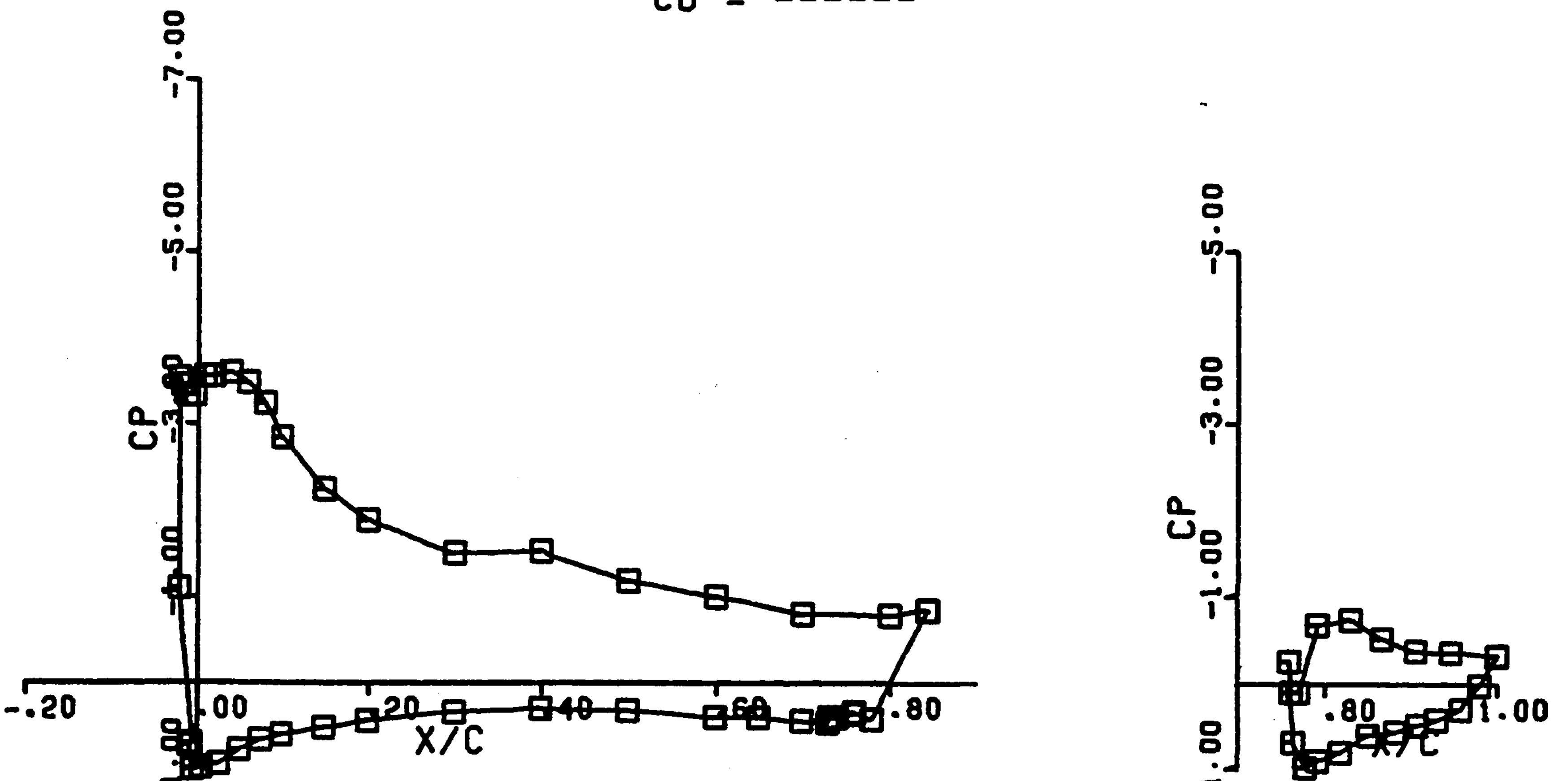

MAIN ELEMENT
CL = 1.745
CM = -0.092

FLAP
CL = 0.189
CM = -0.158

GLAZE 3 ROUGH RUN # 157

AOA = 7.60
FLAP DEF = 30.00
CL = 1.963
CM = -0.261
CD = ------

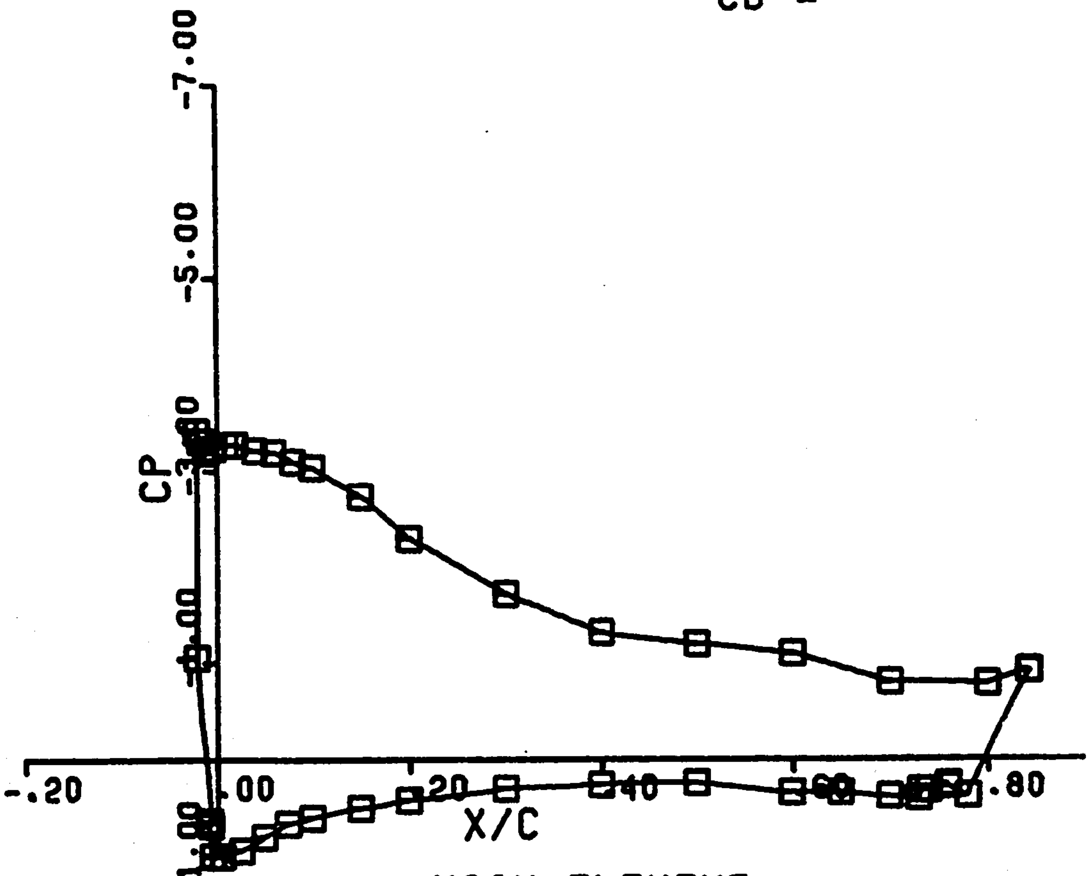

MAIN ELEMENT
CL = 1.763
CM = -0.087

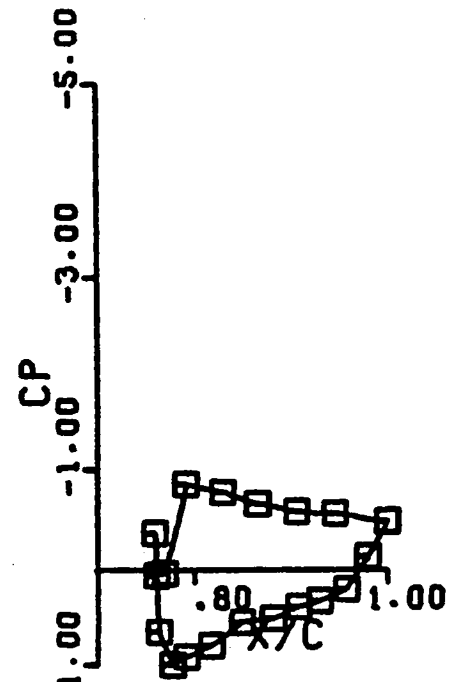

FLAP
CL = 0.200
CM = -0.174

GLAZE 3 ROUGH RUN # 158

AOA = 8.60
FLAP DEF = 30.00
CL = 1.903
CM = -0.277
CD = ------

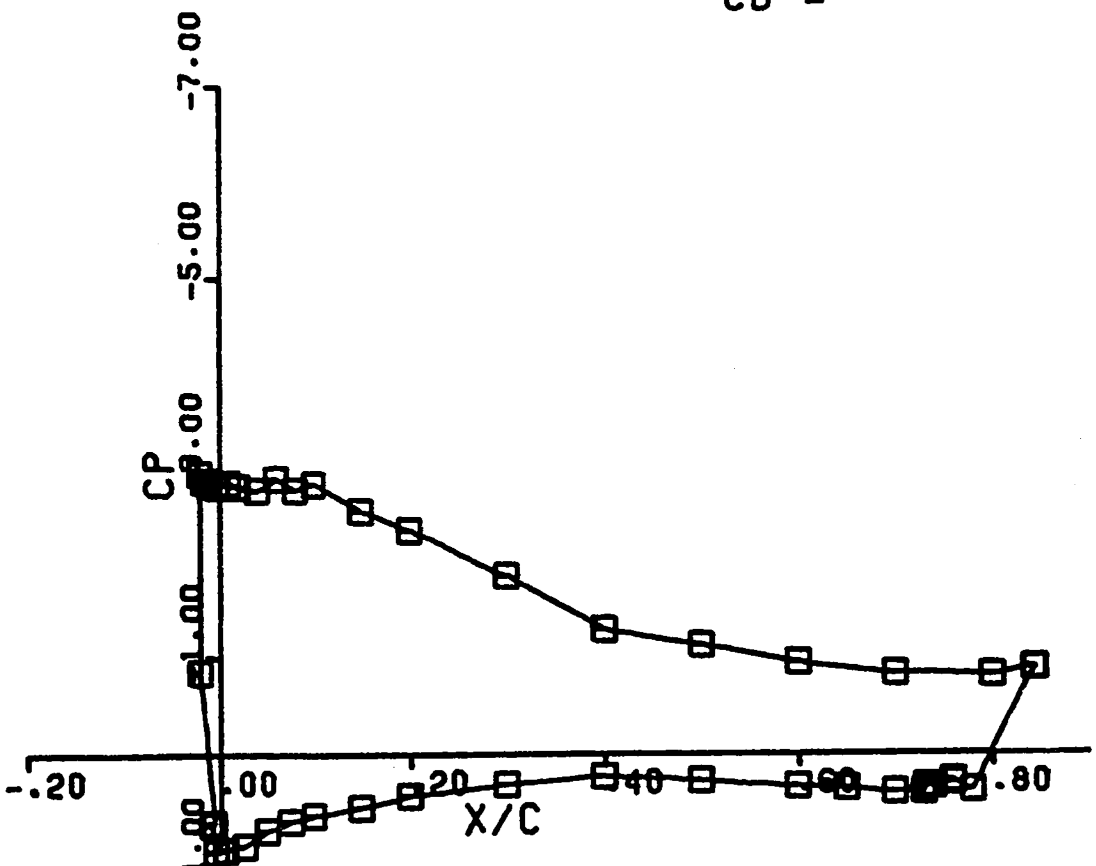

MAIN ELEMENT
CL = 1.700
CM = -0.094

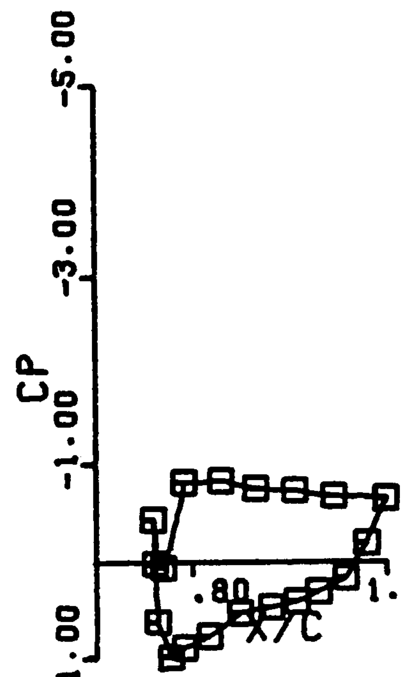

FLAP
CL = 0.203
CM = -0.183

GENERIC ROUGH RUN # 50

AOA = -2.40
FLAP DEF = 0.00
CL = 0.055
CM = -0.060
CD = 0.034

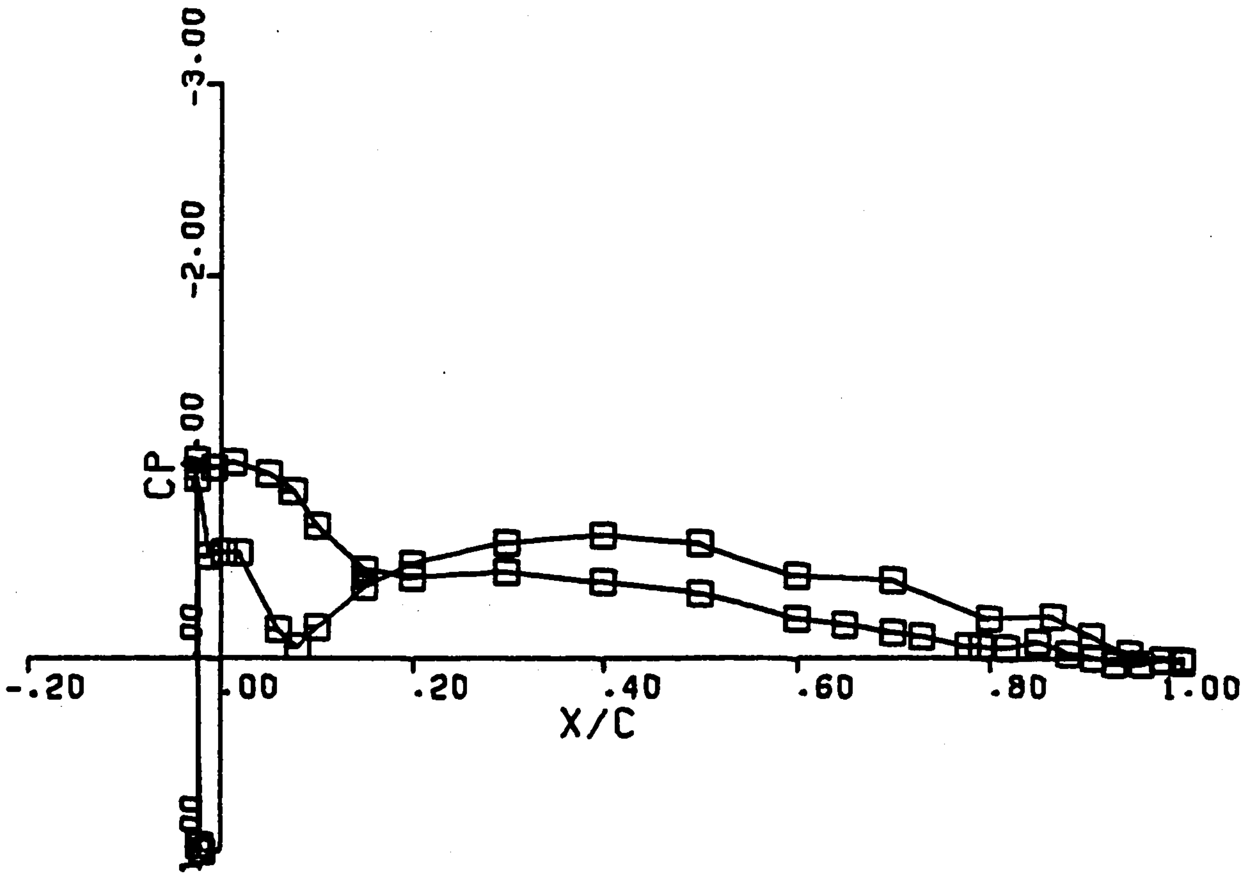

GENERIC ROUGH RUN # 51

AOA = -0.40
FLAP DEF = 0.00
CL = 0.295
CM = -0.042
CD = 0.037

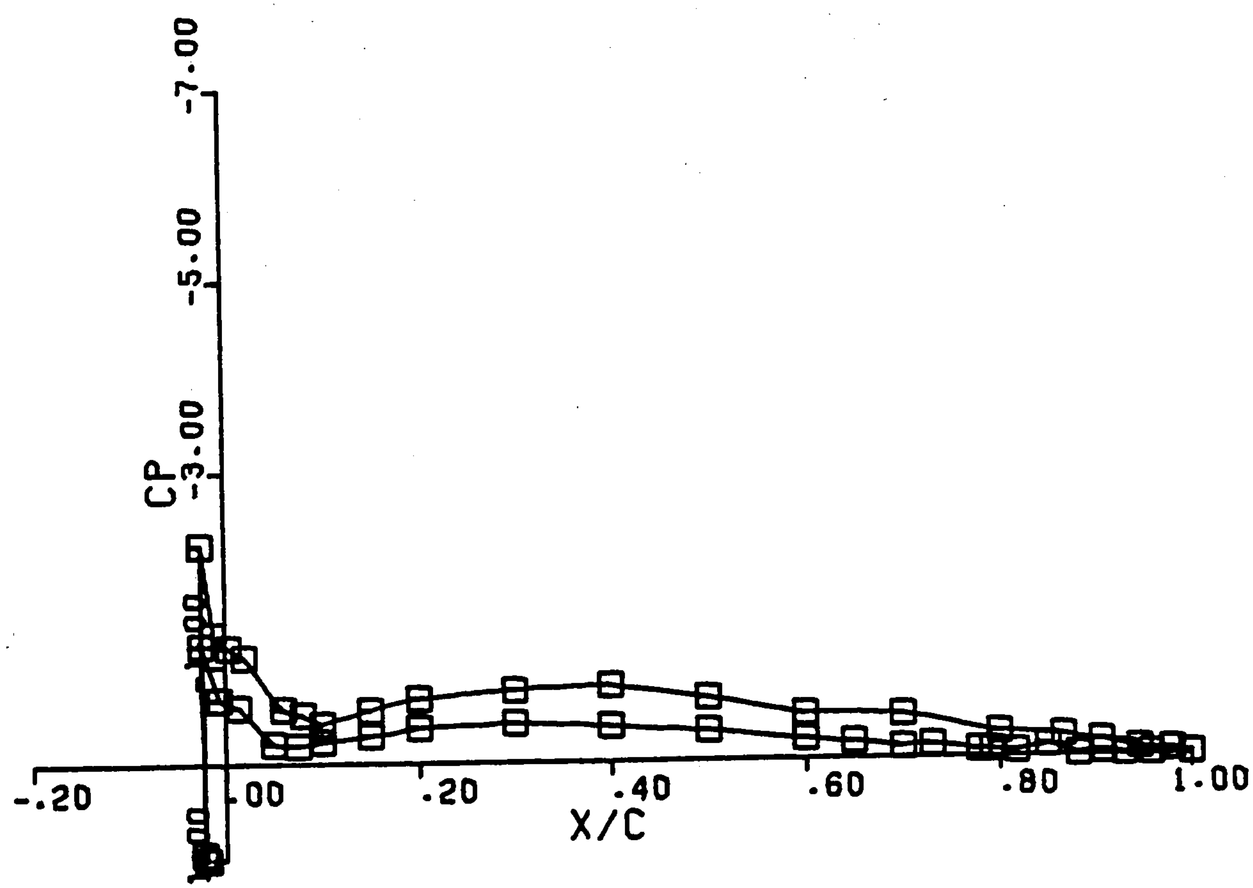

GENERIC ROUGH RUN # 52

AOA = 1.60
FLAP DEF = 0.00
CL = 0.554
CM = -0.035
CD = 0.044

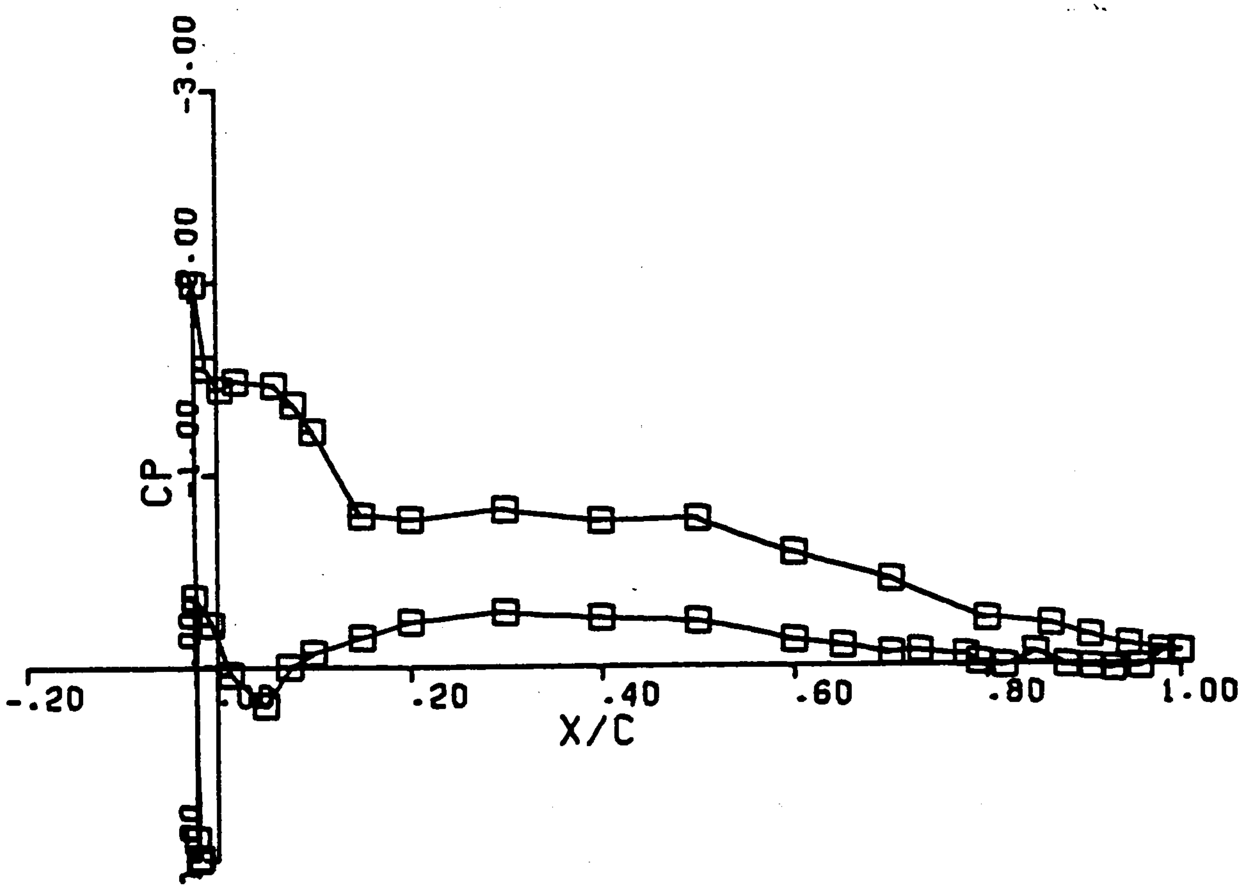

GENERIC ROUGH RUN # 53

AOA = 3.60
FLAP DEF = 0.00
CL = 0.735
CM = -0.021
CD = 0.068

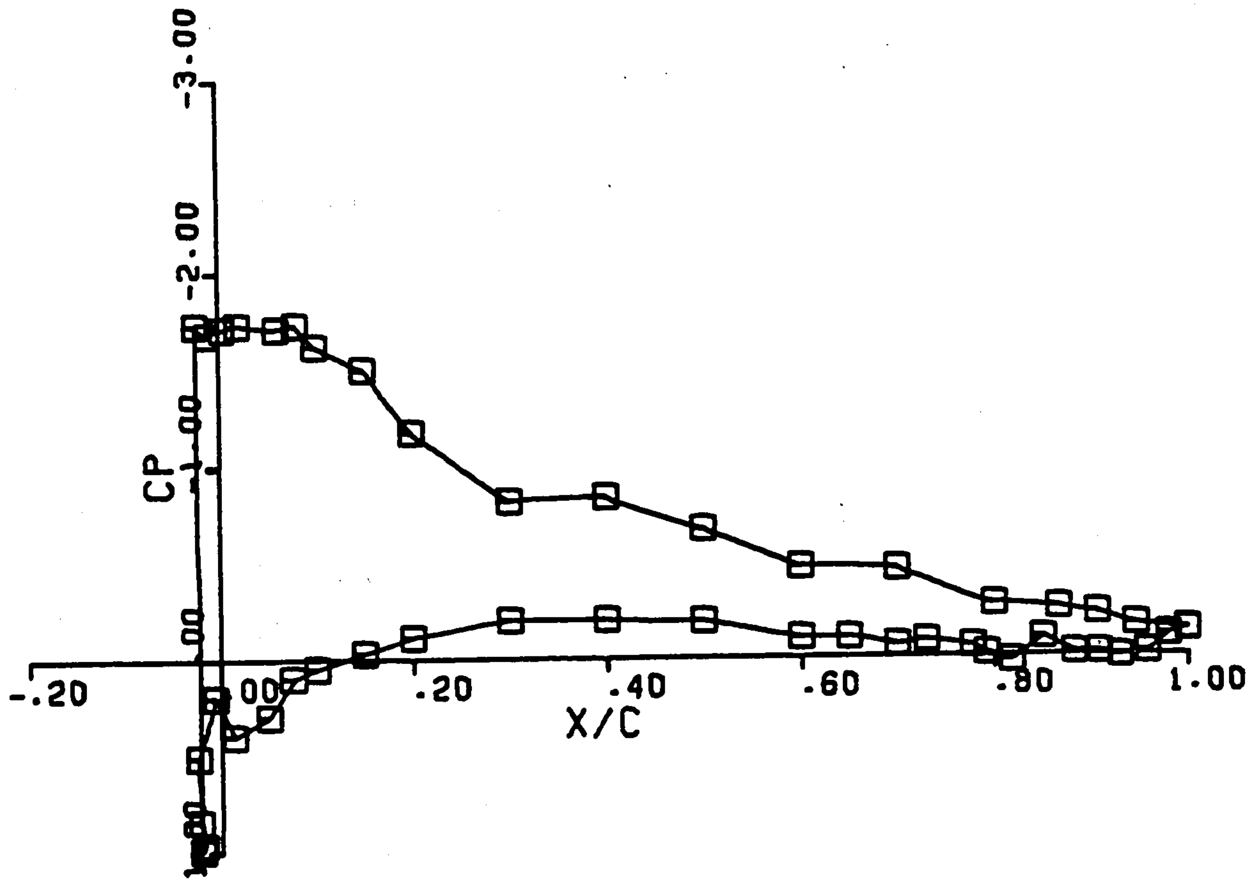

GENERIC SMOOTH RUN # 55

AOA = -2.40
FLAP DEF = 0.00
CL = 0.103
CM = -0.059
CD = 0.035

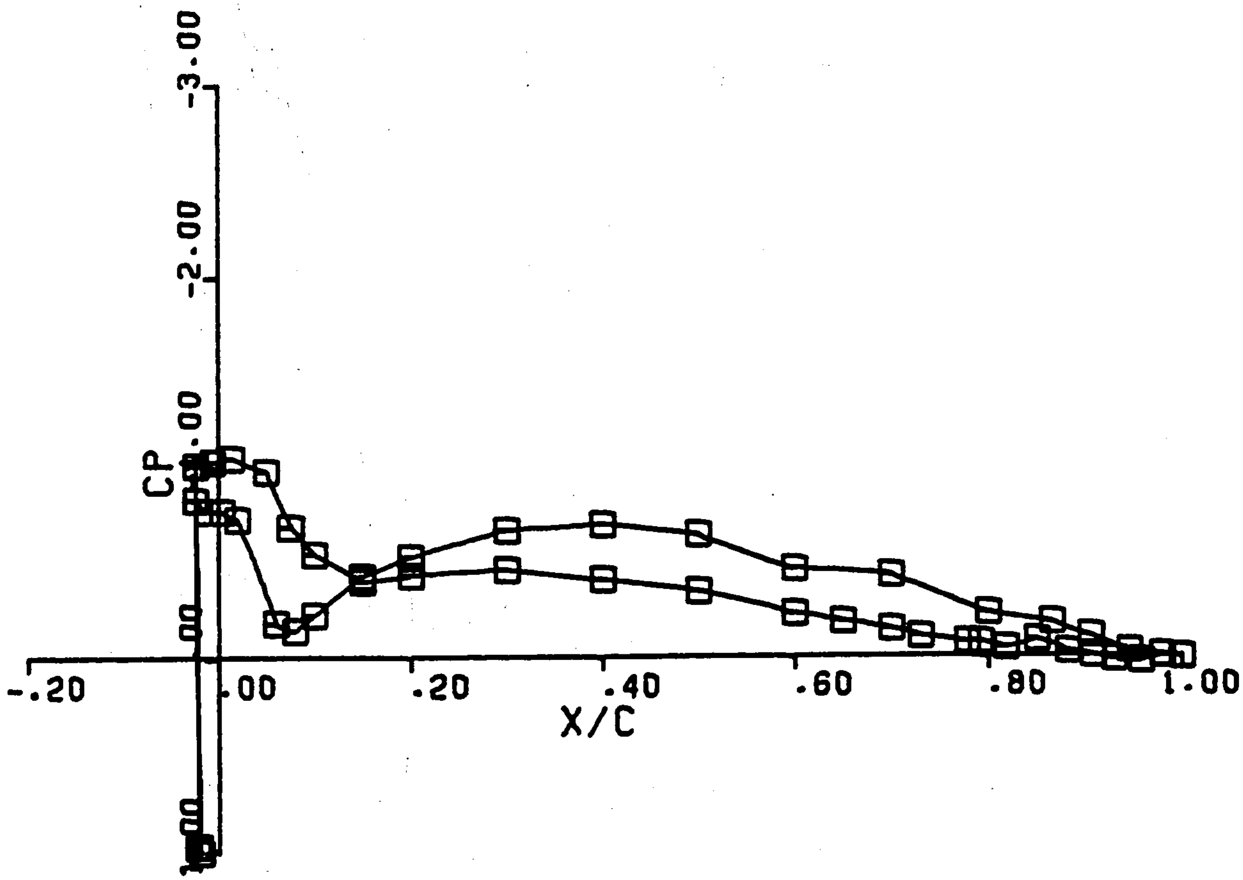

GENERIC SMOOTH RUN # 56

AOA = -0.40
FLAP DEF = 0.00
CL = 0.323
CM = -0.042
CD = 0.036

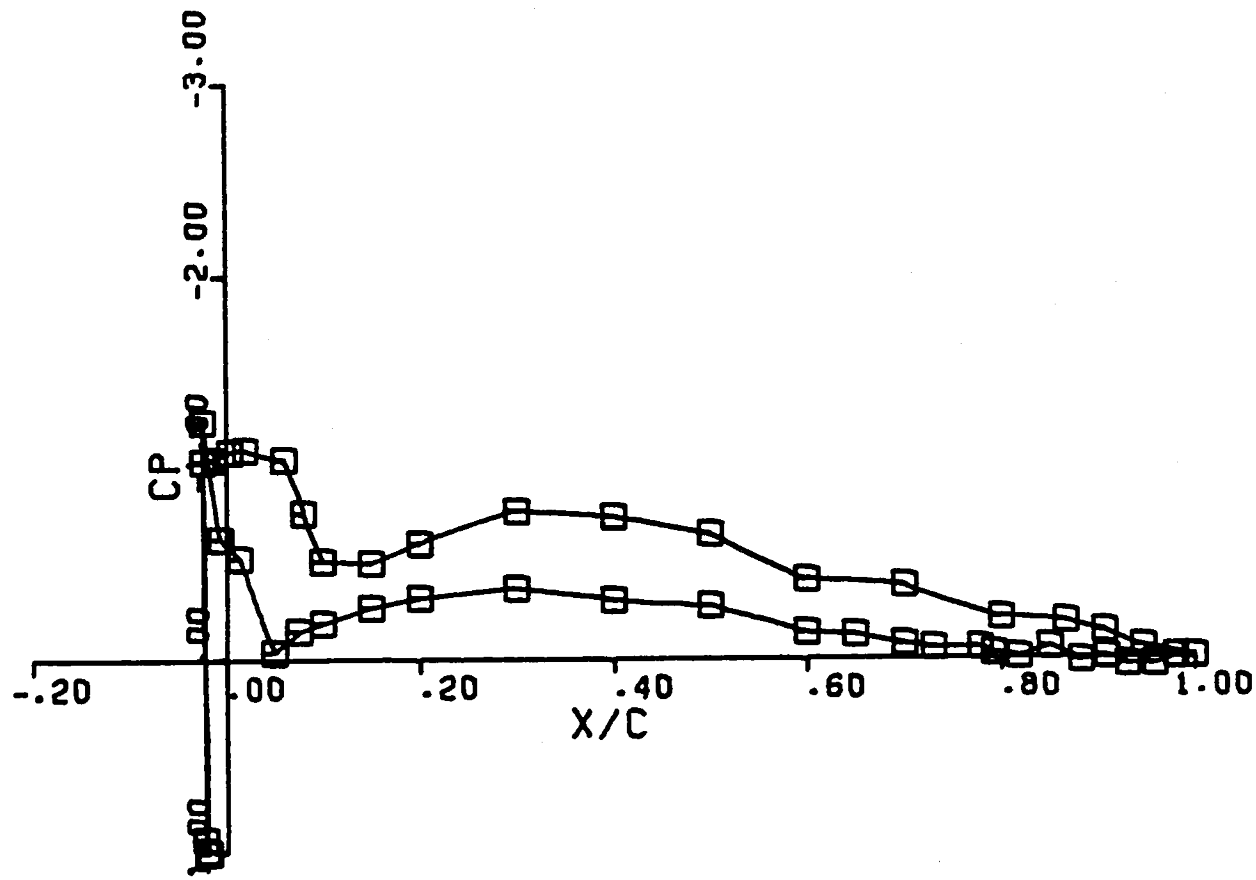

GENERIC SMOOTH RUN # 57

AOA = 1.60
FLAP DEF = 0.00
CL = 0.532
CM = -0.031
CD = 0.043

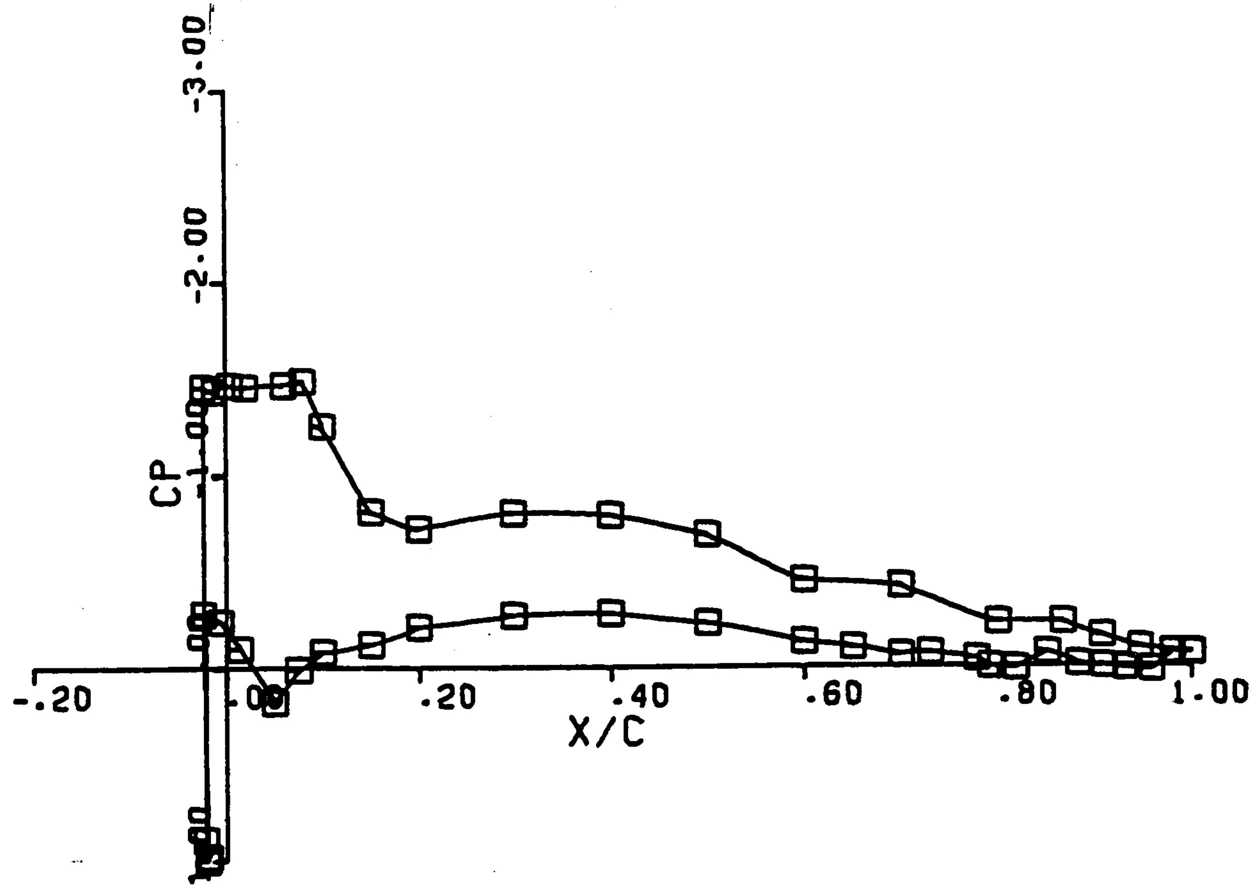

GENERIC SMOOTH RUN # 58

AOA = 3.60
FLAP DEF = 0.00
CL = 0.727
CM = -0.019
CD = 0.062

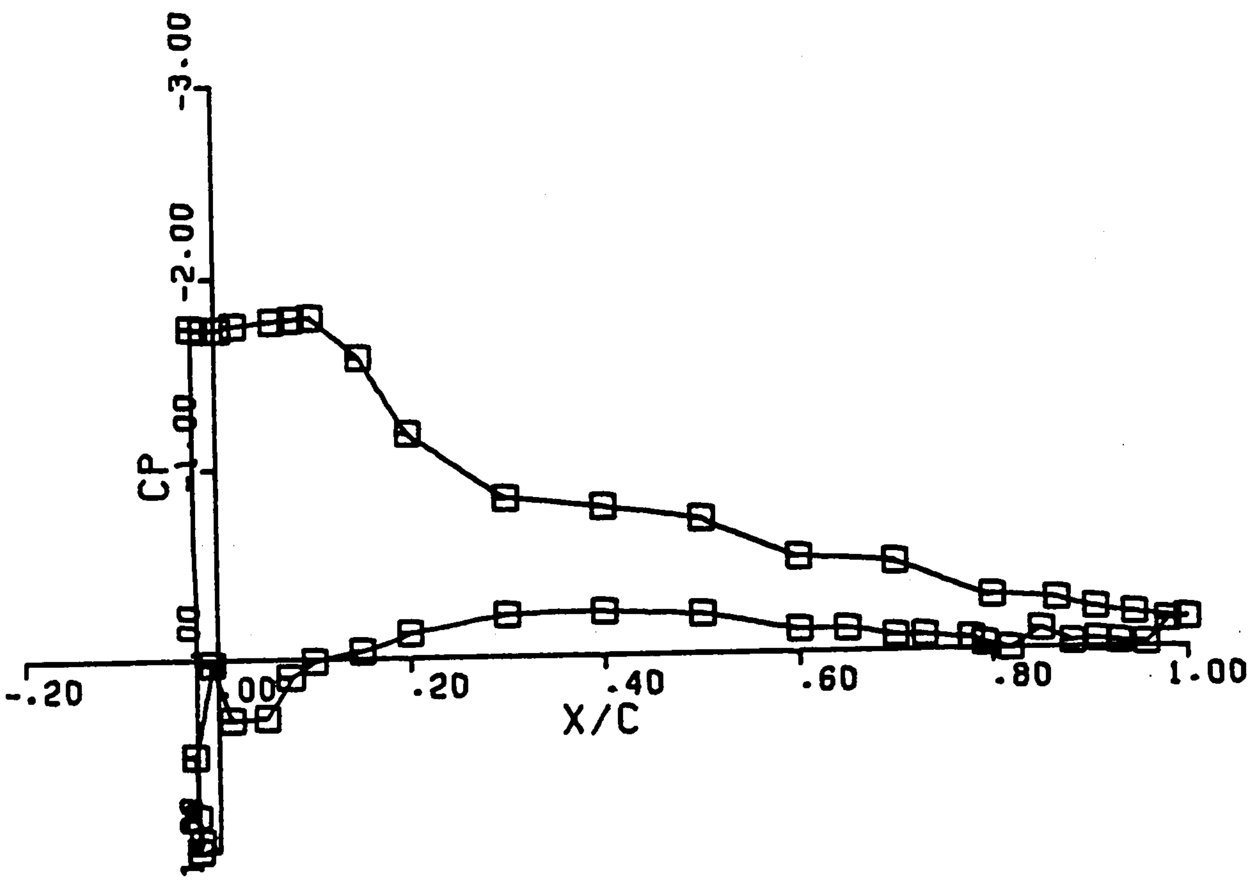

GENERIC SMOOTH RUN # 59

AOA = 5.60
FLAP DEF = 0.00
CL = 0.849
CM = -0.025
CD = ------

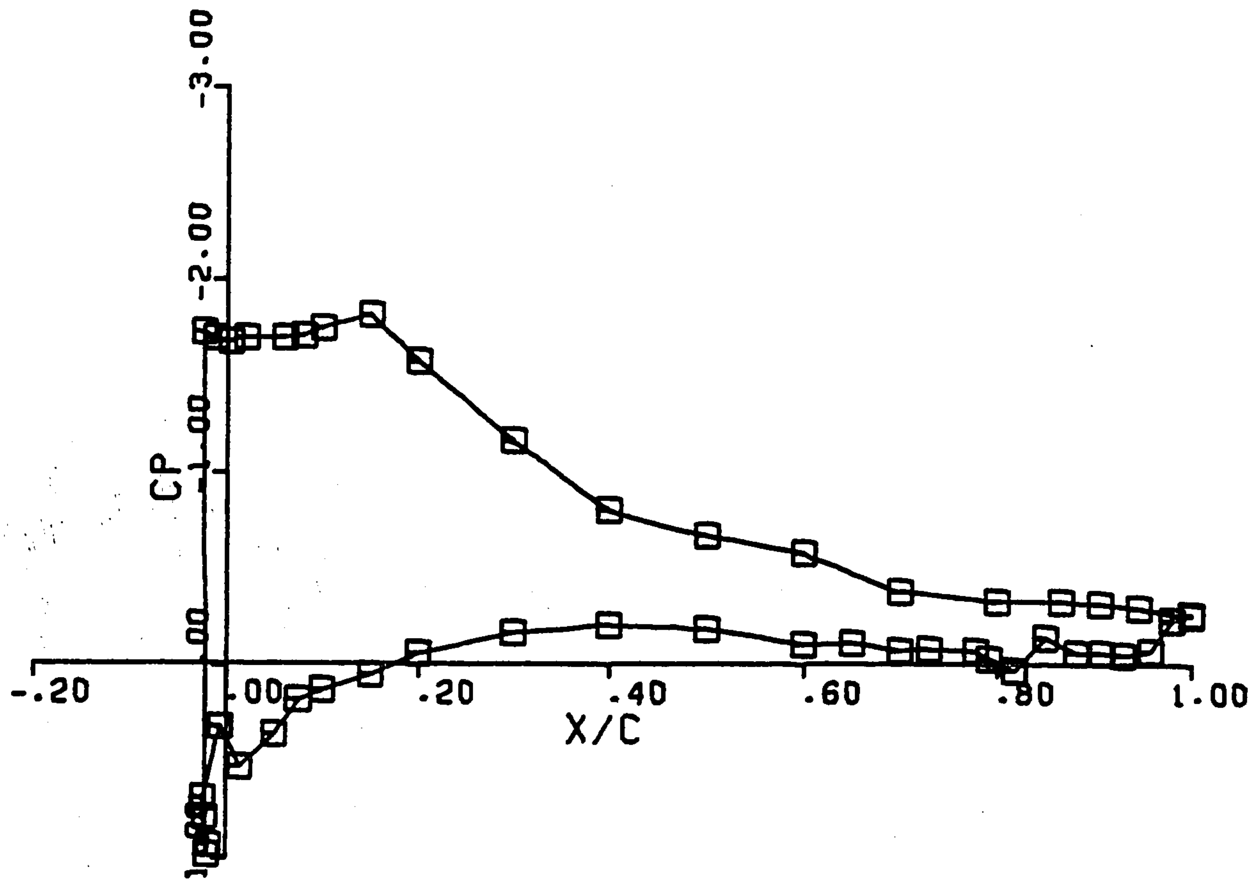

GENERIC SMOOTH RUN # 108

AOA = -2.40
FLAP DEF = 30.00
CL = 1.240
CM = -0.272
CD = ------

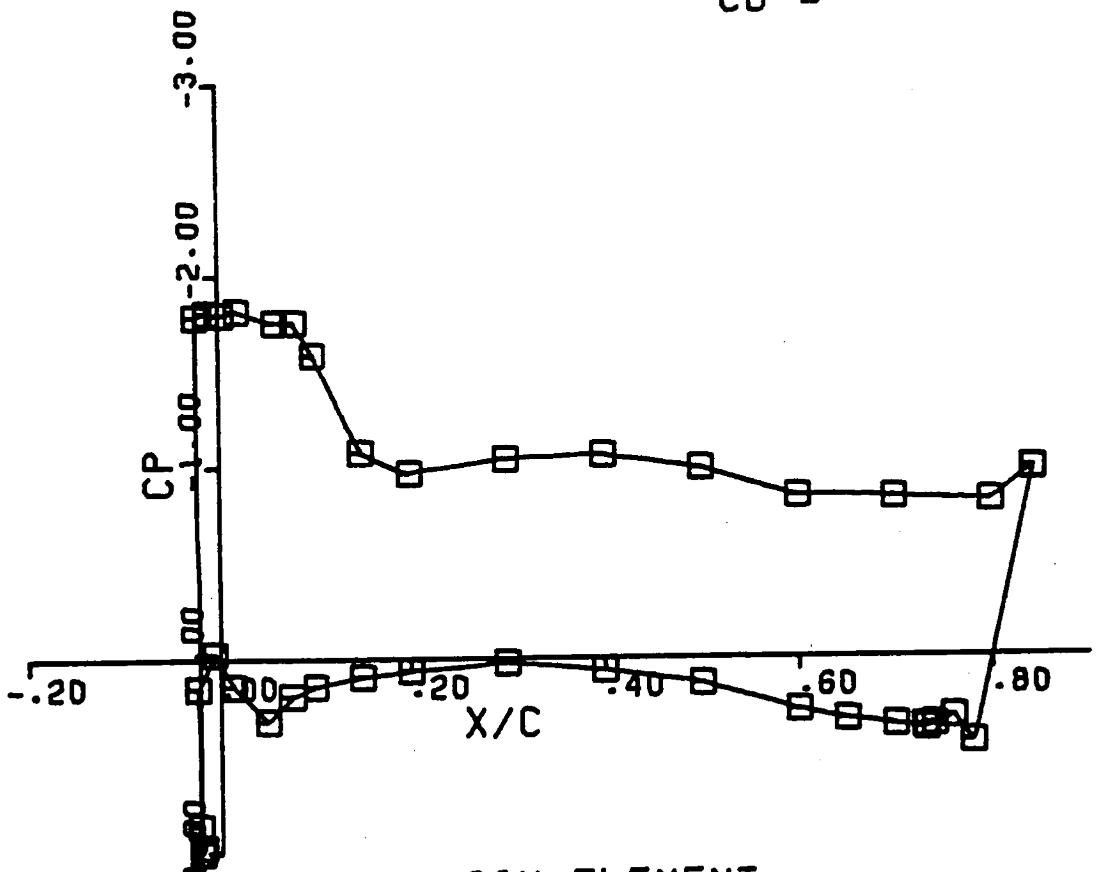

MAIN ELEMENT
CL = 1.039
CM = -0.118

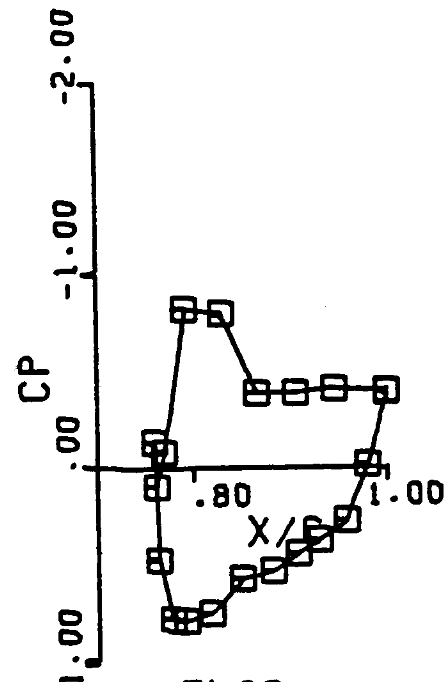

FLAP
CL = 0.201
CM = -0.154

GENERIC SMOOTH RUN # 109

AOA = -8.40
FLAP DEF = 30.00
CL = 0.204
CM = -0.209
CD = -------

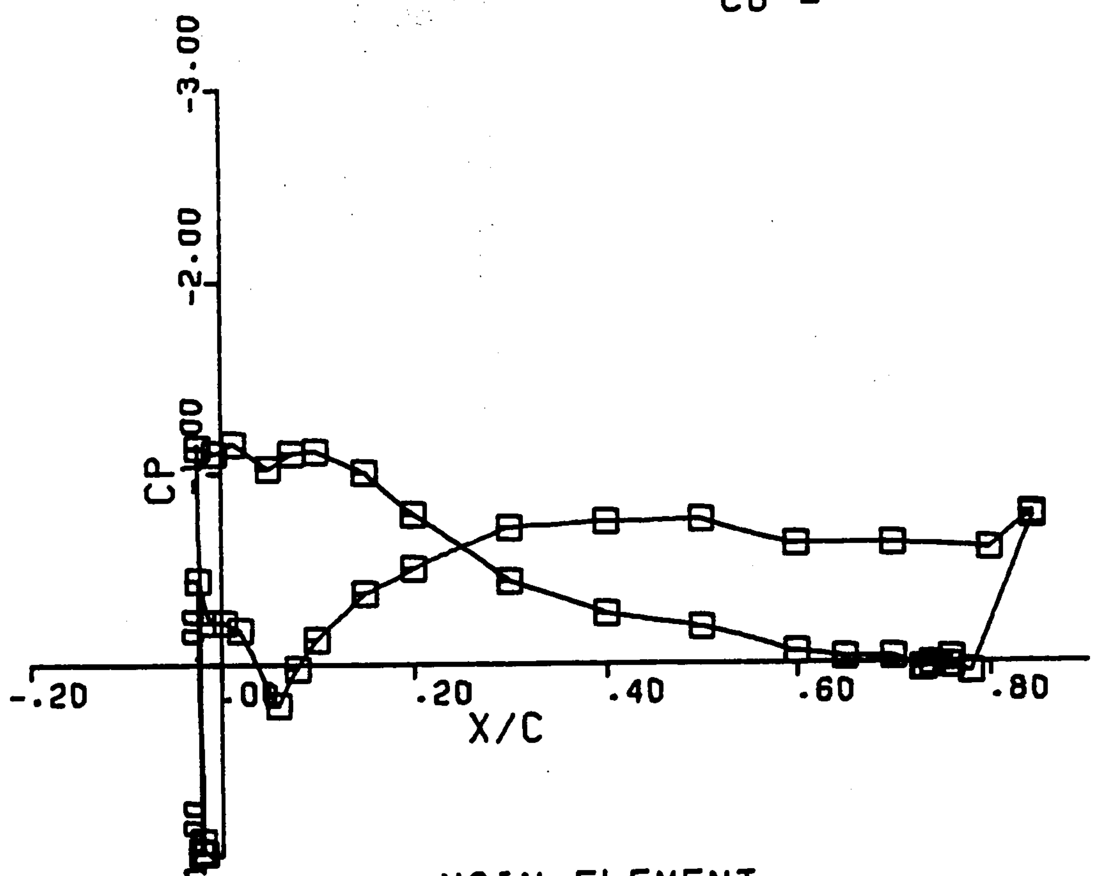

MAIN ELEMENT
CL = 0.080
CM = -0.119

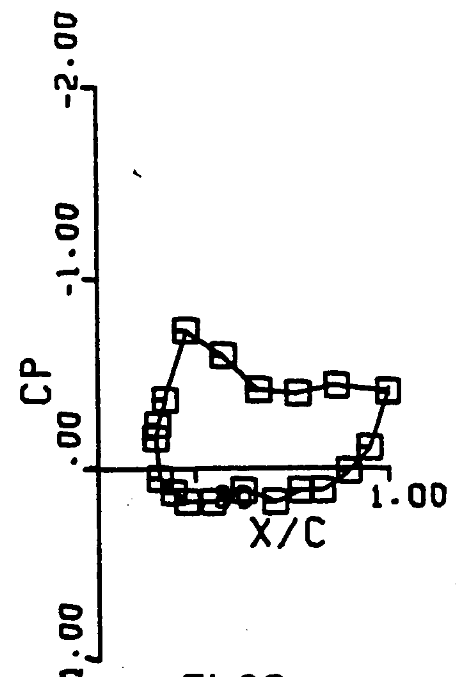

FLAP
CL = 0.124
CM = -0.091

GENERIC SMOOTH RUN # 110

AOA = -5.40
FLAP DEF = 30.00
CL = 0.841
CM = -0.283
CD = ------

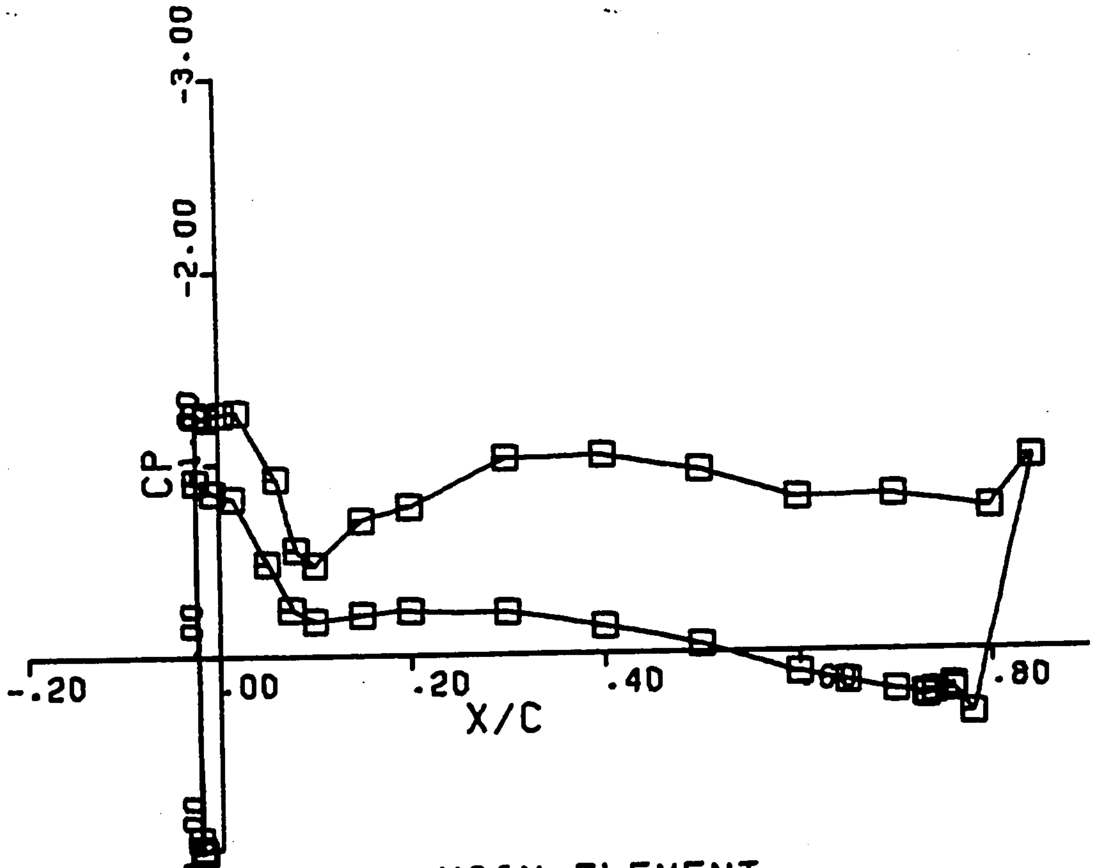

MAIN ELEMENT
CL = 0.639
CM = -0.133

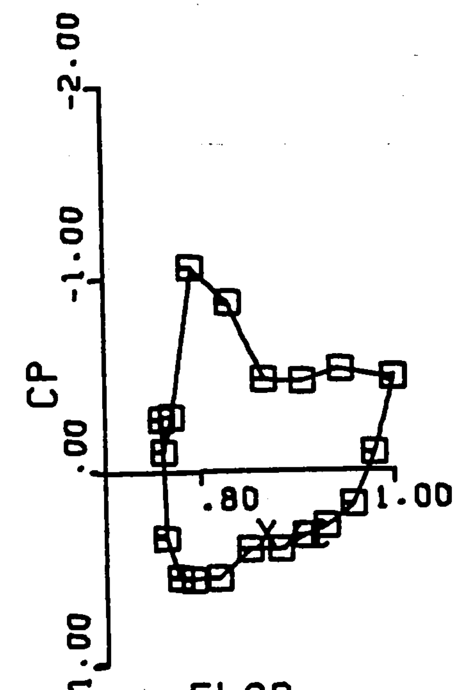

FLAP
CL = 0.203
CM = -0.150

GENERIC SMOOTH RUN # 111

AOA = 1.60
FLAP DEF = 30.00
CL = 1.646
CM = -0.252
CD = ------

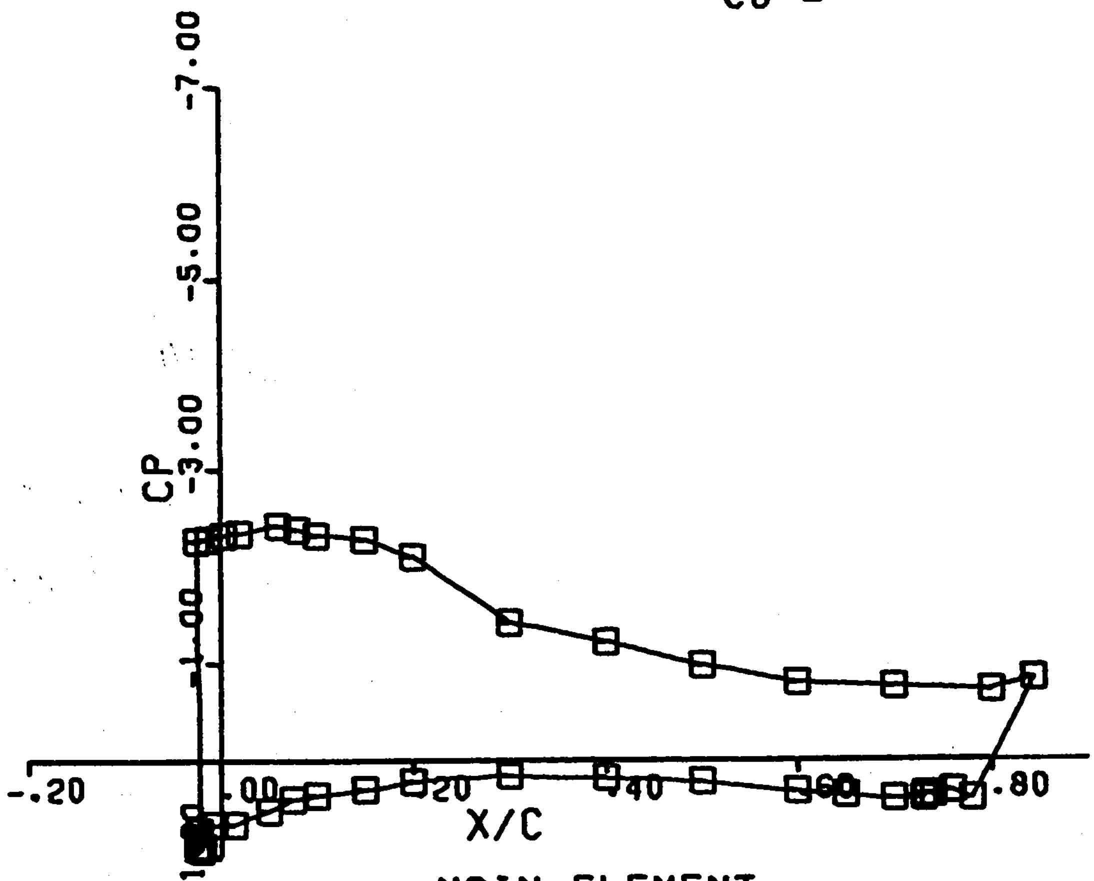

MAIN ELEMENT
CL = 1.438
CM = -0.088

FLAP
CL = 0.208
CM = -0.164

GENERIC SMOOTH RUN # 112

AOA = 5.60
FLAP DEF = 30.00
CL = 1.738
CM = -0.300
CD = -------

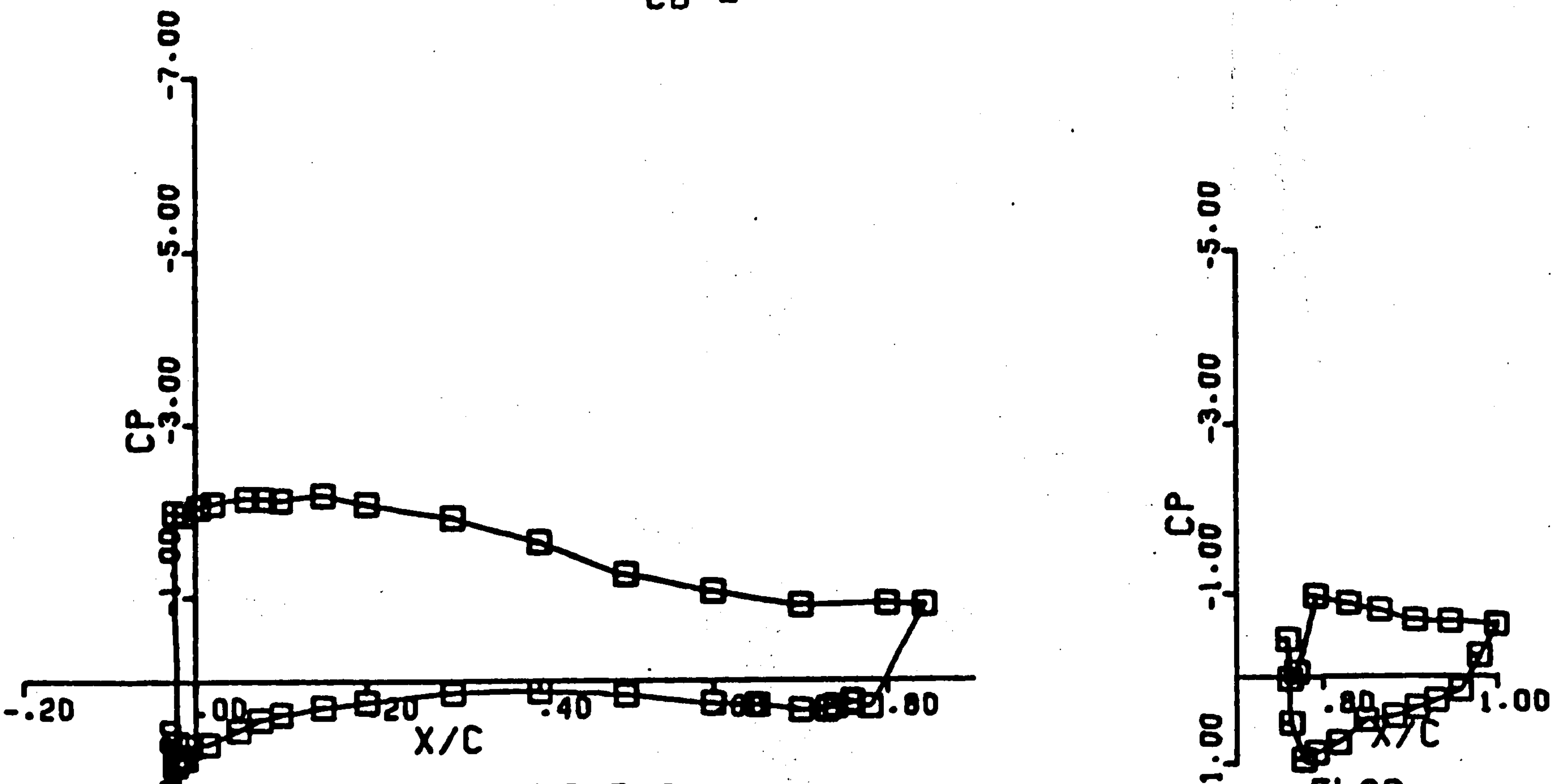

MAIN ELEMENT
CL = 1.527
CM = -0.120

FLAP
CL = 0.212
CM = -0.179

GENERIC SMOOTH RUN # 113

AOA = 7.60
FLAP DEF = 30.00
CL = 1.713
CM = -0.344
CD = ------

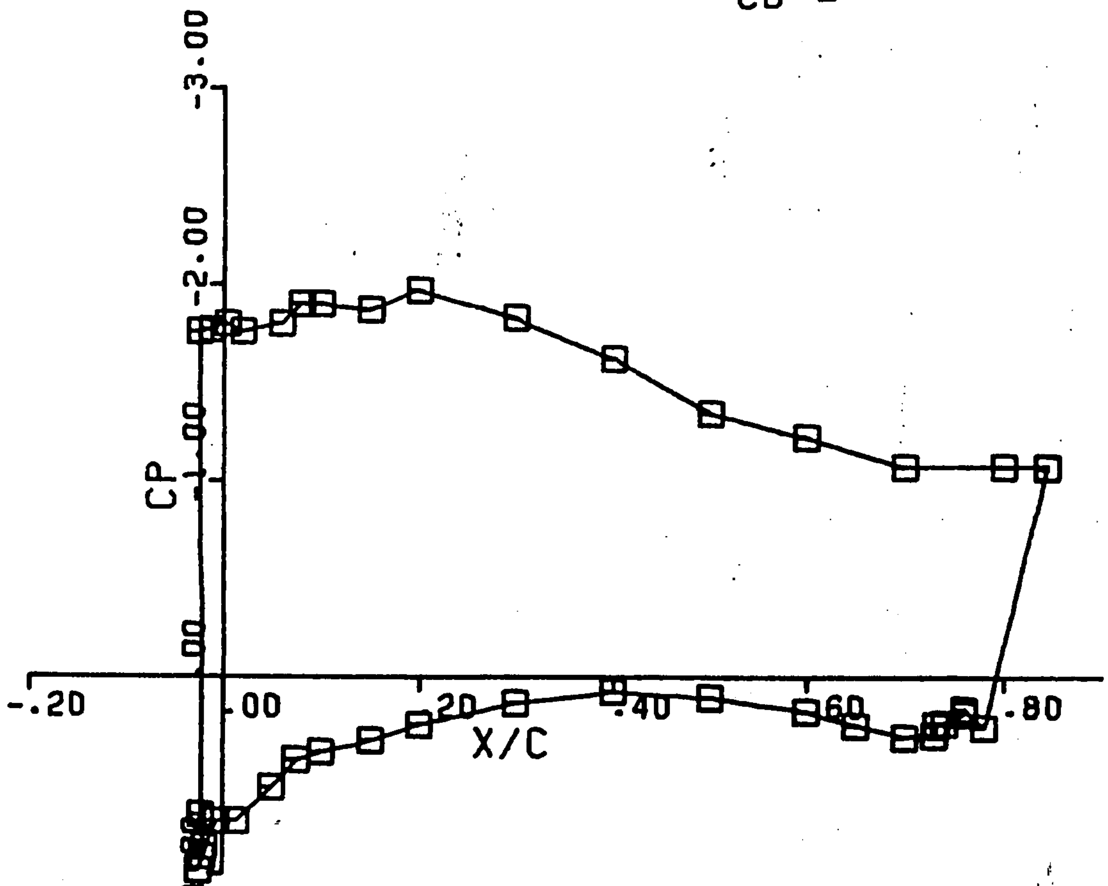

MAIN ELEMENT
CL = 1.481
CM = -0.140

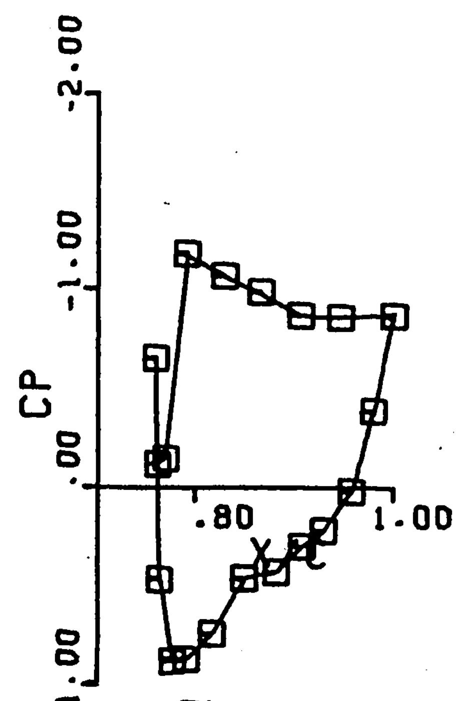

FLAP
CL = 0.232
CM = -0.203

GENERIC SMOOTH RUN # 114

AOA = -6.40
FLAP DEF = 10.00
CL = -0.102
CM = -0.114
CD = -------

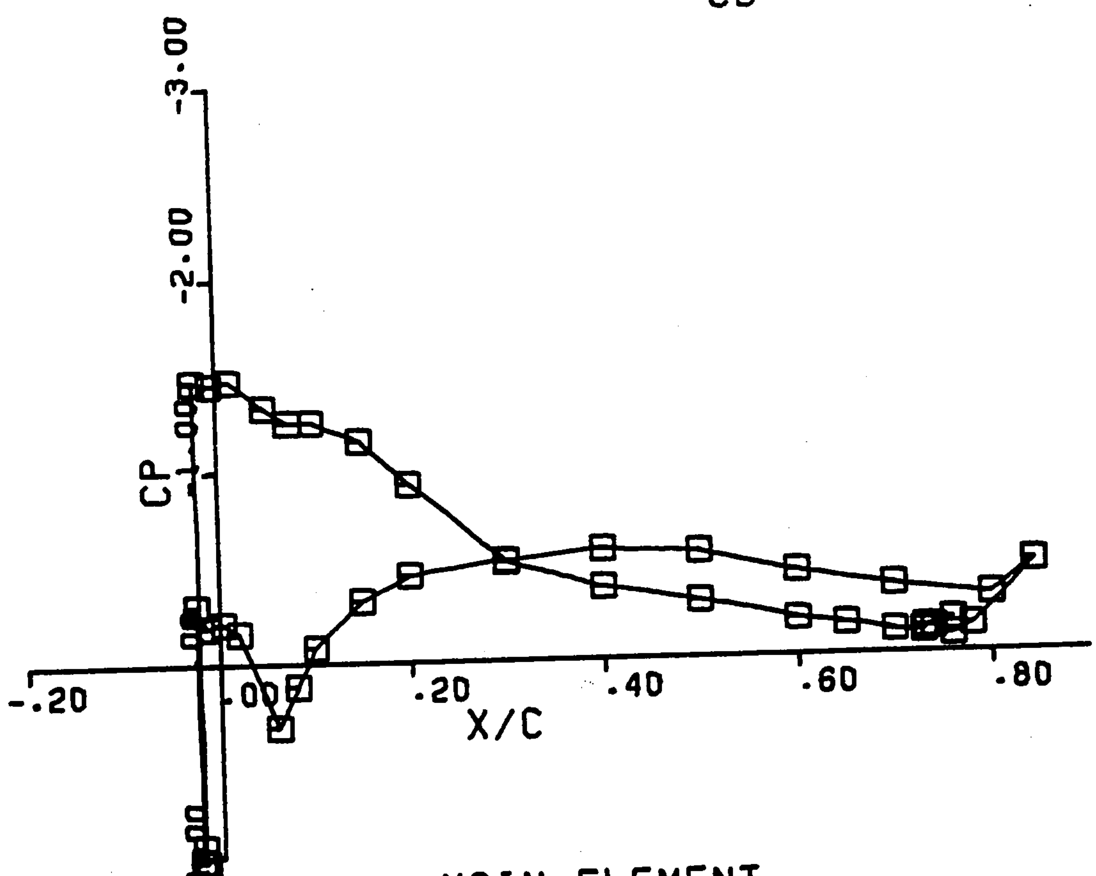

MAIN ELEMENT
CL = -0.162
CM = -0.076

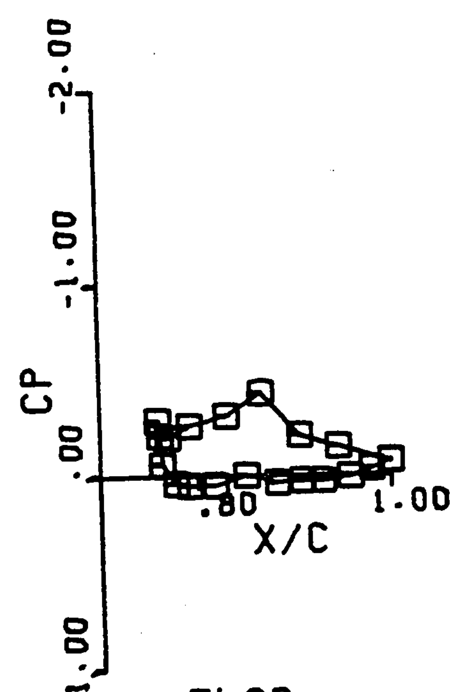

FLAP
CL = 0.060
CM = -0.038

GENERIC SMOOTH RUN # 115

AOA = -2.40
FLAP DEF = 10.00
CL = 0.448
CM = -0.111
CD = ------

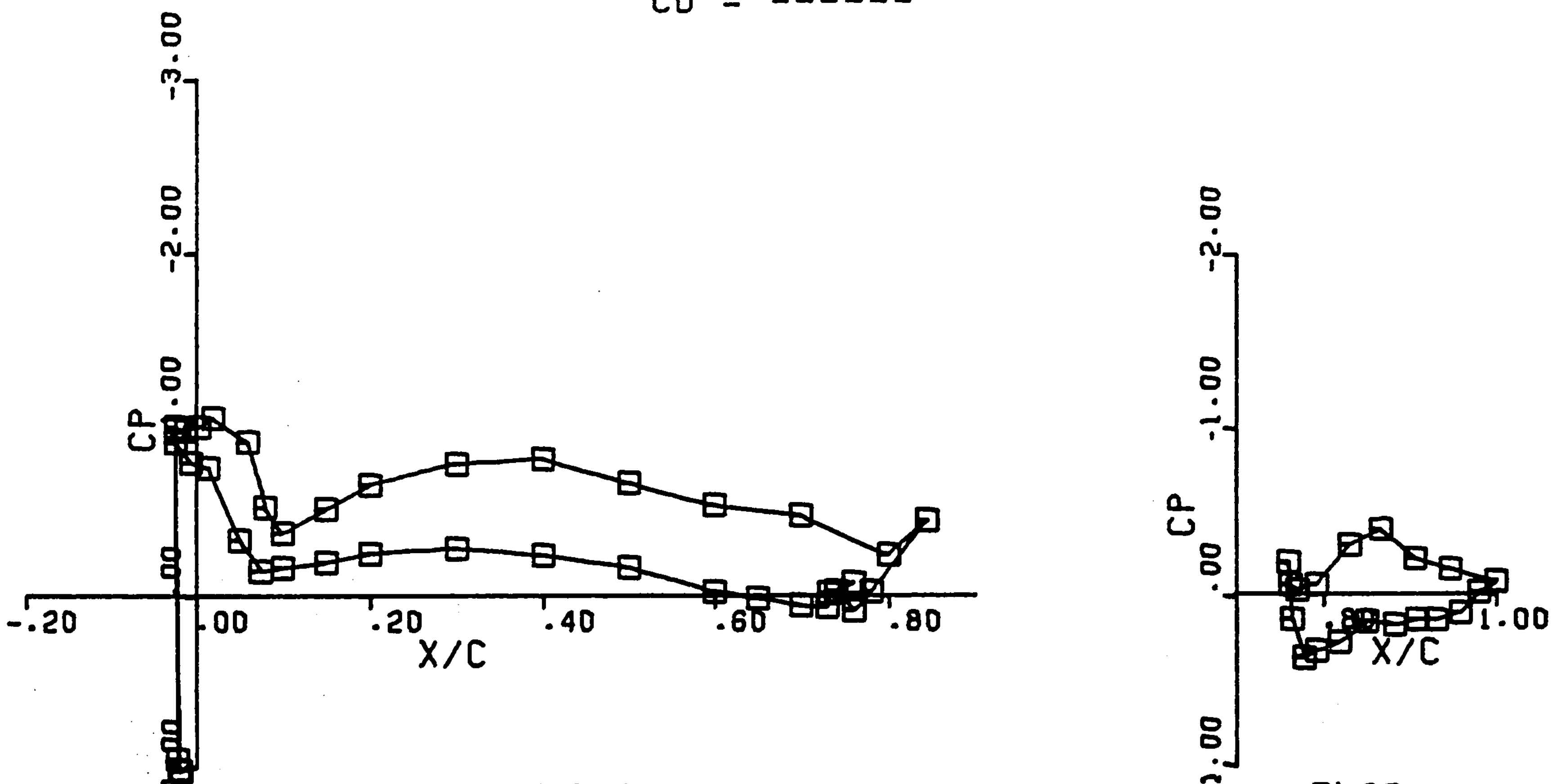

MAIN ELEMENT
CL = 0.366
CM = -0.058

FLAP
CL = 0.083
CM = -0.053

GENERIC SMOOTH RUN # 124

AOA = 5.60
FLAP DEF = 10.00
CL = 1.194
CM = -0.097
CD = ------

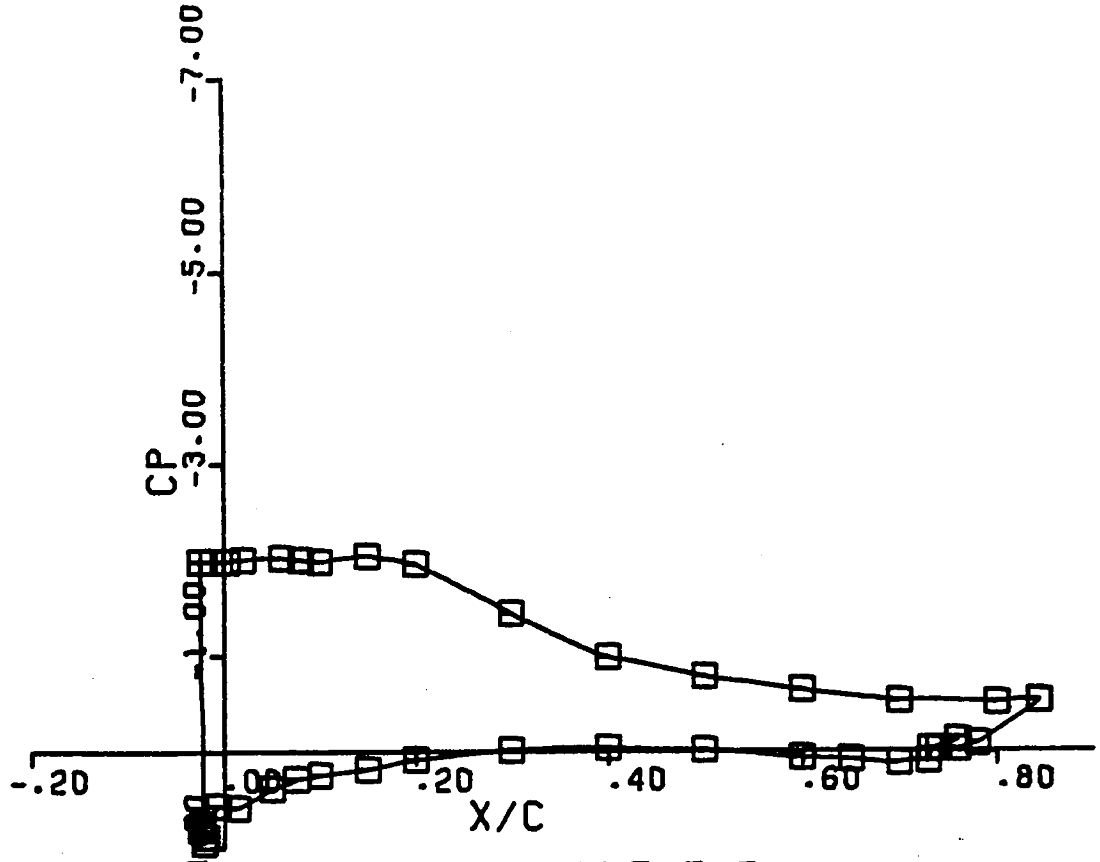

MAIN ELEMENT
CL = 1.084
CM = -0.025

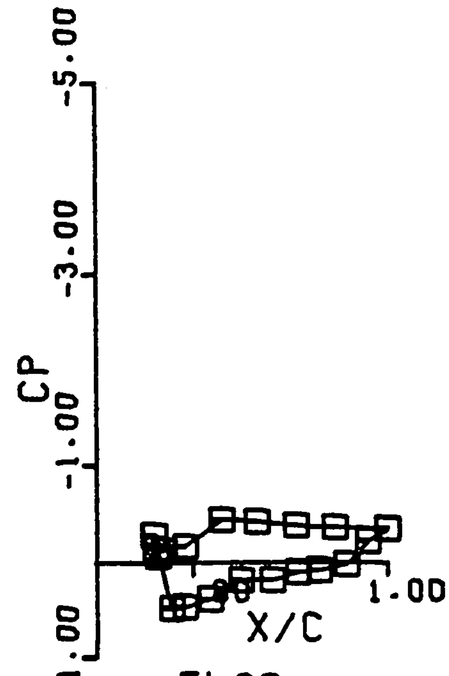

FLAP
CL = 0.110
CM = -0.072

GENERIC SMOOTH RUN # 125

AOA = 7.60
FLAP DEF = 10.00
CL = 1.216
CM = -0.136
CD = ------

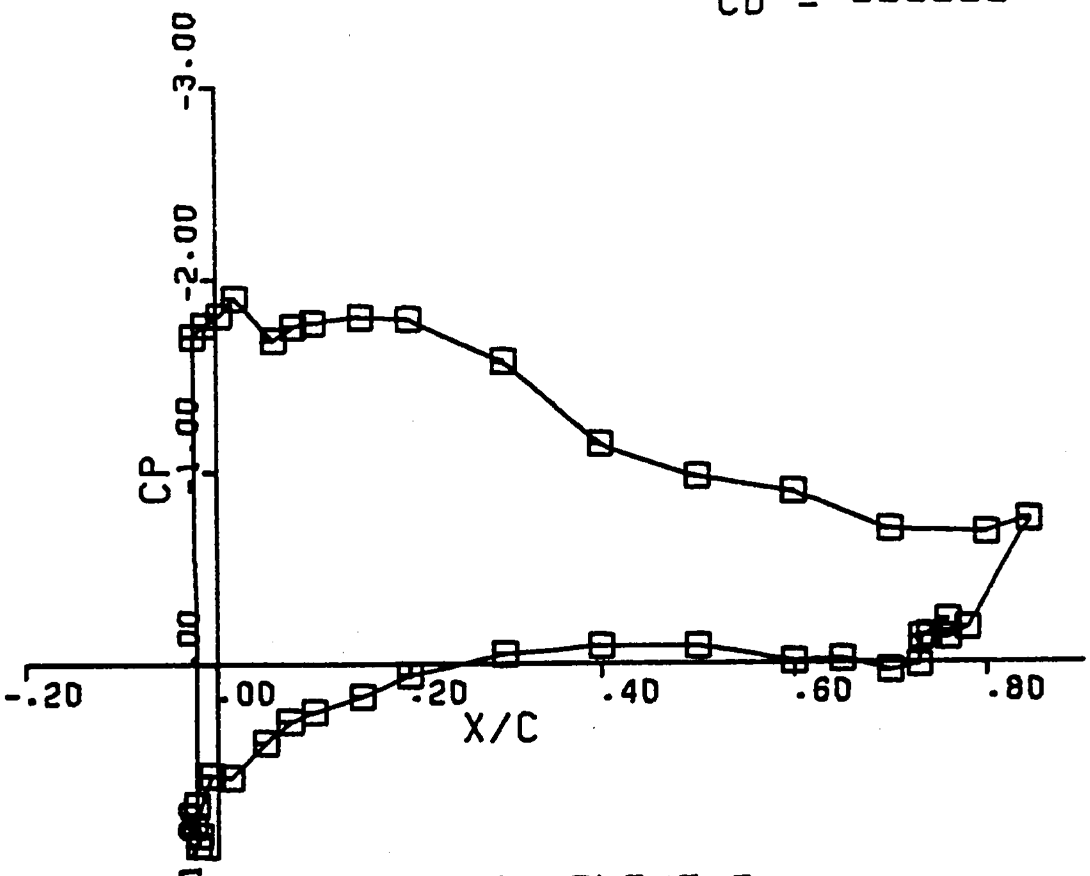

MAIN ELEMENT
CL = 1.085
CM = -0.048

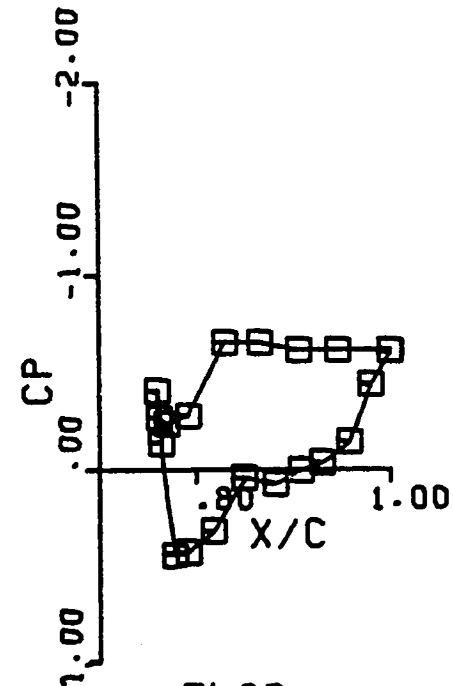

FLAP
CL = 0.131
CM = -0.089

GENERIC SMOOTH RUN # 126

AOA = 5.60
FLAP DEF = 10.00
CL = 1.191
CM = -0.094
CD = ------

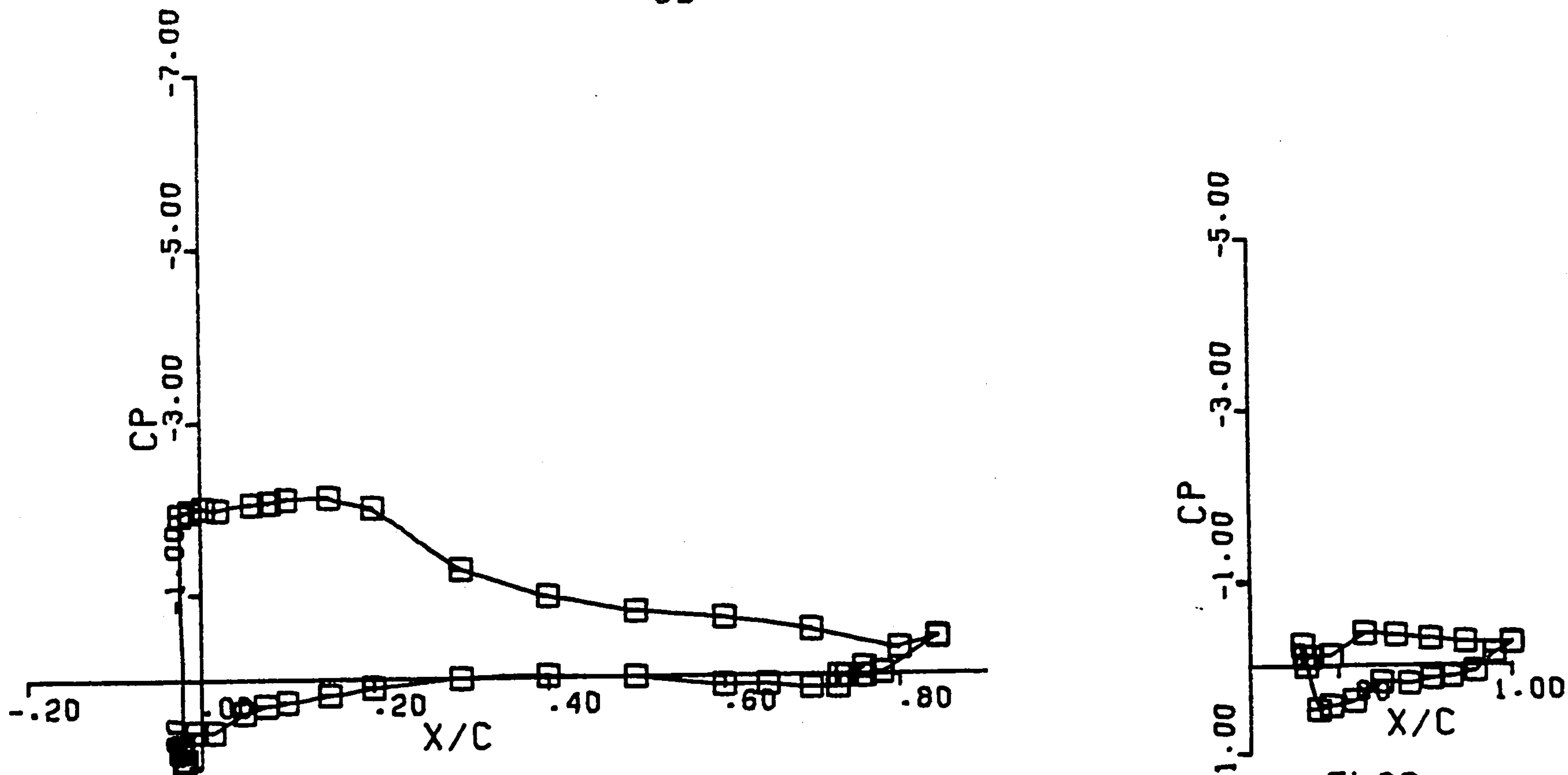

MAIN ELEMENT
CL = 1.084
CM = -0.024

FLAP
CL = 0.107
CM = -0.071

GENERIC SMOOTH RUN # 127

AOA = 9.60
FLAP DEF = 10.00
CL = 1.145
CM = -0.181
CD = ------

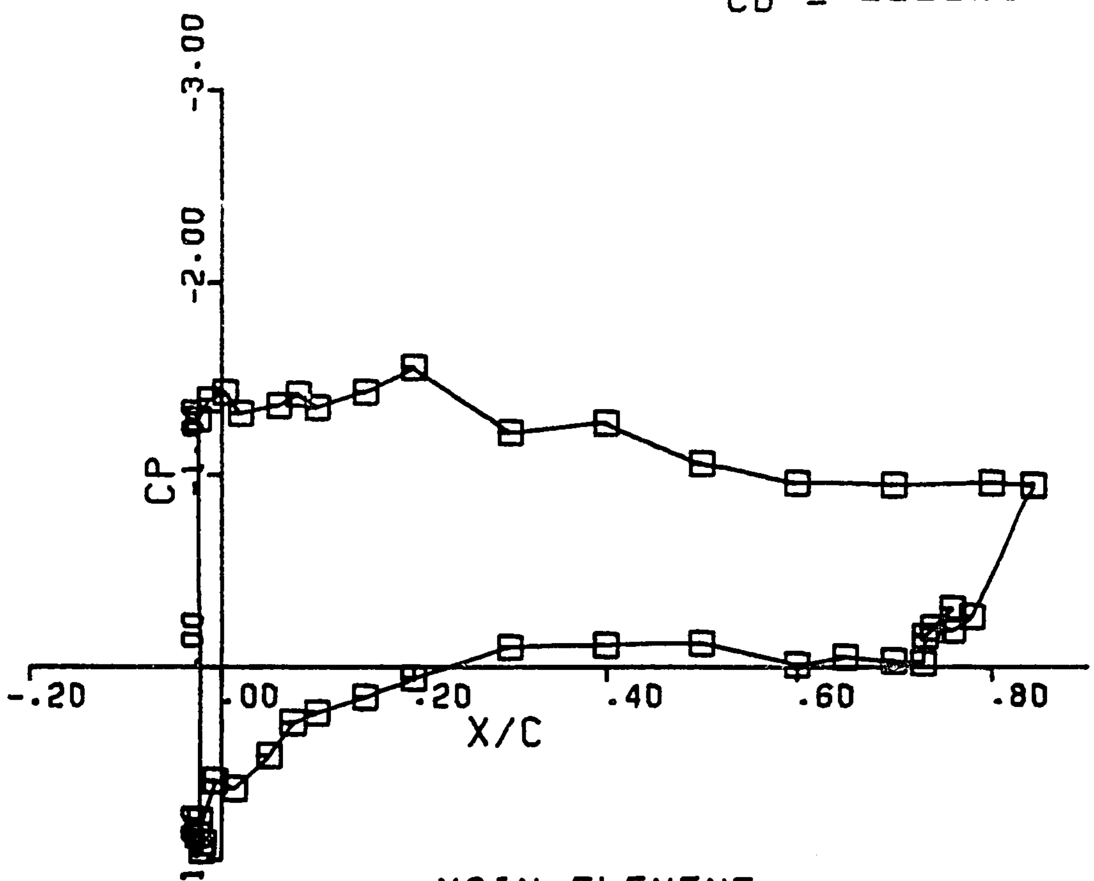

MAIN ELEMENT
CL = 0.998
CM = -0.079

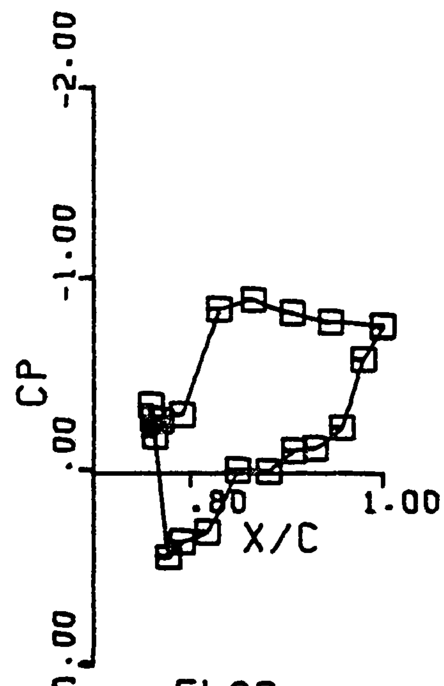

FLAP
CL = 0.147
CM = -0.102

GENERIC SMOOTH RUN # 128

AOA = 5.60
FLAP DEF = 20.00
CL = 1.461
CM = -0.202
CD = ------

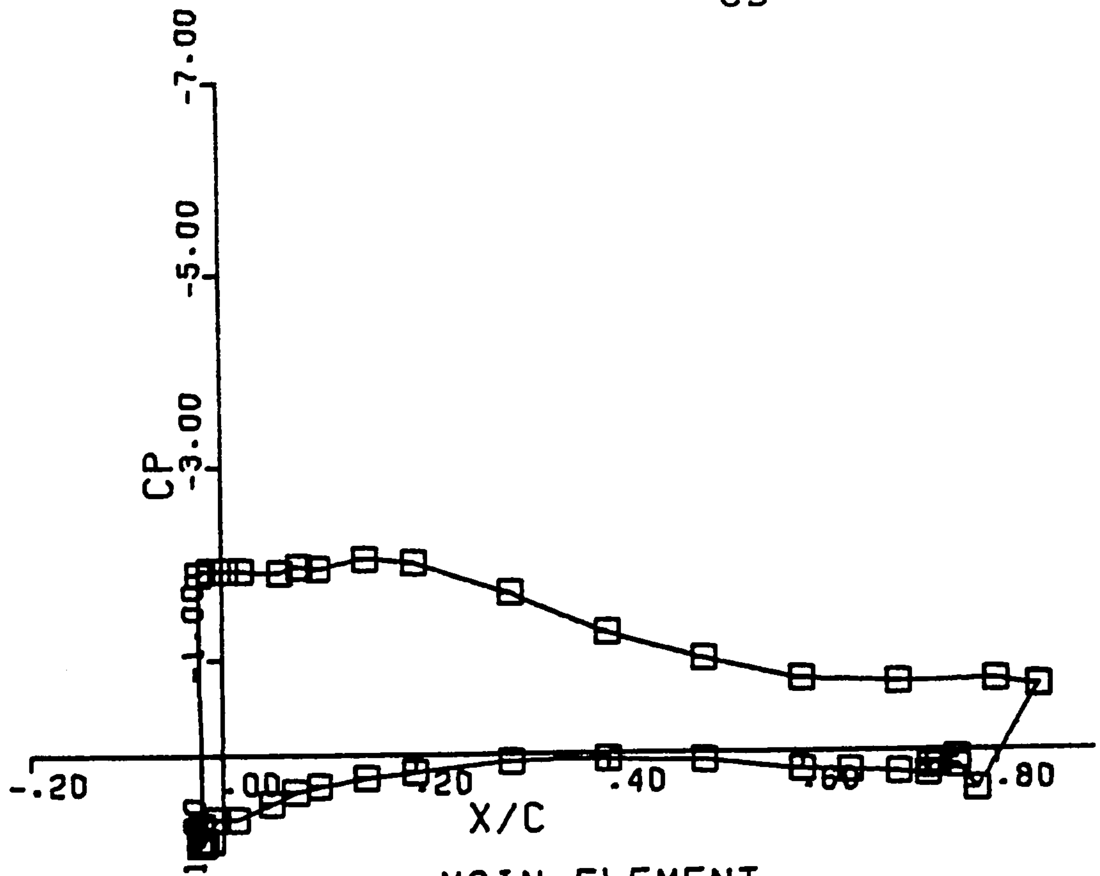

MAIN ELEMENT
CL = 1.301
CM = -0.082

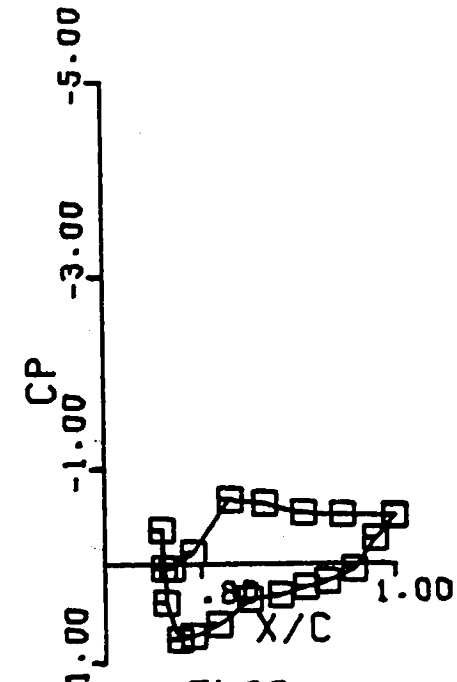

FLAP
CL = 0.159
CM = -0.121

GENERIC SMOOTH RUN # 129

AOA = 7.60
FLAP DEF = 20.00
CL = 1.553
CM = -0.252
CD = ------

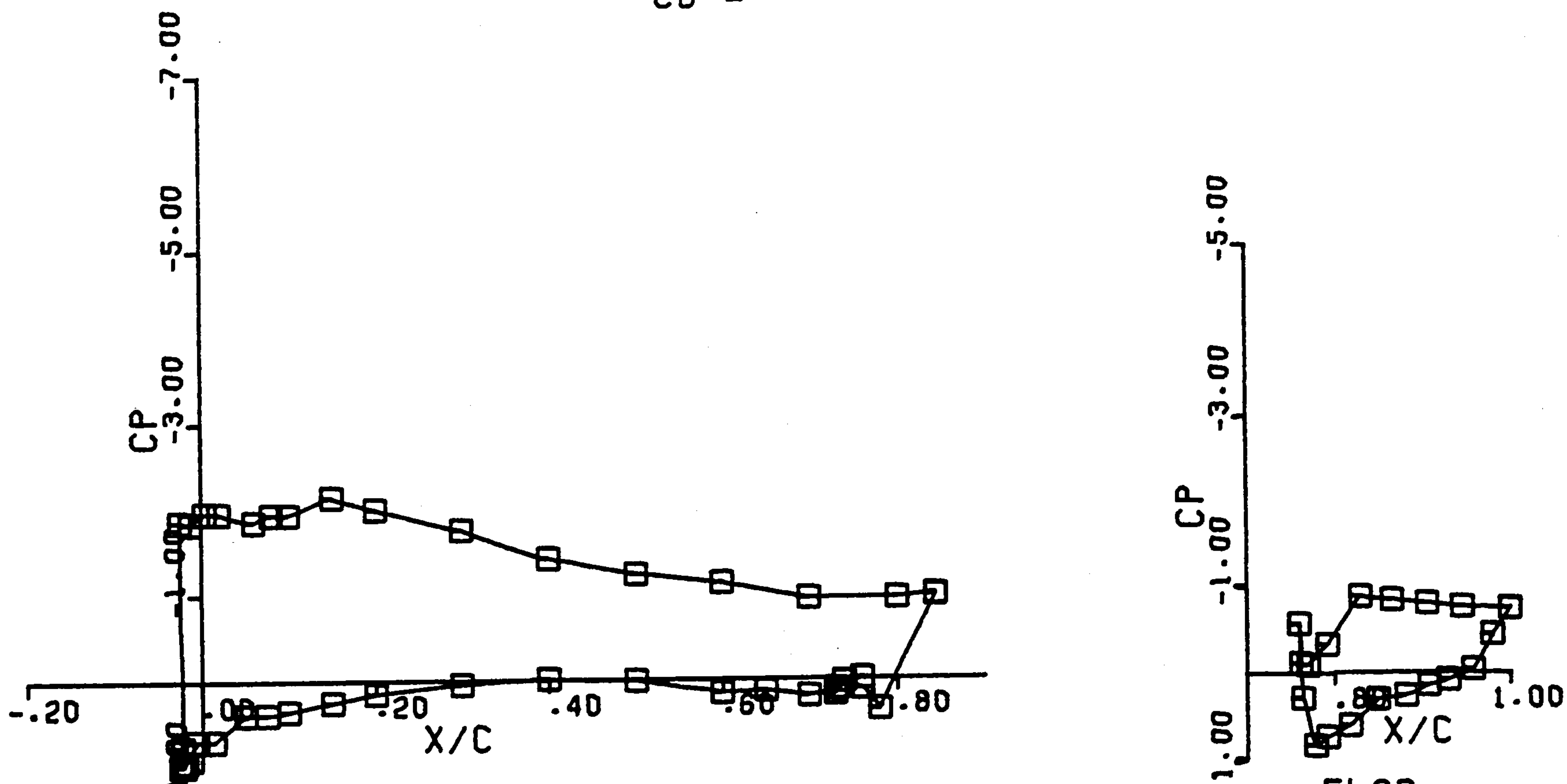

MAIN ELEMENT
CL = 1.368
CM = -0.109

FLAP
CL = 0.185
CM = -0.143

GENERIC SMOOTH RUN # 130

AOA = 9.60
FLAP DEF = 20.00
CL = 1.373
CM = -0.290
CD = ------

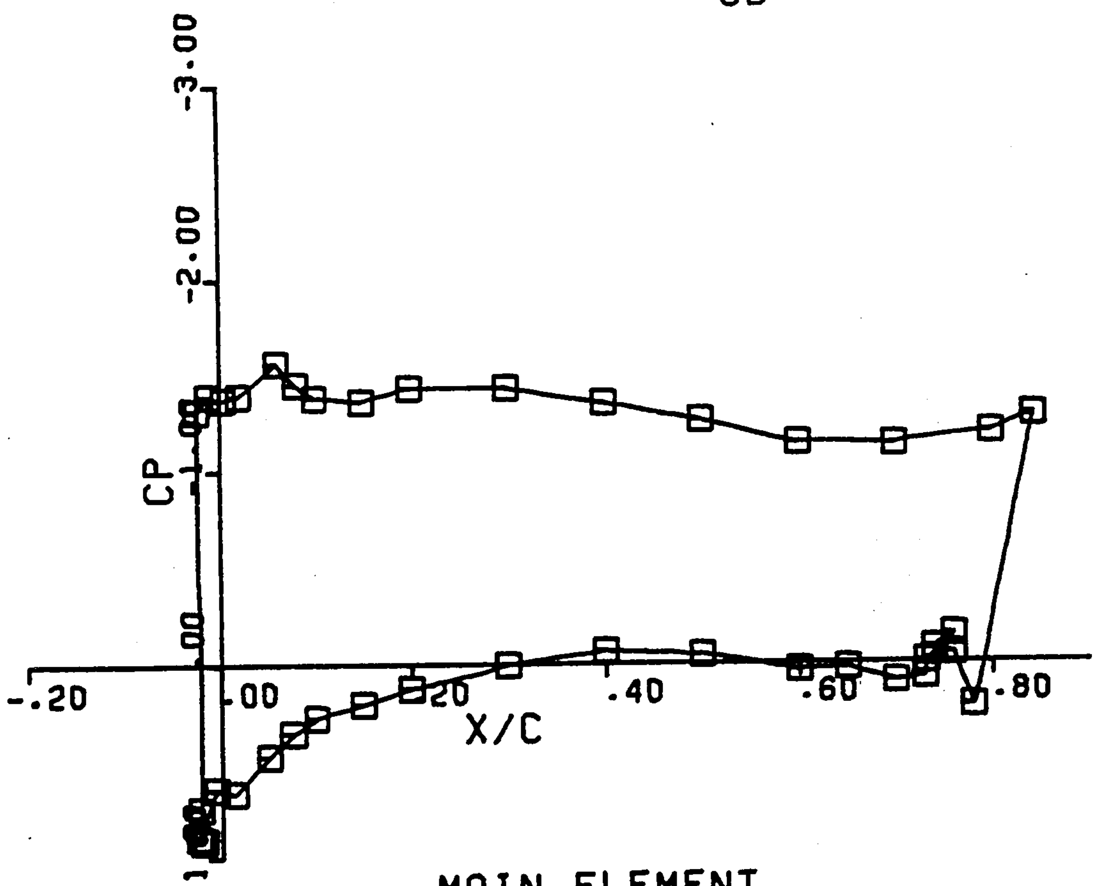

MAIN ELEMENT
CL = 1.168
CM = -0.128

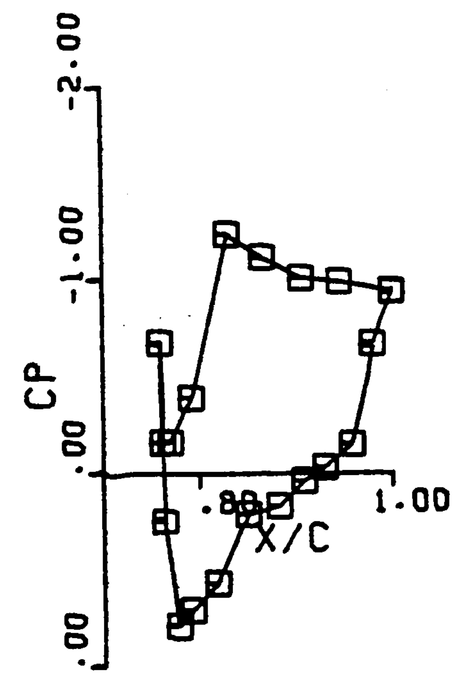

FLAP
CL = 0.205
CM = -0.163

GENERIC SMOOTH RUN # 131

AOA = -2.40
FLAP DEF = 20.00
CL = 0.802
CM = -0.174
CD = ------

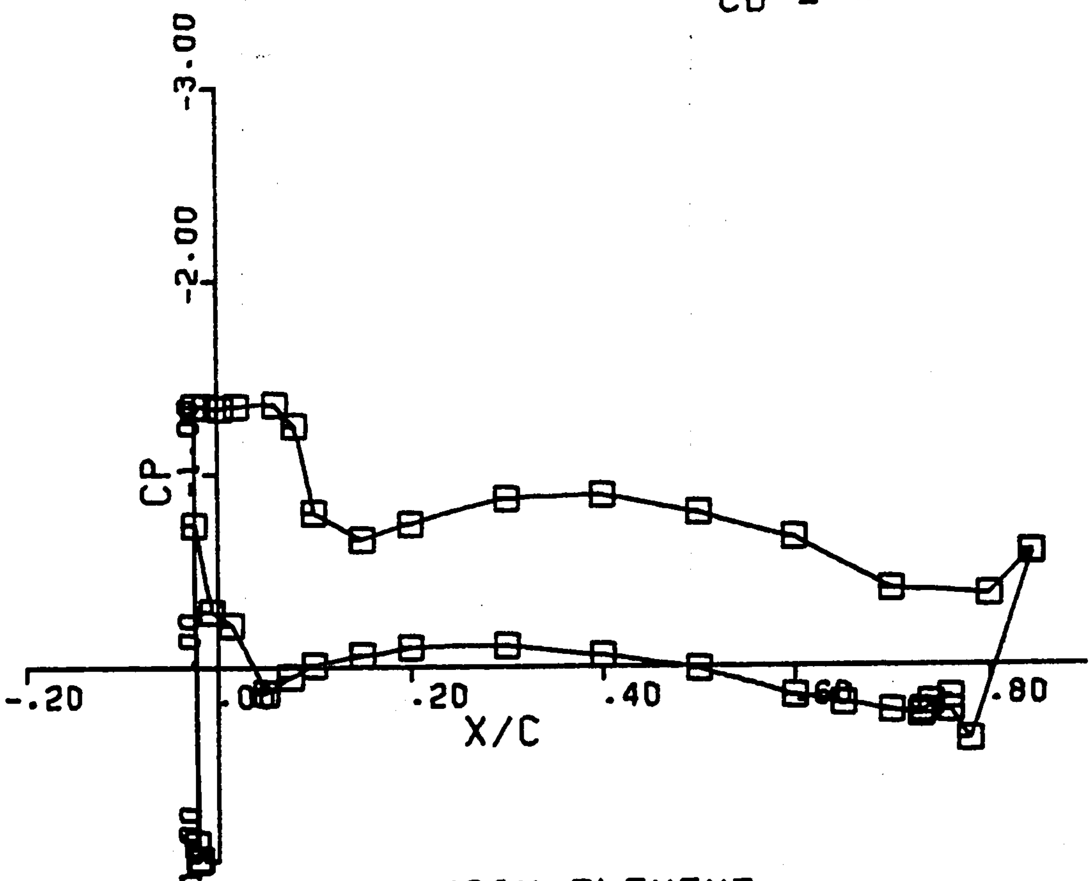

MAIN ELEMENT
CL = 0.667
CM = -0.079

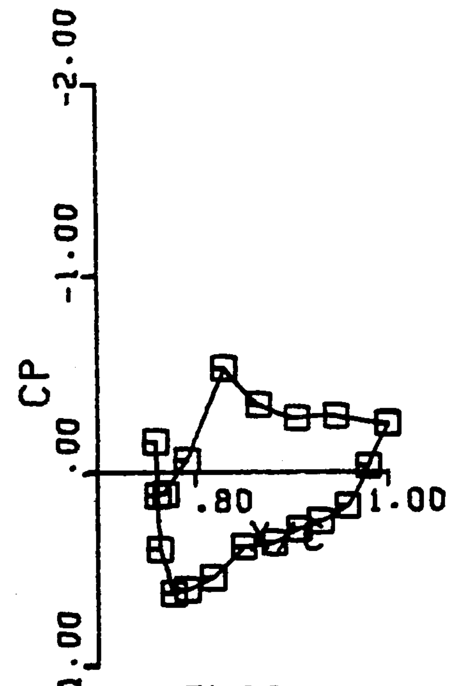

FLAP
CL = 0.135
CM = -0.095

GENERIC SMOOTH RUN # 132

AOA = 7.60
FLAP DEF = 0.00
CL = 0.904
CM = -0.036
CD = ------

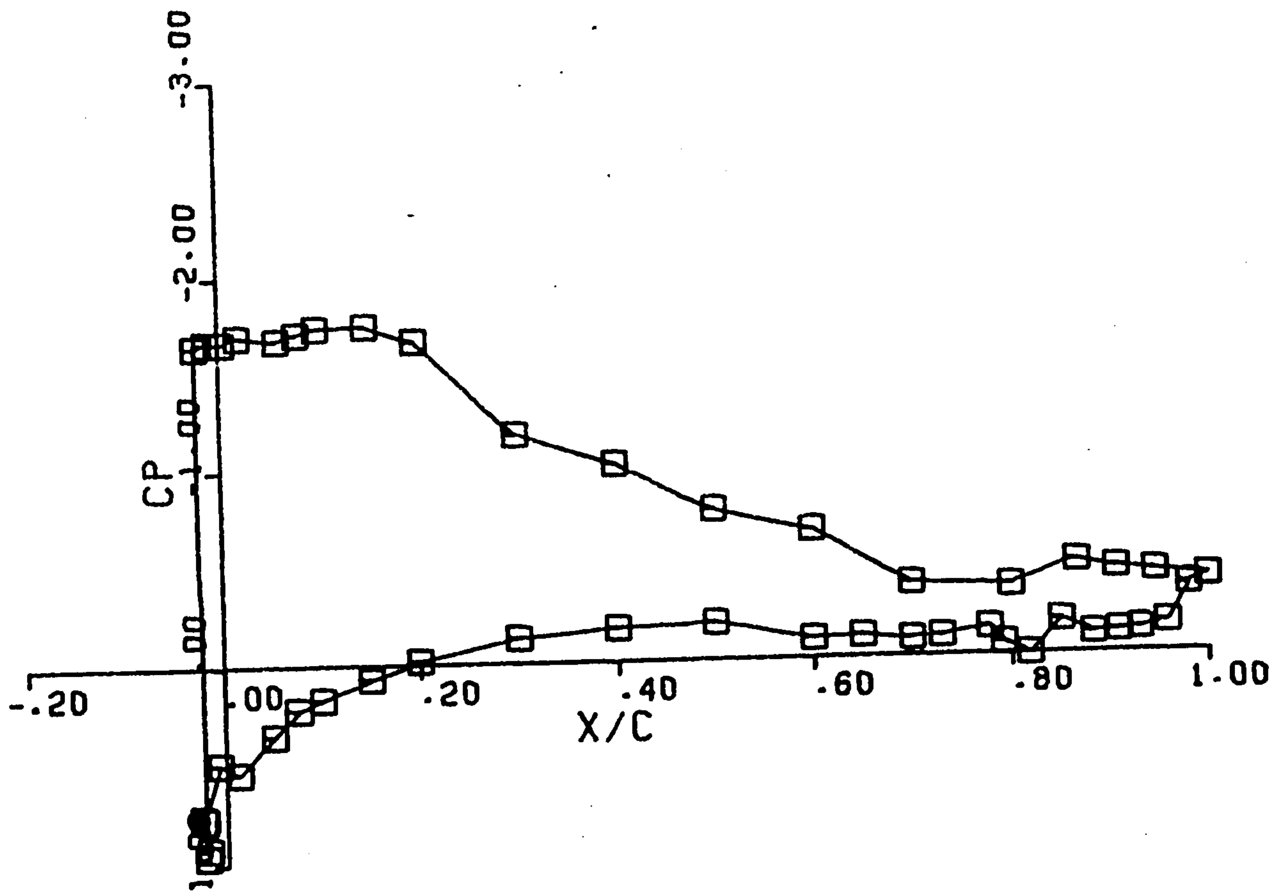

GENERIC SMOOTH RUN # 133

AOA = 9.60
FLAP DEF = 0.00
CL = 0.936
CM = -0.092
CD = ------

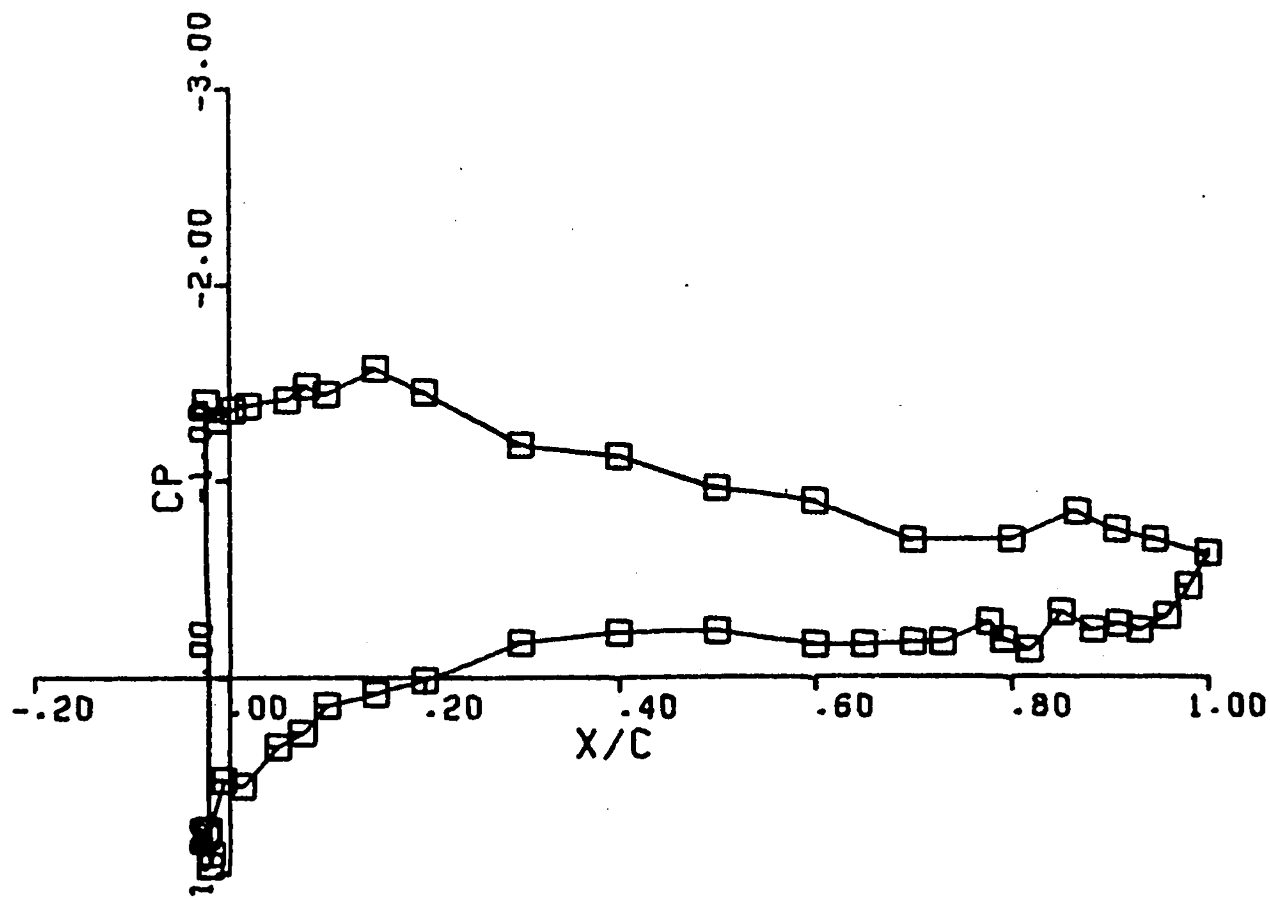

GENERIC SMOOTH RUN * 134

AOA = 11.60
FLAP DEF = 0.00
CL = 0.775
CM = -0.116
CD = ------

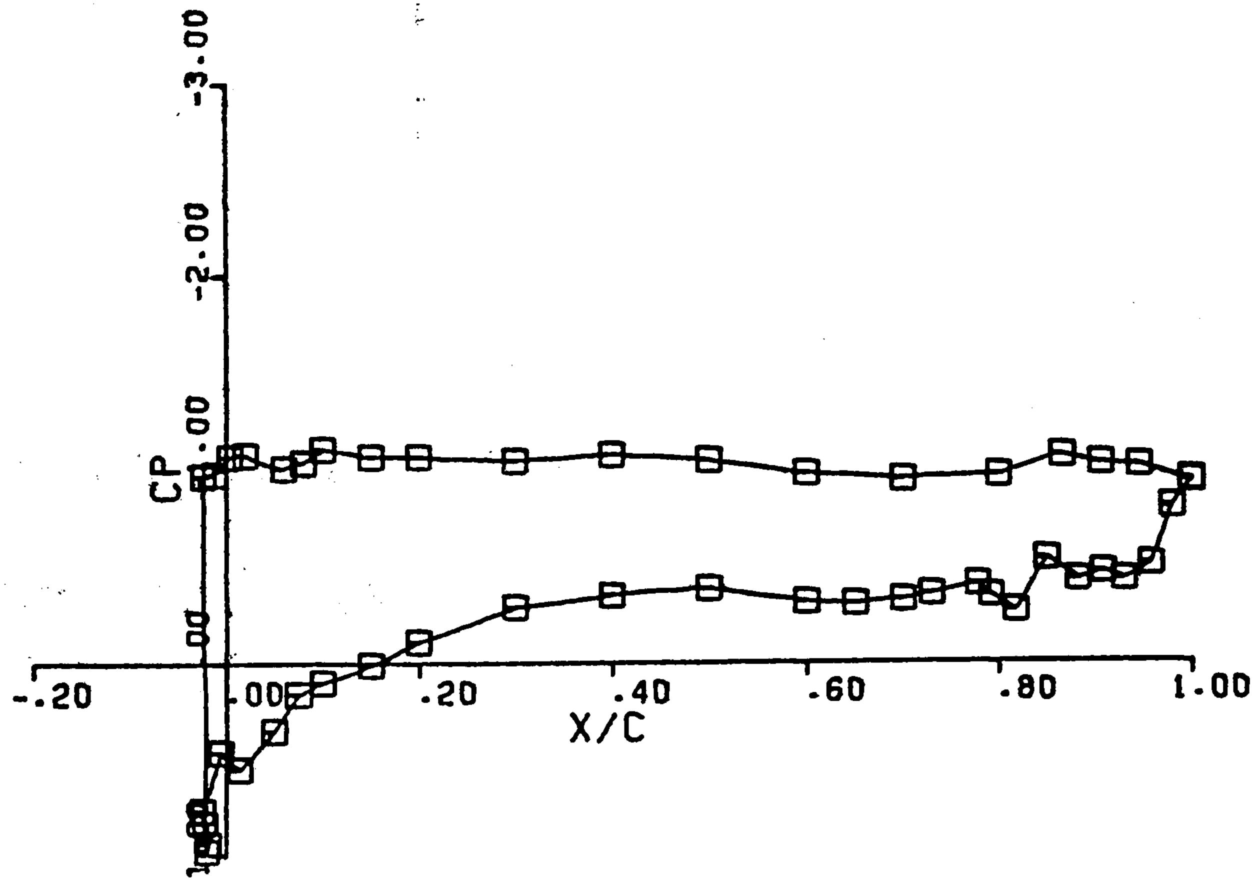

1. Report No.	2. Government Accession No.	3. Recipient's Catalog No.
NASA CR-168288		

4. Title and Subtitle	5. Report Date
Results of an Experimental Program Investigating the Effects of Simulated Ice on the Performance of the NACA 63A415 Airfoil with Flap	January 1984
	6. Performing Organization Code
7. Author(s)	8. Performing Organization Report No.
R. J. Zaguli, M. B. Bragg, and G. M. Gregorek	AARL TR 8302
	10. Work Unit No.
9. Performing Organization Name and Address	11. Contract or Grant No.
The Ohio State University Dept. of Aeronautical and Astronautical Engineering Columbus, Ohio 43212	NAG3-28
	13. Type of Report and Period Covered
12. Sponsoring Agency Name and Address	Contractor Report
National Aeronautics and Space Administration Washington, D.C. 20546	14. Sponsoring Agency Code
	505-45-02

15. Supplementary Notes

Final report. Project Manager, Robert J. Shaw, Propulsion Systems Division, NASA Lewis Research Center, Cleveland, Ohio 44135.

16. Abstract

A test program conducted in the NASA Icing Research Tunnel is described. Aerodynamic data are reported for a NACA 63A415 airfoil, with fowler flap, clean and with simulated ice shapes. The effect of three ice shapes on airfoil performance are presented, two of the simulated ice shapes are from earlier Icing Tunnel tests. Lift, drag, and moment coefficients are reported for the airfoil, clean and with ice, for angles of attack from approximately zero lift to maximum lift and for flap deflections of 0, 10, 20, and 30 degrees. Surface pressure distribution plots for the airfoil and flap are presented for all runs. Some preliminary oil flow visualization data are also discussed. Large drag penalties were measured in all instances. Maximum lift penalties were in general serious, and depend upon the ice shape and flap deflection.

17. Key Words (Suggested by Author(s))	18. Distribution Statement
Airfoil ice accretion Simulated ice accretion Static pressure distributions Airfoil performance	Unclassified - unlimited STAR Category 02

19. Security Classif. (of this report)	20. Security Classif. (of this page)	21. No. of pages	22. Price*
Unclassified	Unclassified	182	A09

*For sale by the National Technical Information Service, Springfield, Virginia 22161

National Aeronautics and Space Administration

Washington, D.C. 20546

Official Business

Penalty for Private Use, $300

SPECIAL FOURTH CLASS MAIL
BOOK

U.S. MAIL

Postage and Fees Paid
National Aeronautics and
Space Administration
NASA-451

NASA

POSTMASTER: If Undeliverable (Section 158 Postal Manual) Do Not Return